ISOFLURANE: INTERACTION WITH HEPATIC MICROSOMAL ENZYMES

by

Jennifer Jean Bradshaw, B.Sc., M.Sc.

Thesis presented for the degree of

DOCTOR OF PHILOSOPHY

in the Department of Medical Biochemistry,

UNIVERSITY OF CAPE TOWN

April, 1992

ACKNOWLEDGEMENTS

There are many people who have either given me tremendous support or assistance with the scientific content with this thesis due to the abnormal circumstances under which it was completed. I would like to express my gratitude especially to the following people:

Dr. Kathryn Ivanetich for her help and guidance for the duration of this thesis.

Dr. Melanie Ziman for all her support, advice on the scientific content of the thesis, and for her technical assistance in the more complex experiments.

Professor Gevers for his support and for taking over supervision of this thesis.

Dr. Cynthia Sikakana for her support and advice on the scientific content of the thesis.

Mr H. Terblanche, Ms. S. Titus, Ms. J. Harper and Ms. R. Mennie for all their technical assistance.

Mrs V. Morris for her help in typing the first draft of this thesis onto disc.

Professor Peter Dold for his encouragement, and assistance in drafting some of the Figures.

M.J. Mountain and Parteners for the use of computer and printing facilities.

I would like to acknowlege with gratitude the financial assistance of the South African Medical Research Council.

Lastly, I would like to thank my husband, Richard, and children, Jenny and David, for their patience, support and encouragement for the duration of this thesis.

Some of the work in this thesis has been published with the approval of Dr. K.M. Ivanetich, one of my supervisors, and can be found as follows:

i) Isoflurane: A Comparison of Its Metabolism by Human and Rat Hepatic Microsomes. J.J. Bradshaw and K.M. Ivanetich. Anesth. Analg., **63**, 805-813, 1984.

ii) Limitations of the Sodium Fusion Assay for Fluorinated Metabolites. K.M. Ivanetich and J.J. Bradshaw. Anesth. Analg., **61**, 61-64, 1980.

ABSTRACT

Isoflurane interacts with cytochrome P-450 in rat and human hepatic microsomes and the Δ6- and Δ5-desaturases in rat hepatic microsomes. The interaction of isoflurane with cytochrome P-450 results in its metabolism to fluoride ion and organofluorine metabolites. The cytochrome P-450 isozymes catalysing the defluorination of isoflurane were assessed in hepatic microsomes from phenobarbital-, β-naphthoflavone- and pregnenolone-16α-carbonitrile-pretreated and untreated rats. One or more of the cytochrome P-450 isozymes induced by phenobarbital and pregnenolone-16α-carbonitrile appear to defluorinate isoflurane, but those induced by β-naphthoflavone do not. From a comparison of the extent of defluorination of isoflurane in hepatic microsomes from phenobarbital- and pregnenolone-16α-carbonitrile-pretreated rats, and their K_m and V_{max} values, it appears that isoflurane is defluorinated by one or more isozymes induced by both phenobarbital and pregnenolone-16α-carbonitrile. The major isozyme is probably cytochrome P-450PCN1.

The metabolites of isoflurane were identified in human and phenobarbital-induced rat hepatic microsomes. In microsomes from phenobarbital-pretreated rats, isoflurane is metabolised to fluoride ion and trifluoroacetaldehyde; trifluoroacetic acid is not produced in measureable amounts. The trifluoroacetaldehyde produced binds to microsomal constituents. In human hepatic microsomes, the organofluorine metabolite is identified as trifluoroacetic acid. It is proposed that isoflurane is metabolised by different pathways in human and phenobarbital-induced rat hepatic microsomes.

The interaction of isoflurane with the cyanide-sensitive factors was assessed by several criteria. Firstly, using the reoxidation of cytochrome b_5 as an index of fatty acid desaturase activity, isoflurane appears to interact with the Δ6- and/or Δ5-desaturases, but not the Δ9-desaturase. Secondly, these results were confirmed and clarified by the use of direct assays to measure the fatty acid desaturase activity. Using the direct assay, we confirmed that isoflurane did not inhibit the Δ9-desaturase and inhibited Δ6-desaturation of linoleic acid, but not the Δ6-desaturation of α-linolenic acid. The inhibition of the Δ6-desaturation of linoleic acid occurred at low millimolar concentrations of isoflurane. Isoflurane inhibits the Δ5-desaturation of eicosa-8,11,14-trienoic acid to a small extent which is only apparent at much higher concentrations of isoflurane than that which inhibits the Δ6-desaturase.

Further studies focussed on measurement of the activity of Δ6-desaturase in order to attempt to study the kinetics of the inhibition of the Δ6-desaturase by isoflurane: Δ6-desaturase activity was assessed using hepatic microsomes as the source of the enzyme and linoleic acid as substrate precursor. In the course of these studies, we identified a number of factors that affected the apparent activity of the Δ6-desaturase in hepatic microsomes. These included significant levels of endogenous substrate and competing reactions in the hepatic microsomes. Endogenous substrate levels were quantified and corrected for. We then resorted to computer modelling to extract the kinetics of the Δ6-desaturase free of contributions from acyl-CoA synthetase and lysophospholipid acyltransferase, as well as enzyme decay. The kinetics of isoflurane inhibition of the Δ6-desaturase were then superimposed and studied by computer modelling.

LIST OF ABBREVIATIONS

V_{max}	Maximal rate of the reaction
K_m	Michaelis Menten constant which is equal to the concentration of the substrate that gives half the numerical maximal rate of the reaction
EDTA	Ethylenediaminetetra acetic acid
NAD(H)	Nicotine adenine dinucleotide (reduced)
NADP(H)	Nicotine adenine dinucleotide phosphate (reduced)
TRIS	Tris(hydroxy methyl)methylamine
U	Units
CoA	Coenzyme A
HCl	Hydrochloric acid
BSA	Bovine serum albumin
$MgCl_2$	Magnesium chloride
GSH	Reduced glutatione
TLC	Thin layer chromatography
HPLC	High pressure liquid chromatography
CO	Carbon monoxide
min	Minute(s)
m-	milli- (10^{-3})

μ-	micro- (10^{-6})
n-	nano- (10^{-9})
p-	pico- (10^{-12})
M	Molar
nm	Nanometers
mol	Mole

Lysophospholipid acyltransferases	Collective name referring to all the acyltransferases
2-Linoleoylphosphatidyl-choline and 2-γ-linolenoyl-phosphatidylcholine	Products of acylation of phospholipids by the lysophospholipid acyltransferases during measurement of the Δ6-desaturase reaction
Fatty acid desaturases	Also known as the fatty acyl-CoA desaturases and refers to the Δ9-, Δ6- and Δ5-desaturases
Acyl-CoA synthetase	also known as the acyl-CoA synthase, or long-chain acyl-CoA synthetase
Acyl-CoA	Fatty acyl-CoA

TABLE OF CONTENTS

LIST OF TABLES

LIST OF FIGURES

1. INTRODUCTION

Since the discovery of the anaesthetic properties of nitrous oxide and diethyl ether during the last century, the quest for a safer, better anaesthetic agent has continued, with two goals in mind: anaesthetic non-flammability and the absence of anaesthetic toxicity (1,2). The non-flammable properties appeared to be achieved by halogenation, but chlorine proved to be unsuitable resulting in enhanced anaesthetic toxicity, as was observed with chloroform (1,2). The development of the atomic bomb provided the necessary chemical technology for the inclusion of fluoride into anaesthetic ethers and led to the synthesis of fluroxene, halothane, methoxyflurane, enflurane and isoflurane (1,2).

Fluroxene was the first halogenated anaesthetic to be synthesised in 1951; it was non-flammable but unstable, and was soon replaced by the highly successful anaesthetic, halothane (3). The structures of the halogenated anaesthetics, halothane, methoxyflurane, enflurane, and isoflurane together with some of their physical properties, are shown in Table 1. Halothane is a non-flammable anaesthetic agent, first introduced into clinical practice in 1956 (5). Halothane has enjoyed great popularity as an anaesthetic agent, but is associated with occasional cases of potentially fatal hepatitis and more frequent cases of abnormal liver function (6,7).

Methoxyflurane was the first of the non-flammable fluorinated ethers to be used as an anaesthetic agent (8). However, it is now seldom used because methoxyflurane anaesthesia is associated with polyuric renal failure (9). The nephrotoxic properties of methoxyflurane are associated with its high rate of

TABLE 1

PROPERTIES OF SOME CURRENTLY AVAILABLE VOLATILE ANAESTHETIC AGENTS *

	Isoflurane	Enflurane	Halothane	Methoxyflurane
	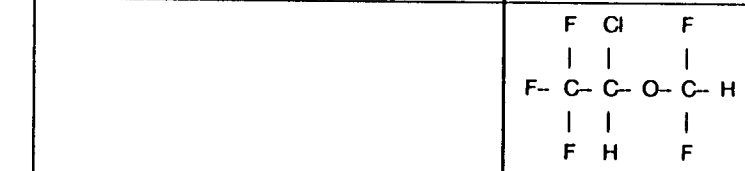	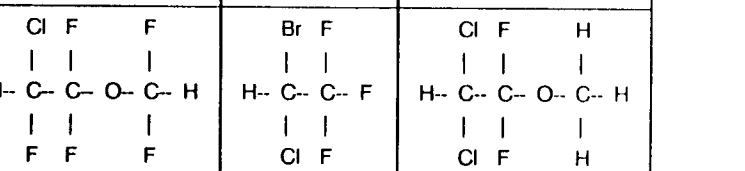		
Molecular weight	184.5	184.5	197.4	165.4
Specific gravity (25 °C)	1.50	1.52	1.86	1.41
Boiling point (°C)	48.5	56.5	50.2	104.7
Vapor pressure at 20 °C (torr)	240	172	244	22.8
Minimum inflammable concentration in 70 per cent N_2O, 30 per cent O_2 (per cent)	7.0	5.8	4.8	> vapor pressure
MAC in O_2 †	1.15	1.68	0.75	0.16
MAC in 70 per cent N_2O †	0.50	0.57	0.29	0.07
Blood/gas partition coefficient (37 °C)	1.4	1.9	2.3	12
Conductive rubber/gas partition coefficient (at room temperature)	62	74	120	630
Preservative	None	None	Thymol	Butylated hydroxytoluene
Stability in soda lime	Stable	Stable	Breaks down	Breaks down
Per cent of uptake recovered as metabolites	0.17	2.4	20	50

* Adapted from reference 4

† In 30- to 55-year-old patients; per cent of 1 atm.

metabolism to fluoride ion; fluoride ion is thought to be the metabolite causing renal dysfunction (10-13).

Enflurane is a non-flammable, stable anaesthetic agent which was first introduced into clinical practice in the mid-1970's (9). Although enflurane, like methoxyflurane, is metabolised to the potentially nephrotoxic fluoride ion, the rate of metabolism of enflurane is so low that toxic fluoride levels (ca. 50 μM urinary fluoride) are seldom, if ever, reached (9,14,15). Isoflurane, a structural analogue of enflurane (Table 1), appears to be virtually devoid of nephrotoxicity also due to the low extent of metabolism to fluoride ion (1,16). Although isoflurane is more costly to manufacture, it appears to be potentially the safest of all the fluorinated anaesthetic agents presently marketed (16).

Isoflurane was first manufactured in 1965, two years after enflurane (1). Following extensive testing in both animal and human subjects, isoflurane showed no signs of organ toxicity and was scheduled for release by the pharmaceutical industry in 1975 (1). Shortly before its release, Corbett implicated isoflurane as the cause of hepatic neoplasia observed in mice (17). Further studies showed that the neoplasia was caused by polybrominated biphenyls contaminating the animals' foodstuff, and isoflurane was finally released in 1981 (1,18,19). From its release until 1987, there were 45 cases of hepatic dysfunction reported following isoflurane anaesthesia (20). These cases have been examined for a possible association between anaesthetic administration and subsequent hepatic dysfunction. The conclusion reached was that, based on current evidence, there does not seem to be any association between isoflurane anaesthesia and post-operative hepatic

dysfunction (20). Therefore, it would appear that isoflurane may represent a major advance in the search for a perfect anaesthetic.

The toxicity resulting from anaesthesia has normally been (i) renal, as in the case of methoxyflurane, which is the result of its conversion to fluoride ion, or (ii) hepatic, as in the case of halothane. Although isoflurane anaesthesia is thought not to result in nephrotoxicity or hepatotoxicity, it is still essential to elucidate the interaction of isoflurane and its metabolites with hepatic enzymes. This thesis has focussed on an investigation of the interaction of isoflurane (and in certain cases, other halogenated anaesthetic agents) with two hepatic microsomal enzyme systems, viz:

i) the cytochrome P-450-dependent drug-metabolising system, which catalyses the defluorination of volatile anaesthetic agents, including possibly isoflurane.

ii) the fatty acid desaturases, which play a role in the biosynthesis of polyunsaturated fatty acids and consequently in the maintenance of membrane structure and function, as well as the biosynthesis of eicosanoids.

The background to both of these hepatic enzyme systems, together with their role in anaesthetic metabolism and, in the case of the fatty acid desaturases, fatty acid metabolism will be discussed.

1.1 DRUG METABOLISM

Organisms are increasingly exposed to foreign chemicals such as drugs, insecticides, environmental pollutants and food additives, which usually have no biological value (21). These chemicals are called xenobiotics (21-23). The body metabolises and then excretes these compounds via urine, faeces or exhaled air. The enzyme systems involved in the metabolism of xenobiotics have been extensively studied over the last 3 to 4 decades.

Xenobiotics are usually of a hydrophobic nature and can undergo several types of reactions in the liver and other tissues to render them more hydrophilic in order that they can be more easily excreted. Such reactions include conjugation, hydrolysis, reduction or oxidation, of which oxidation and conjugation are considered to be qualitatively the most important.

Xenobiotic metabolism often occurs in two phases (Figure 1)(21,24) :

i) Phase 1: The oxidation, reduction or hydrolysis of a non-polar xenobiotic to yield a more hydrophilic or polar metabolite.

ii) Phase 2: Subsequent conjugation of the polar metabolite to a small endogenous, usually highly polar, compound e.g. glutathione, glucuronic acid, sulfate, glycine or water.

The general function of drug metabolism is the conversion of a relatively toxic hydrophobic xenobiotic to a relatively non-toxic hydrophilic compound which the body can easily excrete. However, there are exceptions where

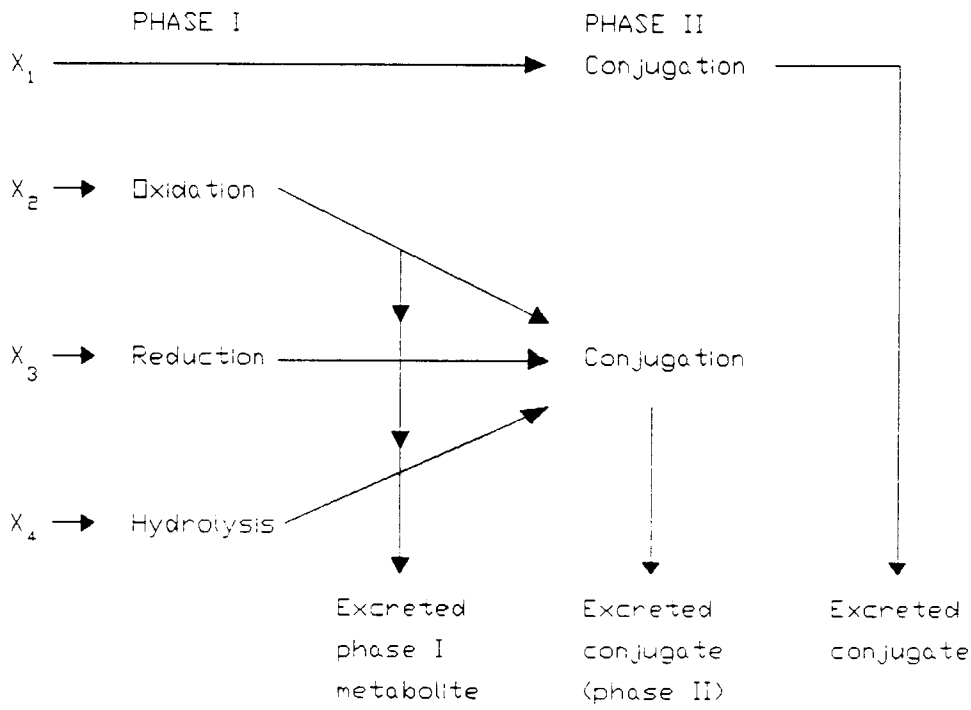

FIGURE 1 **Phase 1 and Phase 2 of drug metabolism**

X, xenobiotic.
Adapted from reference 21

biotransformation of a non-toxic compound by Phase 1 and/or Phase 2 of drug metabolism results in a more toxic reactive compound (25,26).

Ongoing research into chemical carcinogenesis has shown that a large number of chemicals believed to be carcinogens, require metabolic activation by the enzymes of Phase 1 and/or Phase 2 of drug metabolism (25-27). Enzymatic activation of chemical pre-carcinogens usually results in a relatively unstable, electrophilic intermediate which can bind covalently to the nucleophilic centres of membranes and/or macromolecules (25,28); for example, benzo(α)pyrene is metabolised by cytochrome P-450 and epoxide hydrase to the 7,8-diol-9,10-oxide, which is thought to be the ultimate carcinogen (28,29). Similarly, benz(α)anthracene is metabolically activated to the 1,2-3,4-oxide, and aflatoxin B_1, to the 2,3-oxide by cytochrome P-450 (25,28,29). Other types of compounds which are activated by the enzymes of Phase 1 or Phase 2 of drug metabolism include:

i) the nitroso compounds, e.g. dimethylnitrosamine which is activated by cytochrome P-450 resulting in the electrophilic alkyldiazonium ion (27);

ii) the haloalkanes, e.g. carbon tetrachloride which is activated to the trichloromethyl radical and associated oxy radical which cause liver necrosis and lipid peroxidation (30);

iii) the haloethylenes, e.g. vinylchloride which is activated to chloroethylene oxide and chloroacetaldehyde by cytochrome P-450 (31).

Drug metabolism occurs in all organisms except anaerobic bacteria (32,33). In mammals, the liver contains the highest concentration of the drug metabolising enzymes; lower activities are found in most organs and tissues of the body i.e. in the kidneys, lungs, intestine, blood and skin (32,33). Some of the reactions catalysed by the enzymes of Phase 1 of drug metabolism are shown in Table 2. The oxidative reactions are the most common and these are primarily catalysed by a group of enzymes known as cytochrome P-450 (21,25,34).

The conjugation reactions of Phase 2 of drug metabolism are catalysed by a number of different enzymes, which include glucuronyl transferase, glutathione transferase, methyl transferase, sulphotransferase and epoxide hydrase. More details of the reactions of Phase 2 of drug metabolism can be found elsewhere (21).

Sometimes only a single transformation of a xenobiotic occurs, e.g. the oxidative reaction of Phase 1 of drug metabolism, but more frequently two processes are involved, e.g. oxidation followed by conjugation (21). The aspect of drug metabolism investigated herein, viz: the Phase 1 reactions catalysed by cytochrome P-450, will be considered in more detail.

1.1.1 Cytochrome P-450

Cytochrome P-450 is a haem protein found deeply embedded in the lipid bilayer of the endoplasmic reticulum* in association with the other components of an electron transport chain of which cytochrome P-450 is the terminal oxidase (Figure 2) (35-41). Cytochrome P-450 consists of a group of isozymes having a characteristic absorption peak at 450 nm of the ferrous-carbon monoxide

* On homogenisation of the liver, the endoplasmic reticulum becomes fragmented, and the fragments form vesicles, known as microsomes (24).

TABLE 2

PHASE I OF HEPATIC METABOLISM OF XENOBIOTICS *

Reaction	Enzyme	Example
Oxidative metabolism		
Oxidation of a variety of compounds (Table 3)	Cytochrome P-450	(Table 3)
Oxidation and/or reduction of aldehydes and carboxylic acids	Alcohol dehydrogenase, aldehyde dehydrogenase	Ethanol
Reductive metabolism		
Reduction of azo- and nitro-compounds	Flavin enzymes, azo- and nitro-reductases, cytochrome P-450	Sulfanilamide
Reduction of carbonyl compounds, haloalkanes	Cytochrome P-450	Chloral, halothane
Hydrolysis		
Hydrolysis of esters	Esterases	Aspirin

* Compiled from references 21, 24.

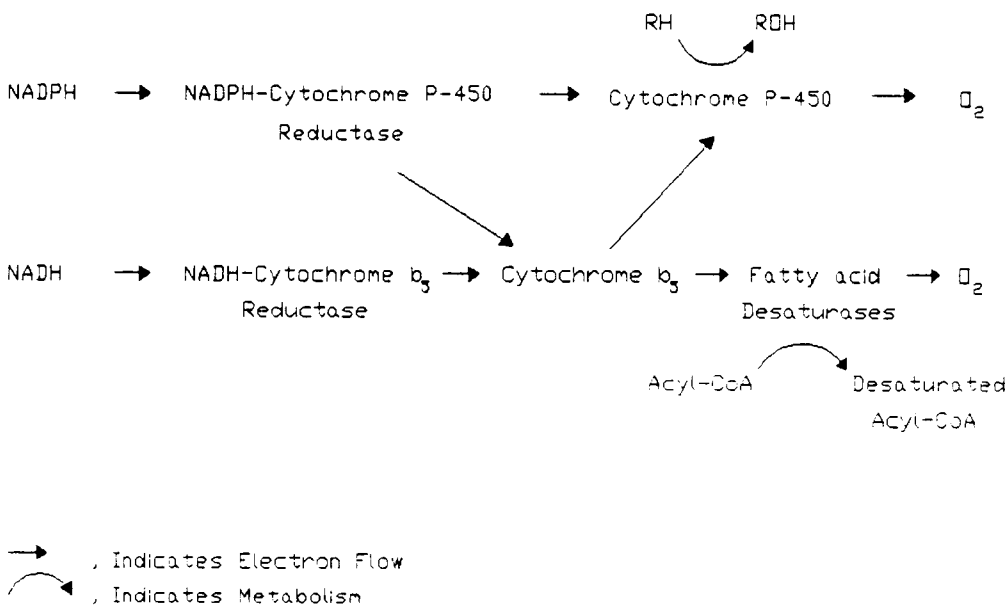

FIGURE 2 **Interaction of two microsomal electron transport pathways**

RH, substrate; ROH, hydroxylated product.
Compiled from references 34 and 92

complex, after which it was named in 1962 by Omura and Sato (35). The molecular weight of the cytochrome P-450 isozymes range from 48,000 to 56,000 daltons (42-44,46-49).

Cytochrome P-450 is a b-type cytochrome with an active centre containing an iron protoporphyrin IX in a large relatively open hydrophobic crevice of the protein (36,50-52). The haem is bound to the apoprotein by non-covalent forces, primarily hydrophobic in nature (50,52). The fifth ligand to the haem iron is provided by the thiolate group of a cysteine residue in the protein, and the sixth ligand is thought to be a relatively weak field ligand, such as water or the hydroxyl group of a neighbouring amino acid residue in the protein, such as serine or threonine (51-58).

The most remarkable features of cytochrome P-450 are its broad substrate specificity, and the wide variety of reactions it catalyses (Table 3). The broad substrate specificity is due, in part, to the existence of isozymes, but even the purified isozymes interact with a number of different substrates (23). Cytochrome P-450 probably first evolved to take on the function of the biosynthesis and degradation of endogenous substrates critical to the organism's life function (58). However, during the course of evolution, the substrate specificity broadened so that cytochrome P-450 now metabolises both endogenous substrates and foreign chemicals (23,58,59).

Substrates for cytochrome P-450 can be considered to be of 3 classes (23), viz:

i) endogenous compounds, e.g. fatty acids, steroids and prostaglandins (60).

TABLE 3

SOME HYDROXYLATION REACTIONS CATALYSED BY CYTOCHROME P-450 *

Aromatic hydroxylation

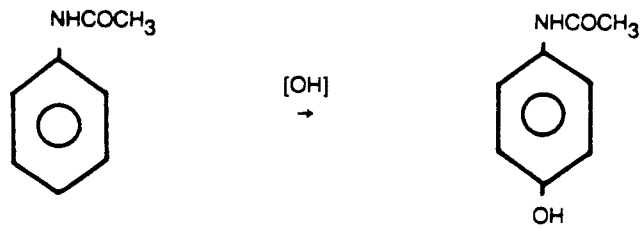

Aliphatic hydroxylation

$$R\text{-}CH_3 \xrightarrow{[OH]} R\text{-}CH_2\text{-}OH + H^+$$

N-Dealkylation

$$R\text{-}NH\text{-}CH_3 \xrightarrow{[OH]} [R\text{-}NH\text{-}CH_2OH] \rightarrow RNH_2 + CH_2O \text{ (Formaldehyde)}$$

O-Dealkylation

$$R\text{-}O\text{-}CH_3 \xrightarrow{[OH]} [R\text{-}O\text{-}CH_2OH] \rightarrow ROH + CH_2O \text{ (Formaldehyde)}$$

Deamination

$$R\text{-}CH(NH_2)\text{-}CH_3 \xrightarrow{[OH]} [R\text{-}C(OH)(NH_2)\text{-}CH_3] \rightarrow R\text{-}CO\text{-}CH_3 + NH_3$$

Sulphoxidation

$$R\text{-}S\text{-}R' \xrightarrow{[OH]} [R\text{-}SOH\text{-}R']^+ \rightarrow R\text{-}SO\text{-}R' + H^+$$

N-Oxidation

$$(CH_3)_3N \xrightarrow{[OH]} [(CH_3)_3NOH]^+ \rightarrow (CH_3)_3NO + H^+$$

* Reproduced from reference 34.

ii) natural products that are found in foodstuffs, or formed on ingestion, e.g. vitamins, steroids, fatty acids, mycotoxins and alkaloids.

iii) xenobiotics, e.g. industrial chemicals, pesticides, drugs and environmental pollutants.

1.1.1.1 Binding of Compounds to Cytochrome P-450

The first step in the oxidative and reductive metabolism of compounds, including xenobiotics and endogenous substances, by cytochrome P-450, is the binding of the substrate to the oxidised form of the enzyme (32,45,61). The binding of a compound to cytochrome P-450 results in a characteristic spectrum which is most often identified by formation of a difference spectrum in microsomes (or with purified cytochrome P-450). The difference spectrum can be measured from the difference in absorbance between hepatic microsomes in which the compound is bound to cytochrome P-450 versus hepatic microsomes in the absence of a compound (61-63). The difference spectrum is thought to arise from a change in spin state of the haem iron (51,64-68). In hepatic microsomes, the cytochrome P-450 isozymes exist in an equilibrium of spin states which are regulated, in part, by the environment of the haem iron, and in part by the binding of endogenous substrates, such as fatty acids (32,51,52). In the high spin form of cytochrome P-450, all 5 d electrons are unpaired and the iron is penta-coordinate; four ligands are provided from the haem pyrrole nitrogens and the fifth ligand is a thiolate anion from a cysteine residue in the protein (32,50-52). In the low spin form, there are 2 electrons in each of the lowest d orbitals, and one unpaired electron in the next highest orbital and the haem is hexacoordinate; the sixth ligand position is either vacant

(pentacoordinate) or occupied by an easily exchangeable ligand, such as water or a hydroxyl group (hexacoordinate) (32,50-52).

The difference spectrum resulting from the binding of a compound to microsomal cytochrome P-450 fall into one of three categories: Type I, Type II or Type IR difference spectra (63,64,69). A Type I difference spectrum arises from the formation of an enzyme-substrate complex, while Type II arises from the binding of a compound (ligand), usually a good electron donor, directly to the haem iron. The spectral and spin state changes associated with these types of difference spectra are illustrated in Figure 3.

1.1.1.2 Oxidative Reactions Catalysed by Cytochrome P-450

The oxidative reactions catalysed by cytochrome P-450 are thought to involve an initial hydroxylation of the compound, which may re-arrange to form a product of different structure (34) (Table 3). The overall reaction for the oxidative metabolism of compounds by cytochrome P-450 is thought to be:

$$NADPH + H^+ + 0_2 + RH \rightarrow ROH + NADP^+ + H_2O \quad \text{.....(1)}$$

where RH represents lypophilic substrate and ROH represents hydroxylated product (32,34,69). As shown here, cytochrome P-450 exhibits 'monooxygenase' activity, i.e. catalyses the incorporation of one atom of dioxygen into the substrate (32,34,69). The other atom of dioxygen is usually reduced to water (32,69)*.

* Cytochrome P-450 is also known as a mixed function oxidase since the reaction involves oxidation of both a substrate and oxygen.

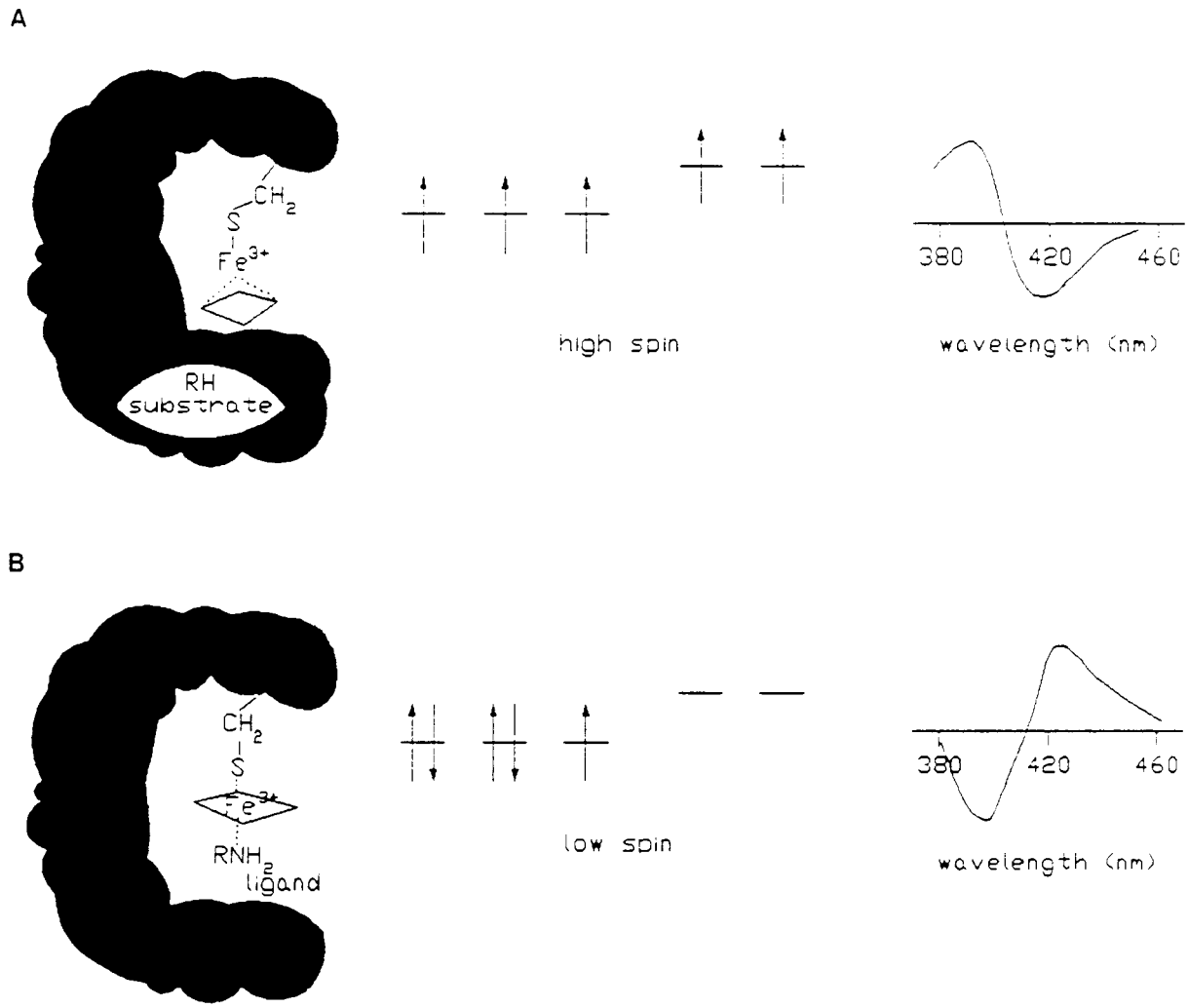

FIGURE 3 **The binding of a substrate (A) and ligand (B) to cytochrome P-450, showing the apoprotein (cloudy) and plane of the porphyrin ring**

The spin state changes and resulting difference spectra which accompany the binding of a substrate (A) and ligand (B) to cytochrome P-450 are also illustrated (83). Reproduced from reference 78

1.1.1.3 Mechanism of Cytochrome P-450 Catalysed Oxidative Reactions

Although cytochrome P-450 consists of a number of isozymes which catalyse the oxidative metabolism a wide variety of substrates, the mechanism of oxidation of all compounds has been assumed to be uniform for all forms of cytochrome P-450 (70). A mechanism for the oxidative metabolism of compounds by cytochrome P-450 which was initially proposed by Estabrook et al (71,72), is outlined in Figure 4 and can be summarised as follows (32,34,50,60,69,73):

Step 1: The binding of the substrate to the substrate-binding site results in a Type I difference spectrum. The binding of the substrate changes the spin state of ferricytochrome P-450 from low to high spin, which facilitates the next step in the pathway (51,64,67,68,75).

Step 2: Reduction of the ferricytochrome P-450-substrate complex to ferrocytochrome P-450-substrate complex by reducing equivalents usually donated from NADPH via NADPH-cytochrome P-450 reductase (See Section 1.1.1.6); this step sets the stage for binding and activation of molecular dioxygen (75).

Step 3: The binding of molecular dioxygen with the ferrous cytochrome P-450-substrate complex yields a ferrous dioxygen complex (32,34). The dioxygen binds to the haem iron trans to the thiolate sulfur atom (fifth axial ligand) (32).

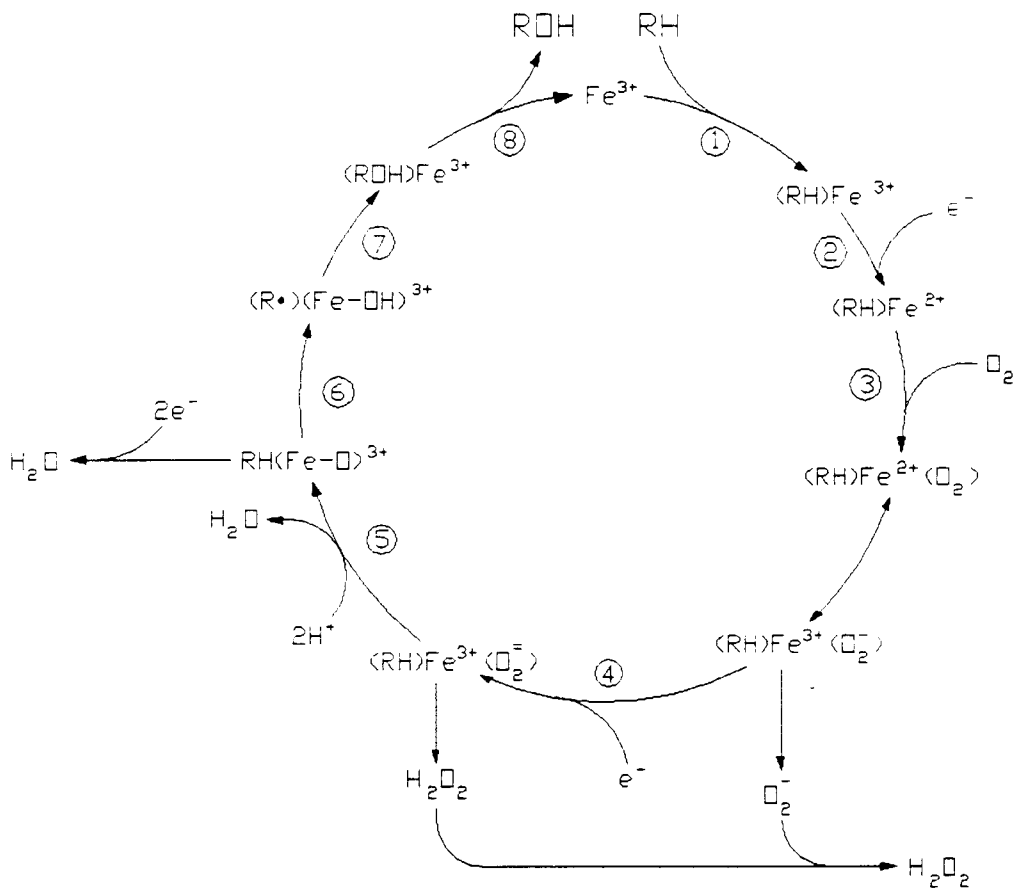

FIGURE 4 **Proposed scheme for the mechanism of action of cytochrome P-450 in xenobiotic hydroxylation**

RH, substrate; ROH, hydroxylated product; Fe^{2+} and Fe^{3+}, haem iron of cytochrome P-450.
Adapted from reference 32

Step 4: A second electron from NADH or NADPH via NADH-cytochrome b_5 reductase and cytochrome b_5 or via NADPH-cytochrome P-450 reductase, reduces the oxyferrocytochrome P-450-substrate complex.

Step 5: The dioxygen bridge is broken resulting in the formation of an activated oxygen.

Steps 6&7: Once the dioxygen bridge has been broken, oxygen insertion into the substrate is thought to occur via hydrogen abstraction by the activated oxygen followed by recombination of the resultant carbon and hydroxyl radicals to give hydroxylated product (32).

Step 8: The last step of the reaction involves dissociation of the hydroxylated product from cytochrome P-450 yielding the hydroxylated product and low spin ferric cytochrome P-450.

Steps 1, 3 and 6 are probably rapid and not rate-limiting (32,74). The rates of the other steps are influenced by a variety of circumstances, such as the association of cytochrome P-450 with cytochrome b_5 and NADPH-cytochrome P-450 reductase, the nature of the substrate, the cytochrome P-450 isozyme, availability of NADPH and type of membrane phospholipid used to reconstitute the cytochrome P-450 complex (32,50,74). It has been postulated that the rate-limiting step varies depending on specific conditions and more than one rate-limiting step may in fact exist (32,50,74).

1.1.1.4 Autooxidation of Cytochrome P-450

The reductive metabolism of dioxygen by cytochrome P-450 gives rise to the formation of active oxygen species, viz: superoxide anion, from a one electron transfer to oxygen and/or peroxide anion from a two electron transfer to oxygen (32,68,75-77) (Figure 4).

During the generation of active oxygen species, cytochrome P-450 exhibits oxidase activity, viz:

$$NADPH^+ + H^+ + 0_2 \rightarrow NADP^+ + H_20_2 \quad .....(2)$$

In the absence of substrate, this process is termed "autooxidation" (75,77). The oxidase activity of cytochrome P-450 is thought to arise from the decay of oxyferrocytochrome P-450 to either superoxide anion or hydrogen peroxide (75-77). Superoxide is usually dismutated viz:

$$2O^-_2 + 2H^+ \xrightarrow[\text{dismutase}]{\text{superoxide}} H_2O_2 + O_2 \quad .....(3)$$

The oxidase activity of cytochrome P-450 gives rise to the formation of active oxygen species with the futile consumption of reducing equivalents. It has been suggested that the spin state of substrate free-cytochrome P-450 regulates the production of active oxygen species by minimising electron flow to the haemoprotein-bound molecular dioxygen; cytochrome P-450 in high spin form does not require substrate binding for rapid reduction (32,68).

The exact mechanism of hydrogen peroxide and superoxide formation in microsomal systems has, as yet, not been resolved (75,78). Cytochrome P-450 appears to play a role in the generation of hydrogen peroxide and superoxide anion in the microsomal system, rather than the other components of the electron transport pathway (79). The involvement of cytochrome P-450 in this process is demonstrated by the inhibition of hydrogen peroxide generation by ligands such as carbon monoxide and cimetidine which bind to the dioxygen binding site (75,78). However, the purified reconstituted system differs in its source of hydrogen peroxide; NADPH-cytochrome P-450 reductase is predominantly responsible for hydrogen peroxide production suggesting that a more intact system such as microsomes or cellular suspensions might be preferable for this type of investigation (82).

1.1.1.5 Stoichiometry of Oxidative Reactions

The stoichiometry of the monooxygenase activity of cytochrome P-450-catalysed reactions (equation 1, page 14) is expected to be: 1 molecule of NADPH consumed : 1 molecule oxygen utilised : 1 molecule product generated. In determining the stoichiometry of cytochrome P-450 monooxygenase reactions, it is necessary to make a correction for the oxidase activity (equation 2, page 19) in which 1 molecule of NADPH and oxygen are consumed for every 1 molecule of hydrogen peroxide generated. Such oxidase activity is found in hepatic microsomes on the addition of reducing equivalents in the absence of substrate. Therefore, by accounting for the oxidase activity in the stoichiometry of the monooxygenase activity of cytochrome P-450, the hydrogen peroxide plus product generated should be in a 1:1:1 ratio with oxygen consumed and NADPH oxidised. The measurement of the stoichiometry of cytochrome P-450

dependent oxidations is further complicated by the proposal that the cytochrome P-450 monooxygenase and oxidase activities may not involve a two electron transfer: a one electron transfer may be involved in the production of superoxide and a four electron transfer has been reported for the oxidation of ethanol to acetaldehyde using a purified cytochrome P-450 isozyme in the reconstituted system (32,75,81,82). Furthermore, a four electron transfer to oxygen has been postulated as a source of water in microsomes, rather than the monooxygenase reaction (equation 1, page 14) (83).

Besides the production of active oxygen species from autooxidation of cytochrome P-450, it has been well documented that some substrates of cytochrome P-450 channel electrons from NADPH into the formation of hydrogen peroxide as well as into making product i.e., these substrates increase the oxidase activity of cytochrome P-450 (32,75,80). The production of active oxygen species by cytochrome P-450 in the presence of a substrate is termed uncoupling. The extent of uncoupling depends on the nature of the substrate, the cytochrome P-450 isozyme and the spin state of cytochrome P-450 (32,84). For example, perfluoro-n-hexane completely uncouples cytochrome P-450, i.e. there is increased hydrogen peroxide generation and NADPH consumption with no measurable product formation (75). Since many substrates partially uncouple cytochrome P-450, the stoichiometry of 1:1:1, for NADPH consumption:oxygen utilisation:product formation expected from the monooxygenase reaction, may seldom be achieved.

In addition to oxidative reactions, cytochrome P-450 also catalyses the reductive metabolism of a number of compounds, including halothane, carbon tetrachloride and hexachlorobenzene (85-88).

1.1.1.6 The Role of the Other Components of the Electron Transport Pathway in Cytochrome P-450-dependent Oxidations

Cytochrome P-450-catalysed oxidative metabolism can be reconstituted with NADPH-cytochrome P-450 reductase, cytochrome P-450, lipid, oxygen and reducing equivalents supplied preferentially by NADPH (Figure 2). The lipid, which is either that of the microsomal membrane or exogenous lipid, such as dilauroylphosphatydyl micelles, influences substrate binding and is required for optimal interaction of the proteins for electron transfer (32,89,90).

Although NADPH is the preferential electron donor, reducing equivalents can be supplied directly to cytochrome P-450 from artificial electron donors such as dithionite and ascorbate, or via cytochrome b_5 and NADH-cytochrome b_5 reductase from NADH (32,45,52,62,91). Although NADH only supports cytochrome P-450-dependent drug oxidations to a limited extent, it has a synergistic effect on drug oxidations when NADPH is also present (34,62,92). The mechanism of this observed synergism is not understood, but it is postulated that NADH can more effectively supply the second electron for oxygen activation via cytochrome b_5 (62,93,94).

A similar stimulatory effect on the cytochrome P-450-dependent oxidations of some substrates is observed in a reconstituted system in the presence of cytochrome b_5. In the purified reconstituted system, the various isozymes of cytochrome P-450 have an absolute, a partial, or no requirement for cytochrome b_5 (95-99). The requirement for cytochrome b_5 depends also on the nature of the substrate. For example, for the oxidation of methoxyflurane (rabbit hepatic cytochrome P-450LM_2) (95) and the O-deethylation of

p-nitrophenetole (rat hepatic cytochrome P-450PB), the phenobarbital-inducible isozymes show an absolute requirement for cytochrome b_5 (96). In contrast, both the phenobarbital- and 3-methylcholanthrene-inducible forms show no requirement for cytochrome b_5 for the oxidation of both aniline and ethylmorphine (rat hepatic cytochrome P-450MC) (96).

Cytochrome b_5 has been shown to bind tightly in a 1:1 stoichiometry to cytochrome P-450 through electrostatic attractions mediated, in part, by cytochrome b_5 haem proprionate groups (100-102). This association between cytochrome P-450 and cytochrome b_5 is thought to be specific for the phenobarbital-induced forms of cytochrome P-450; it has been suggested that only certain cytochrome P-450 isozymes have a cytochrome b_5 binding site (101). The interaction of cytochrome P-450 and cytochrome b_5 is accompanied by a change in the cytochrome P-450 spin state to a relatively higher spin form which increases the rate of the first electron reduction of cytochrome P-450 (100,103).

NADPH-cytochrome P-450 reductase has recently been shown to bind to cytochrome P-450 at a different binding site from that of cytochrome b_5 (104,105); carboxyl groups of NADPH-cytochrome P-450 reductase are involved in charge-pair interactions with two cytochrome P-450LM$_2$ amino groups (106). It has been suggested that both electrostatic interactions and steric constraints play a role in the binding and electron transfer step(s) (107). Cytochrome P-450 reduction by NADPH-cytochrome P-450 reductase is biphasic; the mechanism is complex and currently under investigation (108-110).

1.1.1.7 Inhibitors of Hepatic Microsomal Cytochrome P-450

There are three steps in the cytochrome P-450 catalytic cycle (Figure 4) at which a compound can inhibit cytochrome P-450-dependent reactions (111). A compound can inhibit (i) substrate binding, (ii) the binding of molecular dioxygen subsequent to the first electron transfer, and (iii) the catalytic step at which the substrate is oxidised.

1.1.1.7a Competitive Inhibitors

Compounds which compete with the substrate for the substrate-binding site usually inhibit cytochrome P-450-dependent oxidations in a reversible manner (112). Any compound which is a substrate for cytochrome P-450 will inhibit cytochrome P-450 catalysed reactions in this way, e.g. hexobarbital, ethylmorphine and benzamphetamine (112,113).

1.1.1.7b Non-competitive Inhibitors

Compounds which bind directly to the haem iron inhibit cytochrome P-450-dependent oxidations by preventing dioxygen binding (111). Carbon monoxide and cyanide are examples of this type of inhibitor (111). Because of specificity of carbon monoxide for cytochrome P-450 among microsomal proteins, this inhibitor is commonly used to identify cytochrome P-450-dependent drug oxidations (111). Metyrapone is an inhibitor of cytochrome P-450 oxidations which is shown to bind to both the substrate (Type I) and ligand (Type II) binding sites (111,113). The binding of metyrapone to both ligand and substrate binding sites makes it a more effective inhibitor of

cytochrome P-450 oxidations than those that bind only to a single site (111). The binding of metyrapone to both sites is thought to arise from an allosteric mechanism in which metyrapone has contact with both binding sites (113).

1.1.1.7c Metabolic Intermediate Inhibitors

These inhibitors of cytochrome P-450 oxidations require metabolic activation by cytochrome P-450 giving rise to an intermediate which binds directly to the haem iron, e.g. isosafrole and piperonyl alcohol (114). These inhibitors, unlike metyrapone and carbon monoxide, require the presence of oxygen and NADPH for inhibition to occur, i.e. they inhibit the catalytic step of cytochrome P-450 oxidations. Since the metabolite binds to the haem of cytochrome P-450, the resulting complex has spectral properties similar to those of carbon monoxide, viz: an absorbance maximum of the reduced cytochrome P-450 complex between 448 and 456 nm. The complex, once formed, appears to inhibit cytochrome P-450 catalysed oxidations in a non-competitive manner (114).

1.1.1.7d Suicide Inhibitors

Suicide inhibitors of cytochrome P-450-catalysed oxidations are compounds which usually modify the haem moiety of cytochrome P-450 into an N-alkyl porphyrin; this process requires oxygen and NADPH. This type of compound inhibits the catalytic step of cytochrome P-450 oxidations. Examples include 2-allyl-2-isopropylacetamide, secobarbital and other olefinic compounds (115,116). For 2-allyl-2-isopropylacetamide, inhibition of cytochrome P-450 is as follows: formation of the enzyme-substrate complex is followed by reduction of the haem iron, binding of molecular oxygen and metabolism of the allyl group

of the substrate to a reactive intermediate (111,115,117). The reactive intermediate alkylates the haem moiety to yield a N-alkylated porphyrin derivative which may be released by the apoprotein and can be detected as one or more "green pigments". The cytochrome P-450 apoprotein can take up haem from the hepatic haem pool to reconstitute the cytochrome P-450 (115).

1.1.1.8 Multiple Forms of Cytochrome P-450

The multiplicity of cytochrome P-450 in animal species was first suggested by Conney in 1957 when benzo(α)pyrene was shown to increase the microsomal metabolism of substrates such as benzo(α)pyrene, zoxazolamine, but not meperidine (118). Subsequently, it was reported that liver microsomes isolated from phenobarbital-pretreated rats contained elevated levels of a form of cytochrome P-450 which differed in the carbon monoxide spectral characteristics and substrate specificity from that induced by 3-methylcholathrene. Over the last decade, cytochrome P-450 isozymes from different species have been isolated, sequenced, cloned and assigned to specific chromosomal regions. This remains an area of active research.

The similarity of function of the cytochrome P-450 isozymes plus the great degree of structural divergency has resulted in the proteins being divided into different gene families and subfamilies (119). The cytochrome P-450 gene superfamily presently consists of fourteen gene families, of which nine are from mammals (128). Cytochrome P-450 proteins within a gene family have a certain amount of structural similarity (ca. >50%) (121). The cytochrome P-450 isozymes, which are members of the gene families I to IV, are the primary drug-metabolising enzymes and are found to the greatest extent in the liver (119).

The properties of eight rat liver isozymes* from gene families I to IV are summarised in Table 4. Of particular interest here are the rat liver cytochrome P-450 isozymes induced by the polycyclic aromatic hydrocarbons, phenobarbital and pregnenolone-16α-carbonitrile. These isozymes are members of the gene families I, II and III and will be considered in more detail; the other cytochrome P-450 isozymes are reviewed elsewhere (119,122 and references cited therein).

1.1.1.8a Phenobarbital-Inducible Cytochrome P-450 Isozymes

Pretreatment of animals with phenobarbital raises the levels of hepatic microsomal cytochrome P-450 isozymes which are members of the P450IIB subfamily, together with the levels of NADPH-cytochrome P-450 reductase (34,60,119,134). This is parallelled by an increase in the oxygenation of a large number of lipophilic substrates, both exogenous (e.g. drugs such as methoxyflurane) and endogenous (e.g. steroids) (10,60,134). Initially, phenobarbital was thought to induce only one cytochrome P-450 isozyme, cytochrome P-450b (Table 4) which is the major phenobarbital-inducible form of the enzyme. Subsequently, the phenobarbital inducible gene family has been found to be the largest and most complex (121,124,129); microheterogeneity has been observed in the purified enzyme and the cDNA encoding for the

*The nomenclature of the cytochrome P-450 isozymes is very confusing as every laboratory involved in cytochrome P-450 purification has adopted its own system. Recently, a nomenclature system has been developed based on primary amino acid sequence alignment data, where the cytochrome P-450 proteins are grouped into gene families and subfamilies (122). The nomenclature adopted herein follows that of Levin (132,133) and the corresponding gene family and subfamily of the specific isozymes appear in Table 4.

TABLE 4 PROPERTIES OF SOME OF RAT HEPATIC CYTOCHROME P-450 ISOZYMES

Cytochrome P-450 Gene Family	Cytochrome P-450 Isozyme (cf. 132,133)	MW (Daltons)	CO-binding max. (nm)	Inducing Agent	Examples of Reactions Catalysed	Alternate Nomenclature	References
Phenobarbital	b	51,300	450	Phenobarbital; isosafrole; pregnenelone-16α-carbonitrile	N-Demethylation of benzamphetamine; 3 Hydroxylation of hexabarbital	P450IIB1	32,42,43,44,119, 122,130,131,155
	e		450	Phenobarbital	Same as b	P450IIB2	119,130,131,155
		53,000		Slightly by phenobarbital	S-Warfarin-7-Hydroxylation	P450IIC6	45,119,122,130,131
Polycyclic aromatic hydrocarbons	c	56,000	447	β-Naphthoflavone; 3-Methylcholanthrene	3-and 9-Hydroxylation of benzo-(α)pyrene; O-dealkylation 7-ethoxycoumarin; 6-Hydroxylation Z-oxazolamine	P450IA1	42,43,130,131, 119,122,155
	d	52,000	447	3-Methylcholanthrene; isosafrole	6-Hydroxylation of Z-oxazolamine, 2-Hydroxylation estradiol - 17β	P450IA2	46,119,122, 130,131
Pregnenolone-16α-carbonitrile	P-450PCN	51,000	450	Pregnenolone-16α-carbonitrile; slightly by phenobarbital	N-Demethylation of ethylmorphine Andostrenedione 16β-Hydroxylation	P450IIIA1; P450IIIA2	47,119,122,130 131,155
Clofibrate		51,500	452	Clofibrate and hypolipidemic drugs	ω- and (ω-1)- Hydroxylation of lauric acid	P450IVA1	48,122,123,152
Ethanol	j	51,000	452	Ethanol and imidazole	Oxidation of ethanol and other alcohols; p-Hydroxylation of aniline	P450IIE1	49,122,153,154
Untreated	a	48,000	452	Slightly by phenobarbital	N-Demethylation of benzamphetamine; testosterone-7α-Hydroxylation	P-450IIA1; P-450IIA2	42, 130, 131, 155

phenobarbital-inducible forms in rabbits (135). Cytochrome P-450b has been separated by HPLC into at least three different isozymes which have the same molecular weight and electrophoretic mobility; these isozymes are immunochemically indistinguishable (43,44,124,130,131,136).

In addition to cytochrome P-450b, phenobarbital induces another closely related isozyme, cytochrome P-450e (60,119,132,137). Cytochrome P-450b and e exhibit 97% similarity in content of amino acids (119). They are immunochemically related and show only minor differences in substrate specificities, but are encoded by distinct RNAs, which are transcribed by two closely linked genetic loci (60,127,130,133,136). Although cytochrome P-450b and e are co-induced, the levels of cytochrome P-450b has a 5-fold higher catalytic activity for certain substrates (e.g, benzamphetamine) than cytochrome P-450e (119,138,139). The higher activity of cytochrome P-450b compared to cytochrome P-450e is thought to be related to differences in their haem environments (125).

Phenobarbital regulates cytochrome P-450 induction by increasing the transcriptional rate of the mRNAs for the phenobarbital isozymes. The increase in the transcriptional rate results in an accumulation of a mRNA which is undetectable in control animals (60,119,140).

1.1.1.8b Polycyclic Aromatic Hydrogen-Inducible Cytochrome P-450 isozymes

Compounds which induce the isozymes which are members of P450IA gene family include 3-methylcholanthrene, β-naphthoflavone, benzo(α)pyrene and

isosafrole, all of which induce specific isozymes without increasing proliferation of the endoplasmic reticulum (34,118). The isozymes of this cytochrome P-450 gene family catalyse the hydroxylation of a limited number of exogenous compounds, usually arylhydrocarbons, many of which are carcinogens such as benz(α)athracene, benzo(α)pyrene (34,60,119). Consequently, the isozymes of this gene family play a major role in chemically induced neoplasia and toxicity (141-143). The isozymes induced by the polycyclic aromatic hydrocarbons are cytochrome P-450c and cytochrome P-450d (Table 4) (60,132). They are commonly known as "cytochrome P-448" because of the shift in absorbance maximum of the reduced carbon monoxide complex from 450 nm to 448 nm. 3-Methylcholanthrene, β-naphthoflavone and benzo(α)pyrene preferentially induce cytochrome P450c, whereas isosafrole preferentially induces cytochrome P-450d (60,144,145). These two isozymes show a sequence homology of approximately 70%, and are weakly immunochemically related (146-148). Cytochrome P-450c does not exhibit microheterogeneity (43).

Regulation of the cytochrome P-450c and d genes appears to be complex, and is still being investigated (119). There is, however, evidence that the polycyclic aromatic hydrocarbons induce cytochrome P-450 isozymes by a inducer-receptor complex mechanism (60,120,140).

1.1.1.8c Pregnenolone-16α-carbonitrile-Inducible Cytochrome P-450 Isozymes

Pregnenolone-16α-carbonitrile is a synthetic steroid derivative lacking in hormonal activity which induces cytochrome P-450 isozymes which are members of the P450III gene family, as well as enhancing NADPH-cytochrome

P-450 reductase activity (60,149,119). It has been suggested that these isozymes play a role in the metabolism of endogenous compounds, although the physiological substrate is not known (60,150). Multiplicity of the isozymes of the P450III gene family has been reported (126): cytochrome P-450PCN1 is induced by steroids and phenobarbital, whereas cytochrome P-450PCN2 is induced by only phenobarbital (119,126).

The mechanism of pregnenolone-16α-carbonitrile induction is unknown (60). Since pregnenolone-16α-carbonitrile pretreatment results in an accumulation of mRNA for the pregnenolone-16α-carbonitrile-inducible cytochrome P-450 isozyme, pregnenolone-16α-carbonitrile induction may operate at the transcriptional level (60).

1.1.1.8d Cytochrome P-450 Isozymes in the Liver of Untreated Animals

In addition to the small amounts of phenobarbital-inducible cytochrome P-450b and polycyclic aromatic hydrocarbon inducible-cytochrome P-450c, there is a another isozyme, cytochrome P-450a, in the hepatic microsomes from untreated rats (139). Cytochrome P-450a, a member of the P450IIA gene subfamily, is slighlty inducible by phenobarbital and 3-methylcholanthrene, and is not very active in catalysing the metabolism of exogenous substrates (42,119,120).

1.1.1.8e Cytochrome P-450 Isozymes in Human Liver

The recent availability of fresh material from transplant donors has facilitated the isolation and characterisation of human cytochrome P-450 isozymes (156). At

least 16 microsomal cytochrome P-450 genes have been identified, 11 of which are hepatic (151,158). Some of these have been sequenced, cloned and localised to a chromosome and are reviewed elsewhere (151).

There is evidence that human cytochrome P-450 exhibits polymorphism amongst different individuals, since the cytochrome P-450 isozymes have been linked to the observed polymorphism of drug metabolism in humans (159,160). Genetic polymorphism of drug metabolism has been demonstrated for a variety of drugs (Table 5), but the drug which has been most extensively studied is debrisoquine (162-164). The major metabolite of debrisoquine is the 4-hydroxylated product and there are two phenotypes for debrisoquine metabolism: poor metabolisers (about 10% of caucasian populations), who excrete the drug unchanged and consequently suffer from cardiovascular effects, and extensive metabolisers who excrete debrisoquine metabolites (162). Poor metabolisers of a drug family have either a decreased content of a cytochrome P-450 isozyme, or a functionally altered enzyme (165-167). At present, there appear to be five drug families which exhibit genetic polymorphism in humans (Table 5).

1.1.2 Proteins Associated with Cytochrome P-450-Dependent Oxidations

1.1.2.1 NADPH-Cytochrome P-450 Reductase

Since NADPH-cytochrome P-450 reductase is the only obligatory electron transfer protein for cytochrome P-450, it will be discussed here. The other proteins, NADH-cytochrome b_5 reductase and cytochrome b_5 will be discussed

TABLE 5

HUMAN AND RAT LIVER CYTOCHROMES P-450 ISOSYMES INVOLVED IN POLYMORPHISMS OF OXIDATIVE METABOLISM *

Drug family	Specific cytochrome P-450 involved in humans	Alternate Nomenclature†	Examples of demonstrated substrates
Debrisoquine	$P\text{-}450_{DB}$	P450IID1	Debrisoquine, sparteine, bufuralol (+ and -), encainide, propranolol
Phenacetin	$P\text{-}450_{PA}$	P450IA2	Phenacetin
Mephenytoin	$P\text{-}450_{MP}$	P450IIC9	Mephenytoin
Nifedipidine	$P\text{-}450_{NF}$	P450IIIA3	Nifedipine
Tolbutamide	?	?	

* Compiled from reference 156,157,161

† See references 119,122 and 157.

with the fatty acid desaturases, since they form essential components of the fatty acid desaturase pathway.

NADPH-cytochrome P-450 reductase accepts electrons from NADPH in preference to NADH. NADPH-cytochrome P-450 reductase donates electrons to cytochrome P-450, and a number of artificial electron acceptors, including cytochrome c (62,168). The reduction of the cytochrome P-450 by NADPH proceeds via both one-electron equivalent, and two-electron equivalent mechanisms (62,169). NADPH-cytochrome P-450 reductase is a membrane-bound flavin protein with a molecular weight of about 77,000 daltons, and contains one molecule each of FMD and FMN per molecule of the enzyme (32,170). NADPH-cytochrome P-450 reductase has been purified to homogeneity by several techniques including NADP-sepharose affinity chromatography (171).

The interaction of NADPH-cytochrome P-450 reductase with both cytochrome P-450 and cytochrome b_5 has already been discussed (Section 1.1.1.6).

1.1.3 The Metabolism of Volatile Anaesthetic Agents by Hepatic Microsomal Cytochrome P-450

The metabolism of halothane, methoxyflurane and enflurane by the different cytochrome P-450 isozymes and the metabolic pathways for these drugs have been studied (6,95,172-183). In contrast, the role played by the cytochrome P-450 isozymes in the metabolism of isoflurane and the details of its metabolic pathway, remains to be resolved.

Isoflurane has been shown to be very resistant to biotransformation (1,191,192). In man, more than 95% of the administered dose of isoflurane was recovered unaltered, of which only 0.2% was recovered as urinary inorganic fluoride (1,192). Mean peak serum inorganic fluoride concentration was only 4.4 μM/L following six hours isoflurane anaesthesia in man (1,193). Metabolism of isoflurane in vivo to inorganic fluoride appears to be insufficient to cause renal dysfunction, so that nephrotoxicity is unlikely to be linked with isoflurane anaesthesia (192,194).

The proposed pathways of isoflurane metabolism are illustrated in Figure 5. Of the proposed metabolites, inorganic fluoride has been identified in vitro and in vivo in both rats and humans (184,194). An additional metabolite, trifluoroacetic acid, has been found in the urine of humans following isoflurane anaesthesia (Figure 5) demonstrating that isoflurane is probably metabolised by the dechlorination pathway in humans (which is the pathway favoured by the quantum mechanical considerations of Loew et al) (7,183,195).

At the time of initiation of our studies, the only evidence suggesting that cytochrome P-450 might metabolise isoflurane arises from the enhanced rate of defluorination of the anaesthetic in hepatic microsomes following phenobarbital and ethanol (or isozianid) pretreatment of rats (179,184). However, in contrast to the in vitro results, phenobarbital pretreatment of rats had no effect on the extent of isoflurane defluorination in vivo (184,186,187). 3-Methylcholanthrene pretreatment of rats had no effect on the rate of defluorination of isoflurane in vitro (179,184,186).

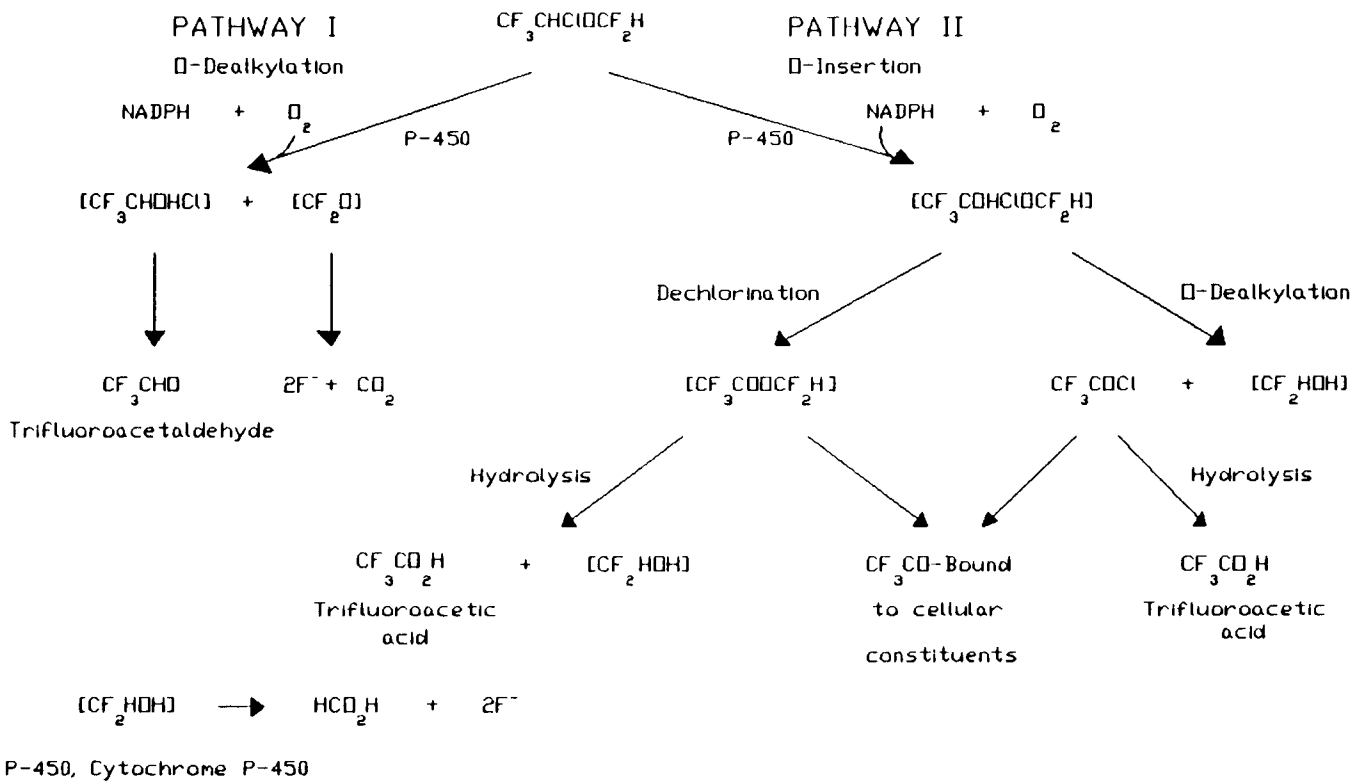

FIGURE 5 **Proposed scheme for the metabolism of isoflurane by cytochrome P-450**

P-450, cytochrome P-450.
Compiled from references 4,181 and 195

Since it is not apparent which enzyme(s) defluorinate isoflurane, and there is only a single report of the identity of the metabolites (195), our study of the metabolism of isoflurane by cytochrome P-450 was undertaken to (i) identify the enzyme(s) catalysing the defluorination of isoflurane and (ii) to confirm the identity of the products of isoflurane metabolism in human and rat hepatic microsomes.

Besides the involvement of cytochrome P-450 in the metabolism of anaesthetic agents, there is also evidence that halothane, methoxyflurane and enflurane interact with hepatic microsomal Δ9-desaturase. For this reason, further studies on isoflurane in hepatic microsomes focussed on its interaction with the fatty acid desaturases and some of the other enzymes involved in fatty acid metabolism. Some of our studies were extended to include halothane, methoxyflurane and enflurane. The next sections, therefore, discuss the pathways of fatty acid metabolism in hepatic microsomes.

1.2 FATTY ACID METABOLISM

1.2.1 Fatty Acids

There are three families of polyunsaturated fatty acids which arise from 18 carbon fatty acid precursors, and these are described by the position of the nearest double bond from the methyl end of the molecule (Figure 6) (196-198) :

i) The n-9 family arises from stearic acid (Table 6) which is not an essential fatty acid as it can be synthesised by the fatty acid synthetase pathway from acetate in mammalian systems (196,199).

ii) The n-6 family arises from the dietary intake of linoleic acid which cannot be synthesised in animals; in plants oleic acid can be desaturated by the Δ12-desaturase to form linoleic acid (Table 6) (196). The Δ12-desaturase activity was lost in vertebrates and invertebrates during metazoan evolution (200). Linoleic acid is, therefore, an essential fatty acid in mammals. Another fatty acid member of the n-6 family is arachidonic acid (Figure 6), which is the most abundant fatty acid in cell membranes and the most important precursor of eicosanoid biosynthesis (201). Arachidonic acid can either be obtained directly from the diet or it can be synthesised from linoleic acid (Figure 6).

iii) The n-3 family arises from dietary α-linolenic acid. The n-3 family of fatty acids is essential in that it cannot be synthesised by animal tissues, but is of a different class to the n-6 family and is found mainly in highly specialised membranes and neural tissue (201,202).

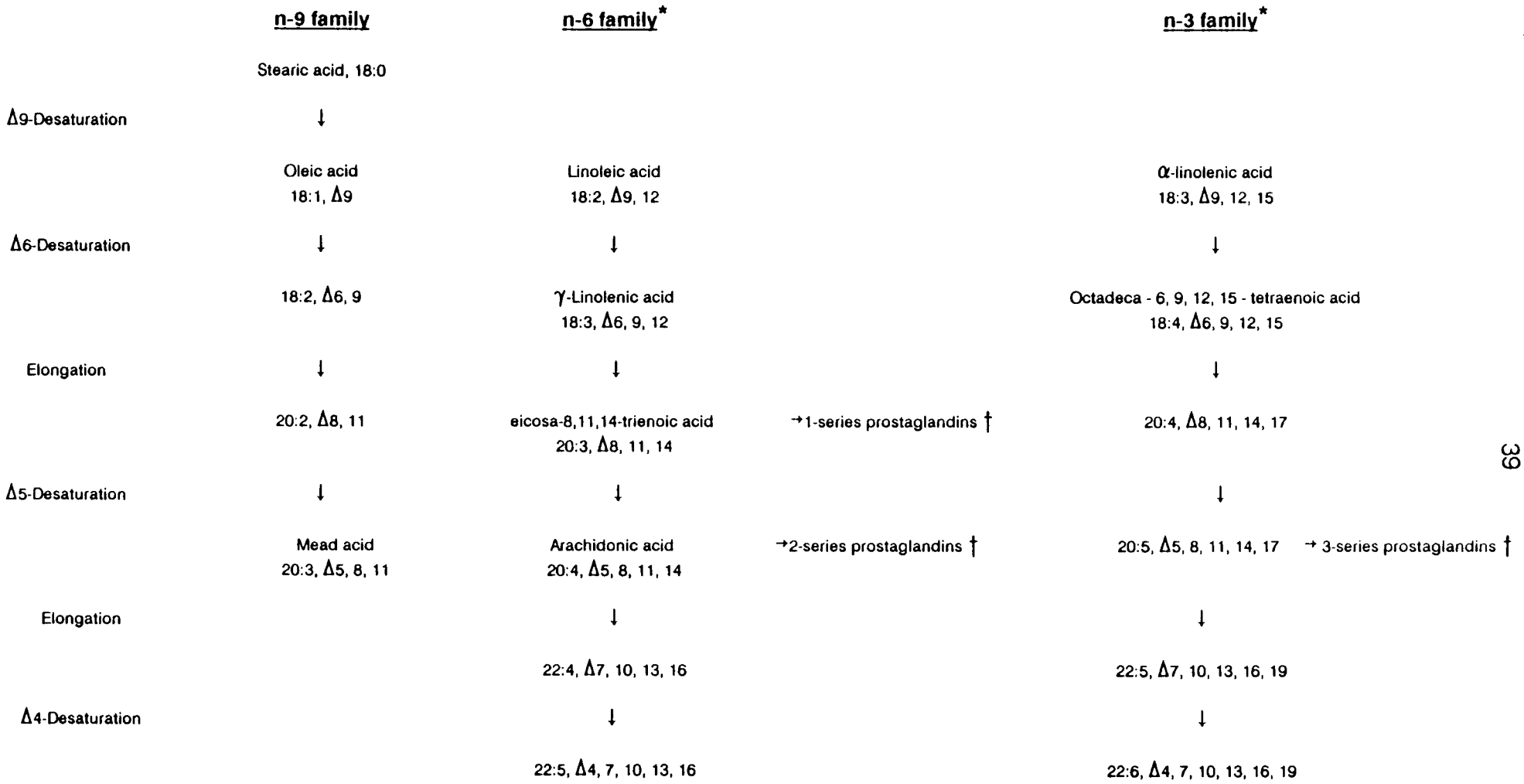

* Essential fatty acid families in mammals

† For more details, see Figure 10

FIGURE 6 The biosynthesis of polyunsaturated fatty acids

compiled from references 197 and 198

TABLE 6

THE TRIVIAL NAMES AND NOMENCLATURE OF SOME FATTY ACIDS

TRIVIAL NAME	NOMENCLATURE
Palmitic acid	16:0
Stearic acid	18:0
Oleic acid	18:1, Δ9
Linoleic acid	18:2, Δ9,12
γ-Linolenic acid	18:3, Δ6,9,12
α-Linolenic acid	18:3, Δ9,12,15
Columbinic acid	18:3, Δ5 trans, 9 cis, 12 cis
Eicosa-8,11,14-trienoic acid (dihomogammalinolenic acid)	20:3, Δ8,11,14
Mead acid	20:3, Δ5,8,11
Arachidonic acid	20:4, Δ5,8,11,14
Eicosa-5,8,11,14,17-pentaenoic acid	20:5, Δ5,8,11,14,17

Fatty acids were first found to be essential constituents of the diet by Burr and Burr in 1929 (203), and have been considered to have the same nutritional status as vitamins (202). Some of the symptoms ascribed to a lack of essential fatty acids in the diet include dermititis, impaired growth and increased water consumption (204).

Fatty acids are thought to be essential components of the diet for two reasons (198,199,202) :

i) Fatty acids are major constituents of cell membranes and exert control over the structural integrity of the membrane. In this capacity, fatty acids regulate the functioning of membrane-bound proteins and enzymes whose activity is dependent on the nature of the surrounding membrane lipids (204-208).

ii) Fatty acids are essential precursors of the eicosanoids, prostaglandins, thromboxanes, and leukotrienes which influence many cellular reactions (201).

Members of the n-6 family of fatty acids which can relieve the symptoms of essential fatty acid deficiency are linoleic acid, found in many vegetable seed oils, and arachidonic acid, obtained predominately from animal foods (199). Another fatty acid which has been found to relieve some of the symptoms of essential fatty acid deficiency is columbinic acid, which is found in columbine seeds (205,209). It has been suggested that columbinic acid may function as linoleic acid or arachidonic acid in epidermal tissues thus relieving some of the essential fatty acid deficiency symptoms related to the skin (204).

The important function of fatty acids in the formation and maintenance of cellular membranes is strongly suggested by many features of the nature of essential fatty acid deficiency disease, such as dermititis and water permeability of the skin (197,205,209).

Fatty acids are found in the lipid component of cellular membranes and play an important role in determining the physical and chemical properties of membranes (206,207). The fatty acid composition of the lipid component of cellular membranes is the net result of complex interrelations of a number of enzyme systems, as well as the composition of dietary fatty acids, most of which are important factors in controlling membrane fluidity (205,206,208). The most important lipid components of microsomal membranes are the phospholipids.

1.2.2 Phospholipids

Phospholipids have the following basic structure:

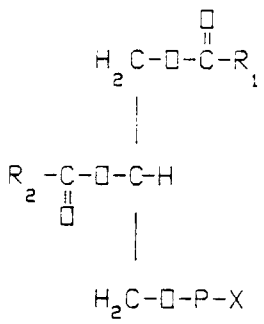

Where R_1 and R_2, fatty acid residues

P, phosphate

X, choline, ethanolamine, serine, inositol or hydrogen

Fatty acid R_1, is usually saturated, e.g. stearic acid or palmitic acid, whereas R_2 is usually unsaturated, predominently arachidonic acid, linoleic acid or oleic acid, but will vary depending on dietary intake of fatty acids and tissue (201,206-208). Phosphoric acid or, more usually, a phosphorylated base (X), may be esterified at the carbon position 3, forming phosphatidic acid phosphatidylcholine, phosphatidylethanolamine, phosphatidylserine or phosphatidylinositol. The phospholipid content of microsomal membranes is shown in Table 7.

The arrangement of the lipid components of microsomal membrane depends on the amphipathic nature of the phospholipids (206,207). The polar head contains the phosphorylated base, and the fatty acid forms the hydrophobic tail. The membranes are arranged in bilayers with the polar heads being exposed to the cytoplasmic surface. The fatty acid composition of the hydrophobic portion of the phospholipid will determine the nature of the hydrophobic interactions and consequently membrane fluidity (206,207).

Some of the enzymes responsible for regulating fatty acid homeostasis and the fatty acid composition of cellular membranes are the acyltransferases, phospholipases, fatty acid desaturases and fatty acid elongases. The formation of the CoA derivative of the fatty acids, which forms the substrate for these enzymes, is catalysed by the long-chain acyl-CoA synthetase These enzymes play an essential role in the pathways of fatty acid metabolism (Figure 7) and will be considered in more detail (Figure 7).

TABLE 7

PHOSPHOLIPID COMPOSITION (%) OF MICROSOMAL MEMBRANES *

Lipid †	Per cent
Phosphatidylcholine	ca. 55
Phosphatidyethanolamine	20-25
Phosphatidylserine	5-10
Phosphatidylinositol	5-10
Sphingomyelin	4-7

* Adapted from reference 207

† These lipids form about 30% of the content of the microsomal membrane which also contains small amounts of cholestrol and triacylglycerol.

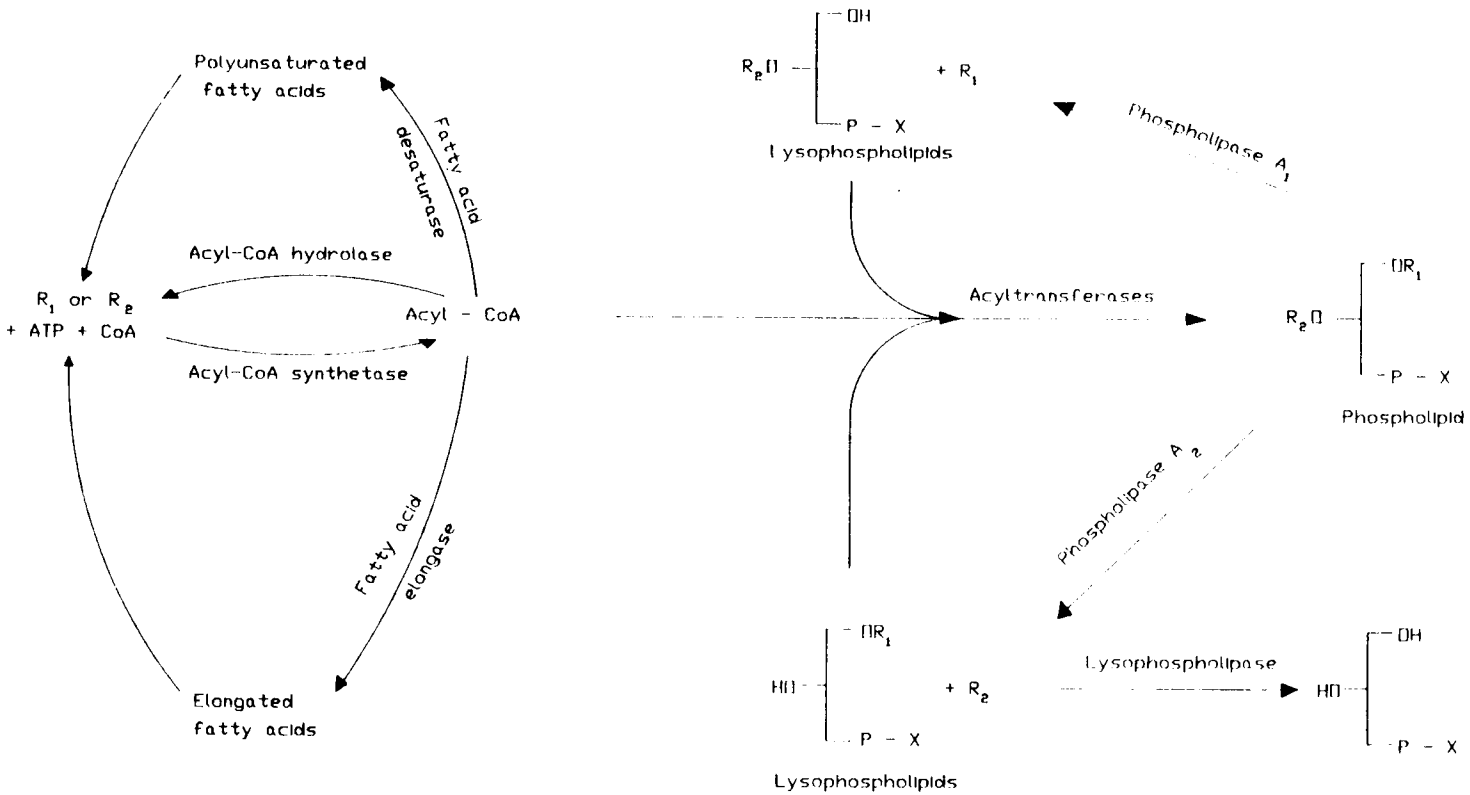

FIGURE 7 **Some of the pathways of fatty acid metabolism in hepatic microsomes**

P, phosphate group; X, base (e.g. choline in phosphatidylcholine); R_1 and R_2, fatty acids
Adapted from reference 210

1.2.3 Long-Chain Acyl-CoA Synthetase

The long-chain acyl-CoA synthetase activates fatty acids as follows:

$$\text{fatty acid} + \text{CoA} + \text{ATP} \xrightarrow[\text{synthetase}]{\text{acyl-CoA}} \text{acyl-CoA} + \text{AMP} + PP_i \qquad \text{.....(4)}$$

The long-chain acyl-CoA synthetase is a membrane-bound enzyme found in microsomes, peroxisomes and mitochondria (211). It has been purified from rat hepatic microsomes and shown to consist of identical subunits (28,000 daltons) which combine to form a catalytic unit of 168,000 daltons (212). Fatty acids of carbon chain length 10 to 18 are activated to CoA derivatives at approximately equal rates, but the rate decreases for longer or shorter chain length fatty acids (213). The mechanism of action of the long-chain acyl-CoA synthetase is proposed to follow Bi Uni Uni Bi Ping Pong kinetics (214,215). The enzyme-bound intermediate has been isolated and contains equimolar amounts of adenylate and fatty acid bound to the enzyme (216).

1.2.4 Acyl-CoA Hydrolase

Acyl-CoA hydrolase catalyses the hydrolysis of the acyl-CoA ester bond (217). This enzyme has a high specificity for fatty acids containing 16 or 18 carbon atoms, and prefers substrates in the micellar form* (218). The acyl-CoA hydrolases are found in most mammalian tissues and the hepatic

*Because of the amphipathic nature of fatty acids and the CoA derivatives thereof, they are only slightly soluble in aqueous medium and, above a certain concentration, tend to aggregate to form micelles.

microsomal enzyme has a molecular weight of 59,000 daltons (217). The presence of an acyl-CoA hydrolase within the cell suggests that an accumulation of acyl-CoA derivatives may not be desired (219). However, the mechanism of regulation of acyl-CoA metabolism is not as yet fully understood (219).

1.2.5 The Acyltransferases

This group of enzymes catalyses the esterification of fatty acids into phospholipids; the specific enzymes are named according to the phospholipid acceptor into which the fatty acid is incorporated. For example, 1-acyl-*sn*-glycero-3-phosphate acyltransferase and 1-acyl-*sn*-glycero-3-phosphatidylcholine acyltransferase esterify a fatty acid into the 2 position of 1-acyl-*sn*-glycero-3-phosphate (lysophosphatidic acid) and 1-acyl-*sn*-glycero-3-phosphatidylcholine (lysolecithin), respectively (220). The enzymes responsible for acylating the 1 carbon position of phospholipids have a high specificity for stearic and palmitic acids and a far lower specific activity than the enzymes acylating the 2-carbon position (221-223). It has been suggested that the relative activities of the acyltransferases towards different acyl-acceptors and donors are responsible for the non-random distribution of fatty acids in membranes (224). Consequently the different specificities of the enzymes towards different donors and acceptors has been extensively studied, especially with regard to the acylation of the 2-carbon position of phospholipids. In rat hepatic microsomes, arachidonic acid is the prefered acyl donor for 1-acyl-*sn*-glycero-3-phosphatidylcholine acyltransferase (225); the mono- and diene fatty acids are esterified by the 1-acyl-*sn*-glycero-3-phosphate acyltransferase (222). Other fatty acids for which 1-acyl-*sn*-glycero-3-phosphate

and 1-acyl-*sn*-glycero-3-phosphatidylcholine acyltransferases show high activity, are linoleic, α- and γ-linolenic, eicosa-8,11,14-trienoic and eicosa-5,8,11,14,17-pentanoic acids. 1-acyl-*sn*-glycero-3-phosphatidylcholine acyltransferase has very low affinity for the long chain fatty acids, viz: 22:2, Δ13,16, 22:3, Δ13,16,19, and 22:4, Δ7,10,13,16; palmitic and stearic acids do not act as acyl donors for the 1-acyl-*sn*-glycero-3-phosphate or 1-acyl-*sn*-glycero-3-phosphatidylcholine acyltransferases (222). Lastly, the polar head group of the acyl acceptor also plays a role in determining the activity of the acyltransferases, e.g. phosphatidylcholine > ethanolamine (224).

The 1-acyl-*sn*-glycero-3-phosphatidylcholine and 1-acyl-*sn*-glycero-3-phosphate acyltransferases are found tightly bound to the endoplasmic reticulum and have been partially purified from rat hepatic microsomes (226-228) and bovine brain microsomes (229).

1.2.6 Phospholipases

The phospholipases are a group of enzymes which catalyse the hydrolysis of phospholipids. There are a number of phospholipases which have been classified according to the position at which they attack phospholipids as illustrated in Figure 8.

It has been established that the phospholipases play an important regulatory role in eicosanoid biosynthesis (230,231). The rate limiting step in prostaglandin biosynthesis is generally thought to be the release of the fatty acid precursor from the membrane phospholipid by phospholipase A_2. The release of arachidonic acid or other polyunsaturated fatty acids on receptor

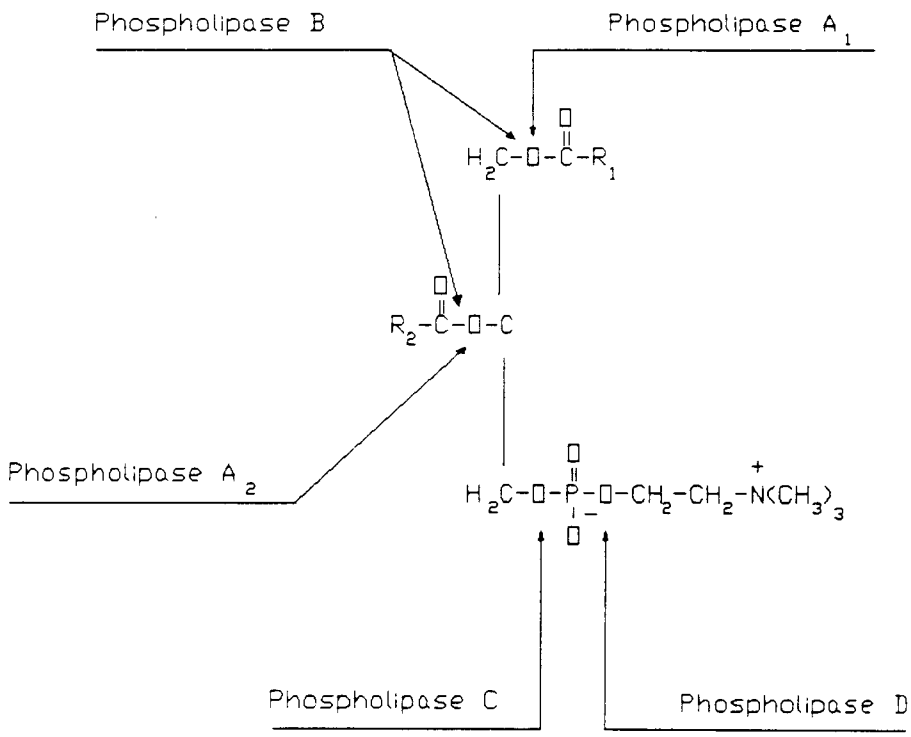

FIGURE 8 **Sites at which the phospholipases attack phosphatidylcholine**

Reproduced from reference 230

activation is not a simple enzyme-catalysed deacylaction by phospholipase A_2, but is the result of a chain of reactions resulting in the activation of phospholipase A_2 (232,233). The polyunsaturated fatty acid, usually arachidonic acid, thus released is available for eicosanoid biosynthesis. The regulatory role of the phospholipases in eicosanoid biosynthesis is currently under intensive investigation. The chain of events from the stimulation of the cell to phospholipase A_2 activation is complex and has been extensively reviewed (210,230,232 and references cited therein).

Phospholipase A_2 has been found in almost every tissue or cell type investigated and is not restricted to a single subcellular site (232,234). Phospholipase A_2 catalyses the release of a fatty acid from the carbon 2 position of phospholipids, such as phosphatidylcholine and phosphatidylethanolamine and has an absolute requirement for calcium (234). In rat liver, phospholipase A_2 activity is found in plasma membranes, endoplasmic reticulum, golgi membranes, mitochondria and lysosymes; it occurs as both a membrane-bound and soluble form (230,234). Phospholipase A_2 has been isolated from, for example, spleen, mitochondria, polymorphonucleocytes, and erythrocytes. The molecular weight and substrate specificity of phospholipase A_2 for a particular phospholipid varies. For example, rat spleen phospholipase A_2 has a specificity for phosphatidylethanolamine whereas that from sheep erythrocyte showed a preference for C-22, mono- and di-unsaturated fatty acids in phosphatidylcholine and phosphatidylethanolamine (234). Although the precise specificity of the reaction varies depending on the source of the enzymes, presumably each enzyme has a specific role to play in lipid metabolism and eicosanoid biosynthesis in mammals.

1.2.7 Fatty Acid Desaturases

The fatty acid desaturases are a group of membrane-bound enzymes which introduce a double bond into fatty acids (197,198). The fatty acid desaturases are defined by the position in the fatty acid chain in which a double bond is introduced with respect to the carboxylic acid end of the molecule, viz: the Δ6-desaturase introduces a double bond between carbon 6 and 7, the Δ9-desaturase between carbon 9 and 10, and the Δ5-desaturase between carbon 5 and 6, from the carboxylic acid end of the molecule. The fatty acid desaturases are the terminal oxidase of an electron transport chain requiring cytochrome b_5, NADH-cytochrome b_5 reductase, oxygen and NADH for activity (235-242). The flow of electrons is from NADH via NADH cytochrome b_5 reductase and cytochrome b_5 to the terminal fatty acid desaturase as follows (see also Figure 1):

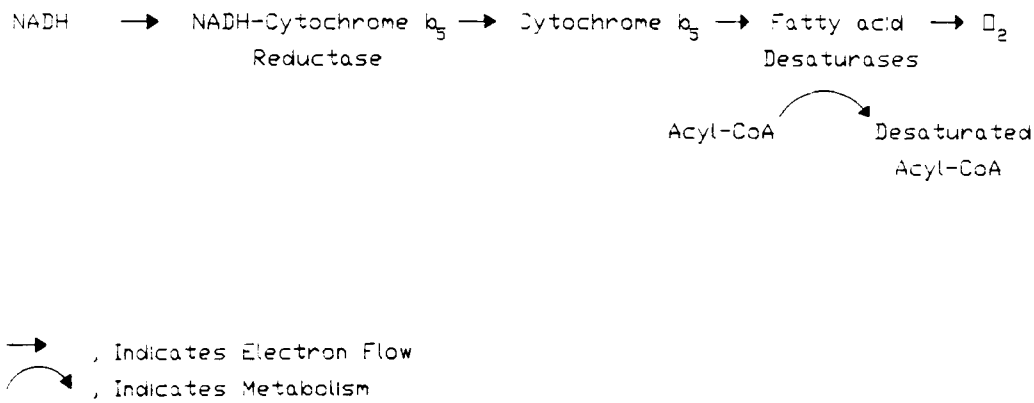

Further requirements for desaturation are a lipid-rich environment and a cytosolic factor (243-249). The lipid appears to play a structural role in desaturation, but the role of the cytosolic factor remains uncertain (244,247). Fatty acid desaturation is inhibited by cyanide, but not by carbon monoxide;

thus the fatty acid desaturases were first referred to as the "cyanide-sensitive factors" (235).

The overall reaction scheme for the desaturation of fatty acids is :

$$\text{acyl-CoA} + O_2 + \text{NADH} + H^+ \xrightarrow[\text{desaturase}]{\text{fatty acid}} \text{desaturated acyl-CoA} + NAD^+ + 2H_2O \quad \text{....(5)}$$

The thioester remains intact during desaturation of the fatty acid substrate; the rate-limiting step of the Δ9- and Δ6-desaturases is the desaturation step (250-252).

The Δ9-, Δ6-, and Δ5-desaturases have been shown to be different enzymes by immunochemical techniques and by isolation of the Δ9- and Δ6-desaturases (253-255). Although both these enzymes have been isolated, the purification has proved difficult to reproduce and this has hampered research into the structure and function of these enzymes.

1.2.7.1 Δ9-Desaturase

The Δ9-desaturase was the first of the fatty acid desaturases to be investigated. The Δ9-desaturase accepts unsaturated fatty acids of chain-length 12 to 19 carbons; the maximum rate of desaturation being for fatty acids of 16 to 19 chain-length, with an abrupt cut-off at 20 (251). The preferred substrate for the Δ9-desaturase is stearic acid (198). The product of the Δ9-desaturation of stearic is oleic acid; further metabolism of oleic acid does not occur except where the essential fatty acids, linoleic acid or α-linolenic acid, are lacking, in which case there is a build-up of mead acid instead of arachidonic acid in the

cell (Figure 6, Table 6), (197,204,256). The ratio of mead acid to arachidonic acid is thought to be an indicator of essential fatty acid deficiency (triene to tetraene ratio) (198,252,256).

The physiological roles of the Δ9-desaturase have been proposed to be as follows:

i) to reduce the melting point of the saturated fatty acids to allow for easier transport (198).

ii) to maintain the correct levels of oleic acid within the cell and hence the physical integrity of the membrane (198,257).

iii) in the biosynthesis of triacylglycerol. In this role, the Δ9-desaturase is involved in carbohydrate-lipid conversion and energy metabolism (257).

The Δ9-desaturase has been isolated from rat liver (251,254) and hen liver microsomes (258,259). Purification of rat liver Δ9-desaturase was achieved by a sequence of extractions of contaminating proteins, followed by solubilisation of the Δ9-desaturase in Triton X-100-calcium deoxycholate. The enzyme is extremley unstable, however, and loses activity on detergent solubilisation (261). Nevertheless, the cDNA for rat hepatic Δ9-desaturase has recently been constructed, from which the protein sequence was deduced (260).

Rat liver Δ9-desaturase is a single polypeptide of 41,500 daltons, containing one molecule of non-haem iron which is necessary for catalytic activity (254,262). The Δ9-desaturase contains a high percentage of hydrophobic residues (62%)

indicating that it is deeply embedded in the hydrophobic region of the membrane bilayer, possibly with only the hydrophilic catalytic site exposed (198,260,262). In the absence of lipid or detergent, the protein tends to form high molecular weight aggregates which suggests that the lipid required for activity serves to provide binding sites for the hydrophobic region of the enzyme (262).

The apparent K_m for the Δ9-desaturation of stearoyl-CoA when the purified enzyme is reconstituted with cytochrome b_5, NADH-cytochrome b_5 reductase, egg lecithin liposomes, and NADH, is 4-5 μM (262). From inhibition studies using unsaturated acids of different configurations, (cis- or trans-isomers), and from the similarity between the K_m for the Δ9-desaturation of stearoyl-CoA and the K_i for the inhibition of this reaction by oleoyl-CoA (4.5 μM) in the purified reconstituted system, it is suggested that upon interaction of stearoyl-CoA with the Δ9-desaturase, stearoyl-CoA assumes a conformation similar to that of oleate, viz: a gauche conformation (251,262). The mechanism of desaturation of the Δ9-desaturase does not involve an oxygenation but rather an extraction of the D-hydrogens, which is the rate-limiting step of the overall reaction (250,251).

1.2.7.2 The Δ6- and Δ5-Desaturases

The physiological substrates for the Δ6- and Δ5-desaturase are primarily unsaturated fatty acids of the n-6 and n-3 fatty acid families, and the n-9 family only in cases of essential fatty acid deficiency, as already discussed (197). Of the physiological substrates for the Δ6-desaturase, α-linolenic acid is desaturated at a greater rate than linoleic acid, which is desaturated at a greater rate than oleic acid (197,198,237).

The physiological role of the Δ6- and Δ5-desaturases is the biosynthesis of polyunsaturated fatty acids which (i) form components of membrane phospholipids necessary for maintaining the physical integrity of the membrane and (ii) are the precursors of eicosanoid biosynthesis (198,201,257).

The Δ6-desaturase is far more readily solubilised in detergents than the Δ9-desaturase, suggesting that the Δ6-desaturase is not as deeply embedded in the microsomal membrane (263). However, only Okayasu et al have reported the successful purification of the enzyme (255). After initial detergent solubilisation, the Δ6-desaturase was purified by ion exchange chromatography followed by cytochrome b_5 affinity chromatography (255). The purified enzyme has a molecular weight of ca. 65,000 daltons. As in the case of the Δ9-desaturase, the Δ6-desaturase is a single polypeptide chain containing one atom of non-haem iron, which is required for catalytic activity (255). The Δ6-desaturase contains only 49% hydrophobic residues compared with the 62% of the Δ9-desaturase; this is a further indication that the Δ9-desaturase is more hydrophobic than the Δ6-desaturase (see also 237,255,261). Both the Δ6- and Δ9-desaturases appear to be located on the cytoplasmic side of the endoplasmic reticulum (264,265).

The apparent K_m for the desaturation of linoleoyl-CoA by the Δ6-desaturase, using the purified reconstituted system, was 45 μM, and the V_{max} value was 83 nmol/mg protein/min (255). In hepatic microsomes, reported apparent K_m values for the desaturation of linoleic acid varied from 0.2 μM to 160 μM (266-270).

The Δ6-desaturase can accommodate a wider variety of chain lengths than the Δ9-desaturase, although the optimum activity is for C-18 fatty acids (271,272). The increasing activity with the greater number of double bonds (oleic acid <linoleic acid <α-linolenic acid) would indicate that the higher activity is due to the increased curvature of the molecule (198,269). The active centre of the Δ6-desaturase cannot bind stearoyl-CoA and thus appears to be significantly different from that of the Δ9-desaturase (237,255,269). The Δ6-desaturase appears to recognise the chain length as well as the number of double bonds (272).

In rat hepatic microsomes, the Δ5-desaturase shows activity towards eicosa-8,11,14-trienoic in two forms: (i) as the CoA derivative of the fatty acid and (ii) the fatty acid esterified in phospholipids (273,274). Separate enzymes for the two reactions have not been identified and both activities have been found following partial purification of the protein by detergent solubilisation (274). The lack of requirement for CoA rules out any possibility that the desaturation measured is a multiple enzyme reaction, viz: release of the fatty acid substrate from the phospholipid (phospholipase), followed by CoA esterification (acyl CoA-synthetase), desaturation and finally transfer of the fatty acid back to the phospholipid (acyltransferase) (Figure 7). Similarly, the Δ12-desaturase in plants and bacteria has also been reported to desaturate oleoyl-CoA as well as oleic acid esterified in phospholipids (275). There are no reports on the structure of the Δ5-desaturases as isolation to homogeneity has not been achieved (274).

1.2.7.3 Factors which Stimulate Fatty Acid Desaturase Activity in Vitro

On reconstitution of the purified Δ9- or Δ6-desaturase with cytochrome b_5, NADH-cytochrome b_5 reductase, lipid, NADH and oxygen, the reaction does not have an absolute requirement for a cytosolic factor. A cytosolic factor stimulates the Δ9-, Δ6- and Δ5-desaturase activities in hepatic microsomes in vitro, however (245-249). The activities of the Δ9-, Δ6- and Δ5-desaturases are lost on repeated washing of crude microsomal extracts, and can be restored on addition of the cytosolic factor (276). A crude extract of the factor has been prepared from cytosol and comprises both a lipid and a protein component (246). The precise role of this factor is uncertain (247), although it has been suggested that it plays a role in product removal (277).

A stimulatory effect on the activities of the Δ9- and Δ5-desaturases, but not the Δ6-desaturase was observed with BSA (247,249). There is, however, a single report where the activity of the Δ6-desaturase was increased by ca. 50% in unwashed microsomes (276). BSA can activate or inhibit the other enzymes which utilise acyl-CoA esters as substrates, viz: the acylhydrolases, elongases and acyltransferases, depending on a complex set of circumstances relating in part to the critical micellar concentration* and K_m values of the enzymes (218,278,279). The activation of the Δ9-desaturase by BSA observed by Jeffcoat et al has been proposed to result from the greater availability of the acyl-CoA for Δ9-desaturation (280); BSA inhibits the formation of micelles from the fatty acid substrate (218,278,279).

* The critical micellar concentration of a fatty acid or CoA derivative thereof, is the concentration in aqueous medium above which it aggregates to form micelles.

1.2.7.4 Other Fatty Acid Desaturases

Besides the Δ9-, Δ6-, and Δ5-desaturases, Δ8-and Δ4-desaturases have been reported in mammals (198,281,282). The Δ4-desaturase shows activity primarily towards members of the n-3 family, giving rise to 22:6, Δ4,7,10,13,16,19, a structural component of brain tissue (201). The Δ8- and Δ4-desaturases are not active in the liver and are found in specialised tissues such as testis, adrenal and brain tissue; little is known about them (198,282,283).

1.2.7.5 Regulation of Fatty Acid Desaturation in Vivo

The activity of the fatty acid desaturases in vivo appears to be regulated by the nutritional and hormonal status of the animal, although the exact mechanism of control is not fully understood (197,257). The Δ9-desaturase has a very short half life in vivo (4 hr), and is induced in response to specific dietary manipulations, e.g. carbohydrate intake (252,257,260). Levels of the Δ9-desaturase are thought to respond to the metabolic requirements of the cell, and control is closely linked to that of carbohydrate metabolism (257,284). Since the Δ6- and Δ5-desaturases are unaffected by dietary intake of carbohydrate (Table 8), it appears that the Δ9-desaturase is regulated by a mechanism different from that of the Δ6- and Δ5-desaturases (208,257). This is in accord with their different physiological roles: the Δ9-desaturase is involved in carbohydrate-lipid and energy metabolism whereas the Δ6- and Δ5-desaturases are on the synthetic pathway for molecules which have specific physiological functions, e.g. the eicosanoids (257).

TABLE 8

THE EFFECTS OF BASIC DIETARY INTAKE ON
Δ9-, Δ6- AND Δ5-DESATURASE ACTIVITY

DIETARY CONDITION	EFFECT ON FATTY ACID DESATURASE ACTIVITY			REFERENCES
	Δ9-Desaturase	Δ6-Desaturase	Δ5-Desaturase	
High-carbohydrate	increases	unaffected	unaffected	284-288
Protein	unaffected	increases	increases	279, 280, 288-290
Fasting	decreases	decreases	increases	252,288,291
Linoleic acid	decreases	decreases	increases	252,292
Fat free		increases	decreases	252,293,294
Cholesterol	increases	decreases	decreases	310

Considerable research has focussed on the effects of dietary fats on the activity of these enzymes, possibly due to concern over increased consumption of processed oils by humans (295). Much of this research is on the effects of isomers of the naturally occurring fatty acids on membrane composition, fatty acid desaturation in vivo and the interaction of these isomers with the fatty acid desaturases in vitro (296-301). Many of these studies on the effects of isomers of naturally occurring fatty acids on the fatty acid desaturases indicate that, although the fatty acid isomers have varying effects on the activity of the fatty acid desaturase, they usually disturb essential fatty acid metabolism by increasing the minimum requirement for linoleic acid in the diet (302-304). Since, during processing of many vegetable oils, isomerisation of the naturally occurring cis-unsaturated fatty acids occurs, the dietary intake of such fatty acids in processed oils may play a central role in regulating essential fatty acid metabolism.

Besides dietary control of the fatty acid desaturases, a number of hormonal factors affect the activity of these enzymes (198,252,305-308). For example, an animal in an experimental diabetic state shows decreased Δ9- and Δ6-desaturase activities; insulin is known to increase the Δ9-desaturase activity (198,252,305-308). Other factors which affect the activity of the fatty acid desaturases include drugs, such as the glucocorticoids and the anti-inflammatory drug, ebselen (309,388), and ethanol (311,388). Ebselen inhibits the Δ9-desaturase by disrupting electron transfer from NADH to NADH-cytochrome b_5 reductase (388). Dietary ethanol reduces the activities of the Δ9-, Δ6- and Δ5-desaturases and alters the acyl composition of subcellular membranes. This suggests that the change in cell morphology observed after

ethanol consumption results from the change in membrane structure and may be related to the change in activity of the desaturases (311,312).

1.2.7.6 The Interaction of Anaesthetic Agents with the Fatty Acid Desaturases

The volatile anaesthetic agents, halothane, methoxyflurane and enflurane have been reported to interact with Δ9-desaturase (313,314). These drugs did not inhibit the conversion of stearate to oleate. However, the interaction of these volatile anaesthetic agents with the Δ9-desaturase was demonstrated by their ability to stimulate cyanide-sensitive electron flow from NADH to oxygen.

The stimulation of electron flow from NADH to oxygen by these anaesthetic agents is measured in hepatic microsomes as follows: cytochrome b_5 is fully reduced by a limited quantity of NADH, and once the NADH supply is exhausted, the pseudo first order rate constant for the re-oxidation of cytochrome b_5 is measured. The rate of electron flow can be measured in the absence and presence of the CoA derivative of a fatty acid or of a compound which stimulates the rate to above that of the background rate. The role of either cytochrome P-450 or the fatty acid desaturases in the stimulation of electron flow can be established through the use of inhibitors (carbon monoxide for cytochrome P-450 or cyanide for the fatty acid desaturases). The complete inhibition by cyanide of the increased electron flow mediated by a compound suggests interaction of the compound exclusively with the cyanide-sensitive factors, which include the Δ9-, Δ6-, and Δ5-desaturases. The stimulated electron flow resulting from the interaction of a compound with the cyanide-sensitive factors does not necessarily mean that it is binding to the substrate-binding site

of the enzyme(s); for example, *p*-cresol has been suggested to stimulate electron flow by increasing the production of active oxygen species (315).

Several local anaesthetic agents have been reported to interact with the Δ9-desaturase, including dibucaine, propianolol and tetracaine; these anaesthetic agents inhibited the conversion of stearic acid to oleic acid by Δ9-desaturase in microsomes from tetrahymena (316).

1.2.7.7 Distribution of the Fatty Acid Desaturases

Fatty acid desaturase activity has been demonstrated in the livers of many species, including rats, mice and humans (237,317-319). One exception is the cat family, which lacks Δ6-desaturase activity (320). Human hepatic microsomes have Δ6-desaturase activity and desaturate both α-linolenic acid and linoleic acid (317). The Δ5-desaturase activity in human hepatic microsomes is far lower than that found in rat hepatic microsomes (317). Although the liver is the main site of the fatty acid desaturases, these enzymes are present in other tissues. For example, Δ9- and Δ6-desaturase activities have been demonstrated in rat kidney (321) and testis (323); bovine mammary glands and the sarcoplasmic reticulum of rabbit muscle both have Δ9-desaturase activity (324,325), and rat adrenal gland has a very active Δ6-desaturase (326). In contrast, rat and human epidermal tissue lack both Δ6- and Δ5-desaturase activities (327,328) and human platelets have low Δ6- and Δ5-desaturase activities (329). Transformed cells, e.g. Morris hepatoma cells and adrenocarcinomas show greatly reduced Δ9- and Δ6-desaturase activities (330-333).

1.2.8 Fatty Acid Chain Elongation

Fatty acid chain elongation involves the condensation of malonyl-CoA with an acyl-CoA in a four step reaction (Figure 9) (334,335). The fatty acid chain elongation is a different system from de novo fatty acid synthetase, although the reactions catalysed are very similar (335). Fatty acid chain elongation takes place in four steps thought to be calalysed by different enzymes (336): the first step in the elongation is a condensation of acyl-CoA and malonyl-CoA to form a β-keto-acyl CoA (Figure 9). This step is reported to be the rate limiting step of the reaction (334,335). The second step is a reduction catalysed by β-keto acyl-CoA reductase, requiring reducing equivalents; NADH and NADPH can act as electron donors via either cytochrome b_5 and/or NADPH-cytochrome P-450 reductase (198,337-339). The third step is a dehydration by β-hydroxy acyl-CoA dehydrase, followed by reduction by trans-2-enol-CoA reductase, giving rise to acyl-CoA, elongated by 2 carbons. The enzymes of this pathway have not been isolated, but are known to be localised on the microsomal membrane (340).

The relative rates of fatty acid desaturation and elongation for each of the fatty acid families have been measured by Bernert and Sprecher (341). Within a fatty acid family, the rate of elongation is far greater than the rate of desaturation, the latter being the rate limiting step in their metabolism (341). However, in vivo the situation could be different, depending on the availability of the different fatty acids for desaturation and elongation.

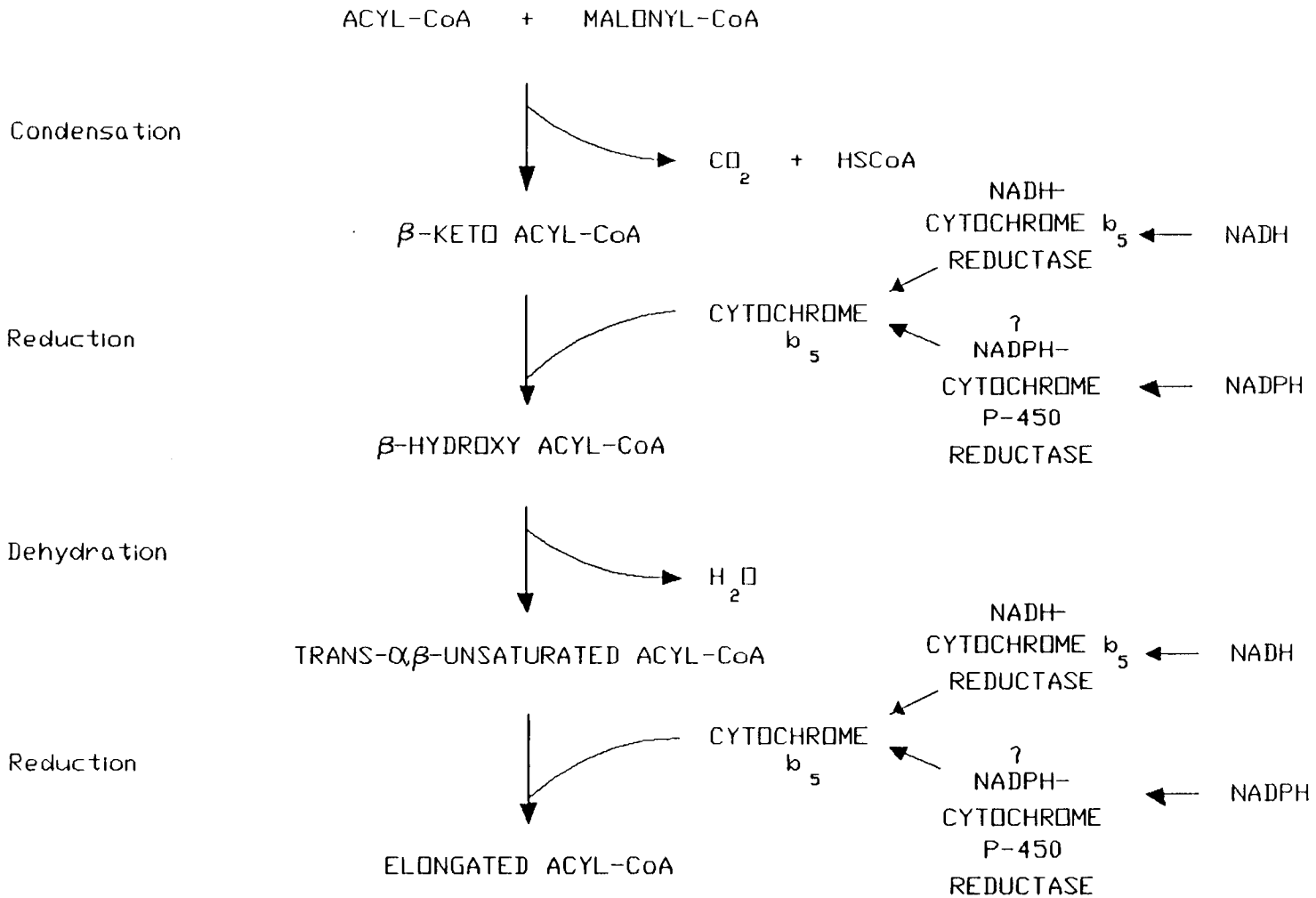

FIGURE 9 **Proposed pathway for the elongation of fatty acids**

Adapted from reference 335

1.2.9 Proteins Associated with Fatty Acid Desaturations and Chain Elongation

1.2.9.1 Cytochrome b_5

Cytochrome b_5 is an essential factor in Δ9- and Δ6-desaturations in rat hepatic microsomes (239,240) and in the purified reconstituted systems (254,255). Cytochrome b_5 also participates in the reduction of cytochrome P-450 during drug oxidation (see Section 1.1.1.6) and in the chain elongation of fatty acids (see Section 1.2.8). Cytochrome b_5 is an amphipathic molecule with a molecular weight of 16,000 daltons (342). The complete amino acid sequence is known; it includes a hydrophobic sequence of 40 amino acid residues which attach the protein to the microsomal membrane, which is predominately α helix in secondary structure, and a hydrophilic catalytic region containing 80 amino acid residues which is located on the cytoplasmic surface of the endoplasmic reticulum (244,342,390). The polar region is also highly helical, but not all α helix (390). The two sections are joined by a short unstructured sequence. The haem crevice is located in the hydrophilic portion of the molecule and the haem is orientated so that one proprionyl side chain is at the surface of the molecule (346,347).

Cytochrome b_5 is easily purified by detergent solubilisation, ammonium sulfate precipitation and DEAE ion exchange chromatography (343). The reduced (ferrous) form of the protein has an absorption peak at 424 nm which shifts to 409 nm in the oxidised (ferric) form. It has recently been cloned and assigned to a specific gene locus in both rats and humans (391).

1.2.9.2 NADH-Cytochrome b_5 Reductase

NADH-cytochrome b_5 reductase is an amphipathic protein attached to the cytosolic surface of the endoplasmic reticulum (344,345). NADH-cytochrome b_5 reductase accepts electrons from NADH in preference to NADPH (371). NADH-cytochrome b_5 reductase has been purified; it has a molecular weight of about 43,000 daltons and contains 1 equivalent of flavin per mol of protein (344,345).

The interaction of cytochrome b_5 with both NADH-cytochrome b_5 reductase and Δ9-desaturase has been studied (346). The proteins involved in the microsomal electron transport chain undergo translational and rotational diffusion in the phospholipid bilayer to produce productive protein-protein contacts (346). The interaction of cytochrome b_5 with NADH-cytochrome b_5 reductase is thought to take place via complementary charge-pair interactions involving carboxylic side chains of glutamic acid residues and the single exposed haem proprionate group (347).

1.2.10 The Role of Fatty Acids in the Biosynthesis of the Eicosanoids, Prostaglandins, Thromboxanes, Leukotrienes and other Derivatives of Carbon-20 Unsaturated Fatty Acids

The eicosanoids are a family of chemically related lipids having a wide variety of different biological activities which modulate practically every function of the body (348,349). The eicosanoids are formed in response to a wide variety of hormonal and non-hormonal stimuli from their fatty acid precursors, which are released from specific fatty acid pools (348). The eicosanoids act locally and

virtually always in competition with other prostanoids and usually stimulate or inhibit key cellular processes (348).

The common fatty acid precursors of the eicosanoids are arachidonic acid, dihomogammalinolenic acid (eicosa-8,11,14-trienoic acid) and eicosa-5,8,11,14,17-pentaenoic acid which can be formed from the essential fatty acids linoleic acid or α-linolenic acid through the pathways illustrated in Figure 10, or can be ingested as a food constituent (201). Of these precursors, arachidonic acid predominates in cellular pools and consequently gives rise to the widest variety and largest amounts of eicosanoids including the prostaglandins of the 2 series (Figure 10) (348,350,351). Considerable attention has been focussed on the chemistry, pharmacology and physiology of the products of arachidonic acid over the last decade and this field has been extensively reviewed (for example, 352-354 and refs. cited therein).

Eicosa-5,8,11,14,17-pentaenoic acid, found predominently in fish oils, is the precursor of the eicosanoids which include the 3-series of prostaglandins (Figure 10). However, eicosa-5,8,11,14,17-pentaenoic acid is a poor substrate for cyclo-oxygenase, the enzyme catalysing the initial step in eicosanoid biosynthesis (Figure 10) (319,348). Consequently, the 3-series of prostaglandins are produced in exceedingly small amounts and are not thought to play an important physiological role (319), although it has been suggested that the 3-series of prostaglandins may have antithrombotic potential (348) and may play a role in preventing ischaemic heart disease (356).

The 1-series of eicosanoids are derived from dihomogammalinolenic acid (eicosa-8,11,14-trienoic acid) (Figure 10) and this series of eicosanoids is

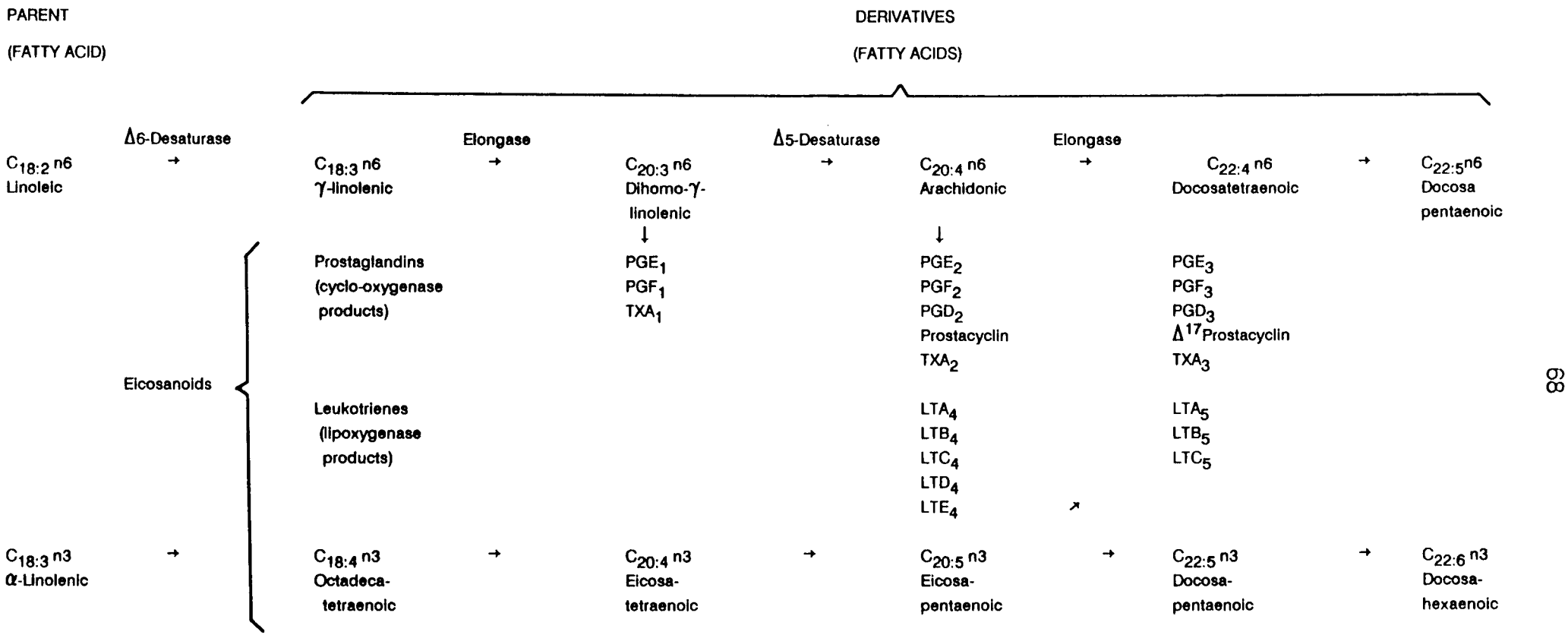

FIGURE 10 **Derivation of prostaglandins and leukotrienes from essential fatty acids**

PG, prostaglandin; TXA, thromboxane; LT, leukotriene.
Adapted from reference 350

produced in small amounts compared to the 2-series, probably because of the small amounts of dihomogammalinolenic acid found in most cellular membranes (351,357). The membranes of vesicular glands, however, contain a large amount of dihomogammalinolenic acid from which the very high quantities of PGE_1 found in semen of man, sheep and baboon are derived (201). The variety of eicosanoid products from dihomogammalinolenic acid is not as great as those from arachidonic acid; the absence of a Δ5-double bond renders this compound incapable of conversion into the leukotriene series (351). The intermediates in thromboxane synthesis from dihomogammalinolenic acid, PGH_1, and PGG_1, are poor substrates for thromboxane synthetase so TXA_1 is a product of very minor consequence (201,351).

The increased biosynthesis of the eicosanoids occurs on reaction to a stimulus, such as neurotransmitters (e.g. norephinephrine), neuropeptides (e.g. somatostasin), various humoral agents (e.g. braydikin), hyperosmolar stimuli and even mechanical strain (349). These stimuli control eicosanoid biosynthesis by regulating the release of the fatty acid precursor from the membrane by phospholipase A_2 (348)*. Subsequent reactions involve either cyclo-oxygenase or lipoxygenase which are the enzymes catalysing the initial steps in the formation of the numerous products shown in Figure 10.

Not all eicosanoid products are formed in every tissue in the body; their distribution depends not only on the fatty acid content of subcellular

*Another source of the fatty acid precursors for eicosanoid biosynthesis is thought to be the inositides. The inositides contain primarily arachidonic acid and stearic acid. The fatty acid precursor is released from the inositides by the action of phospholipase C (Figure 8) and diacylglycerol lipase (354). This reaction is known as the inositol effect (354).

membranes, but also on the relative activities of cyclo-oxygenase and lipoxygenase in the various tissues (349,351).

Because the biological actions of eicosanoids encompass such a wide spectrum of effects, research in this field has made important contributions to a better understanding of diseases such as cardiovascular disease, thrombotic disease, immunity and inflamation, reproduction, nephrology, pulmonary disease, gastroenterology and metabolic disorders (357). Many commonly prescribed drugs exert their therapeutic effects through inhibition of eicosanoid biosynthesis. For example, phospholipase A_2 is inhibited by the glucocorticoids and the antimalarial drug, mepacrine; cyclo-oxygenase is inhibited by aspirin and non-steroidal anti-inflammatory drugs, such as indomethacin, which extend their effect through inhibition of the synthesis of PGE_2, the prostaglandin which is the causitive agent of erythema, oedema and pain associated with inflammation (319,349,358).

1.3 AIMS OF THIS PROJECT

In order to obtain a better understanding of the hepatic metabolism of isoflurane and the effects of this drug on liver processes, the interaction of this anaesthetic agent with the cytochrome P-450 and fatty acid desaturase enzyme systems in the liver were studied. These two enzyme systems were chosen for the following reasons:

i) Cytochrome P-450 was chosen since all fluorinated volatile anaesthetic agents are known to be metabolised by the cytochrome P-450 enzyme system.

ii) The fatty acid desaturases or cyanide-sensitive factors were chosen since several volatile anaesthetic agents have been shown to interact with the Δ9-desaturase (313,314) with unknown physiological consequences.

Firstly, the metabolism of isoflurane by hepatic microsomal cytochrome P-450 was investigated in order to

i) establish whether hepatic microsomal cytochrome P-450(s) catalyse(s) the defluorination of isoflurane in rat hepatic microsomes, and if so, which isozyme(s) of cytochrome P-450 are active in this transformation. This study involves the use of inhibitors and inducing agents specific for isozymes of cytochrome P-450.

ii) elucidate the pathways of isoflurane metabolism in rat and human hepatic microsomes by identification of metabolites.

Secondly, the interaction of isoflurane with the cyanide-sensitive factors was studied as follows:

i) the stimulation of the cyanide-sensitive re-oxidation of cytochrome b_5 in hepatic microsomes was used to assess whether isoflurane interacts with one or more cyanide-sensitive factor.

ii) the effect of isoflurane on the activity of the Δ9-, Δ6- and Δ5-desaturases toward natural fatty acid substrates was assessed.

Since our initial results showed that isoflurane selectively inhibited the Δ6-desaturation of linoleic acid, further studies focussed on an attempt to characterise the interaction of isoflurane with the Δ6-desaturase. While in persuit of this goal, we realised that accurate measurement of the kinetics and activity of the Δ6-desaturase is more complicated than generally appreciated. It was therefore necessary to backtrack and re-investigate the assay system for the Δ6-desaturase in hepatic microsomes. This assay is complicated by the presence of other enzymes competing for the acyl-CoA substrate of the Δ6-desaturase, and several other factors. In an attempt to elucidate the underlying kinetics of the Δ6-desaturase, we investigated the effect of the following on apparent Δ6-desaturase activity:

i) the presence and concentration of endogenous unlabelled linoleic acid in the hepatic microsomes - (was it sufficient to affect Δ6-desaturase activity?).

ii) the activity of phospholipase A_2 - (was it sufficient to release significant amounts of free linoleic acid to affect apparent Δ6-desaturase activity?).

iii) kinetic data for the acyl-CoA synthetase and lysophospholipid acyltransferases - (was the former truely rapid and pre-equilibrium, and thus of insignificant effect on the Δ6-desaturase? Did the latter effectively compete with the Δ6-desaturase for acyl-CoA substrate?).

The influence of these on the apparent Δ6-desaturase activity, and inhibition thereof by isoflurane, were assessed experimentally and the results of this complex system were assessed by computer modelling of a multi-enzyme scheme for fatty acid desaturation.

2. EXPERIMENTAL

2.1 MATERIALS

2.1.1 Materials Used to Study the Interaction of Isoflurane with Hepatic Microsomal Cytochrome P-450

Isoflurane was a gift from Dr Julien Biebuyck, Bell Laboratories, U.S.A., and from Abbott Laboratories, Transvaal, R.S.A. Pregnenolone-16α-carbonitrile was a gift from Searle Laboratories, Chicago, IL., U.S.A. Sodium phenobarbital and β-naphthoflavone were obtained from Maybaker, Port Elizabeth, R.S.A. and Aldrich Chemical Co., Milwaukee, WI., U.S.A., respectively. Isocitrate dehydrogenase was from Sigma Chemicals, St. Louis, MO., U.S.A. NADH, NADPH, NADP and the components of the glucose 6-phosphate-dependent NADPH-generating system were purchased from Bayer-Miles, Cape Town, R.S.A. Sodium fluoride, trifluoroacetic acid, DL-isocitric acid and hydrogen peroxide were obtained from Merck Chemicals, Darmstadt, FDR. Trifluoroacetaldehyde hydrate was from ICN Pharmaceuticals, Plainview, NY, U.S.A. Metyrapone (2-methyl-1,2-bis-(3-pyridyl)-1-propane) was a gift from Ciba-Geigy Ltd, Basle, Switzerland. Cylinders of compressed gases were supplied by Afrox Ltd, Cape Town, R.S.A. All other chemicals were analytical grade reagents supplied by Merck Chemicals, Darmstadt, FDR or BDH Chemicals Limited, Poole, England. Water was distilled and deionized.

2.1.2 Materials Used to Study the Interaction of Anaesthetic Agents with the Enzymes of Fatty Acid Metabolism

The vitamin mixture used in the high-carbohydrate diet was constituted from vitamins received as a gift from Roche (Pty) Ltd., Isando, Transvaal. Cornflour, when used instead of dextrin in the diet, was purchased from African Products (Pty) Ltd., Bellville, Cape, R.S.A. Halothane was obtained from ICI South African Pharmaceuticals Ltd, Johannesburg, R.S.A. and methoxyflurane and enflurane from Abbott Laboratories, Transvaal, R.S.A. Radiochemicals for the fatty acid desaturase, acyl-CoA synthetase and lysophospholipid acyltransferase assays were purchased from Amersham International plc, Buckinghamshire, U.K. The relevant fatty acids and the methyl and CoA esters thereof, as well as glutathione, NADH, ATP and CoA were from Sigma Chemicals, St Louis, MO., U.S.A.

Butylated hydroxytoluene was from Marine Oil Refineries of Africa Ltd, Simonstown, R.S.A. and BSA from Bayer-Miles, Cape Town, R.S.A. All solvents and acids used in the acyl-CoA synthetase, fatty acid desaturase and lysophospholipid acyltransferase assays were analytical reagent grade supplied by Merck Chemicals, Darmstadt, FDR, and Holpro Analytics (Pty) Ltd, Johannesburg, R.S.A. Boron trifluoride-methanol, nicotinamide, 2,7-dichlorofluorescein were from Merck Chemicals.

HPLC supplies were obtained as follows: Zorbax ODS and Golden Series columns were from Dupont, Wilmington, DEL., U.S.A., the Spherisorb column was from Phase Separations Ltd, U.K.; solvents were purchased from

Rathburn Chemicals Ltd, Walkenburn, Scotland and phosphoric acid was from Fischer Scientific Co., Pittsburg, PA., U.S.A.

The solvents and phosphoric acid were filtered through Millipore filters 0.45 and/or 0.22 μm pore size (HVLP 025 00 and/or GVMP 025 00) supplied by Millipore Corp., Bedford, Mass., U.S.A. The C-18 saturation column kit which was used as a pre-column, was purchased from Supelco Inc., Bellefonte, PA., U.S.A.

Gas chromatography supplies were obtained as follows: GP 10% SP-2330 or 100/120 Chromasorb^R W AW was supplied by Supelco Inc., Bellefonte, PA., U.S.A. Nitrogen and hydrogen were extra high purity from Afrox Ltd, Cape Town, R.S.A.

The solvent for liquid scintillation counting, ready-solv, TM EP, was purchased from Beckman Instruments, Cape Town, R.S.A.

All other reagents, e.g. the salts used in buffer solutions, etc., were analytical reagent grade supplied by Merck Chemicals, Darmstadt, FDR, Holpro Analytics (Pty) Ltd, Johannesburg, R.S.A. or BDH Chemicals Limited, Poole, England. Gases were supplied by Afrox Ltd, Cape Town, R.S.A. Water was distilled and deionized.

2.1.3 Instrumentation

For all spectral studies, a Beckman 5230 or a Pye-Unicam SP 1800 UV-visible scanning spectrophotometer was used. The thermostatically controlled

compartment adjacent to the photomultiplier designed to accommodate turbid samples, was used for spectral assays on microsomal samples.

Fluoride ion concentration was measured using an Orion specific ion fluoride electrode (model 94-09) in conjunction with an Orion reference electrode (model 90-01-00) attached to a Radiometer model 22 pH meter.

For all HPLC separations, a Dupont 870 pump module and a series 8800 gradient controller were used. The fatty acids were detected using a Dupont refractive index detector connected to a Perkin-Elmer R100 recorder. Fractions (2 ml) were collected directly into scintillation vials on a LKB 2112 Redirac fraction collector.

Fatty acid methyl esters were separated by gas chromatography, using a Packard 428-series gas chromatograph with a model 907 flame ionisation detector and Hewlett Packard 3390A integrator.

For liquid scintillation counting, samples were dissolved in Ready-solv TM EP (10 ml) and counted in a Packard Tricarb 4640 liquid scintillation counter.

For all analyses of enzyme kinetic data and construction of overlay plots, a Miad personal computer and programs entitled 'Enzfitter' and 'Quattro Pro' were used. 'Enzfitter' is a program for non-linear regression analysis by Robin J. Leatherbarrow, published by Elsevier Science Publishers BV, P.O. Box 1527, 1000 BM Amsterdam. 'Quattro Pro' is by Borland International, Scotts Valley, CA., USA.

2.2 METHODS

2.2.1 Treatment of Animals and Isolation of Hepatic Microsomes

2.2.1.1 Treatment of Animals

Male Long Evans rats were maintained on a diet of Epol laboratory chow (protein minimum 20%, fat 2.5%, fibre maximum 6%, calcium 1.8, phosphorus 0.7%; obtained from Epol Ltd, Johannesburg, R.S.A.) and water, unless otherwise indicated. These rats were used at a weight of 190 ± 10 g for all studies.

2.2.1.1a Induction of Cytochrome P-450

Groups of 3 - 8 rats were used for each experiment. β-Naphthoflavone was administered as a single intraperitoneal injection (80 mg/kg in corn oil) 36 hr before sacrifice (364). Phenobarbital and pregnenolone-16α-carbonitrile were administered intraperitoneally at doses of 80 mg/kg/day in saline and 50 mg/kg/day in corn oil, respectively, for three consecutive days (364). The animals, including control animals which did not receive any pretreatment, were starved for 16 hr before sacrifice by cervical fracture; livers were removed immediately for preparation of subcellular fractions.

2.2.1.1b Induction of Fatty Acid Desaturases

Groups of 2 male Long Evans rats were fed diets to induce the Δ9- and Δ6-desaturases as follows: 3 days prior to use, the animals were starved for

24 hr, and, for induction of the Δ6-desaturase, re-fed a diet of Epol laboratory chow (normal diet) for 48 hr; for induction of the Δ9-desaturase, the animals were re-fed a high-carbohydrate diet containing dextrin or cornflour 126 g, sucrose 30 g, cellulose 4 g, casein 30 g, NaCl 4 g, KCl 2 g, choline chloride 0.2 g and vitamin mixture 6 g (vitamin A, 2.5 g (325 000 I.U./g), vitamin D, 2.0 g (200 000 I.U./g), vitamin B_2, (Riboflavin) 0.5 g, niacin 7.5 g and pantothenic acid 1 g, made up to a total of 500 g with dextrin or cornflour) (314).

2.2.1.2 Human Liver

Human liver samples from three human organ transplant donors were obtained within 20 min of death, but before cessation of the circulation. Liver 1 was from a 52 year-old female motor vehicle accident victim and was used only for hepatic microsomal cytochrome P-450 determination (Section 2.2.2.1) and assessment of the metabolism of trifluoroacetaldehyde by hepatic cytosol (Section 2.2.2.7). Liver 2 was from a 47 year-old female who died of brain haemorrhage, and was stored at -80°C for 2 days before use. Liver 3 was from a 25 year-old male assault victim. Livers 2 and 3 were used to determine cytochrome P-450 levels (Section 2.2.2.1), to assess the in vitro metabolism of isoflurane in hepatic microsomes (Sections 2.2.2.3 and 2.2.2.6), and for the metabolism of trifluoroacetaldehyde by cytosol (Section 2.2.2.7). The histology of livers 2 and 3 was found to be normal.

2.2.1.3 Preparation of Hepatic Microsomes

Hepatic microsomes were isolated in one of two different ways:

2.2.1.3a Method A

Microsomes were isolated from rat or human livers by differential ultracentrifugation essentially as described by Holtzman and Carr (359). The following modification was introduced for human liver: approximately 80 - 150 g of human liver was minced in a Toshiba meat grinder MT-300 prior to homogenisation. Subsequent steps (as described by Holtzman and Carr (359)) were carried out in an identical manner for both human and rat liver. The human or rat liver was homogenised in 3 volumes 0.02 M Tris - 0.15 M KCl, pH 7.4 per gram of wet liver weight. Cell debris and mitochondria were removed by centrifugation at 10,000g for 15 min using a Beckman JA-20 rotor in a Beckman J2-21 centrifuge. The microsomes were sedimented from the supernatant by centrifugation at 105,000g for 1 hr using a Beckman Type 65, 50Ti or 70Ti rotor in a Beckman L-8 ultracentrifuge. The supernatant was used in experiments where cytosol was required (Section 2.2.2.7). The microsomes were resuspended in 0.02 M Tris-HCl, pH 7.4, and pelleted by centrifugation for 45 min at 105,000g. The washed microsomes were resuspended in 0.02 M Tris-HCl, pH 7.4, and assayed for protein by the method of Lowry et al (360) as modified by Chaykin (361), using BSA as a standard. Microsomal suspensions were used at 2 or 4 mg protein/ml, unless otherwise stated. Anaesthetic agents were introduced into microsomal suspensions by vortex mixing for 30 sec prior to the addition of the other components necessary for the assay.

2.2.1.3b Method B

Microsomes were isolated from rat liver by differential ultracentrifugation in a buffer containing sucrose, 0.25 M; KCl, 0.15 M; GSH, 1.5 mM; potassium phosphate, 0.05 M; $MgCl_2$, 5 mM; EDTA, 4 mM, pH 7.4, essentially as described by Mahfouz (297). The method used was as described for Method A except that the microsomes from the first 105,000g spin were not washed, but were resuspended in the above buffer by using gentle agitation to separate the microsomal pellet from the clear glycogen with a vortex mixer, followed by homogenisation. The protein concentration was determined as described for Method A.

2.2.2 METHODS USED IN THE STUDY OF THE IN VITRO METABOLISM OF ISOFLURANE BY RAT AND HUMAN HEPATIC MICROSOMES

2.2.2.1 Determination of Cytochrome P-450 Concentration in Hepatic Microsomes

The concentration of cytochrome P-450 was determined by measuring the difference spectrum between carbon monoxide plus sodium dithionite reduced microsomes (2 mg protein/ml, prepared by Method A) versus sodium dithionite reduced microsomes (2 mg protein/ml) as described by Omura and Sato (36). Samples were assayed within 1 min of dithionite addition. The extinction coefficient of 91 cm^{-1} mM^{-1} for the difference in absorbance between 450 and 490 nm was used to calculate the cytochrome P-450 concentration (36).

2.2.2.2 NADPH Oxidation

The rate of NADPH oxidation in rat hepatic microsomes was measured spectrally at 30°C. Rat hepatic microsomes (2 mg protein/ml, prepared by Method A), were vortexed for 30 sec with 16 mM isoflurane. The reaction was initiated by the addition of 0.12 mM NADPH and the decrease in absorbance at 340 nm due to NADPH oxidation was recorded spectrally against a reaction blank containing only hepatic microsomal suspension. NADPH oxidation was measured both in the absence and presence of $CO:O_2$ (80:20,v/v) and corrected for any non-cytochrome P-450 dependent NADPH oxidation according to the method of Stripp et al (362). Carbon monoxide and oxygen flow were controlled by Matheson Gas Products model 7600 flow meters. The mixture of gases was bubbled through the microsomal suspension for 30 sec at a flow rate of 20 ml/min prior to the addition of isoflurane and NADPH.

2.2.2.3 Measurement of Fluoride Ion Production from Isoflurane in Hepatic Microsomes

Unless otherwise stated, rat or human hepatic microsomes (5 ml, prepared by Method A) at a concentration of 4 mg protein/ml, were incubated with 32 mM isoflurane and NADPH-generating system (0.8 mM NADP, 14.8 mM glucose 6-phosphate, 1 U/ml glucose 6-phosphate dehydrogenase and 10 mM $MgCl_2$), 2 mM nicotinamide and 0.4 mM EDTA. The reaction proceeded at 30°C with shaking at 60 cycles/min, for times ranging from 0 to 30 min. The reaction was stopped by freezing in liquid nitrogen. Reaction mixtures were dried by lyophilisation or rotary evaporation and resuspended in 0.5 ml TISAB IV* for measurement of the concentration of fluoride ion. The electrodes were

*TISAB IV contained 1 M Tris - 0.05 M sodium tartrate adjusted to pH 5.0 with HCl to give a final pH of 6.5 when mixed with the dried reaction mixture.

allowed to equilibrate for approximately 5 min before each reading. The slow response was thought to be due to the low concentration of fluoride and high concentration of protein in the solution. At concentrations above 1 x 10^{-5} μM of fluoride, and in the absence of protein, the slow response was not observed.

Standard curves were drawn up using samples of hepatic microsomes (5 ml) containing four to six known concentrations of sodium fluoride ranging from 2 - 20 μM. The fluoride standards were dried and assayed in exactly the same manner as the reaction mixtures. Standard curves drawn up in this way were compared to standard curves for fluoride plus 10 mM $MgCl_2$. These solutions (5 ml) were lyophilised and dissolved in 0.5 ml TISAB IV as described for reaction samples. $MgCl_2$ was the only component of the NADPH-generating system shown to affect the reading of the fluoride electrode.

To measure the extent to which NADH supported the metabolism of isoflurane, 5 ml rat hepatic microsomes (4 mg protein/ml, prepared by Method A) were incubated with shaking at 30°C for 0, or 5 min with 32 mM isoflurane, 0.2 mM EDTA, 1 mM nicotinamide and 1 mM NADH or NADPH. The production of fluoride ion was measured as described above using a standard curve constructed in the absence of $MgCl_2$.

2.2.2.4 Identification of Organofluorine Metabolites of Isoflurane in Rat Hepatic Microsomes

Hepatic microsomes from phenobarbital-pretreated rats (100 ml at 2 mg microsomal protein/ml, prepared by Method A) were incubated with 16 mM isoflurane, 0.2 mM EDTA, 1 mM nicotinamide, and NADPH-generating system

(0.4 mM NADP, 7.4 mM glucose 6-phosphate, 0.5 U/ml glucose 6-phosphate dehydrogenase, 5 mM $MgCl_2$), for 30 min at 30°C with shaking. Incubated reaction mixtures lacking NADPH-generating system, were used as a control. Zero-time samples were prepared in the same way as reaction mixtures, without incubation. Reaction mixtures were assayed for trifluoroacetic acid or trifluoroacetaldehyde.

2.2.2.4a Identification of Trifluoroacetic Acid

Extraction and thin layer chromatography of trifluoroacetic acid from the microsomal incubation was carried out by modification of the method of Hitt et al (195). After incubation, the reaction mixture was extracted once with chloroform:methanol (1:1,v/v) and the extract discarded. The aqueous layer was acidified to pH 2 - 3 with concentrated sulfuric acid and extracted with 100 ml diethyl ether. The extract was discarded and the aqueous layer was further acidified to a pH of between 0.2 - 0.3 with concentrated sulfuric acid and the trifluoroacetic acid was extracted from the aqueous layer thrice with 20 ml diethyl ether*.

The extracts were concentrated under a stream of nitrogen and chromatographed on silica gel thin layer chromatography plates (Merck, glass backed 20 cm x 20 cm x 0.2 mm without fluorescent indicator) developed in ethanol:chloroform:ammonium hydroxide (5:2:1,v/v/v). Spots were identified by spraying with a solution of 0.5% bromothymol blue in 80% methanol; this solution was treated before use with 1.0 M sodium hydroxide until it just turned blue. Trifluoroacetic acid at concentrations of 0.063 mM and 130 mM was added to 100 ml hepatic microsomes, and taken through the above extraction procedures.

*The pK of trifluoroacetic acid is 0.23 (363).

2.2.2.4b Identification of Trifluoroacetaldehyde

Trifluoroacetaldehyde in microsomal incubation mixtures was oxidised to trifluoroacetic acid as described by Costa et al (364). To 100 ml of reaction mixture, 1.33 ml 10% w/v NaOH, and 10 ml 0.1 M potassium permanganate were added. After the solution was acidified with 2 M sulfuric acid, sodium bisulfite (5% w/v) was added until all excess potassium permanganate was reduced. The precipitated protein was removed by centrifugation for 10 min at 2000g in the MSE 6L centrifuge using the rotor head 62303. The pH was reduced to pH 2 - 3. Further extractions with diethyl ether and the identification of trifluoroacetic acid were carried out as described above (Section 2.2.2.4a). Trifluoroacetaldehyde (0.063 mM and 0.43 mM) was added to hepatic microsomes and taken through the oxidation, extraction and identification procedures described above.

2.2.2.5 Measurement of Organofluorine Metabolites of Isoflurane in Rat and Human Hepatic Microsomes

The method reported by Soltis and Gandolfi (365) (which provided for the analysis of total fluorinated metabolites from volatile anaesthetic agents) was tested in order to find a sensitive method for quantitating the organofluorine metabolites of isoflurane in vitro. Known quantities of trifluoroethanol (0.25 μmol), trifluoroacetic acid (0.25 μmol), trifluoroacetaldehyde (0.25 μmol) and sodium trifluoroacetate (0.25 μmol) were added to 0.5 ml water, buffer (0.02 M Tris-HCl, pH 7.4), microsomes (2 mg/ml, prepared by Method A), or urine. Halothane (20 mM) and fluroxene (15 mM) were added to water or microsomes. To each sample, 50 μl of 0.1 M NaOH was added, and the

mixture was dried by lyophilisation. The dried material was fused with 15-20 mg sodium at high temperatures. Following sodium fusion, excess sodium was removed by the addition of 50 µl methanol and the solution was neutralised by the addition of 2.0 ml water plus 0.5 ml of 6 M potassium acetate, pH 6.0. An aliquot (0.5 ml) of the neutralised solution was added to TISAB IV, and the fluoride concentration determined. Standards of known concentrations of sodium fluoride (10 - 100 µM) were added to a solution (neutralising solution) containing 50 µl methanol, 2.0 ml water and 0.5 ml 6 M potassium acetate, pH 6.0. An aliquot of these neutralising solutions containing known concentrations of sodium fluoride, was added to TISAB IV and the fluoride levels were measured and used as standards.

2.2.2.6 Total Fluoride Analysis

Since the method of Soltis and Gandolfi was shown to be unsatisfactory for measurement of some of the organofluorine metabolites of isoflurane, the modifications outlined in the following sections were introduced in order to measure trifluoroacetic acid and trifluoroacetaldehyde.

2.2.2.6a The Measurement of Trifluoroacetic acid from Isoflurane in Rat and Human Hepatic Microsomes (Method A, Figure 11)

Rat or human hepatic microsomes (2 mg protein/ml) were incubated with 16 mM isoflurane, 0.2 mM EDTA, 1 mM nicotinamide and a glucose 6-phosphate-dependent NADPH-generating system (0.4 mM NADP, 7.4 mM glucose 6-phosphate, 0.5 U/ml glucose 6-phosphate dehydrogenase and

Metabolite		Alteration to reported sodium fusion procedure * and result				Method
	→	+ microsomes	→	remains as free acid	→	volatile = Method C
Trifluoroacetic acid	→	+ Microsomes + NaOH + NH_4OH	→	anionic form	→	non-volatile = Method A
	→	+ Microsomes + NaOH + NH_4OH	→	Schiff's base will not form at high pH	→	volatile = Method A
Trifluoroacetaldehyde	→	+ Microsomes + phenylhydrazine	→	forms Schiff's base with phenylhydrazine	→	non-volatile = Method B
	→	+ Microsomes	→	forms Schiff's base with amine group of macro-molecules	→	non-volatile = Method C

* The reported method was that of Soltis and Gandolfi (365).

FIGURE 11 Outline of experiments to ensure either trifluoroacetaldehyde or trifluoroacetic acid were in a non-volatile form for detection using the sodium fusion assay.

5 mM $MgCl_2$)*.

After 15 min incubation at 30°C with shaking at 60 cycles/min, 10 ml of the reaction mixture was removed and lyophilised to dryness for fluoride ion analysis. A further 10 ml was removed, the pH was adjusted by the addition of 50 μl 0.1 M NaOH and 0.5 ml of 4 M ammonium hydroxide (Method A, Figure 11), and the sample was lyophilised to dryness for analysis of total non-volatile fluoride. The fluoride ion analysis was carried out as already described (Section 2.2.2.3). Standard curves were drawn up as described in Section 2.2.2.3, excepting that sodium fluoride (2 - 20 μM) was added to 10 ml hepatic microsomes containing 5 mM $MgCl_2$ which was lyophilised and reconstituted in 0.5 ml TISAB IV.

For total fluoride analysis, the dried precipitate was fused with 50 - 60 mg sodium, neutralised, and a 0.5 ml aliquot used for fluoride analysis as previously described (Section 2.2.2.5). Aliquots of standard solutions of sodium fluoride (6.4 - 31.8 μM) and trifluoroacetic acid (2.6 - 12.7 μM) added to hepatic microsomes and taken through the same procedure, were used to draw up standard curves to quantify the results.

*For trifluoroacetic acid determination, a glucose 6-phosphate-dependent NADPH-generating system was used, but for the trifluoroacetaldehyde determination an isocitrate-dependent NADPH-generating system was used. It was thought that the aldehyde moiety of the glucose molecule which is present in concentrations far exceeding those of trifluoroacetaldehyde, might interfere with the assay.

2.2.2.6b The Measurement of Trifluoroacetaldehyde from Isoflurane in Rat Hepatic Microsomes (Methods B and C, Figure 11)

Rat hepatic microsomes (2 mg/ml) were incubated with 16 mM isoflurane, 0.2 mM EDTA, 1 mM nicotinamide and an isocitrate-dependent NADPH-generating system (0.4 mM NADP, 6.4 mM isocitric acid, 0.2 U/ml isocitrate dehydrogenase and 5 mM $MgCl_2$) at 30°C with shaking at 60 cycles/min. After 15 min, a 10 ml aliquot was lyophilised and used for fluoride ion analysis. A second and third 10 ml aliquot were lyophilised with (Method B, Figure 11) or without (Method C, Figure 11) 200 μl phenylhydrazine (0.1 mM, final concentration). The total non-volatile fluoride content was determined by sodium fusion (Section 2.2.2.5). Standards of sodium fluoride (6.4 - 47.7 μM fluoride, final concentration) and trifluoroacetaldehyde (2.6 - 19.1 μM trifluoroacetaldehyde, final concentration) were added to rat hepatic microsomes, taken through the same procedure and used to draw up standard curves to quantify the results.

2.2.2.7 The Metabolism of Trifluoroacetaldehyde by Rat and Human Liver Cytosol

The metabolism of trifluoroacetaldehyde by rat and human liver cytosol was assessed as follows: hepatic postmicrosomal supernatant (70-100 ml) was incubated with 7.5 mM NAD, 1 mM nicotinamide with, or without 0.1 or 1.6 mM trifluoroacetaldehyde for 30 min. Reaction mixtures were extracted and subjected to thin layer chromatography as already described (Section 2.2.2.4a).

2.2.2.8 Assay for Hydrogen Peroxide Production

Hepatic microsomes (3.0 ml) from phenobarbital-pretreated rats (2 mg protein/ml, prepared by Method A) were incubated with 16 mM isoflurane, NADPH-generating system (0.4 mM NADP, 6.4 mM isocitric acid, 0.2 U/ml isocitrate dehydrogenase and 5 mM $MgCl_2$), EDTA (0.1 mM) and nicotinamide (1 mM). Following incubation for 15 min, hydrogen peroxide was determined using a slight modification of the method of Hildebrandt et al (366). The reaction was terminated as follows: aliquots (1.5 ml) of the incubation mixture were treated with 1.5 ml of 5% (w/v) trichloroacetic acid and the precipitated protein was removed by centrifugation at 2000g for 10 min in an MSE 6L centrifuge using rotor head 62303. In zero-time samples, reaction mixtures were prepared in the same way and the reaction terminated immediately. To 2 ml of the supernatant, 0.2 ml of 10 mM ferroammonium sulphate was added, followed exactly 2 min later by the addition of 0.1 ml of 2.5 mM potassium thiocyanate. The absorbance at 480 nm was measured exactly 4 min after the last addition. Standards of hydrogen peroxide added to hepatic microsomes and taken through the same procedure were used to prepare standard curves from which the hydrogen peroxide concentration was determined.

Alternatively, hydrogen peroxide was determined by the catalase-methanol method (367). Incubation mixtures of hepatic microsomes (3.0 ml) from phenobarbital-pretreated rats (2 mg/ml, prepared by Method A) included 2000 U/ml catalase and 50 mM methanol as well as 16 mM isoflurane, NADPH-generating system (0.4 mM NADP, 7.4 mM glucose 6-phosphate, 0.5 U/ml glucose 6-phosphate dehydrogenase and 5 mM $MgCl_2$), 0.2 mM

EDTA and 1 mM nicotinamide. After incubation for 15 min at 30°C with shaking, the reaction was terminated by the addition of 1.5 ml of the incubation medium to 1.5 ml ice cold 15% w/v trichloroacetic acid. The precipitated protein was removed by centrifugation for 10 min at 2000g, as described above. The supernatant (1.5 ml) was mixed with 1.5 ml Nash reagent, stirred and heated at 58°C for 8 min. The solution was allowed to cool to room temperature before the absorbance was read at 412 nm. An extinction coefficient of 17.8 cm^{-1} mM^{-1} at 412 nm was used to calculate the hydrogen peroxide concentration (395).

2.2.3 METHODS USED TO STUDY THE INTERACTION OF ISOFLURANE WITH HEPATIC MICROSOMAL CYANIDE-SENSITIVE FACTORS

2.2.3.1 Measurement of the Re-oxidation of Hepatic Microsomal Cytochrome b_5

The re-oxidation of cytochrome b_5 in hepatic microsomes was measured spectrally essentially as described by Oshino et al (236). Complete reduction of cytochrome b_5 in 3.0 ml hepatic microsomes (1.5 mg protein/ml, prepared by Method A (Section 2.2.1.3a) and induced for either Δ6- or the Δ9-desaturase activity) was achieved with NADH (1 - 5 μM). Once the supply of NADH was exhausted, the pseudo-first order kinetics for the re-oxidation of cytochrome b_5 were monitored spectrally against a reference containing only microsomes. The difference in absorbance between 424 nm and 409 nm with time was used to calculate the pseudo-first order rate constant for the auto-oxidation of cytochrome b_5. The pseudo-first order rate constant for the re-oxidation of cytochrome b_5 in the presence of 12 μM stearoyl-CoA, 12 μM linoleoyl-CoA

and 13.3 mM isoflurane was determined in the same way. Linoleoyl-CoA and stearoyl-CoA were added immediately after the NADH, but the isoflurane was vortexed into the microsomes for 30 sec prior to the addition of NADH.

2.2.3.2 Assay for Microsomal Δ6- and Δ5-Desaturase Activities

Incubation conditions are described for Δ5- and Δ6-desaturase activities. Two different assays for the Δ6-desaturase are described here: a modification of the method of Mahfouz (297) (Method 1) and an HPLC assay method devised in our laboratory (Method 2). Method 2 was extended to measure the Δ6-desaturation of α-linolenic acid and the Δ5-desaturation of eicosa-8,11,14-trienoic acid.

2.2.3.2a Incubation Conditions for Assay of Microsomal Δ5- and Δ6-Desaturase Activities

Assays for hepatic microsomal Δ6- and Δ5-desaturases were established in our laboratory based on the method described by Mahfouz (297) and Mahfouz et al (304). Incubation conditions were the same for the measurement of the activities of Δ6- and Δ5-desaturases except for concentrations such as those of microsomal protein, substrate and BSA, and incubation times; these varied depending on the enzyme activity measured, and are outlined below. For the Δ6-desaturation of linoleic acid, hepatic microsomes (0.5 mg protein/ml, prepared by Method B (Section 2.2.1.3b), unless otherwise stated) from rats fed a normal diet were used. Reaction mixtures contained a 0.05 M phosphate buffer, pH 7.4, 0.15 M KCl, 0.25 M sucrose, 1.5 mM GSH, 5 mM $MgCl_2$, 4 mM EDTA, 7.5 mM ATP, 1 mM CoA,

2.6 mM NADH, 40 mM KF, 0.33 mM nicotinamide, BSA (115 or 11.5 μg/μg fatty acid added) and [1-^{14}C] linoleic acid (0.45 - 10.9 nmol, 26 - 632 nCi) in a final volume of 1.0 ml hepatic microsomes. Incubations were at 35°C with shaking at 60 cycles/min for 0 and 10 min, unless otherwise stated. For the Δ6-desaturation of α-linolenic acid, the reaction mixtures were identical to those above except that the radiolabelled fatty acid substrate was [1-^{14}C] α-linolenic acid (0.45 - 10.9 nmol, 25 - 613 nCi), the microsomal protein concentration was 0.5 mg/ml and the reaction time was 0 and 7 min, unless otherwise stated. For the Δ5-desaturation of eicosa-8,11,14-trienoic acid, the radiolabelled fatty acid substrate was [2-^{14}C] eicosa-8,11,14-trienoic acid (0.3 - 1.6 nmol, 3.6 - 19.0 nCi), the microsomal protein concentration was 0.25 mg protein/ml and the reaction time was 0 and 10 min, unless otherwise stated. When the Δ6- or Δ5-desaturase activity was determined in the presence of anaesthetic agents, the anaesthetic agent was suspended in the hepatic microsomes (1 - 2 mg protein/ml) by vortex mixing for 30 sec prior to the addition of the remaining components of the incubation mixture.

Separation and quantitation of the fatty acid substrates and products of the Δ5- and Δ6-desaturation reactions were achieved by TLC after saponification of membrane phospholipids and methylation of the free fatty acid substrates and products as described by Mahfouz (297) (Method 1); or by HPLC following saponification of membrane phospholipids, a method devised in our laboratory (Table 9) (Method 2). The similarities and differences between the two assay methods are summarised in Table 9.

TABLE 9

SUMMARY OF THE SIMILARITIES AND DIFFERENCES BETWEEN THE TWO METHODS OF ASSAY FOR THE Δ6-DESATURASE

Steps in Assay	METHOD 1	METHOD 2
Incubation conditions	Section 2.2.3.2a	Section 2.2.3.2a (Same as Method 1)
Saponification	At 85 °C for 2 hr under argon	At 60 °C for 30 min under argon
Methylation	HCl-methanol, done together with saponification at 85 °C for 2 hr under argon	None
Separation of fatty acids	Argentation TLC separation of fatty acid methyl esters in chloroform:methanol (100:2,v/v)	HPLC of free fatty acids
Reference	Mahfouz (297)	Mahfouz (297), and Aveldano (368)

2.2.3.2b Method 1: Saponification of Membrane Phospholipids followed by Methylation and the Separation of the Fatty Acid Substrate and Product of the Δ6-Desaturase Reaction

The Δ6-desaturase reaction (Section 2.2.3.2a) was terminated by the addition of an equal volume (1 ml) of 5% HCl in methanol. The method of Mahfouz (297) was modified in that free fatty acid carriers (2 mg each of linoleic and γ-linolenic acids) were added prior to methylation, instead of after as methylated fatty acids. Microsomal fatty acids were extracted, saponified and methylated as described by Mahfouz (297,304). Finally, the fatty acid methyl esters were resuspended in 150 μl petroleum ether (bp 60 - 80°C) and stored at -20°C under nitrogen prior to separation by TLC (within 48 hr).

The thin layer chromatography plates (Merck aluminium or glass-backed silica gel 60 (20 cm x 20 cm x 0.2 mm) without fluorescent agent) were dipped in 10% aqueous silver nitrate, air dried, and activated at 110°C for 30 min. Alternatively, the separation of the fatty acid methyl esters was carried out on glass plates which were covered with a slurry of 50% silica gel H in 10% aqueous silver nitrate, air dried and activated for 30 min at 110°C. To each plate, 10 μl samples of the fatty acid methyl ester mixtures were applied. The plates were developed in chloroform:methanol (100:2,v/v) and the separated fatty acid methyl ester bands were identified under ultraviolet light after spraying lightly with a solution of 0.1% 2,7-dichlorofluorescein in ethanol. The methyl esters of linoleic and γ-linolenic acids were identified by comparison of the R_f value with those of authentic methyl ester standards. The bands of methylated fatty acids were cut (aluminium-backed plates) or scraped (glass-backed plates) into counting vials, suspended in 10 ml ready-solv TM EP for liquid scintillation counting (Section 2.1.3).

2.2.3.2c Method 2: Saponification of Membrane Phospholipids and Separation of Free Fatty Acids by HPLC

The Δ5- and Δ6-desaturase reactions were terminated by addition of an equal volume (1 ml) of 10% potassium hydroxide in methanol containing 0.005% butylated hydroxytoluene. Fatty acid carriers were added to facilitate detection by change in refractive index, viz: 1 mg each of the following: linoleic and γ-linolenic acids for the Δ6-desaturation of linoleic acid; α-linolenic acid for the Δ6-desaturation of α-linolenic acid; eicosa-8,11,14-trienoic acid and arachidonic acid for the Δ5-desaturation of eicosa-8,11,14-trienoic acid. The reaction mixtures were saponified for 30 min at 60°C under argon, acidified and extracted thrice with 2 ml hexane. The free fatty acids were dried under a stream of nitrogen at ca. 45°C, resuspended in 0.5 ml methanol, filtered through a 0.45 μm filter (Millipore hydrophilic durapore) and stored under liquid nitrogen. Under these conditions, the fatty acids were stable for at least three to six weeks.

The free fatty acids were separated by HPLC using a modification of the method of Aveldano et al (368). The free fatty acids (50 μl) were applied to one of three HPLC columns : Zorbax ODS (25 cm x 0.45 cm), Zorbax Golden Series (8 cm x 0.62 cm, 3 μm pore size) or Spherisorb ODS (25 cm x 0.45 cm, 10 μm pore size). The columns were equilibrated with acetonitrile:30 mM phosphoric acid (65:35,v/v). The Zorbax ODS column was equilibrated at 35°C and the Zorbax Golden Series and Spherisorb ODS columns were equilibrated at room temperature. The columns were run at a flow rate of 2 ml/min. After each run, the column was washed with acetonitrile (100%) before re-equilibration in acetonitrile:30 mM phosphoric acid (65:35, v/v). Fractions (2 ml) were

collected directly into scintillation vials and mixed with 10 ml of Beckman Ready-Solv TM EP for liquid scintillation counting (Section 2.1.3). The free fatty acids were identified by comparison of their elution profiles* with authentic samples of appropriate free fatty acids.

2.2.3.2d Enzyme Activity Calculations for the Fatty Acid Desaturases used in Both Assay Methods

The fatty acid desaturase activity can be expressed as the ratio:

$$\frac{\text{dpm of product}}{\text{dpm of product + dpm of substrate}}$$

This parameter corrects for variations in the recovery of radioactive fatty acids during the extraction procedures. Since the total number of counts on termination of the reaction, i.e. the dpm in substrate + dpm in product, represents the initial substrate concentration, the ratio can be expressed as follows:

$$\frac{\text{dpm of product}}{\text{dpm of substrate + dpm of product}} = \frac{\text{concentration of product}}{\text{initial substrate concentration}}$$

$$\text{then, product formed } (\mu M) = \frac{\text{concentration of product}}{\text{initial substrate concentration}} \times \text{initial substrate concentration } (\mu M)$$

In the zero time samples, the dpm of the fatty acid product was 50 ± 10 which was comparable to the observed background counts. By subtracting ratios calculated for zero time samples, the small contribution of the background counts to the activity was eliminated. This was only possible when the specific

* The elution profiles for the different fatty acids are illustrated in the results (Figure 18).

activity of the [1-^{14}C] linoleic acid was the same throughout, i.e. substrate concentration was uniform. Where substrate concentration varied, the average background counts were subtracted from each sample counted.

2.2.3.3 Assay for Microsomal Δ9-Desaturase Activity in Hepatic Microsomes

The activity of the Δ9-desaturase in hepatic microsomes (prepared by Method A, Section 2.2.1.3a) was measured essentially as described by Oshino et al (235). Hepatic microsomes (1.0 mg protein) were incubated with 40 μM [1-^{14}C] stearoyl-CoA (12 nCi), 1 mM NADH or NADPH, with, or without 16 mM isoflurane, in a volume of 0.5 ml 0.02 M Tris-HCl, pH 7.4, for 10 min at 30°C with shaking. The reaction was terminated with 0.5 ml 10% potassium hydroxide in methanol, and fatty acid carriers (2 mg each of stearate and oleate) were added.

The reaction mixtures were saponified at 80°C for 30 min under nitrogen, acidified and extracted thrice with 2 ml petroleum ether (bp 60 - 80°C). The extracts were evaporated to dryness under nitrogen at ca. 45°C and the fatty acids were methylated using boron trifluoride (14% w/v in methanol) (369). The fatty acids, suspended in 5 ml boron trifluoride, were heated at 100°C for 15 min under nitrogen. The samples were cooled before 1 ml of water was added, and the methylated fatty acids were extracted thrice with hexane. The methylated fatty acids were taken to dryness under a stream of nitrogen at ca. 45°C and redissolved in 100 μl petroleum ether (bp 40 - 60°C). The methyl esters of stearate and oleate were separated by argentation thin layer chromatography. Silica gel thin layer chromatography plates (Merck,

glass-backed 20 cm x 20 cm x 0.2 mm) were lightly sprayed with an aqueous solution of 10% silver nitrate, air dried and activated at 110°C. The plates were developed in diethyl ether:n-hexane (1:9,v/v) and the spots located by spraying with water; methyl stearate and methyl oleate were identified by comparison of the R_f values with authentic standards. The spots were scraped into counting vials and the radioactivity of the labelled stearate and oleate fractions were determined using liquid scintillation counting (Section 2.1.3).

2.2.3.4 Quantification of the Endogenous Free Fatty Acids present in Hepatic Microsomes

The endogenous free fatty acids in hepatic microsomes from rats fed a normal diet were extracted as follows: to 2 ml of hepatic microsomes (7 - 11 mg protein/ml, prepared by Method B (Section 2.2.1.3b)) 1 μl [1-^{14}C] oleic acid (3.5 nmol, 57.4 nCi) or 1 μl [1-^{14}C] linoleic acid (1.8 nmol, 106 nCi) was added as a radiolabelled standard. The microsomes were acidified to a pH of about 1 with HCl and extracted with 33 ml hexane:2-propanol (3:2,v/v) (370).* The extract was filtered and taken to dryness by rotary evaporation. The residue was dissolved in 0.5 ml chloroform:methanol (2:1,v/v) and the whole sample was applied to silica gel thin layer chromatography plates (Merck, glass-backed 20 cm x 20 cm x 0.2 mm, without fluorescent agent), which had been activated at 110° C for 30 min. The microsomal extract was applied across the central 15 m of the plate, and authentic standards of a free fatty acid (linoleic acid), phospholipid (phosphatidylcholine) and neutral lipid (olive oil) were applied to both sides of the plates. The plates were developed in

*This extraction procedure gave ca. 100% yield of free fatty acids.

petroleum ether (bp 40 - 60° C):diethyl ether:glacial acetic acid (90:10:1, v/v/v) (297).

The free fatty acids were located under ultraviolet light after spraying the sides of the developed plates (viz: the lanes containing the standards) with 0.2% 2,7-dichlorofluorescein in ethanol. The central band with an R_f value corresponding to that of the free fatty acid standard was scraped off and extracted thrice with 10 ml chloroform:methanol (2:1,v/v). The extract was taken to dryness by rotary evaporation, and the residue suspended in 1 ml chloroform:methanol (2:1,v/v).

The fatty acids were methylated using boron trifluoride according to the method of McIntosh et al (369) (Section 2.2.3.3). The extracts were resuspended in 200 µl iso-octane. These samples were stored in liquid nitrogen until they could be separated and quantitated by gas chromatography (Section 2.1.3). The recovery of the radiolabelled fatty acid was determined at several stages of the procedure and used to correct for any loss of free fatty acid which occurred during the lengthy extraction and chromatographic procedures. When [1^{-14}C] linoleic acid was used as an internal standard, the yield of [1^{-14}C] linoleic acid was calculated from the dpm and specific activity, and subtracted from the final concentration of free linoleic acid in the microsomes.

2.2.3.5 Quantification of the Total Fatty Acid Content of the Lipid Fraction of the Hepatic Microsomal Membrane

Hepatic microsomes (0.5 ml of 4 - 7 mg microsomal protein/ml, induced for Δ6-desaturase activity and prepared by Method B (Section 2.2.1.3b)), plus 1 µl [1^{-14}C] oleic acid (3.5 nmol, 57.4 nCi) were saponified as follows: to the

microsomes, an equal volume (0.5 ml) of 10% potassium hydroxide in methanol and butylated hydroxytoluene (0.005%) was added and this mixture was heated at 60° C for 30 min under argon. Following saponification, the microsomes were acidified with HCl and extracted thrice with 2 ml hexane. The hexane extracts were evaporated to dryness under a stream of nitrogen and the residue was resuspended in 1 ml chloroform:methanol, (2:1,v/v). A 10 μl sample was counted to estimate the recovery of the [1-^{14}C] oleic acid (recovery was greater than 90%). The fatty acids were methylated using boron trifluoride as described above (Section 2.2.3.3) and resuspended in 0.5 ml iso-octane. The methylated fatty acids were stored in liquid nitrogen until they could be analysed by gas chromatography.

2.2.3.6 Separation and Quantitation of Fatty Acids by Gas Chromatography

Methyl esters of free fatty acids were separated by gas chromatography as described by Pugh and Kates (371). A glass column (1.8 metre × 0.25 cm), packed with GP 10% SP-2330 on 100/120 Chromosorb W AW (Supelco, Inc.) was run at a temperature of 200°C with nitrogen (20 ml/min) as the carrier gas. The injector temperature was 220°C and the detector temperature 230°C.

The fatty acid methyl esters were identified by comparison of retention times with those of authentic standards. Standard curves were obtained using known concentrations of fatty acid standards (0.13 - 0.66 mM) which were methylated by the boron trifluoride-methanol procedure (Section 2.2.3.3).

The standards curves were used to quantitate the free fatty acid concentration in hepatic microsomes.

2.2.3.7 Assay for Microsomal Phospholipase A_2 Activity

Phospholipase A_2 activity was assessed in hepatic microsomes (prepared by Method B (Section 2.2.1.3b)) isolated from rats induced for Δ6-desaturase activity. The solvents (toluene and ethanol) from a 5 μl volume of radiolabelled L-3-phosphatidylcholine (1-palmitoyl-2-[$1^{-14}C$] linoleoyl-phosphatidycholine, 10.7 nmol, 128 nCi) were removed under a stream of argon at room temperature. The L-3-phosphatidylcholine was resuspended (by vortexing) in 0.1 ml of a 0.05 M phosphate buffer pH 7.4, containing 0.25 M sucrose, 0.15 M KCl, 1 mM GSH, 5 mM $MgCl_2$ and 0.4 mM EDTA. To this was added 0.1 ml hepatic microsomes (0.5 mg/ml) and the mixture was incubated with shaking for 0 or 10 min at 35°C. The concentration of EDTA in some samples was 5.0 mM. The reaction was terminated by the addition of an equal volume of 5% HCl in methanol (0.2 ml) plus butylated hydroxytoluene (0.005%). The microsomal lipids were extracted in chloroform:methanol (2:1,v/v) as described by Folch (372) and separated from the fatty acid fraction by TLC using the solvent system described in Section 2.2.3.4 (297).

2.2.3.8 Measurement of Acyl-CoA Synthetase and Lysophospholipid Acyltransferase Activities in Hepatic Microsomes

The following sections describe methods used to assess the activity of the acyl-CoA synthetase and lysophospholipid acyltransferases in hepatic

microsomes under conditions used to investigate the effect of isoflurane on the Δ6-desaturase.

Reaction mixtures were identical to those used to measure hepatic microsomal Δ6-desaturase activity (Section 2.2.3.2a) and were incubated at 35°C with shaking for 0 to 7 min. Subsequent steps were designed to obtain the best possible separation of neutral lipids, fatty acids, acyl-CoA esters and phospholipids.

2.2.3.8a Extraction and Separation of Microsomal Phospholipids, Neutral Lipids, Fatty Acids and Acyl-CoA Esters

Two different extraction and chromatographic procedures were applied: the first (Method A) separated neutral lipids from fatty acids and phospholipids plus acyl-CoA, the second (Method B), separated acyl-CoA, fatty acids and phospholipids.

Method A: the reaction (Section 2.2.3.2a) was terminated with an equal volume of 5% HCl in methanol (1.0 ml) containing butylated hydroxytoluene (0.005%). The mixture was extracted essentially as described by Folch (372): once with 3 ml of chloroform:methanol (2:1,v/v) and then twice with 3 ml of chloroform. The extracts were pooled and the volume reduced to approximately 0.5 ml under a stream of nitrogen at ca. 45°C.

The extracts were stored in liquid nitrogen prior to the separation of the constituent lipid classes by TLC as follows: an aliquot (50 μl) was applied to TLC plates (Merck aluminium-backed silica gel, 20 cm x 20 cm x 0.2 mm)

which had been activated at 110°C for 30 min under a stream of nitrogen. The plates were developed in petroleum ether (bp 40 - 60° C):diethyl ether:glacial acetic acid (90:10:1,v/v/v) containing 0.005% butylated hydroxytoluene (297). The bands corresponding to the phospholipids, neutral lipids and fatty acids were located under ultraviolet light after spraying with 2,7-dichlorofluorescein and the R_f values were compared with those of authentic standards. The standards used were free fatty acid, linoleic acid; neutral lipid, olive oil and phospholipid, phosphatidylcholine. Identification of the phospholipid was facilitated by the use of molybdenum blue spray (373). Once the lipid classes had been identified, the corresponding bands were cut out and the radioactivity associated with each lipid fraction determined by liquid scintillation counting (Section 2.1.3).

Method B: The reaction (Section 2.2.3.2a) was terminated by the addition of 4 ml diethyl ether containing 0.25 mg butylated hydroxytoluene. All steps in the extraction procedure were carried out under argon or nitrogen. The fatty acids were extracted twice into 4 ml diethyl ether. These extracts were pooled and the volume recorded. An aliquot (0.5 ml) of the diethyl extracts was removed and the radioactivity determined by liquid scintillation counting (Section 2.1.3)

The phospholipid and fatty acyl-CoA fractions remained in the aqueous layer and were separated into organic and aqueous phases essentially as described by Lands (374). To the aqueous layer, 4 ml chloroform:methanol (1:4,v/v) containing 0.005% butylated hydroxtoluene was added, followed by 9 ml chloroform:methanol (4:1,v/v) containing 0.005% butylated hydroxytoluene, and the mixture was vortex mixed. Four ml water was added to wash the

non-lipid material from the organic phase. The organic phase (chloroform:methanol) was removed and the volume of both phases recorded. An aliquot (0.5 ml) of the organic and aqueous phases was used for liquid scintillation counting (Section 2.1.3). This method of separation of the substrates and products of the acyl-CoA synthetase and lysophospholipid acyltransferases is referred to as the assay by differential organic extractions.

Radioactive standards were taken through the extraction procedure described above to assess the percentage recovery and to determine the distribution of the fatty acid, phospholipids and acyl-CoA in the fractions. The standards used were fatty acid, [1-^{14}C] linoleic acid (1.8 nmol, 106 nCi); phospholipid, 1-palmitoyl-2-[1-^{14}C] linoleoyl-phosphatidylcholine (2.2 nmol, 26 nCi) and acyl-CoA, [1-^{14}C] palmitoyl-CoA (0.86 nmol, 50 nCi).

The organic phases (diethyl ether and chloroform:methanol) were taken to dryness under a stream of nitrogen; the residue was resuspended in 0.5 ml chloroform:methanol (2:1,v/v). These samples were stored under liquid nitrogen until their purity could be assessed by TLC. A 50 μl aliquot of sample was applied to the TLC plate (Merck aluminium-backed silica gel, 20 cm x 20 cm x 0.2 mm activated at 110° C for 30 min) under a stream of nitrogen. The plates were developed in chloroform:methanol:glacial acetic acid (66:34:1,v/v/v) containing 0.005% butylated hydroxytoluene*. The bands corresponding to the free fatty acid were located under ultraviolet light after spraying with 2,7-dichlorofluoresein; the phospholipid bands were identified using Molybdenum blue spray and the acyl-CoA band was identified using nitroprusside (after treatment with 10% KOH in methanol to split the

*This solvent system is an adaption of those reported by Emilsson and Sundler (398) and was shown to give optimum separation.

thioester bond) (375). The phospholipid fractions were further identified by comparison of their R_f values with those of authentic standards of phosphatidylcholine, phosphatidylethanolamine, phosphatidylinositol, phosphatic acid and lysophosphatidylcholine. Bands were cut out and counted by liquid scintillation counting (Section 2.1.3).

2.2.3.8b Enzyme Activity Calculations

The activity of the acyl-CoA synthetase was calculated as the ratio of dpm fatty acyl-CoA/total dpm recovered. This ratio corrects for recovery of the radioactivity in the extraction procedure. The amount of fatty acyl-CoA produced (μM) can be calculated from this ratio and specific activity. The concentration of fatty acyl-CoA recovered was corrected for yield of fatty acyl-CoA standards on extraction.

The activity of the lysophospholipid acyltransferases was calculated in the same way as above from the corrected yield of phospholipid.

2.2.3.9 Calculations and Statistical Analyses

Reported values are means ± standard deviations. For the study of the metabolism of isoflurane by cytochrome P-450 (Section 3.1), assays were performed in triplicate on at least two or more preparations of hepatic microsomes from the pooled livers of three to six rats. For the rest of the results (Section 3.2), assays were in triplicate from two or three preparations, and occasionally one preparation, of hepatic microsomes using the pooled livers of two rats. The total number of determinations reported accompany the results in

brackets. Unless otherwise stated, the means are from two or more preparations of microsomes. Daily activity measurements of the fatty acid desaturases varied, however, so that the results of more than one day could not be averaged. In these cases, the results from one day are reported and were chosen so that they were representative of all those obtained on that aspect of the research. When the results of a single, but representative day are reported, this is stated in the text. The Students t-test was utilised to calculate significant differences between means.

Since calculation of the activity of the fatty acid desaturases, acyl-CoA synthetase and lysophospholipid acyltransferases is based on substrate concentration (Sections 2.2.3.2d and 2.2.3.8b) and in the course of the experiments, endogenous substrate was found in the microsomes, the activity of these enzymes was corrected for endogenous substrate as outlined by Segel (376). All substrate concentrations are substrate added plus endogenous substrate and enzyme rates reported are corrected for the effect of endogenous substrate concentration on specific activity, unless otherwise noted.

2.2.3.10 Presentation of Kinetic Data

The kinetic data for the microsomal enzyme reactions were plotted according to the method described by Segel for assays using radiolabelled substrate in the presence of endogenous substrate, i.e. the rate was corrected for endogenous substrate and the substrate concentration used was that of added plus endogenous substrate (376).

Plots of rate versus substrate concentration, Lineweaver-Burk and Eadie-Hofstee plots, were constructed from the experimentally determined data points using a Miad personal computer and the 'Enzfitter' program (Section 2.1.3). Where experimental data points in Lineweaver-Burk plots and Eadie-Hofstee plots looked as if they were linear, these lines were calculated and drawn using the 'Enzfitter' program. Where possible, apparent K_m and V_{max} values were calculated from the Michaelis-Menten equation using the 'Enzfitter' program.

2.2.3.11 Computer Modelling of the Δ6-Desaturase Reaction

A simplified reaction scheme for the Δ6-desaturase and other fatty acid metabolising enzymes was devised (shown in Figure 38). This reaction scheme was simulated using the SLAM II Version 3.0 program on a Univac model 1180 or a Vax 6000-330 computer. The formation of products with time was monitored over 5 min and compared with that obtained experimentally. For each computer run, the simulated data were compared to the experimentally determined data for substrate disappearance or product formation as a function of time by constructing overlay plots using a Miad personal computer and Quattro Pro.

The rate constants in the models were adjusted until the data from the simulated reaction scheme modelled the experimental data for substrate disappearance and product formation versus time for all three enzymes. Once the data from the simulated reaction scheme as a function of time compared favourably with the experimentally determined data for fatty acid disappearance, acyl-CoA formation, Δ6-desaturation and acylation of phospholipids, the constants were

used to simulate the reaction scheme at different concentrations of fatty acid substrate. Fatty acid substrate concentrations were taken as added fatty acid plus endogenous fatty acid. The reaction rate in μM product formed/min was calculated from the amount of product formed at 3 minutes from the output of the simulated reaction scheme, and compared to that obtained experimentally in hepatic microsomes for the acyl-CoA synthetase, Δ6-desaturase and lysophospholipid acyltransferase at the different substrate concentrations used. Concentrations of enzymes and other factors, such as lysophospholipid, were obtained or calculated from the literature.

2.2.3.12 Desaturase System

Details of several aspects of the SLAM model for the desaturase enzyme system are given in this section. The abbreviations used and SLAM definitions are given immediately below (Section 2.2.3.12.1). The differential equations (Section 2.2.3.12.4) are identified and defined in SLAM acceptable language. The variables (Section 2.2.3.12.2) and parameters (Section 2.2.3.12.3) are given. The values of the variables and initial and final values of the parameters are given in the Results and Discussion.

2.2.3.12.1 Key to Abbreviations Used

Abbreviation	Definition	SLAM Definition
F	Added + endogenous fatty acid substrate, i.e. linoleic acid	SS(1)

C*	Coenzyme A (CoA)	
E_1	Acyl-CoA synthetase	SS(2)
FE_1	Complex of F and E_1	SS(3)
FC	CoA derivative of F	SS(4)
E_2	Δ6-Desaturase	SS(5)
FCE_2	Complex of F, C and E_2	SS(6)
U†	Fatty acid product of the desaturation of F	
UC	CoA derivative of U	SS(7)
L	Lysolecithin	SS(8)
E_3	Lysophospholipid acyltransferase	SS(9)
$UCLE_3$	Complex of UC, L and E_3	SS(10)
PU	Phospholipid containing U at 2- position	SS(11)
$FCLE_3$	Complex of FC, L and E_3	SS(12)
PF	Phospholipid containing F at 2- position	SS(13)

* C was present in a large excess and the decay of its concentration was not monitered in the modelled reaction scheme (Figure 38).

† Defined, but U was not an intermediate in the reaction scheme (Figure 38).

Differential	SLAM Definition
$\frac{dF}{dt}$	DD(1)
$\frac{dE_1}{dt}$	DD(2)
$\frac{dFE_1}{dt}$	DD(3)
$\frac{dFC}{dt}$	DD(4)
$\frac{dE_2}{dt}$	DD(5)
$\frac{dFCE_2}{dt}$	DD(6)
$\frac{dUC}{dt}$	DD(7)
$\frac{dL}{dt}$	DD(8)
$\frac{dE_3}{dt}$	DD(9)
$\frac{dUCLE_3}{dt}$	DD(10)
$\frac{dPU}{dt}$	DD(11)
$\frac{dFCLE_3}{dt}$	DD(12)

$\frac{dPF}{dt}$ DD(13)

$\frac{dE_1^*}{dt}$ DD(14)

$\frac{dE_2^*}{dt}$ DD(15)

$\frac{dE_3^*}{dt}$ DD(16)

2.2.3.12.2 Variables

F, E_1, FE_1, FC, E_2, FCE_2, UC, L, E_3, $UCLE_3$, PU, $FCLE_3$, PF, NADH, O_2.

2.2.3.12.3 Parameters

k_1, k_2, k_3, k_4, k_5, k_6, k_7, k_8, k_9, k_{10}, k_{11}, k_{12}, k_{13}, k_{14}, k_{15}, k_{16}.

2.2.3.12.4 Differential Equations

1) $\frac{dF}{dt} = k_2[FE_1] + k_{13}[FC] - k_1[F][E_1]$

DD(1) $= k_2*SS(3) + k_{13}*SS(4) - k_1SS(1)*SS(2)$

2) $\frac{dE_1}{dt} = (k_2 + k_3)[FE_1] - k_1[F][E_1] - k_{14}[E_1]$

DD(2) $= k_2*SS(3) + k_3*SS(3) - k_1*SS(1)*SS(2) - k_{14}*SS(2)$

3) $\frac{dFE_1}{dt} = k_1[F][E_1] - (k_2 + k_3)[FE_1]$

DD(3) $= k_1*SS(1)*SS(2) - k_2*SS(3) - k_3*SS(3)$

4) $\frac{dFC}{dt} = k_3[FE_1] + k_5[FCE_2] + k_{11}[FCLE_3] - k_4[FC][E_2] - k_{10}[FC][E_3][L] - k_{13}[FC]$

$DD(4) = k_3*SS(3) + k_5*SS(6) + k_{11}*SS(12) - k_4*SS(4)*SS(5) - k_{10}*SS(4)*SS(9)*SS(8) - k_{13}*SS(4)$

5) $\frac{dE_2}{dt} = k_5[FCE_2] + k_6[FCE_2] - k_4[FC][E_2] - k_{15}[E_2]$

$DD(5) = k_5*SS(6) + k_6*SS(6) - k_4*SS(4)*SS(5) - k_{15}*SS(5)$

6) $\frac{dFCE_2}{dt} = k_4[FC][E_2] - k_5[FCE_2] - k_6[FCE_2]$

$DD(6) = k_4*SS(4)*SS(5) - k_5*SS(6) - k_6*SS(6)$

7) $\frac{dUC}{dt} = k_6[FCE_2] + k_8[UCLE_3] - k_7[L][E_3][UC]$

$DD(7) = k_6*SS(6) + k_8*SS(10) - k_7*SS(8)*SS(9)*SS(7)$

8) $\frac{dL}{dt} = k_8[UCLE_3] + k_{11}[FCLE_3] - k_7[L][E_3][UC] - k_{10}[FC][L][E_3]$

$DD(8) = k_8*SS(10) + k_{11}*SS(12) - k_7*SS(8)*SS(9)*SS(7) - k_{10}*SS(4)*SS(8)*SS(9)$

9) $\frac{dE_3}{dt} = (k_8 + k_9)[UCLE_3] + (k_{11} + k_{12})[FCLE_3] - k_7[UC][E_3][L] - k_{10}[FC][E_3][L] - k_{16}[E_3]$

$DD(9) = k_8*SS(10) + k_9*SS(10) + k_{11}*SS(12) + k_{12}*SS(12) - k_7*SS(7)*SS(8)*SS(9) - k_{10}*SS(4)*SS(9)*SS(8) - k_{16}*SS(9)$

10) $\frac{dUCLE_3}{dt} = k_7[UC][L][E_3] - k_8[UCLE_3] - k_9[UCLE_3]$

$DD(10) = k_7*SS(7)*SS(8)*SS(9) - k_8*SS(10) - k_9*SS(10)$

11) $\frac{dPU}{dt} = k_9[UCLE_3]$

$DD(11) = k_9*SS(10)$

12) $\frac{dFCLE_3}{dt} = k_{10}[FC][L][E_3] - k_{11}[FCLE_3] - k_{12}[FCLE_3]$

$DD(12) = k_{10}*SS(4)*SS(8)*SS(9) - k_{11}*SS(12) - k_{12}*SS(12)$

13) $\frac{dPF}{dt} = k_{12}[FCLE_3]$

$DD(13) = k_{12}*SS(12)$

14) $\frac{dE_1^*}{dt} = k_{14}[E_1]$

$DD(14) = k_{14}*SS(2)$

15) $\frac{dE_2^*}{dt} = k_{15}[E_2]$

$DD(15) = k_{15}*SS(5)$

16) $\frac{dE_3^*}{dt} = k_{16}[E_3]$

$DD(16) = k_{16}*SS(9)$

3. RESULTS

The results presented herein fall into two sections:

i) an investigation of the metabolism of isoflurane by cytochrome P-450 (Section 3.1); and

ii) the interaction of isoflurane and other anaesthetic agents with the cyanide-sensitive factors, focussing on the fatty acid desaturases. These results are followed by an attempt to characterise the interaction of isoflurane with the Δ6-desaturase, and this study includes an investigation into reactions and other factors which may influence accurate measurement of the activity of the Δ6-desaturase in hepatic microsomes (Section 3.2).

3.1 THE METABOLISM OF ISOFLURANE BY THE CYTOCHROME P-450 DRUG METABOLISM PATHWAY

The metabolism of isoflurane by rat cytochrome P-450 was measured in hepatic microsomes in two ways:-

i) indirectly, by the stimulation of CO-inhibitable NADPH oxidation by isoflurane; and

ii) directly, by fluoride ion production from isoflurane in the presence of a NADPH-generating system and EDTA.

Using both these methods, the rates of isoflurane metabolism were assessed in microsomes from rats pretreated with inducing agents specific for isozymes of cytochrome P-450 which are members of the gene families I, II and III.

3.1.1 Rates of the CO-inhibitable NADPH Oxidation in the Presence of Isoflurane in Rat Hepatic Microsomes

The results of the indirect measurement of the metabolism of isoflurane in hepatic microsomes from rats pretreated with inducing agents for the different cytochrome P-450 isozymes are presented in Table 10. Pretreatment of rats with phenobarbital, β-napthoflavone and pregnenolone-16α-carbonitrile gave increased levels of cytochrome P-450 which were significantly greater ($P<0.01$) than the corresponding levels in control microsomes (Table 10). Initial reaction rates, which were linear for two to three minutes, were utilised in the calculation of rates of NADPH oxidation. The rate of CO-inhibitable NADPH oxidation in the presence of isoflurane was decreased or unchanged per mg microsomal protein and per nmol cytochrome P-450 following β-naphthoflavone and pregnenolone-16α-carbonitrile induction and was increased significantly ($P<0.01$) following phenobarbital induction of cytochrome P-450 (Table 10).

3.1.2 Fluoride Ion Production from Isoflurane in Rat Hepatic Microsomes

Fluoride ion production following incubation of rat hepatic microsomes with isoflurane, NADPH-generating system and EDTA was at or below the limit of detection of the fluoride electrode. Therefore, fluoride ion concentration was elevated by lyophilisation of reaction mixtures. In spite of a resulting ten- to

TABLE 10

THE EFFECT OF INDUCTION ON THE CO-INHIBITABLE NADPH OXIDATION OF ISOFLURANE IN RAT HEPATIC MICROSOMES

Induction of Rats	Cytochrome P-450 (nmol/mg protein)	CO-inhibitable NADPH Oxidation *	
		(nmol/mg protein/min)	(nmol/nmol cytochrome P-450/min)
None	0.95 ± 0.08 (6)	1.9 ± 0.2 (12)	2.0 ± 0.2
β-Naphthoflavone	1.22 ± 0.09 (6) †	1.1 ± 0.4 (20)†	0.9 ± 0.4 †
Pregnenolone-16α-carbonitrile	1.73 ± 0.16 (12) †	1.4 ± 1.1 (24)	1.1 ± 0.6 †
Phenobarbital	2.02 ± 0.26 (6) †	5.7 ± 0.4 (20)†	2.8 ± 0.4 †

* In reaction mixtures containing hepatic microsomes (2 mg microsomal protein/ml 0.02 M Tris-HCl, pH 7.4), isoflurane (16 mM), NADPH (0.12 mM). The values are corrected for non-cytochrome P-450-dependent rates of NADPH oxidation measured in identical reaction mixtures in which the microsomes had been bubbled with $CO:O_2$ (80:20, v/v) for 30 sec.

† Differs significantly from corresponding value for microsomes from untreated rats ($P<0.01$).

twenty-fold increase in fluoride concentration, the levels of fluoride measured were still below the linear portion of the standard curve (data not shown).

During the course of our experiments, we realised that lyophilisation designed to increase the concentration of fluoride ten- or twenty-fold, also increased the final concentration of $MgCl_2$ (from the NADPH-generating system), resulting in interference with the fluoride determination. The effects of increasing concentrations of $MgCl_2$ on the fluoride reading in phenobarbital-induced hepatic microsomes (2 mg protein/ml) incubated with NADPH (1 mM), nicotinamide (1 mM) and EDTA (0.2 mM), are shown in Table 11. It was accordingly necessary to draw up a standard curve for fluoride determination in the presence of $MgCl_2$, in order to correct for the effect of $MgCl_2$ on the fluoride reading. Standard curves of fluoride concentration versus millivolt reading obtained in the presence and absence of $MgCl_2$ are illustrated in Figure 12. Other components of the NADPH-generating system were shown not to interfere with the fluoride reading, including glucose 6-phosphate and glucose 6-phosphate dehydrogenase (Results not shown).

Fluoride ion production from isoflurane as a function of time in rat liver microsomes from the differently pretreated animals, is illustrated in Figure 13. The reported fluoride content has been corrected for the levels of fluoride in zero-time samples consisting of hepatic microsomes (4 mg protein/ml) and isoflurane (32 mM). Negligible levels of fluoride ion (<1.0 pmol/mg microsomal protein/min) were found when the NADPH-generating system was excluded from reaction mixtures (Results not shown). In subsequent experiments, production of fluoride ion from isoflurane was assessed after 15 min incubation of microsomes from β-naphthoflavone-treated and

TABLE 11

THE EFFECT OF $MgCl_2$ CONCENTRATION ON THE DETERMINATION OF FLUORIDE ION FROM ISOFLURANE IN RAT HEPATIC MICROSOMES

[$MgCl_2$] in Reaction Mixture (mM)*	[$MgCl_2$] in Solution for Fluoride Determination (mM) †	Apparent Fluoride Production (nmol fluoride/mg protein/min)
None	None	178.0 ± 42.0
0.2	4	150.0 ± 46.0
1	20	11.6 ± 2.6
5	100	5.2 ± 2.0

* In reaction mixtures containing 10 ml hepatic microsomes (2 mg microsomal protein/ml 0.02 M Tris-HCl, pH 7.4), isoflurane (16 mM), NADPH (1.0 mM), EDTA (0.2 mM), and nicotinamide (1.0 mM). Cytochrome P-450 content of hepatic microsomes was 2.83 ± 0.48 nmol/mg microsomal protein.

† 10 ml reaction mixture lyophilised and resuspended in 0.5 ml TISAB IV. Therefore, concentration of $MgCl_2$ in column 2 is 20× that in column 1.

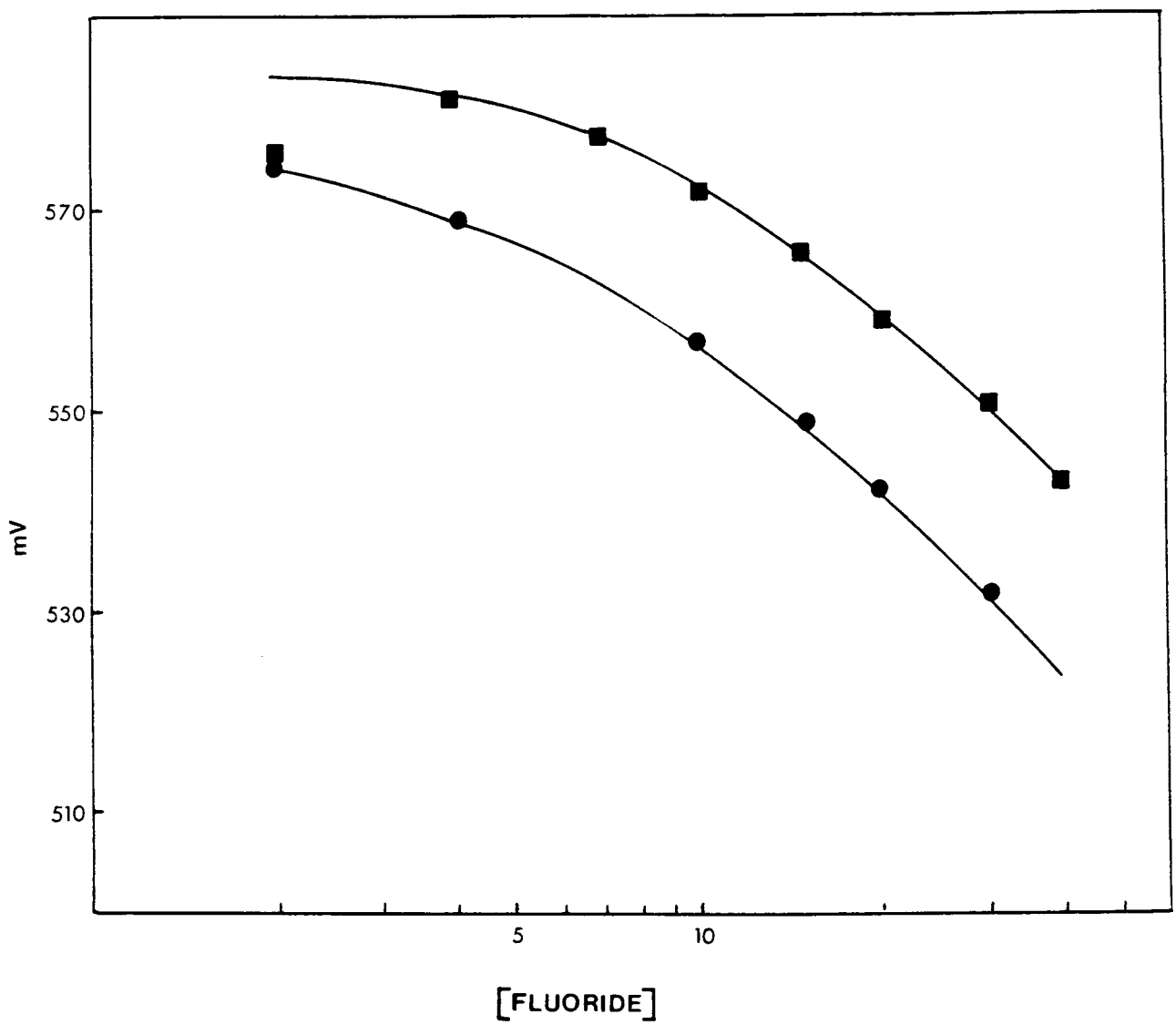

FIGURE 12 **Standard curves of fluoride concentration versus millivolt reading in the presence (■) and absence (●) of $MgCl_2$ (5.0 mM).**

Fluoride concentration, μM on a logarithmic scale.

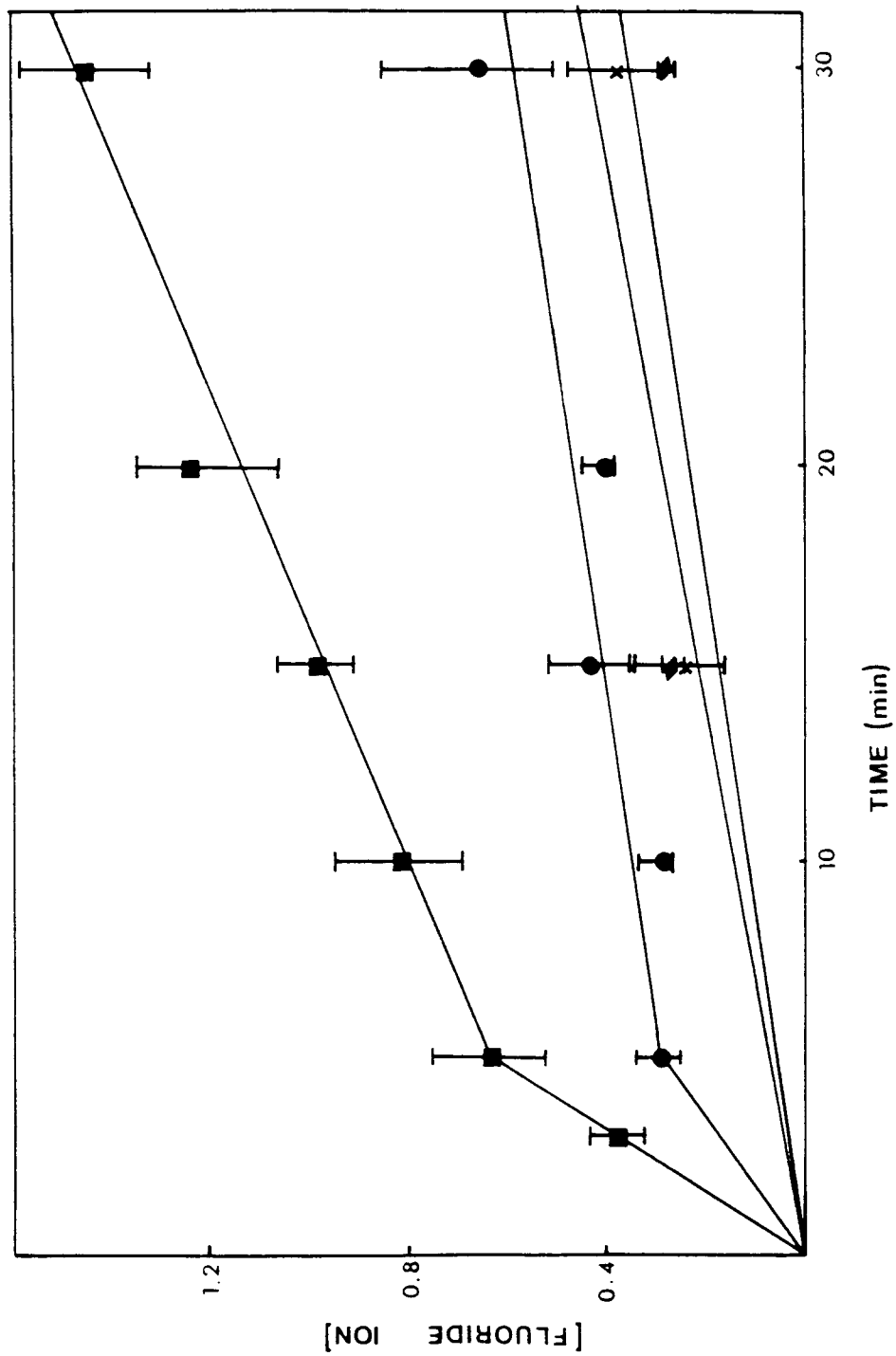

FIGURE 13 **The defluorination of isoflurane as a function of time in hepatic microsomes from untreated rats (X) and rats pretreated with β-naphthoflavone (▬), phenobarbital (●) and pregnenolone-16α-carbonitrile (■).**

Fluoride ion concentration, nmol/mg microsomal protein.

untreated, and 5 min incubation for microsomes from phenobarbital- and pregnenolone-16α-carbonitrile-treated rats, unless otherwise stated (Figure 13). For microsomes from phenobarbital-pretreated rats, this was on the linear portion of the time curve. For microsomes from untreated and β-naphthoflavone-preatreated rats, we used the shortest time over which we could accurately measure fluoride production, without being able to acertain that fluoride production was linear over this time period. This was a compromise that was not fully satisfactory, but we could find no alternative.

A comparison of the production of fluoride ion from isoflurane by microsomes from differently pretreated rats is shown in Table 12. Pretreatment of rats with β-naphthoflavone did not affect fluoride ion production from isoflurane per mg microsomal protein (Table 12). In contrast, both pregnenolone-16α-carbonitrile and phenobarbital pretreatment of rats significantly increased the production of fluoride ion per mg microsomal protein from isoflurane ($P<0.01$) (Table 12). Fluoride ion production per nmol cytochrome P-450 was unchanged following β-naphthoflavone induction but was increased significantly following pregnenolone-16α-carbonitrile and phenobarbital treatment ($P<0.01$) (Table 12).

It was possible to calculate K_m and V_{max} values for the production of fluoride ion from isoflurane only in microsomes from phenobarbital- and pregnenolone-16α-carbonitrile-induced rats. In view of the extremely low levels of fluoride ion produced from isoflurane in hepatic microsomes from β-naphthoflavone-pretreated and untreated rats (Table 12), it was not possible to determine K_m and V_{max} values for the defluorination of isoflurane in microsomes from these rats. Lineweaver-Burk plots for the defluorination of isoflurane in microsomes from phenobarbital- and pregnenolone-16α-

TABLE 12

THE EFFECT OF INDUCTION ON THE FLUORIDE ION PRODUCTION FROM ISOFLURANE IN RAT HEPATIC MICROSOMES

Induction of Rats	Cytochrome P-450 (nmol/mg protein)	Production of Fluoride Ion *	
		(pmol/mg protein/min)	(pmol/nmol cytochrome P-450/min)
None	0.95 ± 0.08 (6)	16 ± 5 (12)	18 ± 4
β-Naphthoflavone	1.22 ± 0.09 (6) †	18 ± 4 (12)	16 ± 7
Pregnenolone-16α-carbonitrile	1.73 ± 0.16 (12) †	126 ± 18 (7) †	72 ± 9 †
Phenobarbital	2.02 ± 0.26 (6) †	59 ± 10 (12) †	24 ± 4 †

* In reaction mixtures containing hepatic microsomes (5 ml at 4 mg microsomal protein/ml 0.02 Tris-HCl, pH 7.4), isoflurane (32 mM), EDTA (0.4 mM), nicotinamide (2 mM), NADP (0.8 mM), glucose 6-phosphate (14.8 mM), glucose 6-phosphate dehydrogenase (1.0 U/ml) and $MgCl_2$ (10.0 mM).

† Differs significantly from corresponding value for microsomes from untreated rats ($P<0.01$).

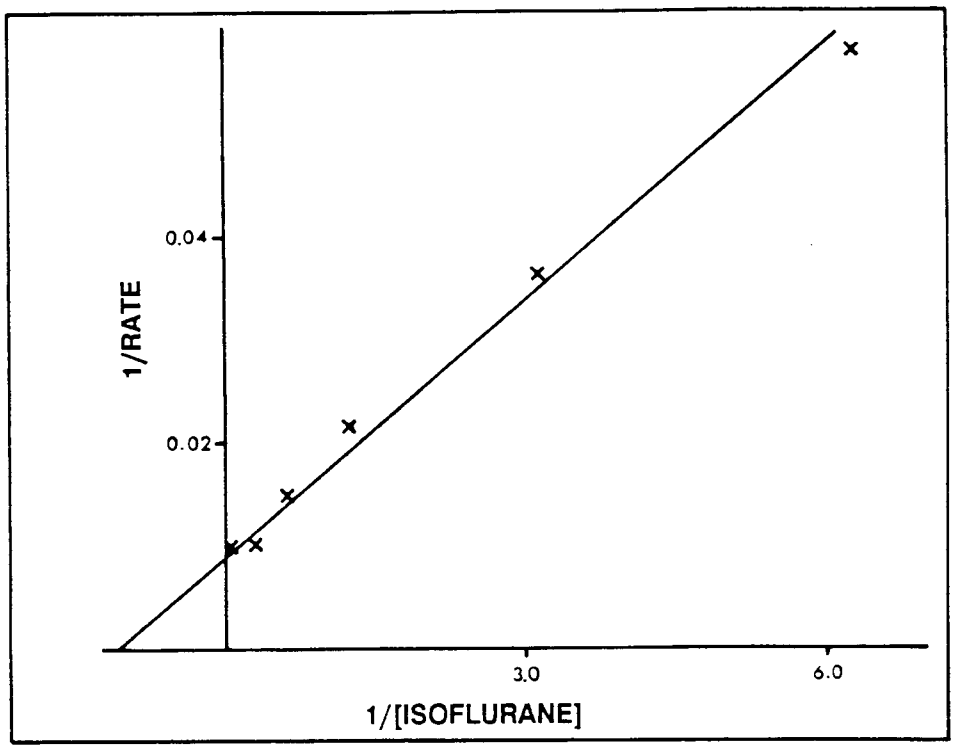

FIGURE 14 **Lineweaver-Burk plot for the defluorination of isoflurane in hepatic microsomes from phenobarbital-pretreated rats.**

Rate, rate of fluoride ion production expressed as a percentage of maximum rate; isoflurane concentration, mM.

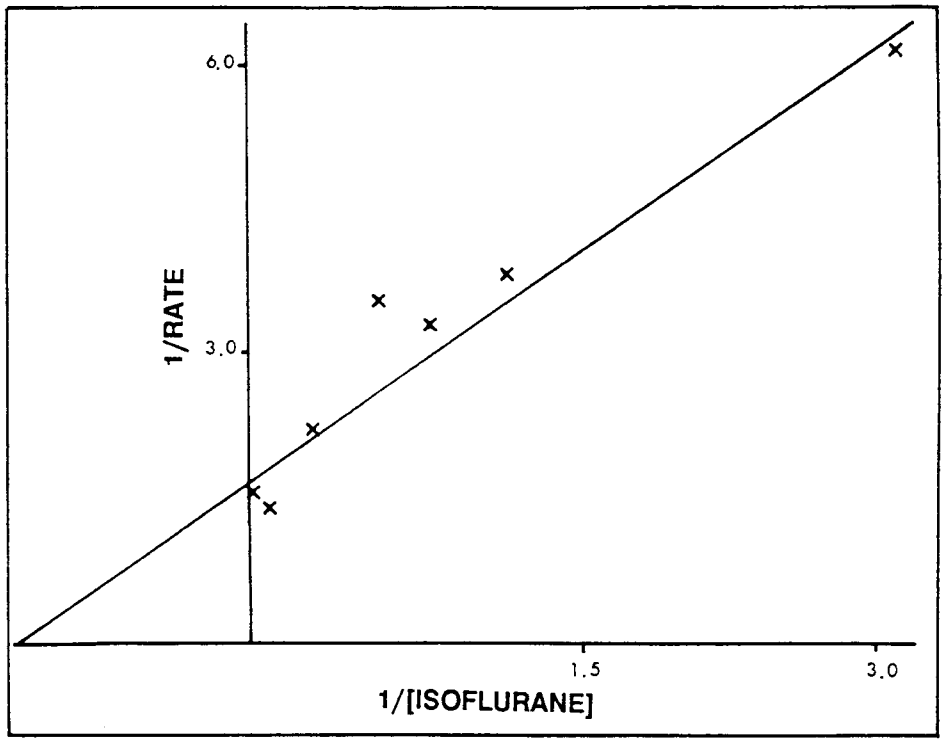

FIGURE 15 **Lineweaver-Burk plot for the defluorination of isoflurane in hepatic microsomes from pregnenolone-16α-carbonitrile-pretreated rats.**

Rate, nmol fluoride ion produced/mg microsomal protein/5 min; isoflurane concentration, mM.

carbonitrile-pretreated rats are illustrated in Figures 14 and 15, respectively. Since incubation times of 5 and 15 min were used in different experiments for the determination of the rate of fluoride ion production from isoflurane in microsomes from phenobarbital-pretreated rats, the reaction rate in the Lineweaver-Burk plot (Figure 14) is expressed as a percentage of the maximum rate. The rate of fluoride ion production expressed in this way was equivalent for both incubation times. The K_m values for the defluorination of isoflurane in microsomes from phenobarbital- and pregnenolone-16α- carbonitrile-pretreated rats were 0.86 ± 0.05 mM for both types of pretreatment. The V_{max} values were 40 and 115 pmol fluoride/mg microsomal protein/min (17 and 68 pmol fluoride/nmol cytochrome P-450/min) for phenobarbital and pregnenolone-16α-carbonitrile induction, respectively.

The production of fluoride ion from isoflurane in hepatic microsomes from phenobarbital-pretreated rats was inhibited by both CO and metyrapone. The extent of the inhibition of fluoride ion production from isoflurane by $CO:O_2$ (80:20),v/v) and metyrapone is shown in Table 13.

The alternate electron donor, NADH, supported the defluorination of isoflurane in hepatic microsomes at a slightly lower rate than NADPH (Table 14). In the presence of both NADH and NADPH, the rate of defluorination of isoflurane in hepatic microsomes from phenobarbital-pretreated rats was significantly higher than in the presence of either electron donors alone ($P<0.01$) (Table 14). Metyrapone inhibited the NADH-supported defluorination of isoflurane to a greater extent than that supported by NADPH (Tables 13 and 14).

Since the rate of isoflurane metabolism by cytochrome P-450 measured via CO-inhibitable NADPH oxidation was significantly greater than that measured

TABLE 13

THE EFFECT OF INHIBITORS OF CYTOCHROME P-450 ON THE DEFLUORINATION OF ISOFLURANE IN HEPATIC MICROSOMES FROM PHENOBARBITAL-PRETREATED RATS

Additions*	Fluoride Ion Production (pmol/mg protein/min)	% Inhibition of Fluoride Ion Production
None	35 ± 3 (15)	--
$CO:O_2$ (80:20, v/v)	27 ± 5 (15) †	24 ± 15
None	35 ± 4 (14)	--
Metyrapone (3.4 mM)	22 ± (14) 9 †	37 ± 8

* To reaction mixtures containing hepatic microsomes (5 ml at 4 mg microsomal protein/ml 0.02 M Tris-HCl, pH 7.4), isoflurane (32 mM), EDTA (0.4 mM) glucose 6-phosphate (14.8 mM), glucose 6-phosphate dehydrogenase (1.0 U/ml), NADP (0.8 mM), $MgCl_2$ (10.0 mM) and nicotinamide (2.0 mM), incubated for 15 min at 30 °C.

† Differs significantly from rate in the absence of inhibitor ($P < 0.01$).

TABLE 14

THE EFFECT OF ELECTRON DONOR AND METYRAPONE ON THE DEFLUORINATION OF ISOFLURANE IN HEPATIC MICROSOMES FROM PHENOBARBITAL-PRETREATED RATS

Additions* (mM)	Fluoride Ion Production (pmol/mg protein/min.)
NADPH (1)	193 ± 40 (8)
NADH (1)	141 ± 41 (8)
NADH (1) + NADPH (1)	249 ± 24 (8) †
NADH (1) + metyrapone (3.4)	19 ± 1 (4) †

* To reaction mixtures containing hepatic microsomes (5 ml at 4 mg microsomal protein/ml 0.02 M Tris-HCl, pH 7.4), EDTA (0.2 mM), nicotinamide (1 mM), and isoflurane (32 mM), incubated for 5 min at 30 ° C.

† Differs significantly from that in the presence of one electron donor, or in absence of inhibitor ($P<0.01$).

directly via fluoride ion production (compare Tables 10 and 12), the production of hydrogen peroxide during the metabolism of isoflurane was measured to see if the production of active oxygen species could account for the discrepancy between NADPH utilised and fluoride ion produced.

3.1.3 Production of Hydrogen Peroxide in Rat Hepatic Microsomes

A number of factors were shown to influence the spectrophotometric measurement of hydrogen peroxide by the method of Hildebrandt (366) (Table 15). EDTA, glucose 6-phosphate-dependent NADPH-generating system and hepatic microsomes lowered the absorbance of known concentrations of hydrogen peroxide significantly ($P<0.01$), whereas isoflurane, nicotinamide and the isocitrate-dependent NADPH-generating system had no effect. Consequently, reaction conditions were selected which had minimal effect on the spectrophotometric measurement of hydrogen peroxide: the isocitrate-dependent NADPH-generating system was used, and EDTA concentration was reduced to 0.1 mM.

The production of hydrogen peroxide was measured by two methods: the method of Hildebrandt (366) and the catalase-methanol method (367) (Table 16). Hepatic microsomes from phenobarbital-pretreated rats in the presence of NADPH-generating system, produced hydrogen peroxide (Table 16). The production of hydrogen peroxide was significantly lower following incubation of hepatic microsomes with NADPH generating system plus isoflurane ($P<0.01$); the results were the same for both methods of analysis (Table 16). Isoflurane in hepatic microsomes incubated without NADPH generating system, did not produce measureable amounts of hydrogen peroxide (Table 16).

TABLE 15

THE EFFECTS OF REAGENTS OF THE REACTION MIXTURE ON THE SPECTROPHOTOMETRIC DETERMINATION OF HYDROGEN PEROXIDE DESCRIBED BY HILDEBRANDT (366)

Medium containing Hydrogen Peroxide *	Incubation Time (min)	A_{480nm}
Buffer	5	0.521 ± 0.031
Microsomes	5	0.397 ± 0.023 †
Microsomes + isoflurane	5	0.407 ± 0.011
Buffer + EDTA (0.2 mM)	5	0.337 ± 0.012 †
Microsomes + EDTA (0.2 mM)	5	0.187 ± 0.010 †
Buffer + glucose 6-phosphate-dependent NADPH-generating system	0	0.407 ± 0.012 †
Buffer + isocitrate-dependent NADPH-generating system	0	0.520 ± 0.016
Buffer + EDTA (0.1 mM) + glucose 6-phosphate-dependent NADPH-generating system	5	0.197 ± 0.026 †
Buffer + EDTA (0.2 mM) + glucose 6-phosphate-dependent NADPH-generating system	5	0.079 ± 0.012 †
Buffer + nicotinamide (1 mM)	5	0.542 ± 0.032

* Buffer, 0.02 M Tris-HCl, pH 7.4; Microsomes, hepatic microsomes from phenobarbital-pretreated rats at 2 mg microsomal protein/ml 0.02M Tris-HCl, pH 7.4; Glucose 6-phosphate-dependent NADPH-generating system, glucose 6-phosphate (7.4 mM), glucose 6-phosphate dehydrogenase (0.5 U/ml), $MgCl_2$ (5 mM), nicotinamide (1 mM) and NADP (0.4 mM); Isocitrate-dependent NADPH-generating system, isocitric acid (6.4 mM), isocitrate dehydrogenase (0.2 U/ml), $MgCl_2$ (5 mM), nicotinamide (1 mM), and NADP (0.4 mM). Hydrogen peroxide concentration was 58 μM.

† Differs significantly from the corresponding value for hydrogen peroxide in buffer or, where relevant, hydrogen peroxide plus microsomes ($P<0.01$).

TABLE 16

THE EFFECT OF ISOFLURANE ON HEPATIC MICROSOMAL HYDROGEN PEROXIDE PRODUCTION

Additions to Hepatic Microsomes * (from Phenobarbital-pretreated Rats)	Method of Assay	Incubation Time (min)	Hydrogen Peroxide (nmol/mg protein/min)
Isoflurane + glucose 6-phosphate-dependent NADPH-generating system	Catalase-methanol	15	2.12 ± 0.13 (4)
Glucose 6-phosphate-dependent NADPH-generating system	Catalase-methanol	15	5.19 ± 0.58 (4) †
Isoflurane	Catalase-methanol	15	0.06 ± 0.02 (4)
Isoflurane + isocitrate-dependent NADPH-generating system	Hildebrandt	5	3.08 ± 0.17 (3) †
		2	2.89 ± 0.19 (3) †
Isocitrate-dependent NADPH-generating system	Hildebrandt	5	6.14 ± 0.07 (3)
		2	5.06 ± 0.69 (3)

* The isocitrate-dependent NADPH-generating system, which contained EDTA (0.2 mM), sodium azide (0.2 mM), isocitric acid (6.4 mM), isocitrate dehydrogenase (0.2 U/ml), NADPH (0.4 mM), $MgCl_2$ (5 mM) and nicotinamide (1.0 mM), was added to reaction mixtures of hepatic microsomes (2 mg microsomal protein/ml 0.02 M Tris-HCl, pH 7.4).

The glucose 6-phosphate-dependent NADPH-generating system, which contained EDTA (0.1 mM), glucose 6-phosphate (7.4 mM) glucose 6-phosphate dehydrogenase (0.5 U/ml), NADPH (0.4 mM), $MgCl_2$ (5 mM) and nicotinamide (1.0 mM) was added to reaction mixtures of hepatic microsomes (2 mg microsomal protein/ml 0.02 M Tris-HCl, pH 7.4).

Isoflurane concentration was 16 mM.

† Differs significantly from the corresponding value in the absence of isoflurane ($P<0.01$).

3.1.4 The Metabolism of Isoflurane by Human Hepatic Microsomes

The metabolism of isoflurane by human hepatic microsomes was measured directly by production of fluoride ion from isoflurane in the presence of EDTA and NADPH-generating system. The levels of fluoride ion produced following incubation of hepatic microsomes from human livers 2 and 3 with isoflurane, NADPH-generating system and EDTA are shown in Table 17, together with the concentrations of cytochrome P-450 found in all three livers.

3.1.5 Detection of Fluorinated Metabolites using the Sodium Fusion Assay

Three possible fluorinated metabolites of volatile fluorinated anaesthetic agents such as fluroxene, isoflurane and halothane, were subjected to the sodium fusion assay of Soltis and Gandfolfi (365). Since the decomposition of fluorinated compounds to fluoride ion is reported to depend on the medium (365), the yield of inorganic fluoride from these organofluorine metabolites was measured in various solutions and physiological fluids (Table 18).

From the results presented in Table 18, it was apparent that the yield of inorganic fluorine from the fluorinated metabolites of volatile anaesthetic agents was not strikingly dependent on the physiological medium. The yield of inorganic fluoride did, however, show striking variation with the volatility of the metabolite during the sodium fusion assay; i.e., if a metabolite is volatile under the conditions of assay, e.g. trifluoroacetaldehyde and trifluoroethanol (Table 18), it is removed during the lyophilisation step in the assay. If not, e.g., sodium trifluoroacetate, yields are good (Table 18).

TABLE 17

THE PRODUCTION OF FLUORIDE ION FROM ISOFLURANE BY HUMAN HEPATIC MICROSOMES

Human Liver No.	Cytochrome P-450 (nmol/mg protein)	Fluoride Ion Production*	
		(pmol/mg protein/min)	(pmol/nmol cytochrome P-450)
1	0.63, 0.64 (2)	N.D.	N.D.
2	0.53, 0.56 (2)	25 ± 6 (4)	45 ± 11
3	0.71, 0.74 (2)	27 ± 10 (4)	37 ± 14

* The reaction mixtures contained hepatic microsomes (4 mg microsomal protein/0.02 M Tris-HCl, pH 7.4), glucose 6-phosphate (14.8 mM), glucose 6-phosphate dehydrogenase (1.0 U/ml), NADP (0.8 mM), $MgCl_2$ (10 mM), EDTA (0.4 mM) and nicotinamide (2.0 mM).

N.D. Not determined.

TABLE 18

RECOVERY OF FLUORINATED METABOLITES OF ANAESTHETIC AGENTS USING THE SODIUM FUSION ASSAY

Metabolite	Medium	Recovery of Fluorinated Metabolites as Inorganic Fluoride	
		μM fluoride	% of Theoretical Yield *
Trifluoroethanol	Water	<1	<2
	Tris-HCl †	<1	<2
	Microsomes §	<1	<2
	Urine	<1	<2
Trifluoroacetaldehyde	Water	<1	<2
	Tris-HCl †	<1	<2
	Microsomes §	<1	<2
	Urine	<1	<2
Trifluoroacetic acid	Water	31 ± 2	26
	Tris-HCl †	22 ± 2	19
	Microsomes §	25 ± 8	20
	Urine	22 ± 5	19
Sodium trifluoroacetate	Water	100 ± 20	83
	Tris-HCl †	120 ± 6	100
	Microsomes §	96 ± 15	80
	Urine	100 ± 5	83
	Phosphate ¶	100 ± 5	83

* Concentrations of metabolites were adjusted to give a final concentration of 120 μM fluoride ion in assay medium assuming 100% recovery after sodium fusion. Assay was that of Soltis and Gandolfi (365).

† 0.02 M, pH 7.4.

§ At a concentration of 2 mg microsomal protein/ml in 0.02 M Tris-HCl, pH 7.4. Microsomes were from phenobarbital-pretreated rats.

¶ 0.05 M, pH 7.4.

We adapted the sodium fusion assay of Soltis and Gandolfi to ensure that in a single sample, one of the fluorinated metabolites of isoflurane, viz: either trifluoroacetic acid or trifluoroacetaldehyde (Figures 5 and 11), was in a non-volatile form for quantitation. The results of the adaptions to the sodium fusion assay on the recovery of trifluoroacetic acid and trifluoroacetaldehyde are outlined in the following section, and have been reported elsewhere (396).

Trifluoroacetic acid in physiological fluids was relatively volatile (ca. 20% recovery as fluoride), but sodium trifluoroacetate, the anionic form of the acid, was relatively non-volatile, giving a yield of approximately 80% (Table 18). Although sodium hydroxide was added to each sample before lyophilisation (Section 2.2.2.5), the amount of sodium hydroxide added was apparently insufficient to ensure complete ionisation of the free acid to sodium trifluoroacetate (Table 18). Complete ionisation of trifluoroacetic acid to the non-volatile form was achieved by the addition of ammonium hydroxide, as well as sodium hydroxide before lyophilisation, as in Method A (Figure 11). The recovery of inorganic fluoride from trifluoroacetic acid (50 μM) was 87 ± 10% (n = 5) under these conditions.

Since trifluoroacetaldehyde, another potential metabolite of isoflurane, was volatile under these conditions and lost during lyophilisation (data not shown), Method A (Figure 11) selectively measured trifluoroacetic acid, even if trifluoroacetaldehyde was produced.

The conversion of trifluoroacetaldehyde to a non-volatile form was achieved by the addition of phenylhydrazine (Method B, Figure 11), which forms a non-volatile phenylhydrazone with trifluoroacetaldehyde. Under these

conditions, since alkali was not added, trifluoroacetic acid remained volatile, and was removed by lyophilisation (data not shown). Therefore, Method B (Figure 11) selectively measured the organic fluoride from trifluoroacetaldehyde, even in the presence of trifluoroacetic acid.

During the course of these experiments, it was observed that inorganic fluoride could be recovered from trifluoroacetaldehyde when added to hepatic microsomes in the absence of sodium hydroxide or ammonium hydroxide (Method C, Figure 11). Trifluoroacetaldehyde (22 μM), added to 10 ml hepatic microsomes (2 mg microsomal protein/ml), lyophilised and taken through the sodium fusion assay, yielded of 68.5 ± 13 μM (n=5) inorganic fluoride (103 ± 19% recovery). Under these conditions (Method C, Figure 11) trifluoroacetaldehyde binds, presumably as a Schiff base, to microsomal constituents. The high pH resulting from the addition of the sodium hydroxide and ammonium hydroxide to hepatic microsomes used to render trifluoroacetic acid non-volatile (Method A, Figure 11) breaks these bonds releasing volatile trifluoroacetaldehyde resulting in the selective recovery of trifluoroacetic acid.

Thus, by altering the conditions under which the reaction mixtures were lyophilised, the sodium fusion assay was adapted to measure the organic fluoride from either trifluoroacetic acid or trifluoroacetaldehyde, as potential metabolites of isoflurane.

As a control, the recovery of organic fluoride from isoflurane was also measured. Isoflurane (32 mM), which was vortexed into microsomes (5 ml at 4 mg microsomal protein/ml) and lyophilised, yielded less than 2.2 nmol fluoride/ml incubation mixture. Any contribution made by isoflurane

to the levels of total organic fluoride was corrected for by including isoflurane in the zero-time samples, the results of which were subtracted from incubated samples.

3.1.6 Identification of the Organofluoride Metabolites of Isoflurane in Rat and Human Hepatic Microsomes

Known concentrations of trifluoroacetic acid and sodium fluoride incubated with human liver microsomes (2 mg microsomal protein/ml) taken through lyophilisation (under conditions where trifluoroacetic acid is non-volatile (Method A, Figure 11)) and sodium fusion, were used to draw up fluoride standard curves (Figure 16). As can be seen from Figure 16, sodium fluoride and trifluoroacetic acid gave rise to different standard curves indicating that the recovery of fluoride ion from hepatic microsomes was different for trifluoroacetic acid and sodium fluoride using the sodium fusion technique. Since both fluoride ion and trifluoroacetic acid were present in reaction mixtures, a single standard curve was selected for quantitation of fluoride, viz: that for fluoride ion (in the form of sodium fluoride) added to human hepatic microsomes and taken through the sodium fusion assay (Method A, Figure 16).

In human liver, Method A was used for measurement of total non-volatile fluoride including trifluoroacetic acid (Table 19). The production of total non-volatile fluoride significantly exceeded that of fluoride ion ($P<0.01$) in both human livers, suggesting that trifluoroacetic acid was produced in measurable quantities following incubation of isoflurane with human hepatic microsomes, NADPH-generating system and EDTA (Table 19). Only Method A was applied to human hepatic microsomes, since insufficient material was available for quantitation of trifluoroacetaldehyde.

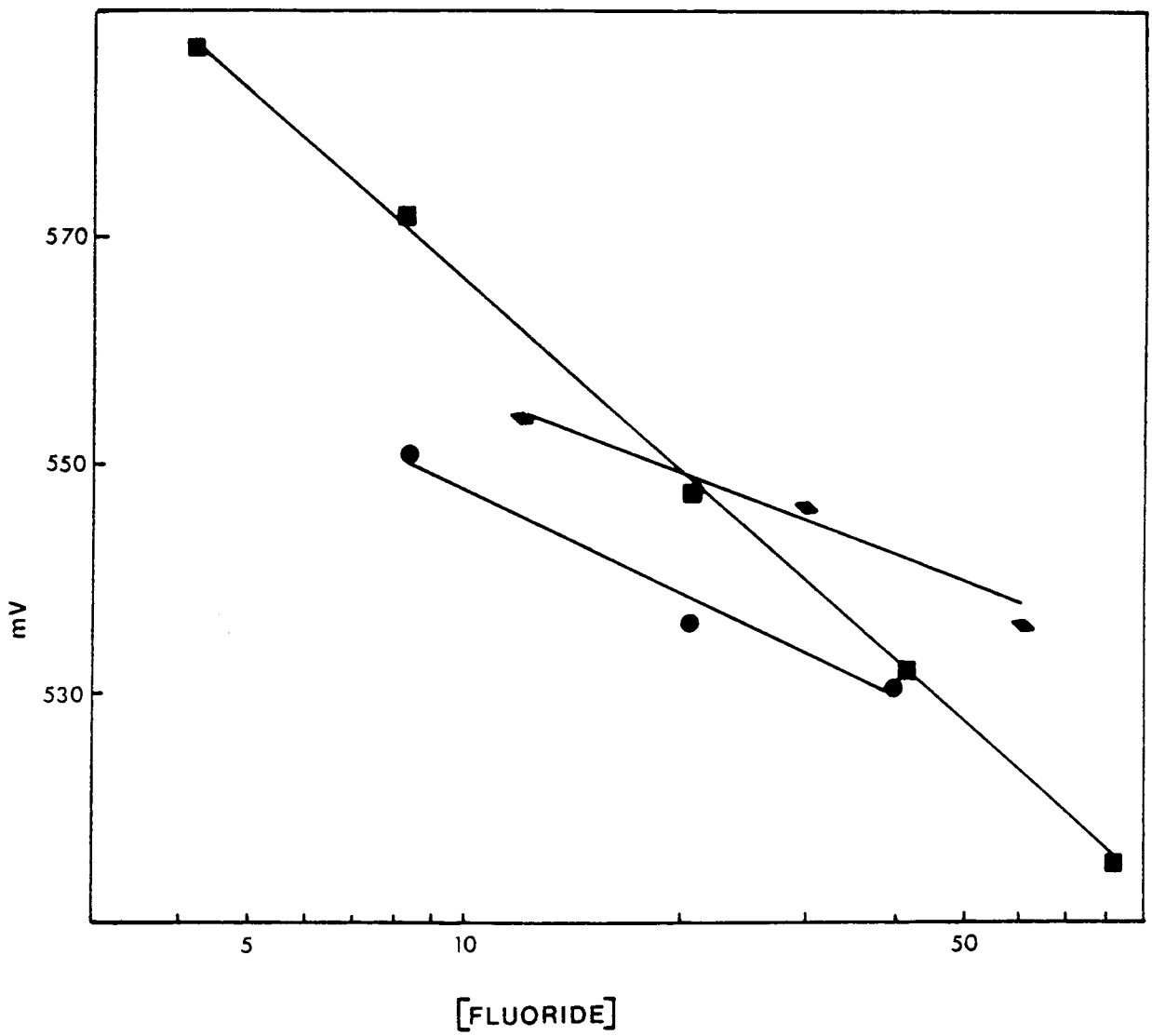

FIGURE 16 **Standard curves of fluoride concentration versus millivolt reading for sodium fluoride (●) and trifluoroacetic acid (▰) added to human hepatic microsomes and taken through the modified sodium fusion assay (Method A, Figure 11), and for sodium fluoride in neutralising solution (■) added to TISAB IV (Section 2.2.2.6).**

Fluoride concentration, μM on a logarithmic scale.

TABLE 19

A COMPARISON OF THE TOTAL NON-VOLATILE FLUORIDE AND FLUORIDE ION PRODUCTION FROM ISOFLURANE IN RAT AND HUMAN HEPATIC MICROSOMES

Species	Method (Figure 11)	Identity of Metabolite in Non-volatile Form	Fluoride Ion *	Total Fluoride §
			(nmol fluoride/mg microsomal protein/15 min)	
Human Liver 2	A	Trifluoroacetic acid	0.40 ± 0.17 (4)	2.5 ± 0.8 (3) †
Human Liver 3	A	Trifluoroacetic acid	0.41 ± 0.07 (4)	0.9 ± 0.5 (5) †
Rat	A	Trifluoroacetic acid	0.35 ± 0.10 (8)	0.2 ± 0.1 (8)
	B	Trifluoroacetaldehyde	0.35 ± 0.10 (8)	4.0 ± 2.0 (5) †
	C	Trifluoroacetaldehyde	0.35 ± 0.10 (8)	2.2 ± 1.4 (5) †

* In 10 ml of reaction mixture containing hepatic microsomes (2 mg microsomal protein/ml 0.02 M Tris-Hcl, pH 7.4), isoflurane (16 mM), EDTA (0.2 mM), nicotinamide (1 mM) and the glucose 6-phosphate-dependent or isocitrate-dependent NADPH-generating system (see Section 2.2.2.6a).

§ Total organic fluoride measured in zero-time samples (0.55 ± 0.31 nmol fluoride/mg microsomal protein) was subtracted from total organic fluoride in incubated samples.

† Significantly greater than fluoride ion production ($P < 0.01$).

Application of Method A to rat hepatic microsomes resulted in no measurable production of non-volatile organic fluoride, i.e. no trifluoroacetic acid (Table 19). Furthermore, trifluoroacetic acid was not produced in measurable amounts as assessed by thin layer chromatography following 30 min incubation of isoflurane, hepatic microsomes from phenobarbital-pretreated rats, NADPH-generating system and EDTA (limit of detection was 0.2 nmol/mg protein/30 min). Known amounts of trifluoroacetic acid (approximately equivalent to the yield of 60 nmol/100 ml of incubation mixture calculated from the fluoride ion production) added to incubation mixtures in which either the NADPH-generating system or isoflurane was omitted, were readily detected.

Treatment of the rat liver incubation mixtures described above with $KMnO_4$, which oxidises acetaldehydes to the corresponding acetic acids, resulted in the production of a metabolite which chromatographed identically to trifluoroacetic acid (R_f = 0.58). Sufficient amounts of this metabolite were produced and extracted from reaction mixtures so that the product could be visually detected relative to reaction mixtures which had not been incubated, or to reaction mixtures incubated for 30 min without NADPH-generating system. The sodium fusion assay was used to confirm the identity of trifluoroacetaldehyde (Methods B and C, Figure 11) as a metabolite of isoflurane in rat hepatic microsomes and to attempt to quantitate the production of this metabolite of isoflurane.

Known concentrations of trifluoroacetaldehyde and sodium fluoride were taken through lyophilisation and sodium fusion as described in Method B (Figure 11) and used to draw up fluoride standard curves (Figure 17). The standard curve obtained for trifluoroacetaldehyde differed from that for sodium fluoride following identical lyophilisation and sodium fusion procedures indicating that

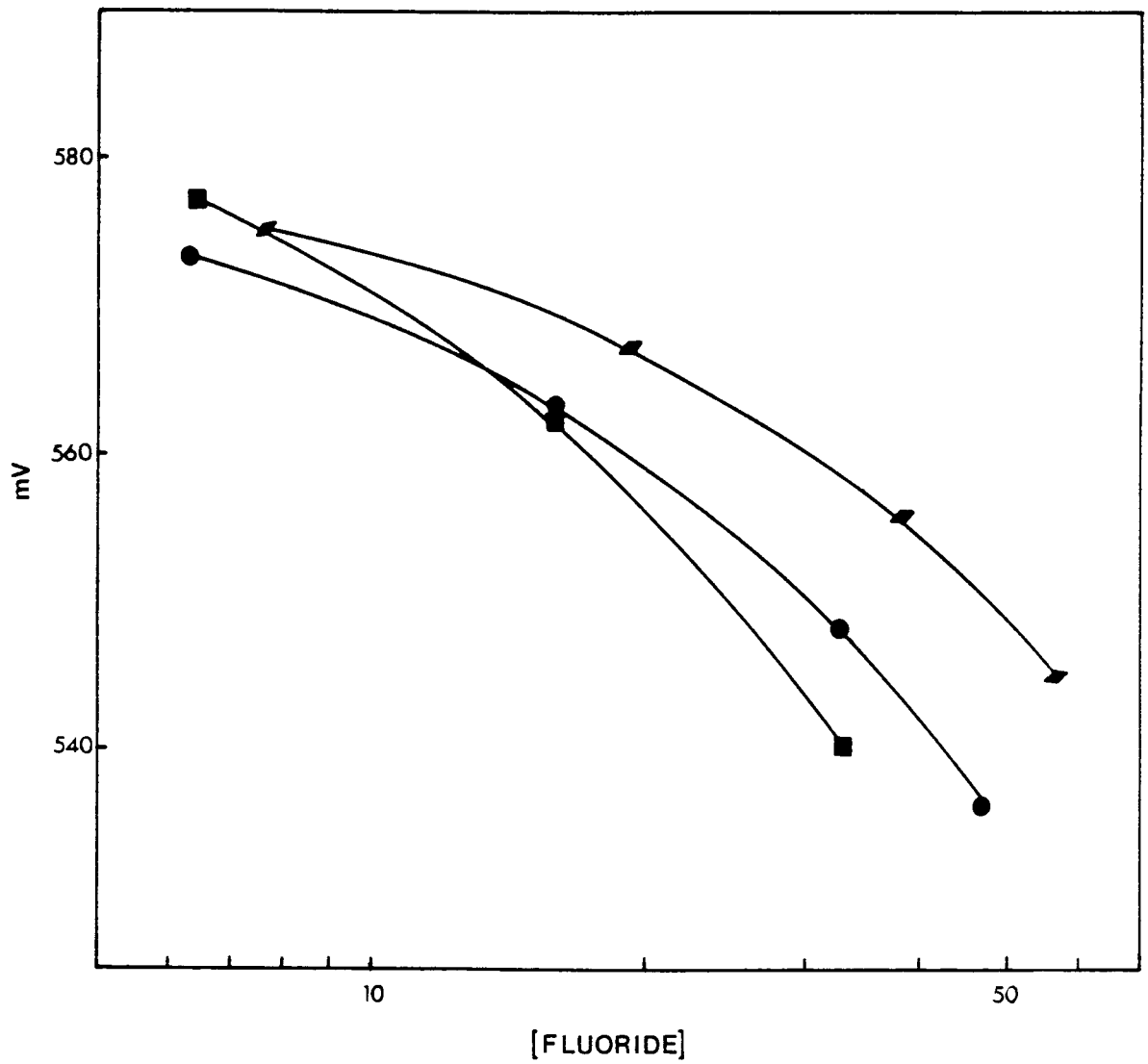

FIGURE 17 **Standard curves of fluoride concentration versus millivolt reading for sodium fluoride (●) and trifluoroacetaldehyde (◢) added to rat hepatic microsomes and taken through the modified sodium fusion assay (Method B, Figure 11), and for sodium fluoride in neutralising solution (■) added to TISAB IV (Section 2.2.2.6).**

Fluoride concentration, μM on a logarithmic scale.

the recovery of fluoride ion from hepatic microsomes was different for trifluoroacetaldehyde and sodium fluoride using this technique. Since quantitation of fluoride was necessary when both trifluoroacetaldehyde and fluoride ion were present, a single standard curve, viz: that for fluoride ion (sodium fluoride) which was added to rat hepatic microsomes and taken through the sodium fusion assay (Method B, Figure 11), was utilised. Both Method B (Figure 11), in which trifluoroacetaldehyde was converted to a non-volatile phenylhydrazone, and Method C, in which trifluoroacetaldehyde was bound to cellular macromolecules, were applied to hepatic microsomes from phenobarbital-pretreated rats, following incubation with isoflurane (16 mM), EDTA and NADPH-generating system. The yields of non-volatile organic fluoride were significantly ($P<0.01$) greater than the fluoride ion measured, or total non-volatile fluoride measured by Method A in which trifluoroacetic acid and not trifluoroacetaldehyde was recovered as a non-volatile metabolite (Table 19).

The results of measurement of total fluorinated metabolites from isoflurane in rat and human hepatic microsomes suggested that in human hepatic microsomes from two transplant donors, isoflurane was converted to fluoride ion and trifluoroacetic acid. In contrast, in hepatic microsomes from phenobarbital-pretreated rats, isoflurane was converted to fluoride ion and trifluoroacetaldehyde. Furthermore, the trifluoroacetaldehyde produced from isoflurane in rat hepatic microsomes appears to bind tightly to microsomal macromolecules, presumably as a Schiff base.

3.1.7 Oxidation of Trifluoroacetaldehyde by Rat and Human Hepatic Cytosol

Rat liver cytosol from phenobarbital pretreated animals in the presence of NADH (7.5 mM) and nicotinamide (1 mM) did not measurably convert trifluoroacetaldehyde (1.6 mM) to trifluoroacetic acid (limit of detection 15 nmol/ml/30 min), i.e. no trifluoroacetic acid was detected visually from the reaction mixtures following extraction and TLC. Similarly, post-microsomal supernatants from human liver 2 and 3 did not measurably convert trifluoroacetaldehyde to trifluoroacetic acid but that from human liver 1 did: trifluoroacetaldehyde was visually detected following extraction and TLC.

3.2 THE INTERACTION OF ISOFLURANE WITH RAT HEPATIC MICROSOMAL CYANIDE-SENSITIVE FACTORS

The interaction of isoflurane with the cyanide-sensitive factors was investigated by assessing the activity of these factors in two different ways:

i) indirectly, by measuring the increased flow of electrons to the cyanide-sensitive factors. This is achieved by measuring the increased rate of reoxidation of cytochrome b_5, an essential component of the fatty acid desaturase electron transport pathway (239,240), as shown in the following reaction:

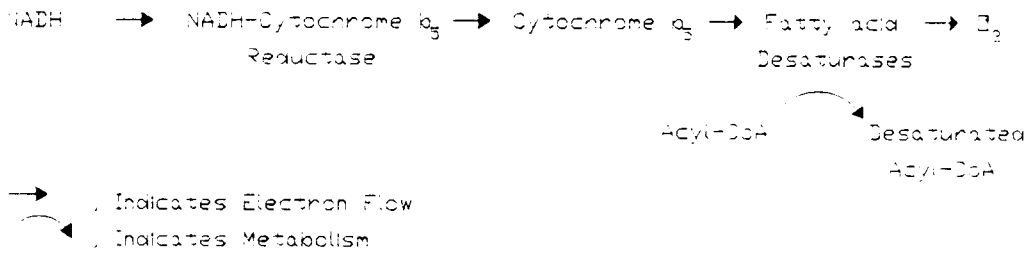

The ability of cyanide to inhibit the observed increased rate of reoxidation of cytochrome b_5 mediated by a compound, indicates metabolism by (or interaction of the compound with) the cyanide-sensitive factors and not with the enzymes of other pathways which also utlilise electron transfer from cytochrome b_5 (Figure 2), but are unaffected by low concentrations of cyanide.

ii) directly, by measuring the effect of isoflurane on fatty acid desaturase activity.

First, it was necessary to establish assay methods for the Δ6-desaturase and some of the other fatty acid desaturases in our laboratory.

3.2.1 Assay for Rat Hepatic Microsomal Δ6-Desaturase Activity

The activity of the Δ6-desaturase was measured in reaction mixtures where the substrate was added as linoleic acid together with an acyl-CoA generating system (Section 2.2.3.2a). After the reaction, the microsomal lipids were saponified. This releases linoleate (substrate) and γ-linolenate (product) from acyl-CoA and lipid derivatives formed concommitant with the Δ6-desaturation of linoleic acid in hepatic microsomes. Under these conditions, the fatty acid desaturase assay described here, and assays reported elsewhere (see e.g. 267-270) measured a composite of reactions, which is illustrated in a simplified form as follows (see also Figure 7):

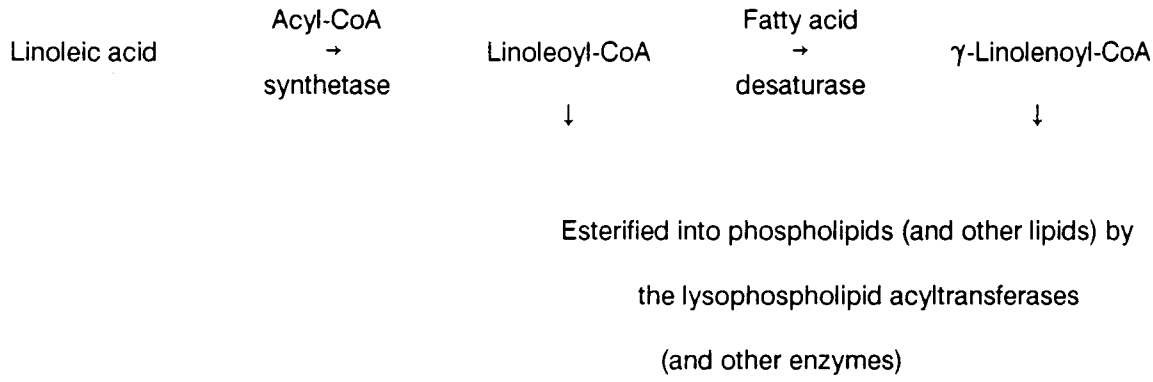

Two different methods of assay were used to measure directly the activity of the hepatic microsomal Δ6-desaturase.

3.2.1.1 Method 1 (Table 9)

This method was based on that reported by Mahfouz (297) with one modification: the fatty acid carriers were added as the free fatty acids immediately upon termination of the reaction in contrast to the reported method, where the carriers were the fatty acyl methyl esters which were added after extraction and methylation, and immediately prior to separation by TLC (297).

Separation of the methyl esters of the fatty acid substrate and product of the Δ6-desaturation of linoleic acid by Method 1 resulted in five UV-detectable spots (Table 20). Two of the five had R_f values corresponded to authentic standards of methyl linoleate and methyl γ-linolenate which chromatographed as single spots. The other three spots remained unidentified. Linoleic acid and γ-linolenic acid, added to hepatic microsomes and taken through the methylation and saponification procedures, also gave rise to five UV-detectable spots. These five spots were always present and had similar R_f values, irrespective of whether the TLC was run on Merck glass-backed or aluminium-backed silica gel plates, or glass-backed plates prepared in our laboratory from a slurry of silica gel H (Section 2.2.3.2b). Therefore, the five UV-detectable spots appeared to result from the methylation and saponification procedures, rather than the argentation TLC. Had the fatty acid carriers been added as the corresponding methyl esters just prior to the TLC, as in the reported method (297), it is possible that only the two spots corresponding to methyl linoleate and methyl γ-linolenate would have been detected visually under UV irradiation.

TABLE 20

THE DISTRIBUTION OF RADIOACTIVITY IN THE UV-DETECTABLE SPOTS FOLLOWING TLC OF THE METHYL ESTERS OF THE SUBSTRATE AND PRODUCT OF THE Δ6-DESATURATION OF LINOLEIC ACID

UV-Detectable Spot	R_f Value	Radioactivity * (% of total radioactivity recovered †)
Unknown 1	0.77	4.6 ± 1.7 (9)
Methyl linoleate	0.58	79.2 ± 2.4 (9)
Methyl γ-linolenate	0.49	12.8 ± 3.2 (9)
Unknown 2	0.20	2.5 ± 0.9 (9)
Unknown 3	0.03	0.2 ± 0.2 (9)

* Values were taken from four different preparations of microsomes. The distribution of radioactivity between methyl linoleate and methyl γ-linolenate varied depending on (a) whether the reaction mixture was a zero time or incubated sample, and (b) incubation conditions, e.g. time, protein concentration. The data presented here are from reaction mixtures containing 0.5 mg protein/ml, corrected substrate concentration of 4.7 μM linoleic acid, and were incubated for 10 min.

† Of the radioactivity applied to the plates, 90 ± 1 % was recovered. The distribution of the radioactivity in the spots is expressed as a percentage of the recovered radioactivity.

Of the radioactivity applied to the TLC plates, 90 ± 1% was recovered in the five UV-detectable spots. Of the recovered radioactivity, > 90% was in the spots corresponding to methyl linoleate and methyl γ-linolenate (Table 20). The distribution of radioactivity among the unidentified spots remained constant during the course of several experiments, and did not vary between zero-time and incubated reaction mixtures (Table 20). Therefore, we did not count the three extraneous spots and used only data from the methyl linoleate and methyl γ-linolenate spots in our calculations. This method for the Δ6-desaturase activity was used for some of the results presented herein; it is referred to as Method 1.

3.2.1.2 Method 2 (Table 9)

In Method 2, the step in Method 1 thought to give rise to the multiple spots following separation of the substrate and product, was eliminated, i.e., methylation of the fatty acids. The substrates and products of the reaction were separated as free fatty acids by HPLC. A chromatogram illustrating the separation of the fatty acid substrate and product of the Δ6-desaturation of linoleic acid by HPLC is illustrated in Figure 18. Of the radioactivity applied to the column, 100 ± 2% was recovered in fractions which eluted at times corresponding to those of authentic standards of linoleic acid and γ-linolenic acid. This HPLC method was extended to measure the Δ6-desaturation of α-linolenic and the Δ5-desaturation of eicosa-8,11,14-trienoic acid. Chromatograms illustrating the separation of the substrates and products by HPLC for the last two reactions are also shown in Figure 18. The product of the Δ6-desaturation of α-linolenic acid, octadeca-6,9,12,15-tetraenoic acid, was not available commercially, and it was therefore only detected radiochemically (Figure 18).

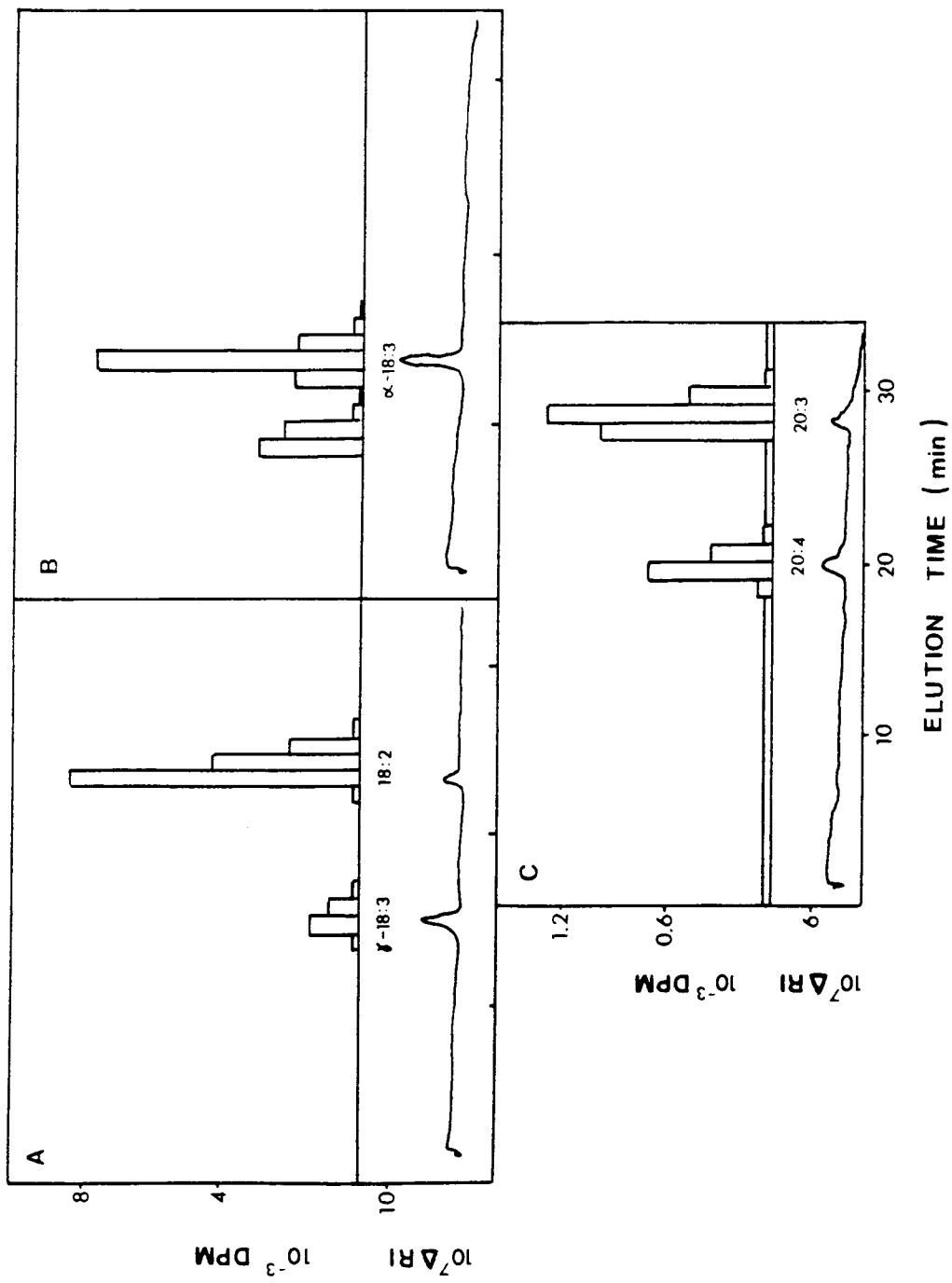

FIGURE 18 **Chromatograms illustrating the separation by HPLC on the Zorbax ODS column of extracts of reaction mixtures of the Δ6-desaturation of linoleic acid (A), Δ6-desaturation of α-linolenic acid (B) and the Δ5-desaturation of eicosa-8,11,14-trienoic acid (C).**

The substrates (18:2, α-18:3 and 20:3) and products (γ-18:3, 18:4 and 20:4) were detected radiochemically (dpm) and by change in refractive index (ΔRI), with the exception of 18:4, which was only detected radiochemically.

For the Δ6-desaturation of α-linolenic acid, 100 ± 2% of the radioactivity applied to the column was recovered in two fractions: one eluted at a time corresponding to that of an authentic standard of α-linolenic acid and the other, which remained unidentified, was assumed to be octadeca-6,19,12,15-tetraenoic acid. For the Δ5-desaturation of eicosa-8,11,14-trienoic acid, only ca. 90% of the radioactivity was recovered in fractions corresponding to authentic standards of the substrate and product, a low recovery compared to the recovery for the Δ6-desaturase assays by this method. Since both the substrate and product of the Δ5-desaturation of eicosa-8,11,14-trienoic acid are substrates for cyclo-oxygenase (Figure 10), we investigated whether the low recovery of radioactivity following Δ5-desaturation of eicosa-8,11,14-trienoic acid could be accounted for by the formation of eicosanoids. No further radioactivity was found in any other fractions. The following percentage recoveries, 94 ± 5% (n=3), 92 ± 0% (n=2) and 85 ± 4% (n=3) were calculated for zero time reaction mixtures, full reaction mixtures incubated for 10 min with and without NADH, respectively. Subsequently, the recovery of [2-^{14}C] eicosa-8,11,14-trienoic acid from the HPLC column (Spherisorb ODS) was found to be 90 ± 2% (n=3), indicating that impurities in the substrate, rather than deficiencies in the chromatographic procedure resulted in the relatively low recovery of the radioactivity for the Δ5-desaturase assay.

The chromatograms illustrated in Figure 18 were obtained after HPLC separation of the substrates and products of the Δ6- and Δ5-desaturases using a Zorbax ODS HPLC column (Section 2.2.3.2c). During the course of approximately five hundred chromatographic separations, the elution times gradually became shorter. Ultimately, separation of the substrate and product

of the Δ6-desaturation of α-linolenic acid was no longer achievable. The Zorbax ODS column could be replaced by a Spherisorb ODS column for assay of the Δ6-desaturation of linoleic acid and Δ5-desaturation of eicosa-8,11,14-trienoic acid. On the latter column, elution times for linoleic acid and γ-linolenic acid were 14 to 17 min and 10 to 12 min, respectively, and for eicosa-8,11,14-trienoic acid and arachidonic acid were 14 to 17 min and 10 to 12 min, respectively. The substrate and product of the Δ6-desaturation of α-linolenic acid were not fully resolved using the Spherisorb ODS column (elution times of 7 to 12 min and 6 to 8 min for substrate and product, respectively). Consequently, a Zorbax Golden Series column was used to assay the Δ6-desaturation of α-linolenic acid. Although initial studies of the Δ6-desaturation of linoleic acid and Δ5-desaturation of eicosa-8,11,14-trienoic acid in hepatic microsomes were performed using the Zorbax ODS column, the bulk of the assays were conducted using the Spherisorb ODS column.

The effects of microsomal protein concentration and time on the activity of the Δ6-desaturation of linoleic acid as measured by Method 1, are shown in Figure 19, and on Δ6- and Δ5-desaturase activities measured by Method 2, in Figures 20, 21 and 22. For the Δ6-desaturase, the rate of product formation was linear up to a protein concentration of 0.5 mg microsomal protein/ml for both substrates; for the Δ5-desaturase, the rate of product formation was linear up to a protein concentration of 0.25 mg microsomal protein/ml (Figures 20, 21 and 22). The Δ6-desaturase activity with linoleic acid as substrate was linear over a period of 10 min, but when α-linolenic acid was the substrate, the rate of product formation was linear for only 7 min (Figures 20 and 21). The Δ5-desaturase activity was linear over a time period of 14 min (Figure 22). The effects of time and protein on the Δ6-desaturation of

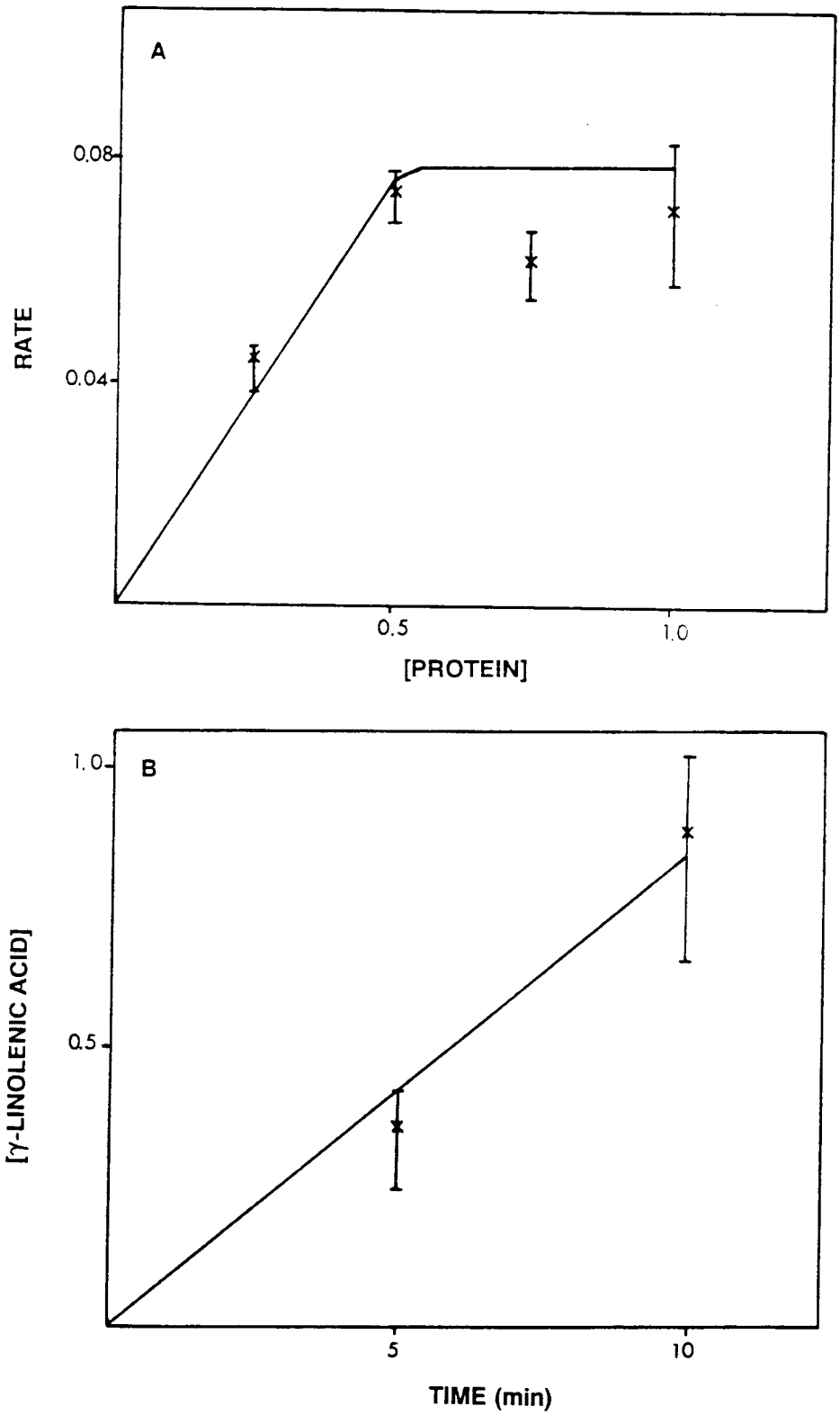

FIGURE 19 **The effect of microsomal protein concentration (A) and time (B) on the Δ6-desaturation of linoleic acid measured using Method 1.**

Protein concentration, mg microsomal protein/ml reaction mixture (Section 2.2.3.2a); rate, μM γ-linolenic acid produced/min; γ-linolenic acid concentration, μM. Corrected substrate concentration was 4.7 μM. BSA concentration was 11.5 μg/μg linoleic acid added. Results are from a single preparation of hepatic microsomes, but are typical of those from three preparations.

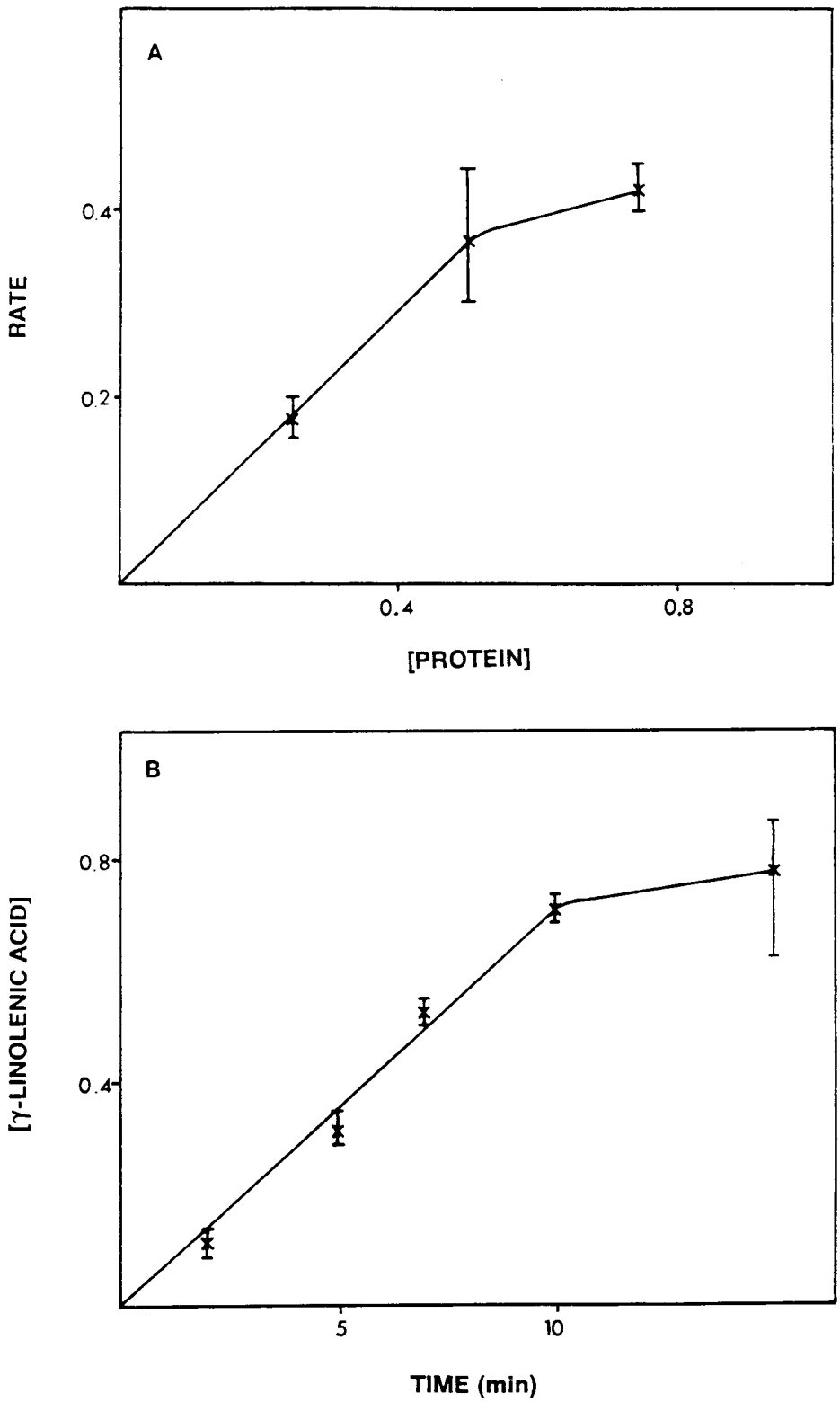

FIGURE 20 **The effect of microsomal protein concentration (A) and time (B) on the Δ6-desaturation of linoleic acid measured using Method 2.**

Protein concentration, mg microsomal protein/ml reaction mixture (Section 2.2.3.2a); rate, μM γ-linolenic acid produced/min; γ-linolenic acid concentration, μM. Corrected substrate concentration was 4.7 μM. BSA concentration was 115 μg/μg linoleic acid added. Results are from a single preparation of hepatic microsomes, but are typical of those from three preparations.

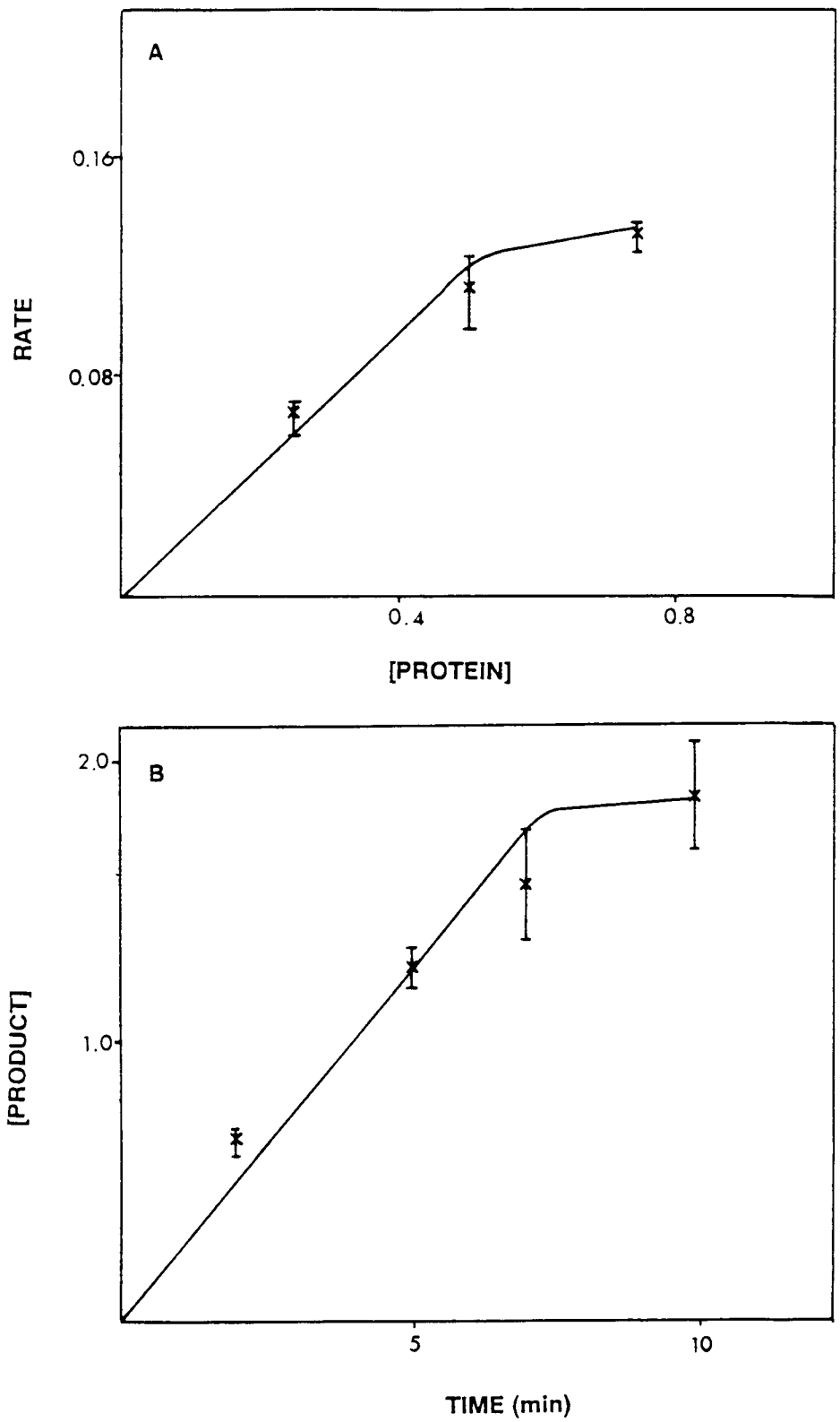

FIGURE 21 **The effect of microsomal protein concentration (A) and time (B) on the Δ6-desaturation of α-linolenic acid measured using Method 2.**

Protein concentration, mg microsomal protein/ml reaction mixture (Section 2.2.3.2a); rate, μM octadeca-6,9,12,15-tetraenoic acid produced/min; product concentration, μM octadeca-6,9,12,15-tetraenoic acid. Corrected substrate concentration was 2.1 μM. BSA concentration was 115 μg/μg linoleic acid added. Results are from a single preparation of hepatic microsomes, but are typical of those from three preparations.

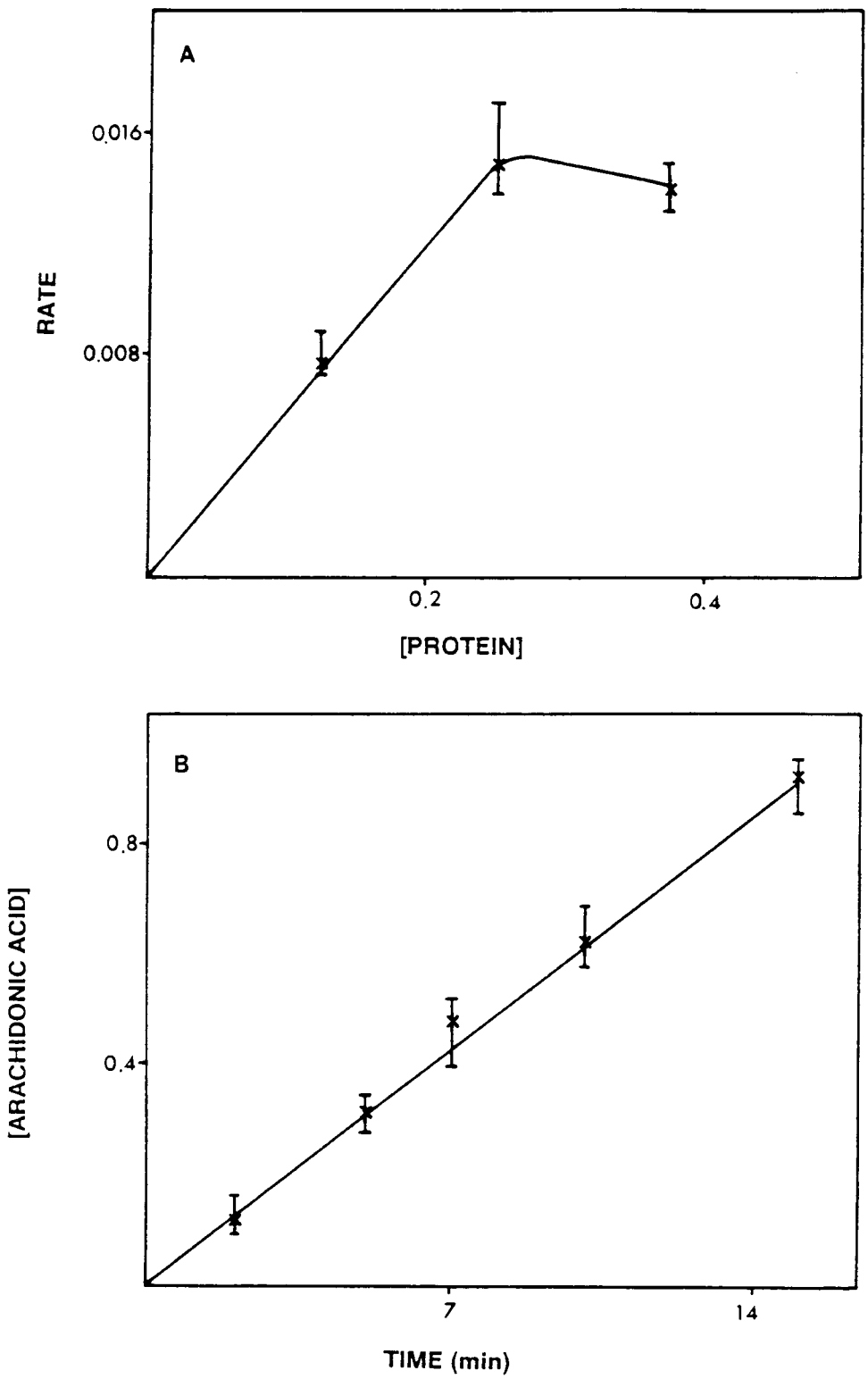

FIGURE 22 **The effect of microsomal protein concentration (A) and time (B) on the Δ5-desaturation of eicosa-8,11,14-trienoic acid measured using Method 2**

Protein concentration, mg microsomal protein/ml reaction mixture (Section 2.2.3.2a); rate, μM arachidonic acid produced/min; arachidonic acid concentration, μM. Corrected substrate concentration was 0.75 μM. BSA concentration was 115 μg/μg linoleic acid added. Results are from a single preparation of hepatic microsomes, but are typical of those from three preparations.

linoleic acid were identical for measurement of the Δ6-desaturase activity by the Methods 1 and 2 (compare Figures 19 and 20).

As previously reported (237), the Δ5- and Δ6-desaturase activities in hepatic microsomes required NADH (Table 21). In the absence of NADH, the activities were relatively low compared to those observed in the presence of NADH, especially for the Δ6-desaturase, where rates were ≤ 5% in the absence of NADH (Table 21). Interestingly, ca. 15% activity was observed for the Δ5-desaturase in the absence of added NADH (Table 21). This result may have been an artifact or may represent the presence of a suitable endogenous electron donor for the Δ5-desaturase in hepatic microsomes.

Although the results of the measurement of the Δ6-desaturase activity appeared to be comparable whether measured by Method 1 (TLC) or Method 2 (HPLC), the results from Method 2 were more reproducible. This is demonstrated by a comparison of the coefficients of variation of the two methods. For the analysis of a single reaction mixture for the Δ6-desaturation of linoleic acid, the coefficient of variation was 3.5% (n=6) for Method 1 and 0.3% (n=5) for Method 2. Consequently, Method 2 was the preferred method for analysis, especially as the activity of the Δ6-desaturase was low.

During the course of our experiments, we became aware that endogenous free fatty acids are present in significant concentrations in hepatic microsomes (see e.g. 397). From results in our laboratory, the levels of free fatty acid substrates for the fatty acid desaturases were found to be sufficiently plentiful to affect the calculation of fatty acid desaturase activity by diluting out the specific activity of the radiolabelled substrate (see the following sections).

TABLE 21

THE EFFECT OF NADH ON FATTY ACID DESATURASE ACTIVITY IN HEPATIC MICROSOMES FROM RATS FED A NORMAL DIET

Reaction	Substrate * Added (μM)	Activity † (pmol/mg protein/min.)	
		- NADH	+ NADH (2.6 mM)
Δ6-Desaturation	Linoleic acid (1.8)	9.1 ± 0.5	202.0 ± 19.1
Δ6-Desaturation	α-Linolenic acid (1.8)	4.1 ± 5.1	92.9 ± 8.6
Δ5-Desaturation	Eicosa - 8, 11, 14 - trienoic acid (0.3)	16.8 ± 5.3	109 ± 5.3

* Reaction mixtures contained hepatic microsomes (0.5 mg protein/ml for the Δ6-desaturase, and 0.25 mg protein/ml for the Δ5-desaturase) and BSA (115 μg/μg free fatty acid substrate added). Incubations were for 10 min (for the Δ6-desaturation of linoleic acid and the Δ5-desaturation of eicosa-8,11,14-trienoic acid) or 7 min (Δ6-desaturation of α-linolenic acid) and assayed using Method 2. Corrected substrate concentrations were linoleic acid, 4.7 μM; α-linolenic acid, 2.1 μM; eicosa-8,11,14-trienoic acid, 0.75 μM. Other incubation conditions are given in the Methods. (Section 2.2.3.2a).

† Results were from a single preparation of hepatic microsomes (n=3), but were typical of results obtained on two or more microsomal preparations.

3.2.2. Fatty Acid Content of Rat Hepatic Microsomes

3.2.2.1. Analysis of the Fatty Acid Content of the Microsomal Membrane

In order to establish the technique for fatty acid analysis in our laboratory, I initially measured the total fatty acid content of the microsomal membrane, including free fatty acid plus fatty acid covalently bound in microsomal lipids. Alkaline saponification of the microsomal membrane was used to hydrolyse the fatty acids from lipids; the resulting fatty acids were extracted, methylated and analysed by gas chromatography. A typical chromatogram illustrating the separation of the fatty acids of the microsomal membrane by gas chromatography is shown in Figure 23. The major fatty acids found in these membranes were quantitated and are listed in Table 22, together with their microsomal concentrations. Palmitic acid was also identified as one of the main fatty acid components of the microsomal membrane, but was not quantitated. Other unidentified fatty acids occurred in small amounts (Figure 23). There was a variation in the fatty acid content of the microsomal membrane from microsomal preparation to preparation. This was noticable especially for arachidonic acid, the level of which has been reported to be related to changes in daily dietary intake (197,206). These differences in the fatty acid content of the microsomal membrane may have influenced the activity of the Δ6-desaturase (206). Whatever the cause, the observed daily variation in Δ6-desaturase activity was substantial and has affected the way in which the results are presented herein, viz: the results obtained on more than one day could not always be averaged because of differing Δ6-desaturase activity of the microsomal preparation. For example, the Δ6-desaturase activities in

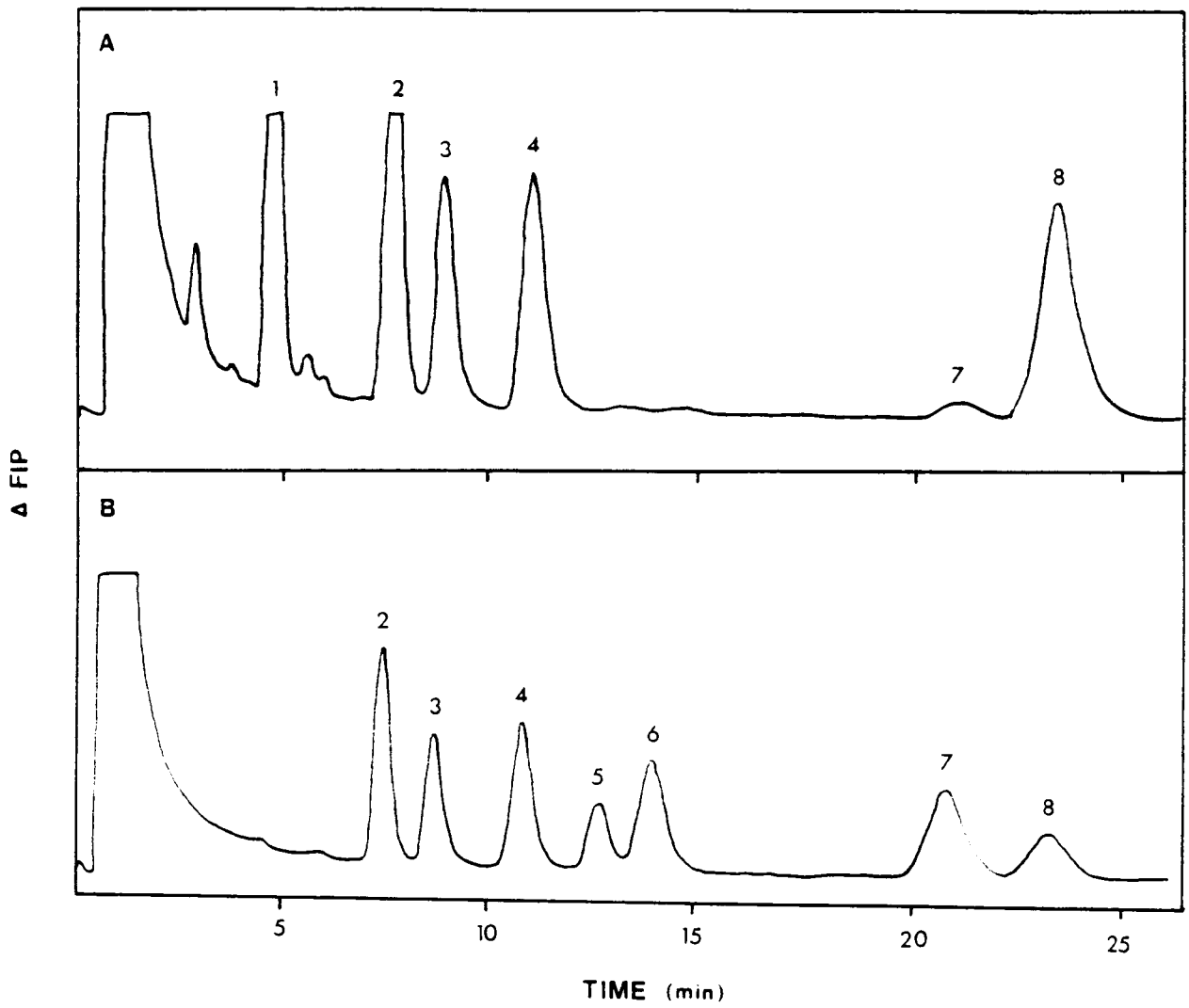

FIGURE 23 **Chromatogram illustrating the separation by gas chromatography of (A) the methyl esters of the fatty acids of hepatic microsomal membranes and (B) a mixture of fatty acid methyl ester standards.**

The fatty acids were detected by the change in flame ionisation potential (ΔFIP). Fatty acid peaks were identified as follows: 1: palmitic acid, 2: stearic acid, 3: oleic acid, 4: linoleic acid, 5: α-linolenic acid, 6: γ-linolenic acid, 7: eicosa-8,11,14-trienoic acid and 8: arachidonic acid.

TABLE 22

ANALYSIS OF THE TOTAL FATTY ACIDS CONTENT OF A PORTION OF THE RAT HEPATIC MICROSOMAL MEMBRANE

Fatty Acid	Fatty Acid Concentration (μM)*		
	Experiment 1	Experiment 2	Experiment 3
Stearic acid	76 ± 18 (3)	92 ± 21 (8)	148 ± 68 (7)
Oleic acid	63 ± 46 (5)	73 ± 14 (3)	54 ± 6 (2)
Linoleic acid	49 ± 8 (6)	59 ± 10 (10)	78 ± 27 (10)
Eicosa - 8, 11, 14 - trienoic acid	5.1 ± 2.1 (6)	9.7 ± 4 (6)	6.7 ± 3 (6)
Arachidonic acid	616 ± 84 (3)	85 ± 9 (5)	154 ± 55 (9)
γ-Linolenic acid	ND	ND	ND
α-Linolenic acid	ND	ND	ND

* In hepatic microsomes at a concentration of 0.5 mg microsomal protein/ml. Total fatty acid concentration includes free fatty acids plus those esterified into lipids. Each experiment used a different preparation of hepatic microsomes from identically treated rats.

ND = Not detected.

experiments 1 and 2 shown in Table 28 differed by a factor of 2 in the absence isoflurane. This extent of variability was typical of Δ6-desaturase activity in the absence of inhibitors. Therefore, the results of desaturase assays on a single, but representative microsomal preparation, are often reported. This data is generally supported by similar results on one or more other microsomal preparations.

3.2.2.2. Analysis of the Free Fatty Acid Content of the Microsomal Membrane

In contrast to the previous section (3.2.2.1), the fatty acids measured in this section were not esterified into lipids, but were non-covalently bound to the microsomal membrane and were, therefore, a potential source of endogenous fatty acid substrate for the fatty acid-metabolising enzymes including the fatty acid desaturases. These free fatty acids were extracted from microsomes (without saponification), separated from the phospholipids by TLC, methylated and then analysed by gas chromatography (Sections 2.2.3.4 and 2.2.3.6). A typical chromatogram illustrating the gas chromatographic separation of extracted microsomal fatty acid methyl esters is shown in Figure 24. Also shown is the chromatogram for fatty acid methyl ester standards (Figure 24 B). Quantitation of the microsomal free fatty acids on two to three microsomal preparations is shown in Table 23. It can be seen that linoleic acid, one of the substrates for the Δ6-desaturase, was present in amounts comparable with added linoleate concentrations used in the assay of the Δ6-desaturase (0.45 - 10.9 μM) (Table 23). The amount of free linoleic acid did not vary significantly ($P>0.1$) in three different preparations of hepatic microsomes. Similarly, the amount of free α-linolenic acid, another substrate for the Δ6-desaturase, and

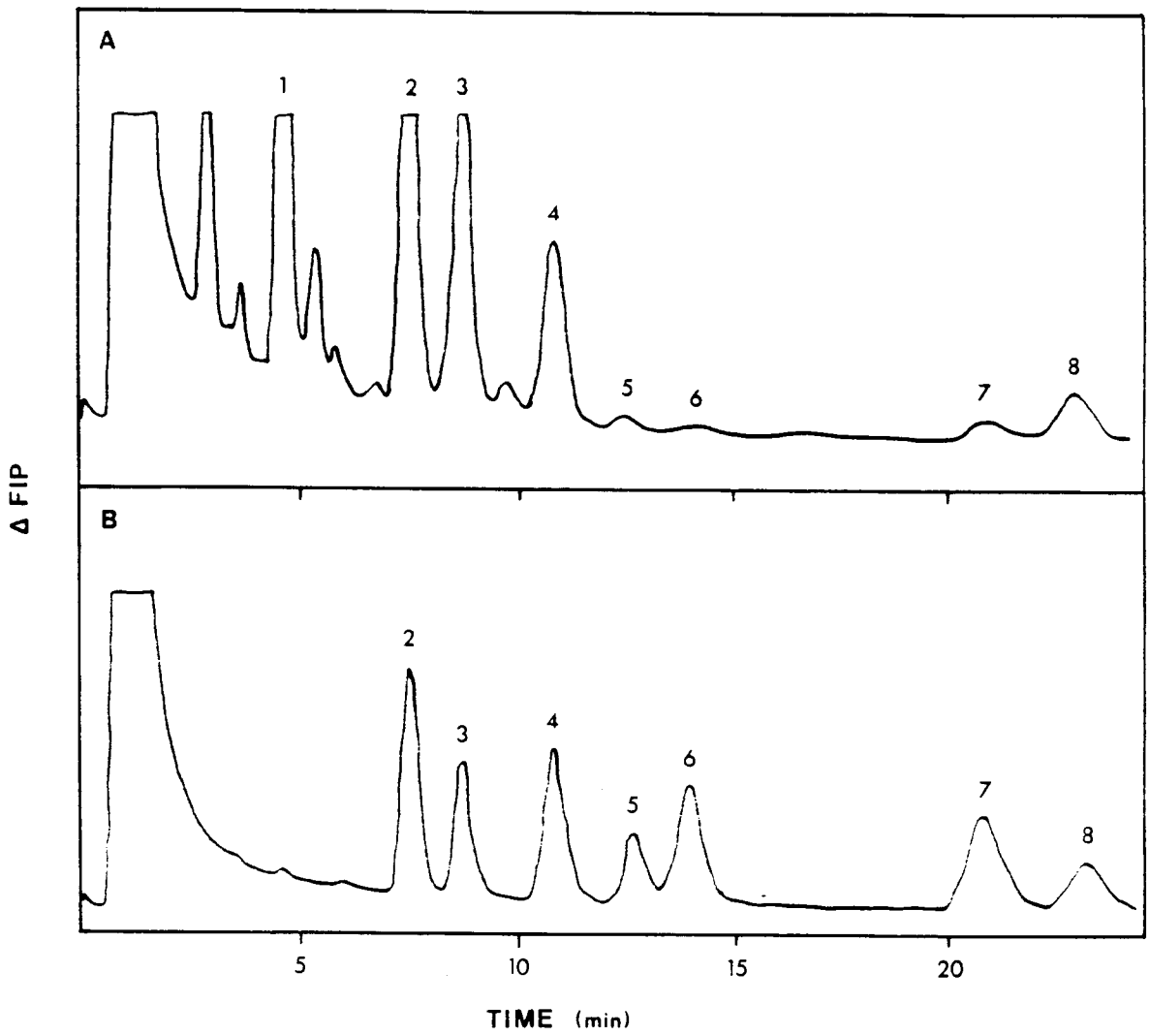

FIGURE 24 **Chromatogram illustrating the separation by gas chromatography of (A) the methyl esters of free fatty acids extracted from hepatic microsomes and (B) a mixture of fatty acid methyl ester standards.**

The fatty acids were detected by the change in flame ionization potential (ΔFIP). Fatty acid peaks were identified as follows: 1: palmitic acid, 2: stearic acid, 3: oleic acid, 4: linoleic acid, 5: α-linolenic acid, 6: γ-linolenic acid, 7: eicosa-8,11,14-trienoic acid and 8: arachidonic acid.

TABLE 23

ANALYSIS OF THE FREE FATTY ACID CONTENT OF RAT HEPATIC MICROSOMES

Fatty Acid	Free Fatty Acid Concentration (μM) *		
	Experiment 1	Experiment 2	Experiment 3
Linoleic acid	2.9 ± 0.8 (4)	3.1 ± 1.3 (6)	2.9 ± 0.9 (8)
α-Linolenic acid	0.6 ± 0.4 (3)	0.4 ± 0.3 (3)	
γ-Linolenic acid	0.4 ± 0.1 (4)	0.7 ± 0.3 (2)	0.5 ± 0.1 (3)
Eicosa - 8, 11, 14 - trienoic acid	0.4 ± 0.9 (4)	0.5 ± 0.1 (4)	
Arachidonic acid	2.0 ± 0.9 (4)	0.8 ± 0.1 (2)	

* In hepatic microsomes at a concentration of 0.5 mg microsomal protein/ml. Each experiment used a different preparation of hepatic microsomes from identically treated rats.

eicosa-8,11,14-trienoic acid, a substrate for the Δ5-desaturase, showed no significant variation in two preparations of hepatic microsomes ($P > 0.1$) (Table 23). The concentrations of these fatty acids in hepatic microsomes were considerably lower than the free linoleic acid present (Table 23). Of the free fatty acids quantitated, only γ-linolenic acid and arachidonic acid showed significant daily variation ($P < 0.01$) (Table 23).

The impact of endogenous substrate on the accurate calculation of enzymic reaction rates has been demonstrated clearly and elegantly by Segel (376). Therefore, as indicated in the Methods (Section 2.2.3.9), we have corrected the fatty acid desaturase, acyl-CoA synthetase and lysophospholipid acyltransferase activities for endogenous fatty acid concentrations. The effect of dilution of the added radiolabelled fatty acid substrate with endogenous unlabelled fatty acid on fatty acid desaturase activity is illustrated in Figure 25. Two different reaction rate versus substrate concentration curves were obtained for the Δ6-desaturase when the results were or were not corrected for endogenous substrate concentrations (Figure 25). The corresponding Lineweaver-Burk plots for these curves showed the substantial effect of correcting for endogenous substrate in calculation of enzyme activity on the apparent K_m value for the enzyme (Figure 25).

As a consequence of this striking effect of endogenous substrate levels on apparent fatty acid desaturase activity, all reaction rates and substrate concentrations for the fatty acid desaturases are reported as corrected values. To our knowledge no other investigators have corrected fatty acid desaturase activity measured with hepatic microsomes for endogenous substrate levels (266-270). The Δ5-desaturase activity is reported at a single substrate

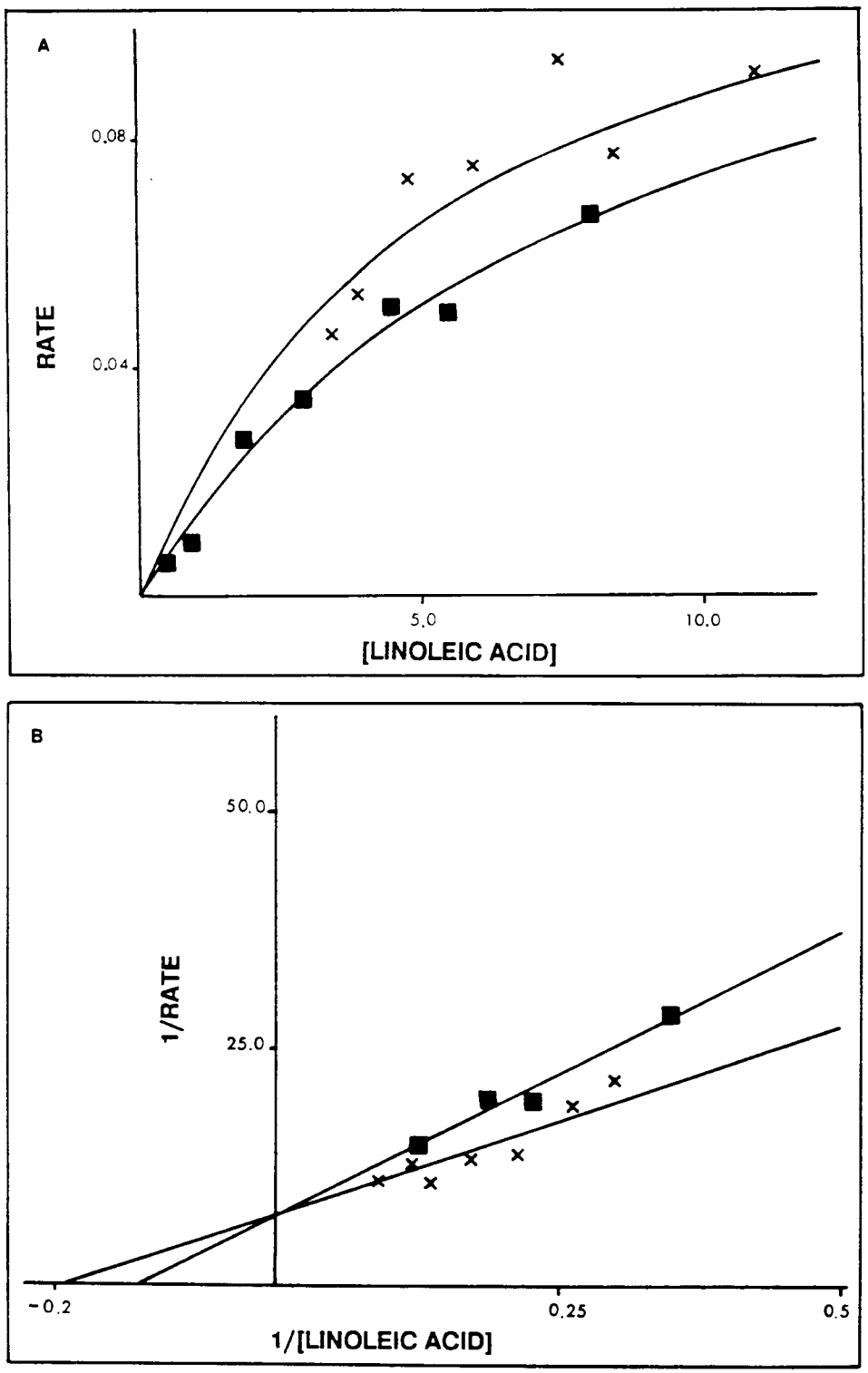

FIGURE 25 **The effect of correcting for endogenous substrate on the rate versus substrate concentration curve (A) and Lineweaver-Burk plot (B) for the Δ6-desaturation of linoleic acid in rat hepatic microsomes. Rate was calculated from the concentration of added + endogenous substrate (corrected) (X), and added substrate (uncorrected) (■). Substrate concentration is that of added + endogenous substrate for corrected data (X) and added substrate for uncorrected data (■)**

Rate, μM [1^{-14}C] γ-linolenoyl-CoA + [1^{-14}C] 2-γ-linolenoyl-phospholipid formed/min; linoleic acid concentration, μM linoleic acid. BSA concentration was 115 μg/μg linoleic acid added. Δ6-Desaturase activity was measured using Method 2. Curves and lines were drawn by Enzfitter (Section 2.2.3.10)

concentration and is corrected for endogenous substrate. For the Δ6-desaturation of α-linolenic acid, both reaction rates and substrate concentrations are reported as corrected values. The Δ9-desaturase activity was determined using stearoyl-CoA as substrate so there was no need to correct for endogenous stearic acid levels.

Since the same substrates and incubation conditions were used for measurement of acyl-CoA synthetase and lysophospholipid acyltransferase activities in hepatic microsomes, these rates were also corrected for endogenous fatty acid levels and are reported in this way. For the lysophospholipid acyltransferase, acyl-CoA is usually used as substrate (371), so activities reported in the literature do not correct for endogenous substrate. For a single report on activity of the acyl-CoA synthetase, the presence of endogenous fatty acids in hepatic microsomes was acknowledged, and the microsomes were treated in such a way as to remove these fatty acids (386). Besides this report, to our knowledge no other studied of the activity of the acyl-CoA synthetase in hepatic microsomes corrected for endogenous substrate.

3.2.3 The Effect of Isoflurane on Indirect Assay for Fatty Acid Desaturase Activity in Rat Hepatic Microsomes

Using the indirect method of assessment of activity of the fatty acid desaturases (the reoxidation of cytochrome b_5), isoflurane was shown to interact with one or more of these enzymes: isoflurane significantly increased the pseudo first order rate constant for the re-oxidation of cytochrome b_5 ($P<0.01$) in hepatic microsomes from rats fed a high-carbohydrate diet (Table 24); potassium

TABLE 24

THE EFFECT OF CYANIDE ON THE ISOFLURANE-STIMULATED RE-OXIDATION OF CYTOCHROME b_5 IN HEPATIC MICROSOMES FROM RATS FED A HIGH-CARBOHYDRATE DIET

Additions to Reaction Mixture*	Pseudo First Order Rate Constant for the Re-oxidation of Cytochrome b_5 (x 10^{-2} sec^{-1})
None	1.30 ± 0.06 (2)
KCN (0.5 mM)	1.30 ± 0.01 (2)
Isoflurane (13.3 mM)	2.24 ± 0.38 (10) †
Isoflurane (13.3 mM) + KCN (0.5 mM)	1.32 ± 0.31 (5) §

* Reaction mixtures contained 3.0 ml hepatic microsomes (1.5 mg microsomes protein/ml 0.02 M Tris - HCL, pH 7.4) and NADH (2.5 μM).

† Differs significantly from the rate constant for no additions ($P < 0.01$).

§ Differs significantly from the rate constant in the presence of isoflurane alone ($P < 0.01$).

cyanide significantly decreased the pseudo first order rate constant for re-oxidation of cytochrome b_5 in the presence of isoflurane ($P<0.01$), but did not affect the reoxidation of cytochrome b_5 in the absence of isoflurane (Table 24). Futher studies were aimed at investigating the effect of isoflurane on the fatty acid desaturases both indirectly, using the reoxidation of cytochrome b_5 as an index of fatty acid desaturase activity, and directly, measuring drug effects on the desaturation of fatty acid substrates.

3.2.3.1 The Effect of Diet and Isoflurane on the Indirect Assay for Fatty Acid Desaturase Activity

The effect of diet on microsomal desaturase activity, as assessed by cytochrome b_5 reoxidation, is given in Table 25. Stearoyl-CoA and linoleoyl-CoA were used as the substrates for the Δ9- and Δ6-desaturases, respectively, thus eliminating any interference from endogenous free fatty acid substrates. The high-carbohydrate diet was used to induce Δ9-desaturase activity (314). The induction of the Δ9-desaturase by a high-carbohydrate diet in our studies is confirmed by the significant increase in the pseudo first order rate constant for the re-oxidation of cytochrome b_5 in the presence of stearoyl-CoA in hepatic microsomes from rats fed on a high-carbohydrate diet, compared to that in hepatic microsomes from rats fed a normal diet ($P<0.01$) (Table 25). In contrast, the pseudo first order rate constants for the re-oxidation of cytochrome b_5 by linoleoyl-CoA in the hepatic microsomes from rats fed a normal diet and from rats fed a high-carbohydrate diet are similar ($P>0.1$) (Table 25). The pseudo first order rate constant for the re-oxidation of cytochrome b_5 in hepatic microsomes from rats fed a normal or a high-carbohydrate diet was increased significantly by isoflurane ($P<0.01$).

TABLE 25

THE EFFECT OF DIET ON THE STEAROYL-CoA, LINOLEOYL-CoA AND ISOFLURANE-STIMULATED RE-OXIDATION OF CYTOCHROME b_5 IN RAT HEPATIC MICROSOMES

Diet	Additions to Reaction Mixture*	Pseudo First Order Rate Constant for the Re-oxidation of Cytochrome b_5 (x 10^{-2} sec^{-1})
HCD	None	1.30 ± 0.16 (7)
Normal	None	1.50, 1.50 (2)
HCD	Stearoyl-CoA (12 μM)	6.87 ± 0.68 (4) †
Normal	Stearoyl-CoA (12 μM)	2.20, 2.42 (2) †
HCD	Linoleoyl-CoA (12 μM)	1.90, 2.20 (2) †
Normal	Linoleoyl-CoA (12 μM)	1.78, 1.80 (2) †
HCD	Isoflurane (13.3 mM)	2.24 ± 0.38 (10) †
Normal	Isoflurane (13.3 mM)	2.13 ± 0.12 (3) †

HCD, High-carbohydrate diet

* Reaction mixtures contained 3.0 ml hepatic microsomes (1.5 mg microsomes protein/ml 0.02 M Tris - HCl, pH 7.4) and NADH (2.5 μM).

† Differs significantly from that in absence of additions to reaction mixture for identical dietary pretreatment ($P<0.01$).

There was no difference in the effects of isoflurane in the microsomes from rats treated with the two diets in spite of the induction of the Δ9-desaturase by the high-carbohydrate diet ($P > 0.1$) (Table 25).

These results confirm that isoflurane stimulates electron transfer perhaps by interacting with a microsomal terminal oxidase. Since a high-carbohydrate diet did not increase the magnitude of the effect of isoflurane on cytochrome b_5 reoxidation (Table 25), isoflurane was probably not stimulating electron flow via the Δ9-desaturase. To obtain more conclusive evidence on which fatty acid desaturase(s) could be involved, the effect of isoflurane on the desaturation of fatty acid substrates by the Δ9-, Δ6- and Δ5-desaturases was studied.

3.2.3.2 The Effect of Isoflurane on the Hepatic Microsomal Δ9-Desaturation of Stearoyl-CoA

The effect of isoflurane on the activity of the Δ9-desaturase in hepatic microsomes from rats fed a high-carbohydrate diet, was investigated using electron donors NADH and NADPH. Isoflurane had no effect on the activity of the Δ9-desaturase when the desaturation of stearoyl-CoA was supported by NADH (Table 26). However, isoflurane did slightly, and probably significantly, diminish the activity of the Δ9-desaturase using NADPH as electron donor ($P < 0.05$) (Table 26). The small magnitude of this effect precluded further studies.

TABLE 26

THE EFFECT OF ISOFLURANE ON THE Δ9-DESATURATION OF STEAROYL-CoA IN HEPATIC MICROSOMES FROM RATS FED A HIGH-CARBOHYDRATE DIET

Additions* (mM)	Electron Donor	Activity of Δ9-Desaturase § (nmol oleate/mg protein/min.)
None	NADH	1.96 ± 0.08 (6)
Isoflurane (16)	NADH	1.96 ± 0.18 (6)
None	NADPH	2.05 ± 0.36 (6)
Isoflurane (16)	NADPH	1.66 ± 0.10 (6) †

* To reaction mixtures containing hepatic microsomes (0.5 mg/ml, 0.02 M Tris-HCl, pH 7.4), stearoyl-CoA (40 μM, 12 nCi) and NADH or NADPH (1 mM), incubated for 10 min at 30 °C.

† Significantly different from that in the absence of isoflurane ($P < 0.05$).

§ The substrate was added as stearoyl-CoA so there was no need to correct the activity for endogenous substrate (Section 2.2.3.9).

3.2.3.3 The Effect of Isoflurane on the Hepatic Microsomal Δ6-Desaturation of α-Linolenic Acid

Isoflurane had no effect on the Δ6-desaturation of α-linolenic acid in hepatic microsomes from rats fed a normal diet: in the presence of 1 mM isoflurane *, the rate of Δ6-desaturation of α-linolenic acid was 0.22 ± 0.03 nmol octadeca-6,9,12,15-tetraenoic acid produced/mg protein/min compared to 0.22 ± 0.01 nmol octadeca-6,9,12,15-tetraenoic acid produced/mg protein/ min in the absence of isoflurane. In these experiments, hepatic microsomes (0.5 mg protein/ml) were incubated with BSA (115 μg/μg α-linolenic acid added) and [1^{-14}C] α-linolenic acid (1.8 μM, 121 nCi) for 7 min as described in Section 2.2.3.2a. The corrected substrate concentration was 2.1 μM α-linolenic acid.

3.2.3.4 The Effect of Isoflurane on the Hepatic Microsomal Δ5-Desaturation of Eicosa-8,11,14-trienoic acid

The effect of isoflurane on the activity of the Δ5-desaturase in hepatic microsomes from rats fed a normal diet is shown in Table 27. At low concentrations (0.4 mM - 2.0 mM), isoflurane had no effect on Δ5-desaturase activity in hepatic microsomes. However, at the highest concentration used (8.0 mM), isoflurane decreased the activity of the Δ5-desaturase in hepatic microsomes slightly, and significantly ($P<0.05$) (Table 27).

* This concentration of isoflurane significantly inhibited the Δ6-desaturation of linoleic acid (Figure 26).

TABLE 27

THE EFFECT OF ISOFLURANE ON THE Δ5-DESATURATION OF EICOSA - 8, 11, 14 - TRIENOIC ACID IN RAT HEPATIC MICROSOMES

Isoflurane * Concentration (mM)	Activity of Δ5-Desaturase † (nmol arachidonic acid formed/mg protein/min)
0	97.1 ± 3.2
0.4	95.7 ± 6.9
2.0	103.2 ± 6.9
8.0	81.6 ± 4.8 §

* In reaction mixtures of hepatic microsomes (0.25 mg protein/ml) incubated as described in the methods (Section 2.2.3.2a) with BSA (115 μg/μg fatty acid substrate added), and [2-^{14}C]-eicosa-8,11,14-trienoic acid (0.3 μM, 3.6 nCi) for 10 min. The corrected substrate concentration was 0.75 μM.

† Results were from a single preparation of hepatic microsomes (n=3).

§ Significantly different from that in the absence of isoflurane ($P<0.05$).

3.2.3.5 The Effect of Isoflurane on Hepatic Microsomal Δ6-Desaturation of Linoleic acid

The effect of isoflurane on hepatic microsomal Δ6-desaturation of linoleic acid by two direct assay Methods is shown in Figure 26. Isoflurane was shown to inhibit the Δ6-desaturation of linoleic acid in a concentration-dependent manner. The inhibition was evident when either Method 1 or 2 was used to measure enzyme activity (Figure 26). The inhibition of the Δ6-desaturase activity by isoflurane was observed at low isoflurane concentrations; half-maximal inhibition of the Δ6-desaturase occurred at approximately 0.6 mM isoflurane (Figure 26).

Since cyanide completely inhibited the stimulation of the reoxidation of cytochrome b_5 by isoflurane at a concentration that inhibits fatty acid desaturase activity but not cytochrome P-450-dependent drug oxidations (235) (Table 24), electron flow to cytochrome P-450 appeared to play no direct role in the ability of isoflurane to stimulate microsomal electron transfer. However, it was not clear whether the cytochrome P-450-dependent metabolism of isoflurane could have resulted in products which affected the Δ6-desaturase. To investigate this possibility, the effect of the specific inhibitors of cytochrome P-450, CO and metyrapone, on the Δ6-desaturase in the presence and absence of isoflurane were assessed.

Neither metyrapone nor $CO:O_2$ (80:20,v/v) significantly affected the extent to which isoflurane inhibited Δ6-desaturase activity in hepatic microsomes ($P>0.1$) (Table 28). The results with metyrapone are difficult to interpret since this compound significantly inhibits the Δ6-desaturase (Table 28). These results

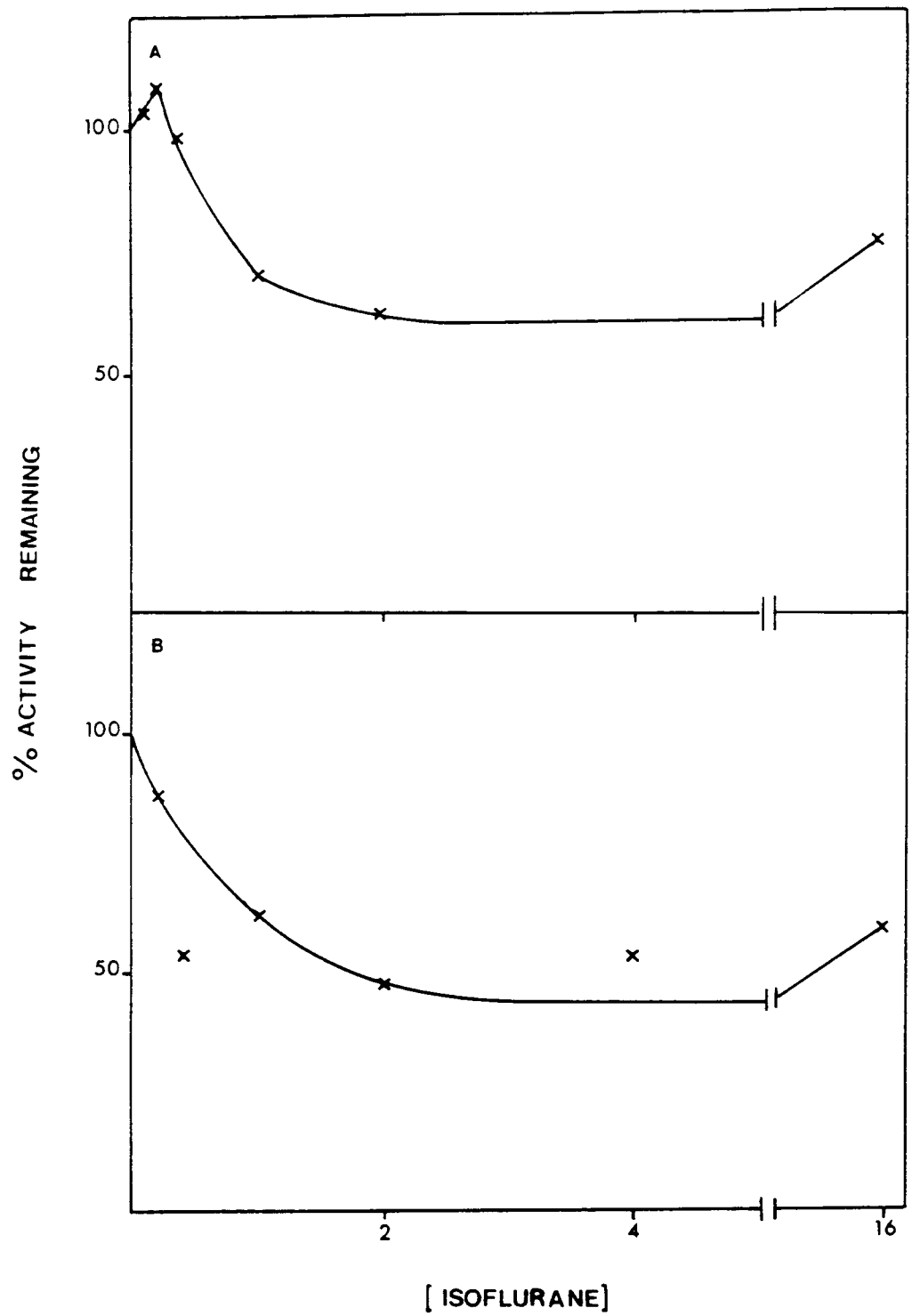

FIGURE 26 **The effect of isoflurane concentration on the Δ6-desaturation of linoleic acid measured using Method 2 (A) and Method 1 (B).**

Isoflurane concentration, mM. Results for Method 2 are from a single hepatic microsomal preparation (n=3). BSA concentration was 115 (Method 1) and 11.5 (Method 2) μg/μg fatty acid added. Corrected substrate concentration was 4.7 μM.

TABLE 28

THE EFFECT OF METYRAPONE AND $CO:O_2$ ON THE INHIBITION OF THE Δ6-DESATURATION OF LINOLEIC ACID BY ISOFLURANE IN RAT HEPATIC MICROSOMES

Additions * (mM)	Activity of Δ6-Desaturase (pmol/mg protein/min) †	% Inhibition of Δ6-Desaturase
EXPERIMENT 1		
None	269 ± 26	
Isoflurane (0.8)	188 ± 3	30.1§
Metyrapone (3.4)	195 ± 3	27.2§
Metyrapone (3.4) + isoflurane (0.8)	177 ± 21	34.0
EXPERIMENT 2		
None	148 ± 13	
Isoflurane (0.8)	109 ± 8	26.3§
$CO:O_2$ (80:20, v/v)	135 ± 10	8.8
$CO:O_2$ (80:20, v/v) + isoflurane (0.8)	88 ± 18	34.6¶

* In reaction mixtures of hepatic microsomes (0.5 mg protein/ml) incubated as described in the methods (Section 2.2.3.2a), with BSA (115 μg/μg fatty acid substrate added), ([$1^{-14}C$] linoleic acid (1.8 μM, 106 nCi) for 10 min, and assayed using Method 2. The corrected substrate concentration was 4.7 μM linoleic acid.

† Results were from a single preparation of hepatic microsomes (n=3). Experiment 1 was performed on a different preparation of microsomes from experiment 2.

§ Significant from that in the absence of additions ($P<0.05$).

¶ Significantly different from that in the absence of isoflurane ($P<0.01$).

suggest that cytochrome P-450 played no role in the effect of isoflurane on Δ6-desaturase activity, viz: that the effect was not caused by a cytochrome P-450 metabolite of isoflurane.

To investigate whether the inhibition of the Δ6-desaturation of linoleic acid by isoflurane was reversible, the following experiment was performed: hepatic microsomes were pre-incubated with or without isoflurane (0.8 mM) for 5 min at 35°C (Table 29). In an attempt to remove the isoflurane, the microsomes were bubbled with air for 10 min at 0 - 4°C before incubation with the components necessary for Δ6-desaturase activity (Table 29). Microsomes without isoflurane were treated in the same manner. Inhibition of the Δ6-desaturase was not diminished significantly by the pretreatment (Table 29).

The inhibition of the Δ6-desaturase activity by isoflurane was observed in hepatic microsomes whether or not the incubation mixture was bubbled with air (Table 29), which suggested that isoflurane (i) may not have been effectively removed by our procedure, or that (ii) isoflurane binding to its site of action may be tight - either reversible or essentially irreversible.

3.2.3.6 The Interaction of Other Volatile Anaesthetic Agents with Rat Hepatic Microsomal Δ6-Desaturase

The effect of the volatile anaesthetic agents, methoxyflurane, enflurane and halothane on the Δ6-desaturation of linoleic acid in hepatic microsomes from rats fed a normal diet, was investigated. None of the anaesthetic agents, including enflurane, a close structural analogue of isoflurane (Table 1), had a significant effect on Δ6-desaturase activity at concentrations far higher than that

TABLE 29

THE EFFECT OF PRE-INCUBATION WITH, AND SUBSEQUENT REMOVAL OF ISOFLURANE ON THE Δ6-DESATURATION OF LINOLEIC ACID IN RAT HEPATIC MICROSOMES

Pre-incubation * at 30 °C for 5 min	Additions † (mM)	Bubbled with air or left on ice for 10 min	Activity of Δ6-Desaturase (pmol/mg protein/min) §	% Activity Remaining
Yes	None	Bubbled with air for 10 min	99 ± 29	
Yes	Isoflurane	Bubbled with air for 10 min	71 ± 5 ¶	74
Yes	None	Left on ice	122 ± 3	
Yes	Isoflurane	Left on ice	75 ± 16 ¶	62
No	None	---	150 ± 13	
No	Isoflurane	---	110 ± 8 ¶	71

* Reaction mixture for pre-incubation contained hepatic microsomes (0.5 mg protein/ml), nicotinamide (1 mM), potassium fluoride (0.04 M) and bovine serum albumin (115 μg/μg fatty acid substrate added). Reaction mixtures were prepared from pre-incubated samples after they had been left on ice or bubbled with air for 10 min, and were incubated as described in the methods (Section 2.2.3.2a) with [1^{-14}C] linoleic acid (1.8 μmol, 106 nCi) with or without isoflurane (0.8 mM) for 10 min. The corrected substrate concentration was 4.7 μM linoleic acid. Results were obtained using Method 2.

† Additions made before pre-incubation.

§ Results were from a single preparation of hepatic microsomes (n = 3), but were typical of results obtained from two microsomal preparations.

¶ Differs significantly from that in absence of isoflurane ($P < 0.01$).

TABLE 30

THE EFFECT OF ANAESTHETIC AGENTS ON THE Δ6-DESATURATION OF LINOLEIC ACID IN RAT HEPATIC MICROSOMES

Anaesthetic Agent * (mM)	% of Activity in Absence of Anaesthetic Agent †
Methoxyflurane (1.7)	90
Methoxyflurane (4.3)	89
Enflurane (1.6)	97
Enflurane (4.1)	102
Halothane (1.9)	90
Isoflurane (0.4)	69 §

* In reaction mixtures of hepatic microsomes (0.5 mg protein/ml) incubated as described in the methods (Section 2.2.3.3b) with bovine serum albumin (115 μg/μg fatty acid substrate added) and [1-^{14}C]-linoleic acid (1.8 μM, 106 nCi) for 10 min at 30 ° C, and assayed using Method 1 (Section 2.2.3.2b). The corrected substrate concentration was 4.7 μM linoleic acid .

† Results were for a single preparation of microsomes (n=3-4).

§ Differs significantly from that in absence of additions ($P<0.01$).

at which isoflurane inhibited Δ6-desaturase activity (Table 30). Isoflurane (0.4 mM) was included as a positive control.

3.2.4. Kinetic Data for Hepatic Microsomal Δ6-Desaturase in the Presence and Absence of Isoflurane

Δ6-Desaturation of linoleic acid was measured at two different BSA concentrations in the presence and absence of isoflurane. Lineweaver-Burk plots for the Δ6-desaturation of linoleic acid in the presence and absence of isoflurane at both BSA concentrations are illustrated in Figures 27 and 28. The inhibition of the Δ6-desaturase by isoflurane was evident at both BSA concentrations.

Kinetic data for the Δ6-desaturation of α-linolenic acid at the lower BSA concentration (11.5 μg BSA/μg free fatty acid added) is illustrated in Figure 29. The kinetic data confirmed that isoflurane did not inhibit of the Δ6-desaturation of this substrate (Figure 29).

The kinetic data for the inhibition of the Δ6-desaturase in hepatic microsomes was measured under conditions where the Δ6-desaturase activity is probably influenced by a number of other enzymatic reactions (Figure 7). Further experiments were aimed at clarifying the role of other reactions, which are shown in Figure 7, in the Δ6-desaturase assay in hepatic microsomes. It was, therefore, necessary to measure the activity of phospholipase A_2, acyl-CoA synthetase and lysophospholipid acyltransferase under the conditions of the Δ6-desaturase assay.

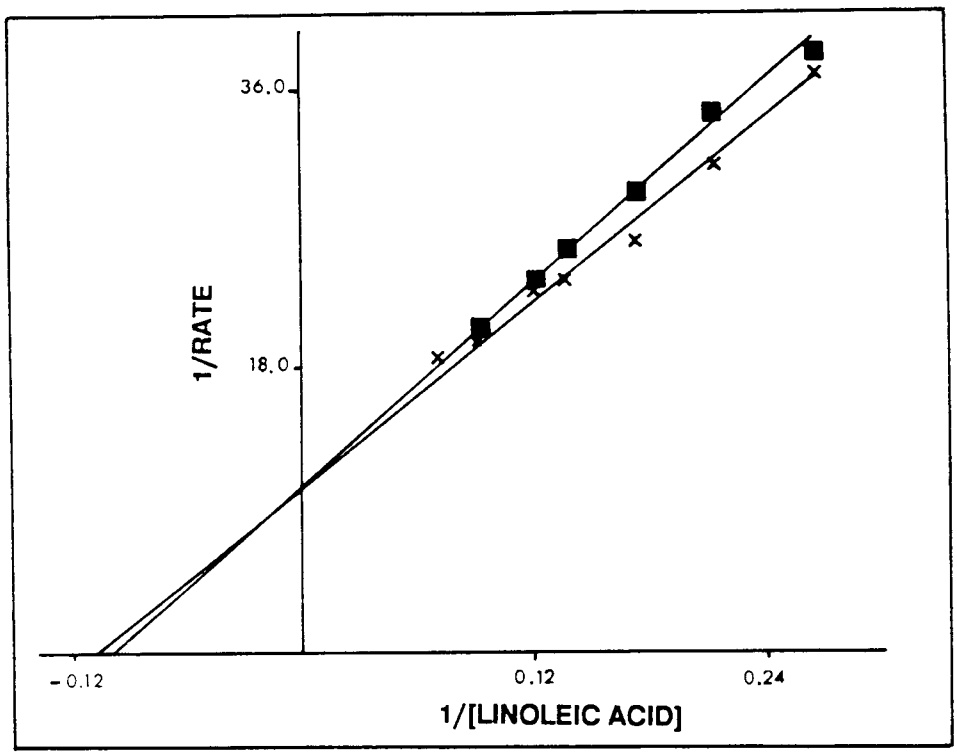

FIGURE 27 **Lineweaver-Burk plot of the Δ6-desaturation of linoleic acid in the presence (■) and absence (X) of isoflurane (2 mM) in rat hepatic microsomes at the low BSA concentration.**

Rate, μM [1^{-14}C] γ-linolenoyl-CoA + 2-[1^{-14}C] γ-linolenoyl-phospholipid formed/min; linoleic acid concentration, μM linoleic acid. BSA concentration was 11.5 μg/μg linoleic acid added. Δ6-Desaturase activity was measured using Method 2. Data represents the average of that obtained in triplicate from three preparations of hepatic microsomes. Lines were drawn by Enzfitter (Section 2.2.3.10).

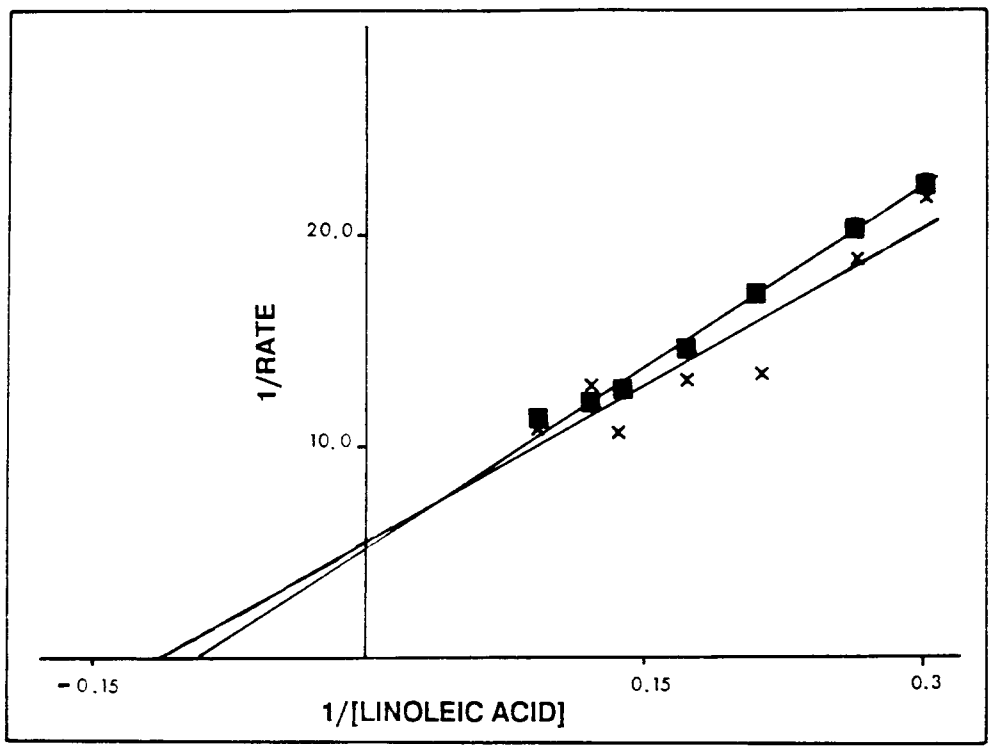

FIGURE 28 **Lineweaver-Burk plot of the Δ6-desaturation of linoleic acid in the presence (■) and absence (X) of isoflurane (2 mM) in rat hepatic microsomes at the high BSA concentration.**

Rate, μM [1^{-14}C] γ-linolenoyl-CoA + 2-[1^{-14}C] γ-linolenoyl-phospholipid formed/min; linoleic acid concentration, μM linoleic acid. BSA concentration was 115 μg/μg linoleic acid added. Δ6-Desaturase activity was measured using Method 2. Data represents the average of that obtained in triplicate from two preparations of hepatic microsomes. Lines were drawn by Enzfitter (Section 2.2.3.10).

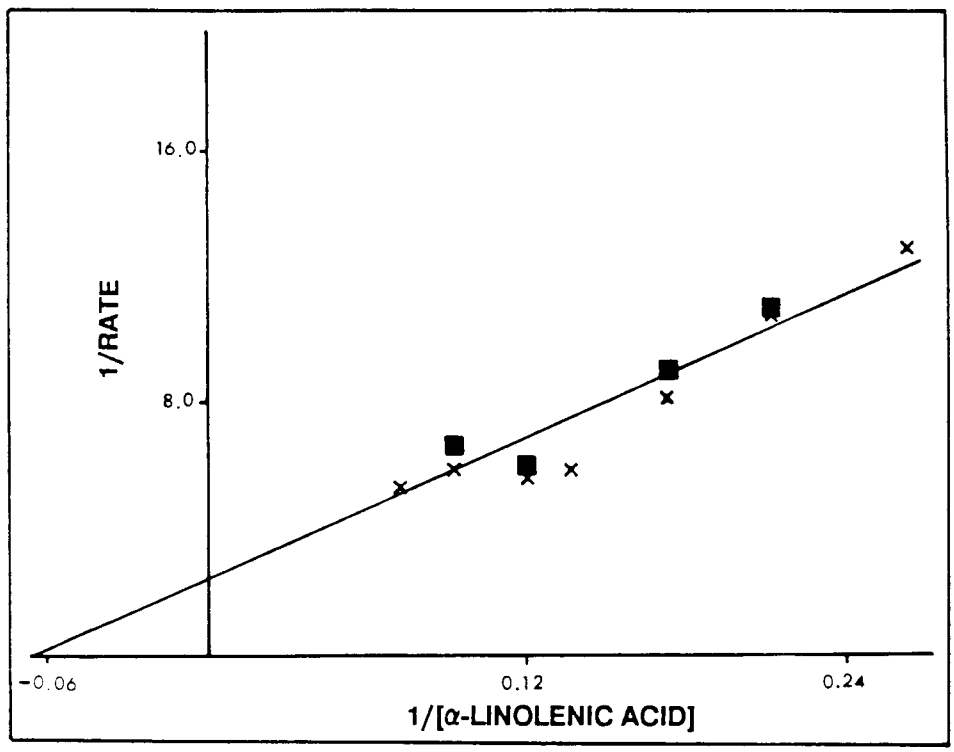

FIGURE 29

Lineweaver-Burk plot of the Δ6-desaturation of α-linolenic acid in the presence (■) and absence (X) of isoflurane (0.8 mM) in rat hepatic microsomes at the low BSA concentration.

Rate, μM [1-^{14}C] octa-6,9,12,15-decatetraenoyl-CoA + 2-[1-^{14}C] octa-6,9,12,15-decatetraenoyl-phospholipid formed/min; α-linolenic acid concentration, μM α-linolenic acid. BSA concentration was 11.5 μg/μg α-linolenic acid added. Δ6-Desaturase activity was measured using Method 2. Results are from a single preparation of hepatic microsomes, but are representative of those obtained from two preparations. Line was drawn by Enzfitter (Section 2.2.3.10).

3.2.5 Measurement of Reactions Which Could Influence the Δ6-Desaturase Activity in Hepatic Microsomes Under the Conditions of Our Experiments

3.2.5.1 Phospholipase A_2 Activity in Rat Hepatic Microsomes

Phospholipase A_2 activity was measured in hepatic microsomes which contained EDTA (4 μM) (Section 2.2.3.7); EDTA acts as a scavenger of calcium ions, an essential component for phospholipase A_2 activity (234). The phospholipase A_2 activity measured under these conditions was extremely low compared to the Δ6-desaturase substrate concentration, viz: 0.035 ± 0.014 μM [1-^{14}C] linoleic acid was released from the radiolabelled phospholipid over a period of 10 min, compared to the substrate concentration range of 3.4 to 10.8 μM, which includes endogenous substrate. Therefore, linoleic acid released from phospholipids during the Δ6-desaturase incubation time was unlikely to significantly dilute the radiolabelled plus endogenous substrate. No further activity measurements on phospholipase A_2 were attempted since phospholipase A_2 activity appeared too low to influence the measurement of the Δ6-desaturase activity in hepatic microsomes.

3.2.5.2 Separation of Fatty Acid (Substrate), Phospholipid and Acyl-CoA (Products) for Measurement of Activity of Fatty Acid-Metabolising Enzymes in Rat Hepatic Microsomes

In order to measure the activity of acyl-CoA synthetase and lysophospholipid acyltransferase in hepatic microsomes, separation of the radiolabelled fatty acid, acyl-CoA and phospholipid in good yield, had to be achieved. This

section outlines the results of the techniques used in the attempt to achieve this separation. A number of different literature methods were attempted for the separation of the three types of compounds mentioned. Although literature methods are well established for measuring one of the three components, our difficulties reflected trying to measure all three concurrently in the same reaction mixture. The methods attempted are outlined in Table 31. The reasons why the methods were unsuitable for our purposes are also given.

The first four methods cited in Table 31 were unsuitable in that they did not achieve separation of the requisite lipid classes in good yield. The fourth method did achieve separation using extraction plus TLC, but was rejected in view of the development of the final method which gave satisfactory results by a shorter method involving differential extraction without chromatography. Useful data was obtained from Method A (Section 2.2.3.8a) which is a combination of the first two methods in Table 31, and Method B (Section 2.2.3.8a) which is the last method in Table 31. The latter Method is referred to as the method of differential organic extraction.

Although the Method A was unsuitable for separation of fatty acids, acyl-CoA and phospholipids, it did, nevertheless, separate neutral lipids from phospholipids, acyl-CoA and fatty acids (R_f values for neutral lipid, fatty acid, and phospholipid plus acyl-CoA were 0.44, 0.22 and 0, respectively). This enabled us to establish that only a small amount (<5%) of the radiolabelled linoleic acid added to reaction mixtures was incorporated into neutral lipids during incubation (data not shown).

TABLE 31

METHODS USED IN AN ATTEMPT TO SEPARATE FATTY ACID, ACYL-CoA AND PHOSPHOLIPID

Procedure	Result	Why the Method was Rejected or Used	Ref.
Extraction from acidified microsomes using Folch Method (chloroform:methanol;2:1; v/v)	ca. >90% yield [1-^{14}C] linoleic acid, ca.> 80% yield 1-palmitoyl-2-[1-^{14}C] linoleoyl-phosphatidylcholine and ca. only 50% yield [1-^{14}C] palmitoyl-CoA standards.	Rejected: the acyl-CoA was not recovered in good yield. TLC of the Folch extract was required to separate overlap of the fatty acid, acyl-CoA and phospholipid in extracts.	266
TLC (Petroleum ether:diethyl ether:glacial acetic acid; 90:10:1,v/v/v) of Folch extract.	Phospholipid and acyl-CoA remained at point of origin. ca. 35% of [1-^{14}C] stearoyl-CoA chromatographed with fatty acid.	Rejected: unable to separate phospholipid and acyl-CoA.	266
Extraction from microsomes using Dole reagent, followed by extraction with Folch.	Fatty acid extracted into heptane, acyl-CoA and phospholipid remained in aqueous layer, and were co-extracted into Folch reagent.	Rejected: TLC of Folch extract was required to separate acyl-CoA and phospholipid. Part of the acyl-CoA chromatographed with the fatty acid using the TLC system chloroform:methanol:glacial acetic acid; 66:34:1; v/v/v.	Adapted from 211, 266 and 398
Extraction of fatty acid and phospholipid from microsomes at alkaline pH with chloroform: methanol followed by water washes to remove acyl-CoA	The acyl-CoA was partly extracted into chloroform:methanol, and remained partly in the aqueous layer. Fatty acid and phospholipid were extracted into chloroform:methanol.	Rejected: TLC of the chloroform:methanol extracts was required to completely separate the phospholipid and acyl-CoA.	Adapted from 374
Extraction of fatty acid with diethyl ether, phospholipid with chloroform:methanol, leaving acyl-CoA in aqueous layer.	[1-^{14}C] Linoleic acid extracted exclusively into diethyl ether, 1-palmitoyl-2-[1-^{14}C] linoleoyl-phosphatidylcholine primarily extracted into the chloroform:methanol layer and [1-^{14}C] palmitoyl-CoA remained primarily in the aqueous layer (Table 32).	Used: although there was some overlap of phospholipid and acyl-CoA with the fatty acid, this could easily be corrected for using the data in Table 32. This method is referred to as the Method by differential organic extraction.	Adapted from 374 and 392

The method developed to separate fatty acid, acyl-CoA and phospholipid involved differential extraction of the components (final method in Table 31 (adapted from 374,392)) as follows: first, the fatty acid was extracted from reaction mixtures into diethyl ether, and then the phospholipids into chloroform:methanol*; the acyl-CoA remained primarily in the aqueous layer. The total recovery of radioactivity from reaction mixtures in all three fractions was 89.0 ± 5.6% (n = 20).

The amount of overlap of the components in the organic phases was assessed by following the distribution of radioactivity in the three phases on extraction of radioactive standards from hepatic microsomes (Table 32).

The fatty acid standard, [1-^{14}C] linoleic acid was extracted measurably only into diethyl ether. Overall recovery was excellent (ca. 90%). The acyl-CoA standard, [1-^{14}C] palmitoyl-CoA remained exclusively (>95%) in the aqueous layer when extracted from buffer. However, only approximately 65% of the acyl-CoA remained in the aqueous layer when the acyl-CoA standard was extracted from hepatic microsomes (Table 32); the remainder was extracted into the diethyl ether layer. The recovery of radioactive acyl-CoA in the diethyl ether layer does not appear to reflect enzymic hydrolysis of the acyl-CoA by hepatic microsomal acyl-CoA hydrolase since the use of heat-treated microsomes did not alter the separation pattern (Table 32).

The phospholipid was also found in significant amounts in two phases: ca. 75% of the phospholipid was extracted into chloroform:methanol, while ca. 20% extracted with diethyl ether and thus would be co-extracted with fatty acid.

* Using this method, the final proportions of chloroform and methanol in the extract are unknown. Therefore, it will be referred to as the chloroform:methanol extract.

TABLE 32

RECOVERY OF RADIOACTIVITY ASSOCIATED WITH RADIOACTIVE STANDARDS IN THE THREE PHASES USED FOR MEASUREMENT OF PRODUCT FORMATION DURING ASSAY FOR LYSOPHOSPHOLIPID ACYLTRANSFERASE AND ACYL-CoA SYNTHETASE ACTIVITY

Radioactive Standard *	Phase	% Recovery †	Total % Recovery †
[1-^{14}C] Linoleic acid in hepatic microsomes	Diethyl ether	89.3 ± 5.6 (5)	89.3 (5)
[1-^{14}C] Palmitoyl-CoA in buffer	Diethyl ether	None	>95 (3)
	Chloroform: Methanol	None	
	Aqueous	>95 (3)	
[1-^{14}C] Palmitoyl-CoA in microsomes	Diethyl ether	32.3 ± 10.1 (5)	90.2 (5)
	Chloroform: methanol	None	
	Aqueous	58.5 ± 10.3 (5)	
[1-^{14}C] Palmitoyl-CoA in microsomes which had been heat-treated (Section 3.2.5.2)	Diethyl ether	32.6 ± 10.5 (4)	90.4 ± 8.1 (4)
	Chloroform: methanol	None	
	Aqueous	56.7 ± 8.5 (4)	
1-Palmitoyl-2-[1-^{14}C] linoleoyl-phosphatidylcholine in hepatic microsomes	Diethyl ether	22.4 ± 3.7 (5)	92.9 (5)
	Chloroform: methanol	70.5 ± 7.0 (5)	

* The radioactive standard was extracted from the medium described above as outlined in Section 2.2.3.8a, Method B

† Expressed as a percentage of the radioactivity added to the medium.

After incubation of hepatic microsomes with [1-^{14}C] linoleic acid (Section 2.2.3.8), the total radioactivity recovered in the three phases was 89 ± 5.6%; the amount of radioactivity in each phase varied with substrate concentration, viz: 20 - 60%, 8 - 30% and 30 - 60% of the radioactivity recovered was in the diethyl ether, chloroform:methanol and aqueous phases, respectively. This reflected that the disappearance of substrate and formation of products was dependent on substrate concentration. In contrast, within each organic phase, the distribution of the radioactivity, which was analysed by TLC, was independent of substrate concentration (data not shown). This showed that the overlap of fatty acid, acyl-CoA and phospholipid within the organic phases was independent of substrate concentration. Therefore, a simple correction for the loss of acyl-CoA and phospholipid into the diethyl ether phase can be made. In all further experiments, the yields of fatty acid, acyl-CoA and phospholipid were corrected for the recoveries seen in Table 32, as follows:

i) radioactivity recovered in chloroform:methanol was equal to 76% of the recovered phospholipids and was corrected accordingly to yield 100% (Table 32).

ii) radioactivity recovered in aqueous phase was equal to 65% of the acyl-CoA and was corrected accordingly to yield 100% (Table 32).

Where necessary, the amount of substrate remaining (free fatty acid) was calculated from the radioactivity associated with the diethyl ether phase minus the amount of radioactivity associated with the acyl-CoA and phospholipid in this phase.

Following incubation of [1-^{14}C] linoleic acid with hepatic microsomes (Section 2.2.3.8a), TLC analysis of the diethyl ether and chloroform:methanol phases was also performed. Since hydrolysis of the thioester bond has been reported to occurr during TLC of acyl-CoA, this TLC analysis was not used to quantitate fatty acid, acyl-CoA and phospholipid during assay for acyl-CoA synthetase and lysophospholipid acyltransferase activity, but only to analyse the distribution of the radioactivity in organic phases after incubation and extraction, in particular, the distribution of the radioactivity in the different phospholipids. In contrast to the TLC system mentioned in the first method in Table 31 (petroleum ether:diethyl ether:glacial acetic acid; 90:10:1, v/v/v), this TLC system (chloroform:methanol:glacial acetic acid; 66:34:1; v/v/v), achieved separation of the acyl-CoA from the phospholipid and fatty acid (Section 2.2.3.8a, Method B). Authentic standards of linoleoyl-CoA, linoleic acid phosphatidylcholine, phosphatidylethanolamine and phosphatidylinositol were used to analyse the TLC system; the acyl-CoA and phospholipids were further identified using the nitroprusside and molubdenum blue sprays, respectively (Section 2.2.3.8a) (373,375).

Of the radioactivity recovered in the diethyl ether phase, ca. 77% was associated with the fatty acid fraction (Table 33). Together the acyl-CoA and phospholipid contributed the remaining 20% of the radioactivity recovered in this phase (Table 33). The acyl-CoA recovered in the diethyl ether phase after TLC of this phase (Table 33) was considerably less than that associated with acyl-CoA standard ([1-^{14}C] palmitoyl-CoA) extracted from microsomes into the same phase (Table 32), suggesting that splitting of the thioester bond during TLC may have occurred. TLC analysis of the aqueous layer of reaction mixtures

TABLE 33

TLC ANALYSIS OF ORGANIC EXTRACTS OF REACTION MIXTURES FOR MEASUREMENT OF LYSOPHOSPOLIPID ACYLTRANSFERASE AND ACYL-CoA SYNTHETASE ACTIVITY IN RAT HEPATIC MICROSOMES *

Organic Phase	Fraction	R_f Value	% Radioactivity Recovered in Corresponding Organic Phase †
Diethyl ether	Acyl-CoA	0	14.3 ± 11.4 (7)
	Phosphatidylcholine + Phosphatidylethanolanine	0.09 0.82	8.6 ± 4.3 (7)
	Linoleic acid	0.93	77.1 ± 13.0 (7)
Chloroform: methanol	Acyl-CoA	0	0
	Phosphatidylcholine (lecithin)	0.09	69.7 ± 4.8 (15)
	Phosphatidylinositol	0.20	0
	Phosphatidylethanolamine	0.82	8.2 ± 2.9 (15)
	Linoleic acid	0.93	21.9 ± 4.9 (15)

* In reaction mixtures of hepatic microsomes (0.5 mg protein/ml) incubated as described in the Methods (Section 2.2.3.2a), with BSA (115 μg/μg fatty acid substrate added), ([1-^{14}C] linoleic acid (1.8 μM, 106 nCi) for 3 min, and analysed using differential organic extractions and TLC (Section 2.2.3.8a, Method B). Corrected substrate concentration was 4.7 μM

† Total recovery of added radioactivity in all three phases (diethyl ether, chloroform:methanol plus aqueous) was 89 ± 5.6% (20); the distribution of the radioactivity recovered in the different phases was dependent on the initial substrate concentration, but was in the following ranges: 20 - 60% in the diethyl ether phase, 8 - 30% in the chloroform:methanol phase and 30 - 60% in the aqueous phase. The distribution of radioactivity within a phase was independent of substrate concentration (data not shown)

was not performed. However, since >90% of the radioactivity associated with the standards [1-^{14}C] linoleic acid and 1-palmitoyl-2-[1-^{14}C] linoleoylphosphatidylcholine was recovered in the organic phases (Table 32), it was assumed that neither the fatty acid nor the phospholipid contributed to the radioactivity in the aqueous layer of reaction mixtures (after diethyl ether and chloroform:methanol extraction). Therefore, the radioactivity in the aqueous phase was assumed to be acyl-CoA.

In the chloroform:methanol phase, approximately 80% of the radioactivity recovered in this phase was associated with the phospholipid (phosphatidylcholine plus phosphatidylethanolamine); the remaining radioactivity was recovered as fatty acid (which may be released from phospholipid during chromatography), but not acyl-CoA (Table 33). The radioactivity associated with the phospholipid was recovered primarily as phosphatidylcholine; a small amount of radioactivity was also associated with phosphatidylethanolamine (Table 33). Therefore, the activity of the acyltransferases measured is primarily that of lysolecithin acyltransferase, with only a small contribution from the enzyme acylating phosphatidylethanolamine.

3.2.5.3 Measurement of Acyl-CoA Synthetase and Lysophospholipid Acyltransferase Activity in Rat Hepatic Microsomes

The activities of the acyl-CoA synthetase and lysophospholipid acyltransferase were measured as a function of time at two different substrate concentrations (4.7 μM and 10.8 μM linoleic acid (corrected concentration)) by the method using differential organic extractions (Section 2.2.3.8a, Method B)(Figures 30 and 31). The data for both enzymes is corrected for

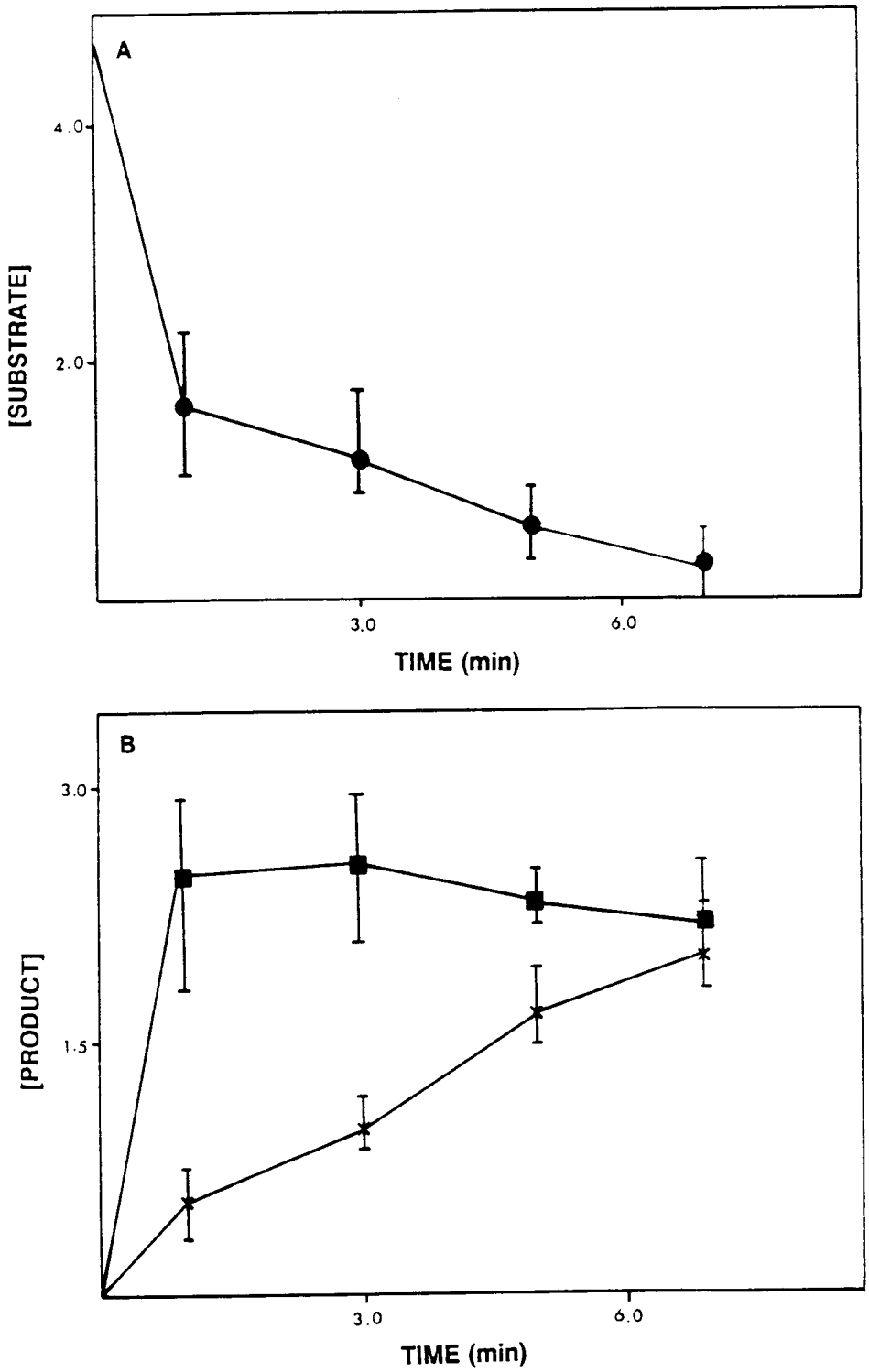

FIGURE 30 **The effect of time on the disappearance of fatty acid (substrate) (A) and on the formation of acyl-CoA (■, B) and the products of acylation of phospholipids (X, B) measured during the metabolism of linoleic acid (4.7 μM) in hepatic microsomes.**

Substrate concentration, μM [1^{-14}C] linoleic acid + endogenous linoleic acid; product concentration, μM [1^{-14}C] linoleoyl-CoA + γ-linolenoyl-CoA (■) and 2-[1^{-14}C] linoleoyl- + 2-[1^{-14}C] γ-linolenoyl phospholiphid formed (X). BSA concentration was 11.5 μg/μg linoleic acid. Corrected substrate concentration was 4.7 μM. Separation of the fatty acid, phospholipid and acyl-CoA was carried out by differential organic extractions (Section 2.2.3.8a, Method B). Data represents quintupulate determinations on one preparation of hepatic microsomes.

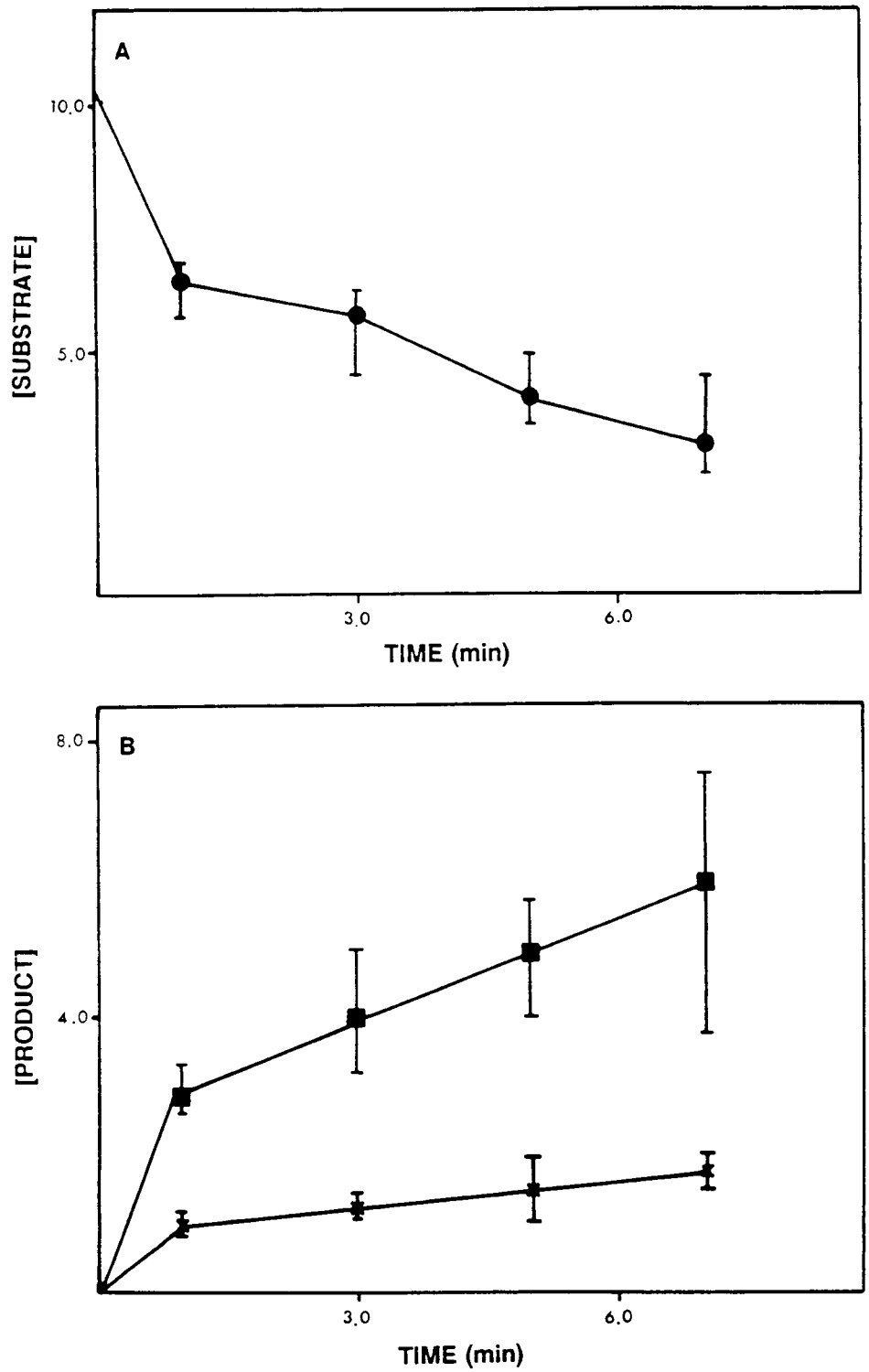

FIGURE 31 **The effect of time on the disappearance of fatty acid (substrate) (A) and on the formation of acyl-CoA (■ , B) and the products of the acylation of phospholipids (X, B) measured during the metabolism of linoleic acid (10.8 μM) in hepatic microsomes.**

Substrate concentration, μM [1^{-14}C] linoleic acid + endogenous linoleic acid; product concentration, μM [1^{-14}C] linoleoyl-CoA + γ-linolenoyl-CoA (■), and 2-[1^{-14}C] linoleoyl- + 2-[1^{-14}C] γ-linolenoyl-phospholipid formed (X). BSA concentration was 11.5 μg/μg linoleic acid added. Corrected substrate concentration was 10.8 μM. Separation of the fatty acid, phospholipid and acyl-CoA was carried out by differential organic extractions (Section 2.2.3.8a, Method B). Data represents quintupulate determinations on one preparation of hepatic microsomes.

endogenous substrate levels. The activity of the acyl-CoA synthetase, measured by acyl-CoA formation (■), was not linear with time at either substrate concentration, except, possibly, for an undetermined period within the first minute. At the lower substrate concentration (4.7 μM linoleic acid) there was no further increase in acyl-CoA formation after the first minute, although there was still unesterified fatty acid present (●) (Figure 30). The activity of the acyl-CoA synthetase as a function of time was greater at the higher substrate concentration (10.8 μM linoleic acid) than at the lower substrate concentration (4.7 μM linoleic acid), but not in the proportion to the two-fold increase in total substrate concentration (Figure 30 and 31)).

The activity of the lysophospholipid acyltransferase did not increase linearly with time over the time period utilised; the activity was comparable at both concentrations of linoleic acid (4.7 μM and 10.8 μM, Figures 30 and 31, respectively). A time period of 3 min was chosen for subsequent experiments because shorter time would have resulted in increased inaccuracy in the determination of lysophospholipid acyltransferase activity, which was low, with no guarantee of being on the linear portion of either the acyl-CoA synthetase or lysophospholipid acyltransferase activity versus time curve.

3.2.5.4 Kinetic Data for the Acyl-CoA Synthetase, Δ6-Desaturase and Lysophospholipid Acyltransferases in Rat Hepatic Microsomes

The experimentally determined reaction rate versus substrate concentration curves for the acyl-CoA synthetase, Δ6-desaturase and lysophospholipid acyltransferases are illustrated in Figures 32, 33, and 34. The double reciprocal

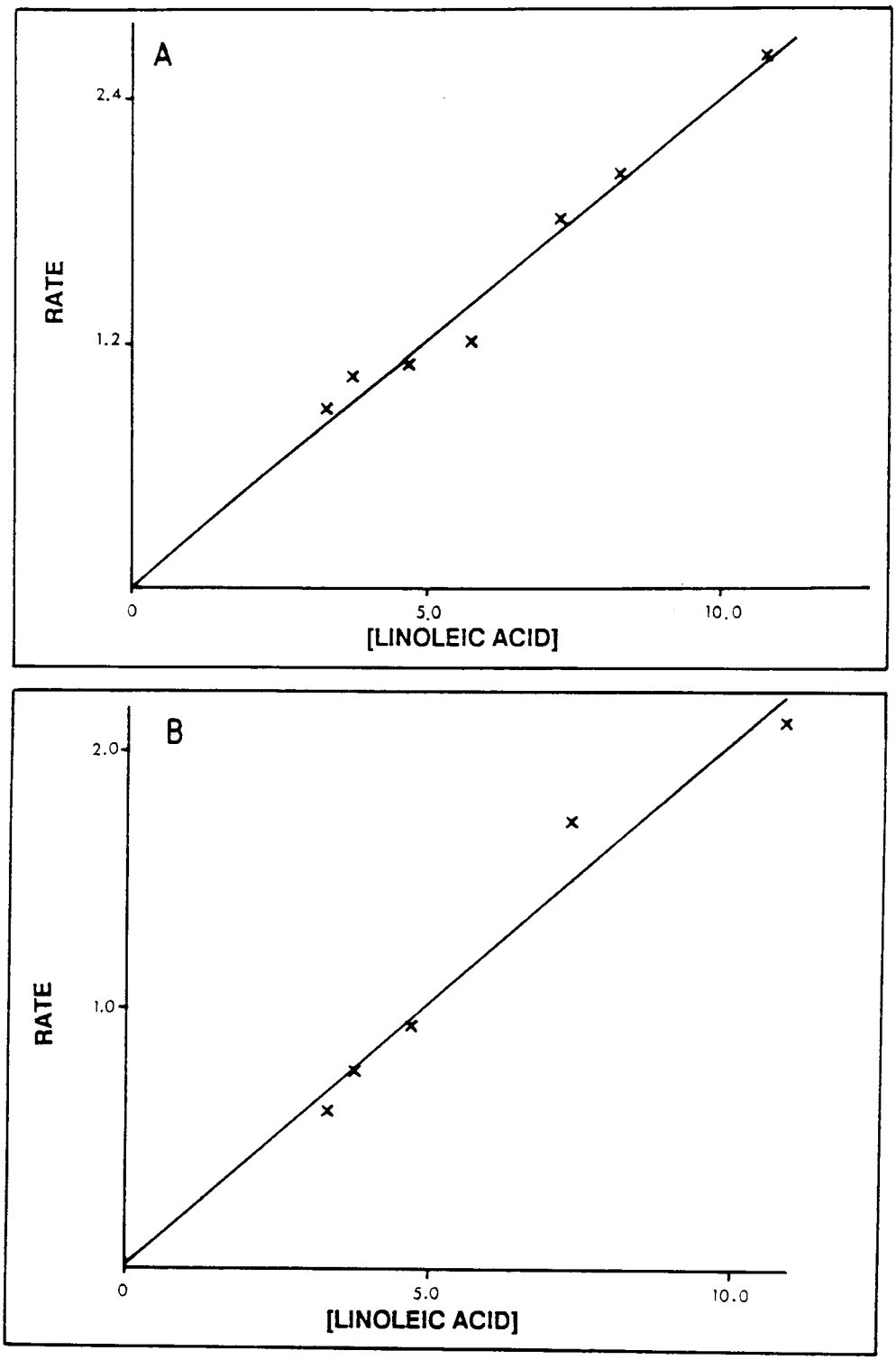

FIGURE 32 **Plot of rate of formation of acyl-CoA versus linoleic acid concentration by rat hepatic microsomal acyl-CoA synthetase at the high (A) and low (B) BSA concentrations.**

Rate, μM [1-^{14}C] linoleoyl-CoA + [1-^{14}C] γ-linolenoyl-CoA formed/min; linoleic acid concentration, μM linoleic acid. Product formation was measured at 3 min and was normalised to 1 min by dividing by 3. BSA concentration was 115 (A) and 11.5 (B) μg/μg linoleic acid added. Separation of the fatty acid, phospholipid and acyl-CoA was carried out by differential organic extractions (Section 2.2.3.8a, Method B). Curve was drawn by Enzfitter (Section 2.2.3.10). Data represents the average of that obtained in triplicate from two preparations of hepatic microsomes (A) and three to five determinations from three preparations of hepatic microsomes (B).

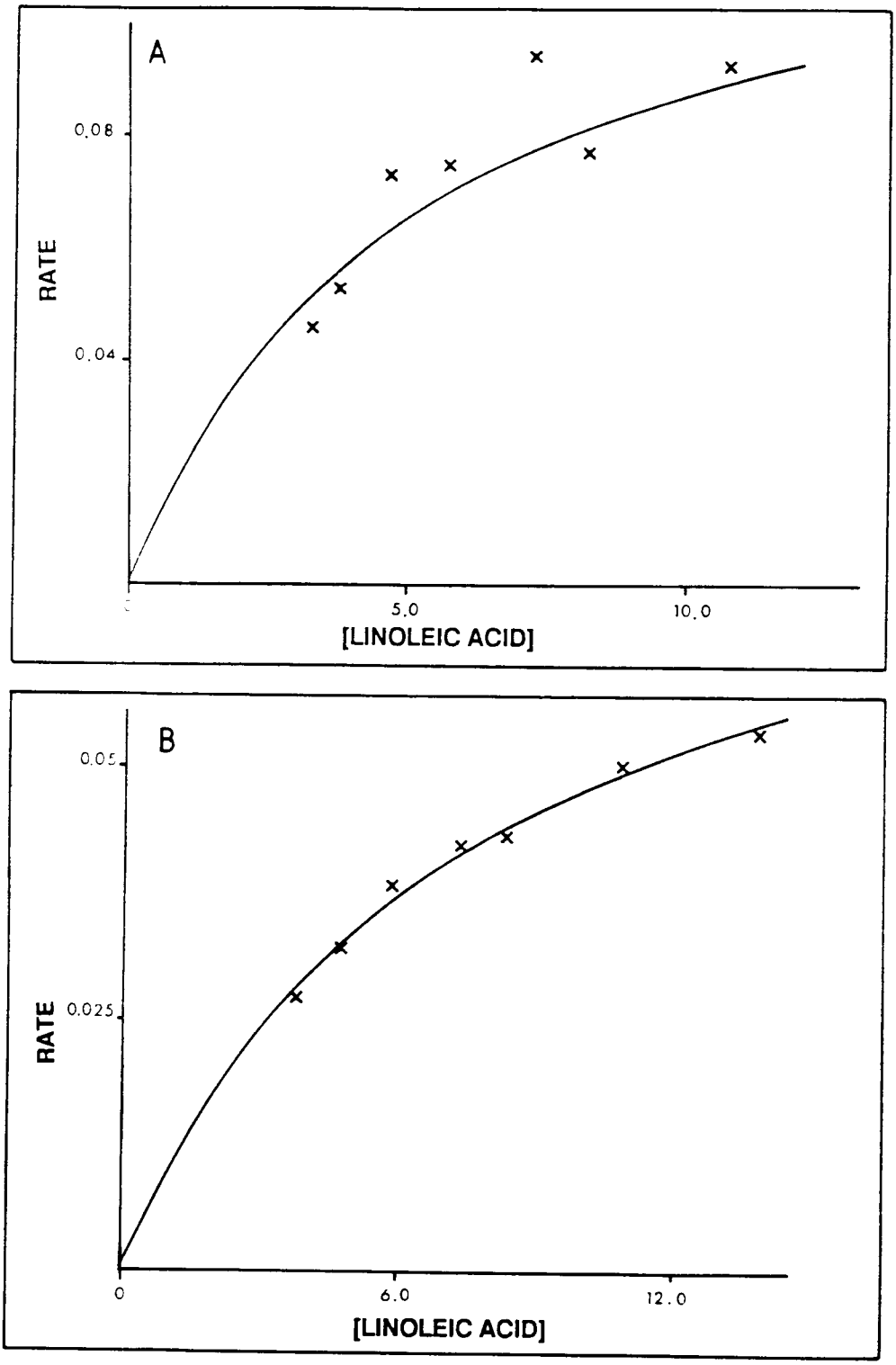

FIGURE 33 **Plot of rate of formation of γ-linolenic acid versus linoleic acid concentration by rat hepatic microsomal Δ6-desaturase at the high (A) and low (B) BSA concentrations.**

Rate, μM [1-^{14}C] γ-linolenoyl-CoA + 2-[1-^{14}C] γ-linolenoyl-phospholipid formed/min; linoleic acid concentration, μM linoleic acid. BSA concentrations were 115 (A) and 11.5 (B) μg/μg linoleic acid added. Δ6-Desaturase activity was measured by Method 2. Curves were drawn by Enzfitter (Section 2.2.3.10). Data represents the average of that obtained in triplicate from two preparations of hepatic microsomes for the high BSA concentration (A), and three preparations for the low BSA concentration (B).

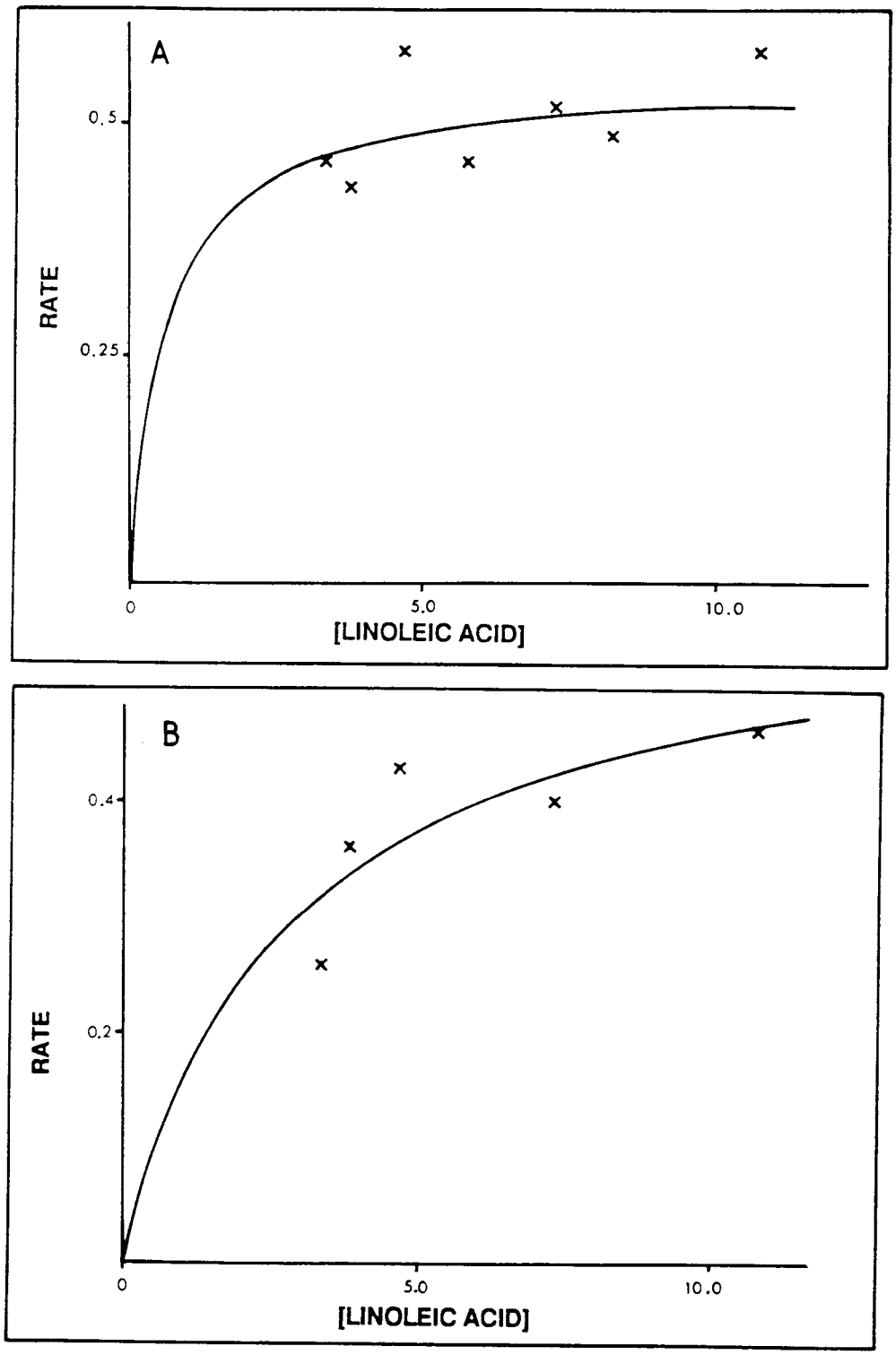

FIGURE 34 **Plot of rate of acylation of phospholipids versus linoleic acid concentration by rat hepatic microsomal lysophospholipid acyltransferases at the high (A) and low (B) BSA concentrations.**

Rate, μM 2-[1-^{14}C] linoleoyl-phospholipid + 2-[1-^{14}C] γ-linolenoyl-phospholipid formed/min; linoleic acid concentration, μM linoleic acid. Product formation was measured at 3 min and was normalised to 1 min by dividing by 3. BSA concentration was 115 (A) and 11.5 (B) μg/μg linoleic acid added. Separation of the fatty acid, phospholipid and acyl-CoA was carried out by differential organic extractions (Section 2.2.3.8a, Method B). Curve was drawn by Enzfitter (Section 2.2.3.10). Data represents the average of that obtained in triplicate from two preparations of hepatic microsomes (A) and three to five determinations from three preparations of hepatic microsomes (B).

plots for all three enzymes were linear (Figures 35,36 and 37). The apparent K_m and V_{max} values for these enzymes were calculated using the Michaelis-Menten equation on the data in Figures 32, 33, 34, 35, 36 and 37, and these values are given in Table 34. These estimations of the apparent K_m and V_{max} values for the acyl-CoA synthetase and lysophospholipid acyltransferase are only approximate because of the inappropriate substrate concentration range used in their determination; it does not span the apparent K_m value. In the case of the acyl-CoA synthetase, the substrate concentration range (3.35 - 10.8 μM) is too low, and for the lysophospholipid acyltransferase, it was too high. For these two enzymes, the rate versus substrate concentration curves illustrated in Figures 32 and 34 were used in further analysis of the kinetics of the Δ6-desaturase, and therefore more accurate determination of the apparent K_m and V_{max} values was not pursued.

3.2.5.5 The Effect of Isoflurane on Rat Hepatic Microsomal Acyl-CoA Synthetase and Lysophospholipid Acyltransferase

Isoflurane had no effect on the acyl-CoA synthetase or lysophospholipid acyltransferase activities in rat hepatic microsomes. The activity of the acyl-CoA synthetase was 1.44 ± 0.04 μM acyl-CoA formed/min in the presence or absence of isoflurane (2 mM) using a substrate concentration of 5.8 μM (corrected) linoleic acid. Similarly, the lysophospholipid acyltransferase activity at the same substrate concentration (5.8 μM linoleic acid) was 0.38 ± 0.02 μM and 0.43 ± 0.01 μM phospholipid formed/min in the presence and absence of 2 mM isoflurane. These results represent the average of at least three sets of experiments on a single preparation of hepatic microsomes.

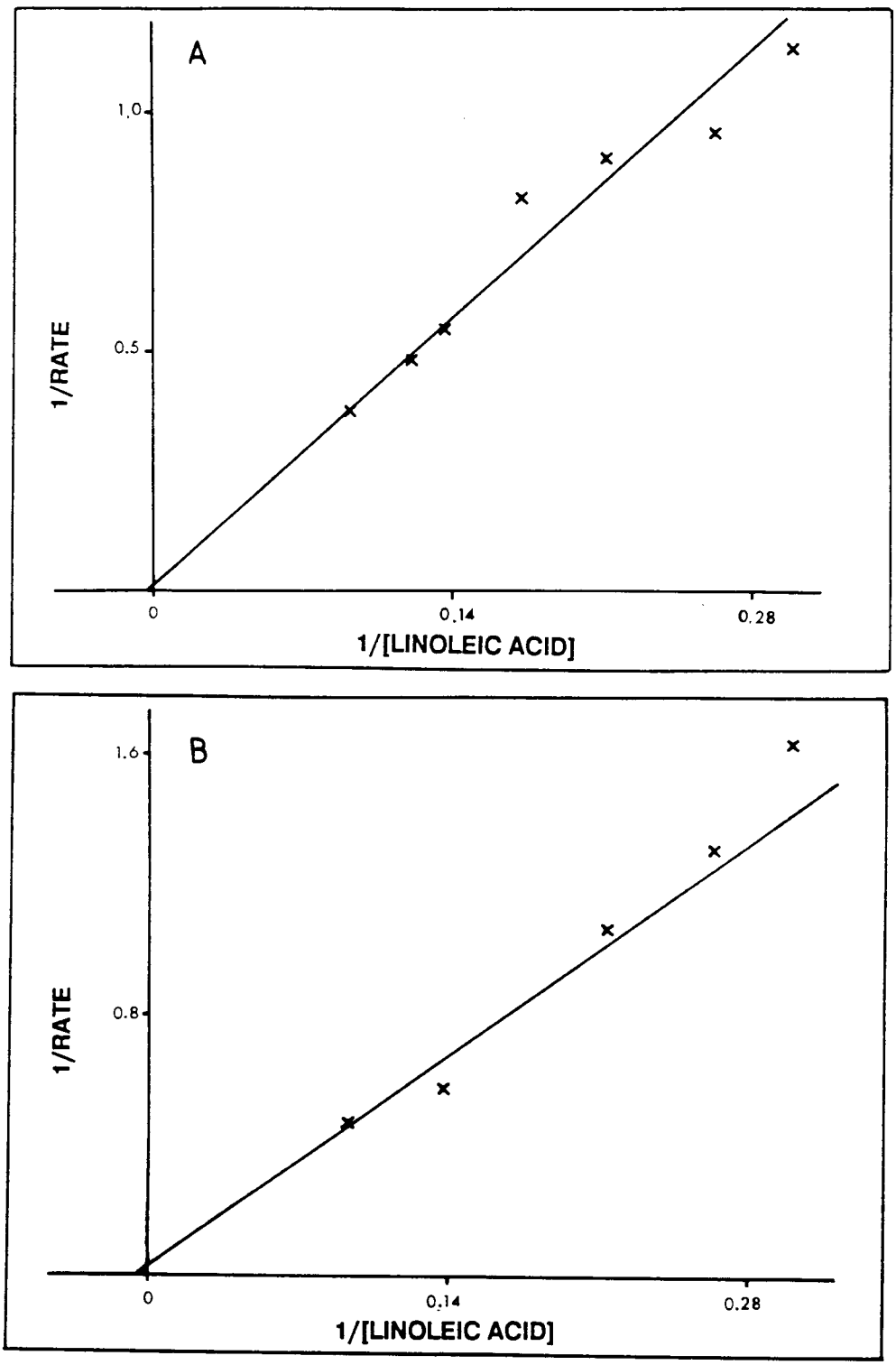

FIGURE 35 **Lineweaver-Burk plot of the formation of acyl-CoA by the acyl-CoA synthetase in rat hepatic microsomes at the high (A) and low (B) BSA concentrations.**

Rate, μM [1-^{14}C] linoleoyl-CoA + [1-^{14}C] γ-linolenoyl-CoA formed/min; linoleic acid concentration, μM linoleic acid. Product formation was measured at 3 min and was normalised to 1 min by dividing by 3. BSA concentration was 115 (A) and 11.5 (B) μg/μg linoleic acid added. Separation of the fatty acid, phospholipid and acyl-CoA was carried out by differential organic extractions (Section 2.2.3.8a, Method B). Lines were drawn by Enzfitter (Section 2.2.3.10). Data represents the average of that obtained in triplicate from two preparations of hepatic microsomes (A) and three to five determinations from three preparations of hepatic microsomes (B).

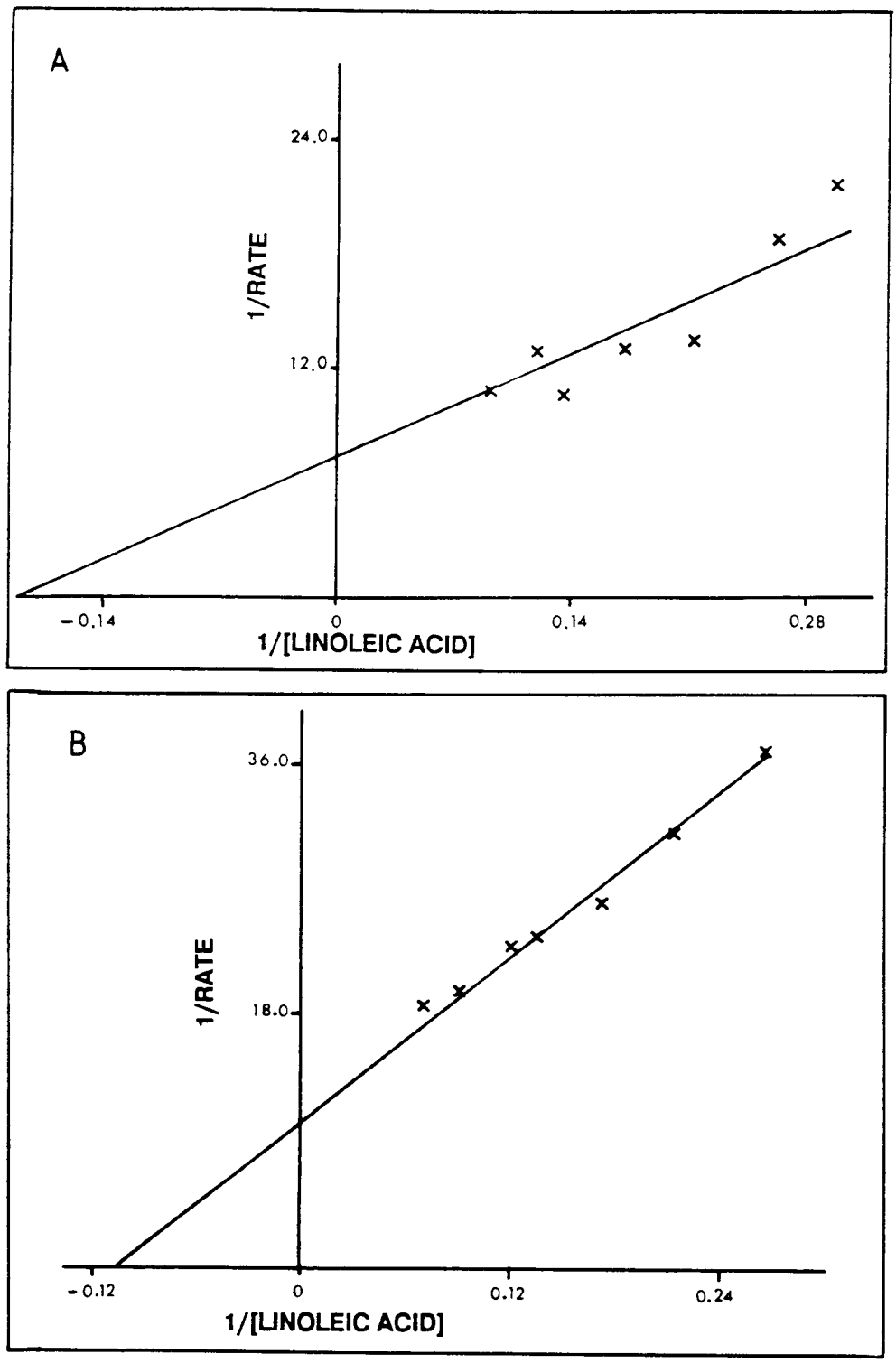

FIGURE 36 **Lineweaver-Burk plot of the Δ6-desaturation of linoleic acid in rat hepatic microsomes at the high (A) and low (B) BSA concentrations.**

Rate, μM [1-^{14}C] γ-linolenoyl-CoA + 2-[1-^{14}C] γ-linolenoyl-phospholipid formed/min; linoleic acid concentration, μM linoleic acid. BSA concentration was 115 (A) and 11.5 (B) μg/μg linoleic acid added. Δ6-Desaturase activity was measured by Method 2. Lines were drawn by Enzfitter (Section 2.2.3.10). Data represents the average of that obtained in triplicate from two preparations of hepatic microsomes for the high BSA concentration (A) and three preparations for the low BSA concentration (B).

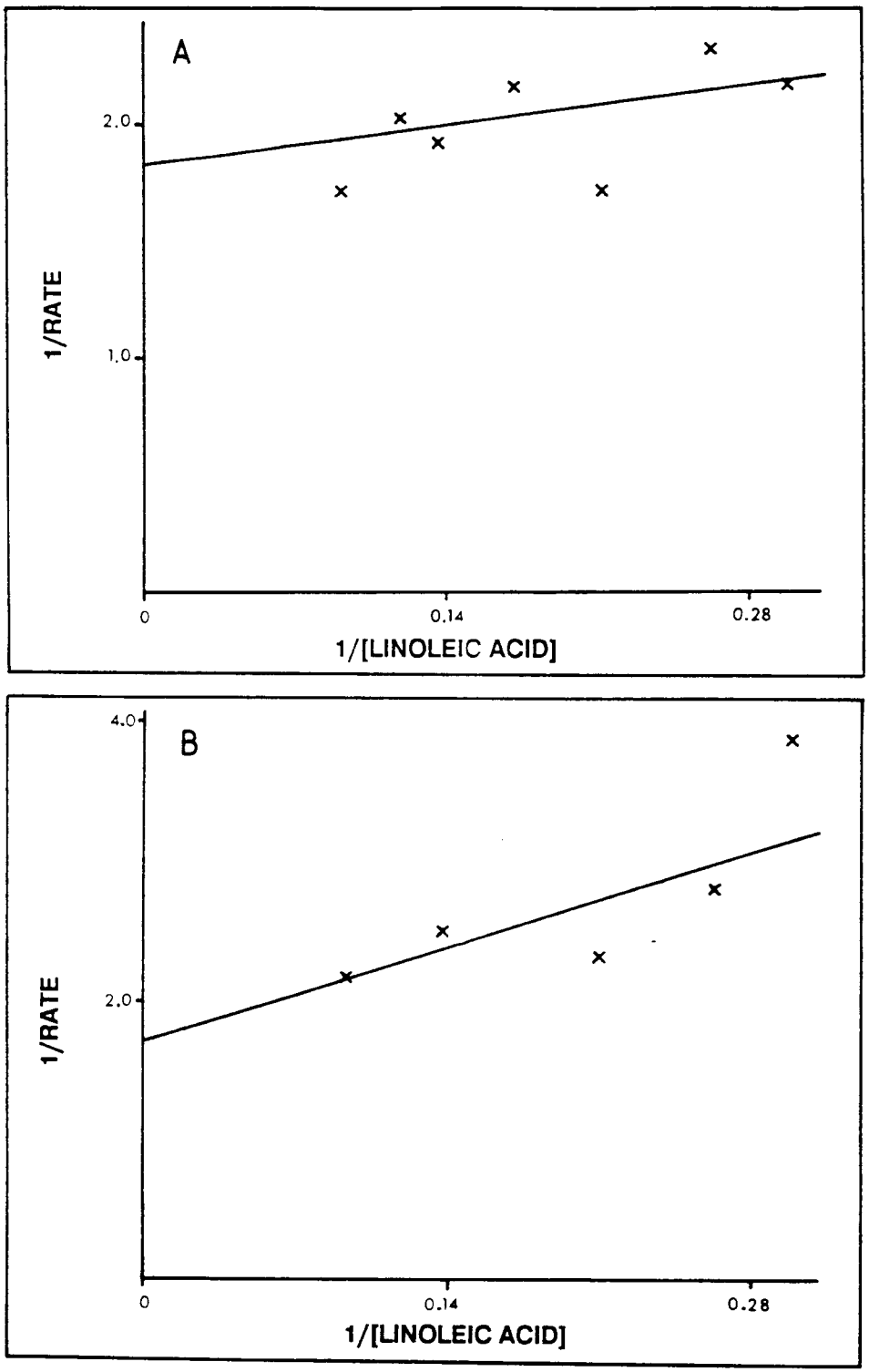

FIGURE 37 **Lineweaver-Burk plot for the acylation of phospholipids by the lysophospholipid acyltransferases in rat hepatic microsomes at the high (A) and low (B) BSA concentrations.**

Rate, μM 2-[1-^{14}C] linoleoyl-phospholipid + 2-[1-^{14}C] γ-linolenoyl-phospholipid formed/min; linoleic acid concentration, μM linoleic acid. Product formation was measured at 3 min and was normalised to 1 min by dividing by 3. BSA concentration was 115 (A) and 11.5 (B) μg/μg linoleic acid added. Separation of the fatty acid, phospholipid and acyl-CoA was carried out by differential organic extractions (Section 2.2.3.8a, Method B). Lines were drawn by Enzfitter (Section 2.2.3.10). Data represents the average of that obtained in triplicate from two preparations of hepatic microsomes (A) and three to five determinations from three preparations of hepatic microsomes (B).

TABLE 34

APPROXIMATE APPARENT K_m AND V_{max} VALUES FOR THE ACYL-CoA SYNTHETASE, Δ6-DESATURASE AND LYSOPHOSPHOLIPID ACYLTRANSFERASE IN RAT HEPATIC MICROSOMES

Enzyme	[BSA] (μg/μg free fatty acid added)	Apparent K_m value (μM) *	Apparent V_{max} value (μM product(s) formed/min) *
Acyl-CoA Synthetase	115	440 ± 530	100 ± 130
	11.5	266 ± 1232	56.5 ± 254
Δ6-Desaturase †	115	7.9 ± 0.8	0.15 ± 0.01
	11.5	9.6 ± 0.4	0.09 ± 0.01
Lysophospholipid Acyltransferases †	115	1.04 ± 0.84	0.59 ± 0.07
	11.5	2.73 ± 1.77	0.58 ± 0.12

* Measured in reaction mixtures containing hepatic microsomes (0.5 mg protein/ml) and linoleic acid (3.35 -10.8 μM). Incubations were for 10 min for the Δ6-desaturase, which was assayed using Method 2, and 3 min for the acyl-CoA synthetase and lysophospholipid acyltransferase, which were assayed by differential organic extractions (Section 2.2.3.8a, Method B). Other incubation conditions are given in the Methods (Section 2.2.3.2a). Values were obtained using the data illustrated in Figures 32, 33, 34, 35, 36 and 37 and Enzfitter (Section 2.2.3.10).

† Linoleic acid was the substrate.

3.2.6. Simulation of the Reaction Scheme by Computer Modelling Using Experimentally Obtained Data

The reaction scheme outlined in Figure 38 was simulated using information available from the literature (Table 35) and the experimentally obtained data for the acyl-CoA synthetase (Figure 30), Δ6-desaturase (Figures 19 and 20) and lysophospholipid acyltransferases (Figure 30) (Section 3.2.5.4). The model required the concentrations (μM) of lysolecithin, and the enzymes acyl-CoA synthetase, Δ6-desaturase and lysophospholipid acyltransferase. The concentrations of these molecules used in the modelling were chosen or calculated as described in the comments in Table 35. All values are normalised to microsomes at 0.5 mg protein/ml, the experimental conditions used in all of the experiments relevant to this modelling. The rate constant for hydrolysis of acyl-CoAs by acyl-CoA hydrolase is also included therein. This constant was equated with k_{13} in the model. Product formation with time for the various reactions is the experimentally determined data referred to below.

The experimentally determined curves for fatty acid disappearance (Figure 30), acyl-CoA formation (Figure 30), Δ6-desaturation of linoleic acid (Figures 19 and 20) and acylation of phospholipids (Figure 30) versus time were used as a criterion of the success of the computer modelling as follows:

i) For the disappearance of fatty acid, the rate constants in the simulated reaction scheme were altered until the sum of linoleic acid and linoleic acid bound to acyl-CoA synthetase (linoleic acid plus [linoleic acid.E_1] in Figure 38) modelled the experimentally determined disappearance of

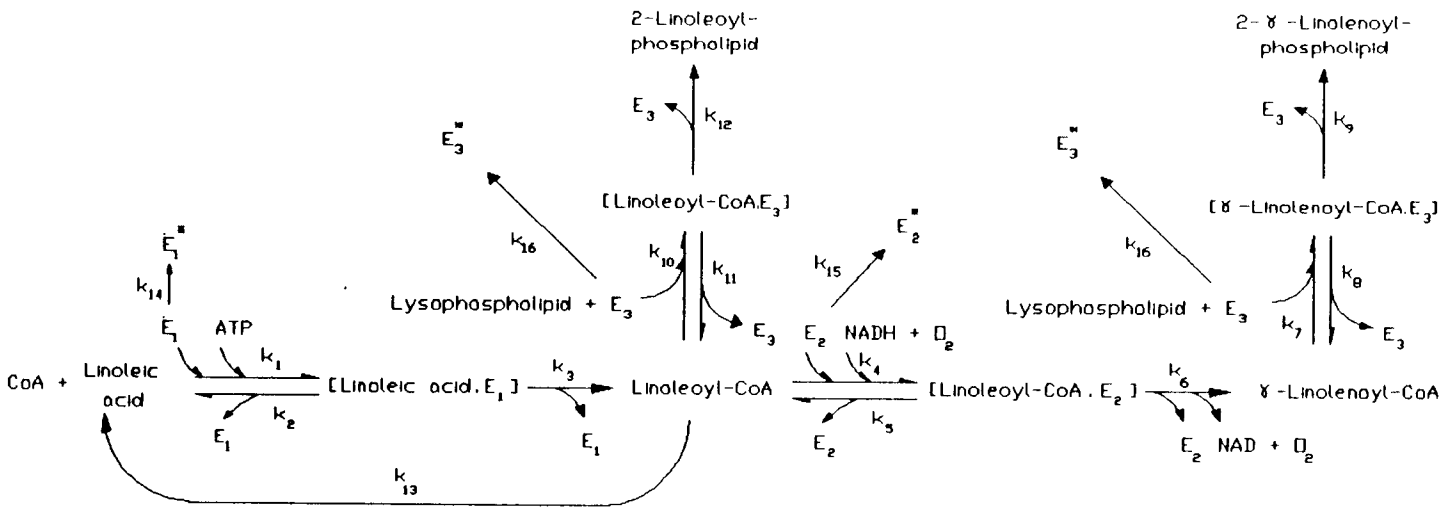

FIGURE 38 **Reaction scheme for the metabolism of linoleic acid in hepatic microsomes used in the computer modelling of the kinetics of the Δ6-desaturase.**

E_1, acyl-CoA synthetase; E_2, Δ6-desaturase; E_3, lysophospholipid acyltransferases. 2-linoleoyl-phospholipid and 2-γ-linolenoyl-phospholipid are the products of acylation of lysophospholipids by the acyltransferases using linoleoyl-CoA and γ-linolenoyl-CoA as substrates, respectively. E_1^*, E_2^* and E_3^* are the products of decay of E_1, E_2 and E_3, respectively.

TABLE 35

LITERATURE DATA USED IN COMPUTER MODELLING OF THE METABOLISM OF LINOLEIC ACID IN HEPATIC MICROSOMES

Component	Value Used	Comments (references)
Lysolecithin	Concentration = 11 μM*§	This value was higher than the literature values of 2.2 μM (400).
Acyl-CoA Synthetase	Concentration = 0.65 μM*	Calculated using MW = 168,000 (212), and specific activities of 55 nmol/min/mg protein in rat hepatic microsomes (355) and 250 nmol/min/mg protein using the purified enzyme (394).
Δ6-Desaturase	Concentration = 0.05 μM*	Within the range calculated using MW = 65,000 (263) and specific activities of 0.108 and 0.428 nmol/min/mg protein in rat hepatic microsomes † and 34.4 nmol/min/mg protein for the purified enzyme (263).
Lysophospholipid Acyltransferases	Concentration = 1.0 μM*§	This value was higher than the values calculated (ca. 0.5 μM) using MW = 225,000 (228) and specific activities of 51.9 nmol/min/mg protein in rat hepatic microsomes and 2303 nmol/min/mg protein after a 30-fold purification (228), and specific activities of 46.7 nmol/min/mg protein in rat hepatic microsomes and 10,000 nmol/min/mg protein after 140-fold purification (226).
Acyl-CoA hydrolase	Rate Constant = 0.11 min^{-1}	Calculated from initial reaction rates (219); equal to k_{13} in reaction scheme (Figure 38).

* At the microsomal protein concentration used in reaction mixtures: 0.5 mg protein/ml.

§ From model 30 on, the concentrations of lysolecithin and lysophospholipid acyltransferases were 2.2 μM and 0.5 μM, respectively.

† The maximum and minimum specific activities obtained for the Δ6-desaturase herein.

linoleic acid with time as closely as possible at 4.7 μM linoleic acid concentration (Figure 30).

ii) For the formation of acyl-CoA, the rate constants in the simulated reaction scheme were altered until the sum of all the acyl-CoA species, free or enzyme-bound (linoleoyl-CoA, γ-linolenoyl-CoA, [linoleoyl-CoA.E_2], [linoleoyl-CoA.E_3] plus [γ-linolenoyl-CoA.E_3] in Figure 38) modelled the experimentally determined production of acyl-CoA with time as closely as possible at 4.7 μM linoleic acid concentration (Figure 30).

iii) For the Δ6-desaturation of linoleic acid, the rate constants in the simulated reaction scheme were altered until the sum of γ-linolenoyl-CoA plus γ-linolenoyl-CoA bound to the lysophospholipid acyltransferases as the enzyme substrate complex, and that incorporated into phospholipids following acylation thereof by lysophospholipid acyltransferase (γ-linolenoyl-CoA, [γ-linolenoyl-CoA.E_3], plus 2-γ-linolenoyl-phospholipid in Figure 38), modelled the experimentally determined rate of Δ6-desaturation of linoleic acid with time as closely as possible at 4.7 μM linoleic acid concentration (Figures 19 and 20).

iv) For the acylation of phospholipids, the rate constants in the simulated reaction scheme were altered until the sum of 2-linoleoyl-phospholipid and 2-γ-linolenoyl-phospholipid (Figure 38) mimicked the experimentally determined acylation of phospholipids with time as closely as possible at 4.7 μM linoleic acid concentration (Figure 30).

For the simulated data, the enzyme-bound products were added to the relevant unbound products; in early models, some of these intermediates were found to present in significant concentrations. For example, in model 23, after 1 min reaction time, ca. 30% of the acyl-CoA was bound to the lysophospholipid acyltransferase in a reversible complex (data not shown).

Prior to modelling the reaction scheme using the above data to obtain calculated values for the kinetic constants k_1 to k_{12}, it was necessary to make certain assumptions to simplify the kinetic treatment. Firstly, we assumed that E_1, E_2 and E_3 followed rapid equilibrium kinetics. Therefore, k_3/k_2 (for E_1), k_6/k_5 (for E_2) and k_{10}/k_9 and k_{12}/k_{11} (for E_3) were equated to 0.1 (399). Secondly, we assumed that the release of radiolabelled fatty acids from the phospholipids was negligible. This assumption was based on our results showing phospholipase A_2 activity to be insignificant under our experimental conditions (see Section 3.2.5.1). The effect of endogenous alternate fatty acid substrates or endogenous fatty acid competitive inhibitors of E_1 or the corresponding acyl-CoA as alternate substrates/competitive inhibitors of E_2 and E_3, was ignored in the model.

The initial values of K_m for E_1, E_2, and E_3 were set at 2 μM, 10 μM and 3 μM, respectively, and of k_{cat} were set at 41 min^{-1}, 2 min^{-1} and 26 min^{-1}, respectively (calculated from data/references in Tables 34, 35, 40 and 42).

After ca. 14 modelling runs, we were still unable to closely mimic the shapes of the curves for the disappearance of linoleic acid and for the formation of acyl-CoA and phospholipid with time (Figure 30); we felt that it was not possible to simulate the experimental data closely with the existing reaction scheme.

Therefore, rate constants for the decay of E_1, E_2 and E_3 were introduced. These unimolecular rate constants were k_{14}, k_{15} and k_{16}, respectively. Pathways allowing for the decay of these enzymes were thus introduced into the reaction scheme and are shown in Figure 38 (See below).

Typical output from SLAM II is shown in Table 36. The rate constants used in the computer output in Table 36 are given at the bottom of page 210 in the order of k_1, k_2, k_3, k_4, k_5, k_6, k_7, k_8, k_9, k_{10}, k_{11}, k_{12}, k_{13}, k_{14}, k_{15} and k_{16}. Also on this page are the initial values of the components of the reaction scheme (Figure 38 and Section 2.2.3.12). The differential equations in SLAM II language are given in Section 2.2.3.12. The disappearance of substrate and formation of eight products as a function of time are shown on page 215 (see Section 2.2.3.12.1 for definition of abbreviations) and the data is illustrated graphically in low resolution on page 216.

In Table 37 are shown the values of the rate constants used in each run in the computer modelling*. Values in boldface indicate that they were changed relative to the previous run or relative to the reference run indicated at the top of the Table. At the bottom of Table 37, are given the values calculated from the indicated run for the equilibrium constants and k_{cats} for acyl-CoA synthetase (E_1), Δ6-desaturase (E_2) and lysophospholipid acyltransferase (E_3).

Overlay plots of the outputs from selected runs are shown in Figures 39 to 80. Separate plots are shown for fatty acid (linoleic acid) disappearance, acyl-CoA formation, Δ6-desaturation of linoleic acid and phospholipid formation with time.

* The initial 15 preliminary modelling runs, which were performed prior to the 37 runs reported in Table 37, are not shown.

TABLE 36

OUTPUT OBTAINED FROM THE SLAM II FOR MODEL 35


```
**********************************************************************
*                                                                    *
*                                                                    *
*                    * * * * * * * * * * * * * *                     *
*                    *                         *                     *
*                    *    SLAM II VERSION 4.02 *                     *
*                    *                         *                     *
*                    * * * * * * * * * * * * * *                     *
*                                                                    *
*                                                                    *
*      C   COPYRIGHT 1983 BY PRITSKER AND ASSOCIATES, INC.           *
*                        ALL RIGHTS RESERVED                         *
*                                                                    *
*                                                                    *
*   THIS SOFTWARE IS PROPRIETARY TO AND A TRADE SECRET OF PRITSKER & *
*   ASSOCIATES, INC. ACCESS TO AND USE OF THIS SOFTWARE IS GRANTED   *
*   UNDER THE TERMS AND CONDITIONS OF THE SOFTWARE LICENSE AGREEMENT *
*   BETWEEN PRITSKER & ASSOCIATES, INC. AND LICENSEE, IDENTIFIED BY  *
*   NUMBER AS FOLLOWS:                                               *
*                                                                    *
*   SERIAL NUMBER: 201313                                            *
*                                                                    *
*   THE TERMS AND CONDITIONS OF THE AGREEMENT SHALL BE STRICTLY      *
*   ENFORCED.  ANY VIOLATION OF THE AGREEMENT MAY VOID LICENSEE'S    *
*   RIGHT TO USE THE SOFTWARE.                                       *
*                                                                    *
*                                                                    *
*                    PRITSKER AND ASSOCIATES, INC.                   *
*                          P.O. BOX 2413                             *
*                    WEST LAFAYETTE, INDIANA 47906                   *
*                          (317)463-5557                             *
*                                                                    *
*                                                                    *
**********************************************************************
```

TABLE 36 CONTINUED

```
_MSC000$JU4:[USERS.MBI.SIC]MODEL35.LOG;1          19-SEP-1991 11:08          Page 3

GEN,ZIMAN,DESAT MODEL,24/10/89
      1  GEN,ZIMAN,DESAT MODEL,24/10/89
INITIALIZE,0.,5.;
      2  INITIALIZE,0.,5.;
CONTINUOUS,18,,,0.005,0.2,H,0.001,0.001;
      3  CONTINUOUS,18,,,0.005,0.2,H,0.001,0.001;
INTLC,SS(1)=4.7,SS(2)=6.5E-1,SS(3)=0.,SS(4)=0.,SS(5)=5.0E-2,SS(6)=0.,
      4  INTLC,SS(1)=4.7,SS(2)=6.5E-1,SS(3)=0.,SS(4)=0.,SS(5)=5.0E-2,SS(6)=0.,
SS(7)=0.,SS(8)=2.2E+0,SS(9)=5.0E-1,SS(10)=0.,SS(11)=0.,SS(12)=0.,
      5  SS(7)=0.,SS(8)=2.2E+0,SS(9)=5.0E-1,SS(10)=0.,SS(11)=0.,SS(12)=0.,
SS(13)=0.,SS(14)=0.,SS(15)=0.;
      6  SS(13)=0.,SS(14)=0.,SS(15)=0.;
INTLC,SS(16)=0.,SS(17)=0.,SS(18)=0.;
      7  INTLC,SS(16)=0.,SS(17)=0.,SS(18)=0.;
RECORD,TNOW,TIME,,8,0.5;
      8  RECORD,TNOW,TIME,,8,0.5;
VAR,SS(1),A,F;
      9  VAR,SS(1),A,F;
VAR,SS(3),B,FE1;
     10  VAR,SS(3),B,FE1;
VAR,SS(4),C,FC;
     11  VAR,SS(4),C,FC;
VAR,SS(6),D,FCE2;
     12  VAR,SS(6),D,FCE2;
VAR,SS(7),E,UC;
     13  VAR,SS(7),E,UC;
VAR,SS(10),F,UCLES;
     14  VAR,SS(10),F,UCLES;
VAR,SS(11),G,PU;
     15  VAR,SS(11),G,PU;
VAR,SS(12),H,FCLES;
     16  VAR,SS(12),H,FCLES;
VAR,SS(13),I,PF;
     17  VAR,SS(13),I,PF;
FIN;
     18  FIN;
.150000+003;
.150000+004;
.250000+002;
.550000+002;
.450000+002;
.140000+001;
.550000+001;
.550000+001;
.200000+001;
.550000+001;
.550000+001;
.200000+001;
.110000+000;
.500000+000;
.000000+000;
.100000+001;
.000000+000;
.000000+000;
```

TABLE 36 CONTINUED

S L A M I I E C H O R E P O R T

SIMULATION PROJECT DESAT MODEL BY ZIMAN

DATE 24/10/1989 RUN NUMBER 1 OF 1

SLAM II VERSION AUG 87

GENERAL OPTIONS

PRINT INPUT STATEMENTS (ILIST):	YES
PRINT ECHO REPORT (IECHO):	YES
EXECUTE SIMULATIONS (IXQT):	YES
WARN OF DESTROYED ENTITIES:	YES
PRINT INTERMEDIATE RESULTS HEADING (IPIRH):	YES
PRINT SUMMARY REPORT (ISMRY):	YES

CONTINUOUS VARIABLES

NUMBER OF DD EQUATIONS (NNEQD):	18
NUMBER OF SS EQUATIONS (NNEQS):	0
MINIMUM STEP SIZE (DTMIN):	3.5000E-04
MAXIMUM STEP SIZE (DTMAX):	3.5000E-02
TIME BETWEEN SAVE POINTS (DTSAV):	3.2000E+00
ACCURACY ERROR SPECIFICATION (LLERR):	WARNING
ABSOLUTE ERROR LIMIT (AAERR):	3.1000E-02
RELATIVE ERROR LIMIT (RRERR):	3.1000E-02

RECORDING OF PLOTS/TABLES

PLOT/TABLE NUMBER 1

INDEPENDENT VARIABLE:	TNOW
IDENTIFIER:	TIME
DATA STORAGE UNIT:	NSET/QSET
DATA OUTPUT FORMAT:	PLOT AND TABLE
TIME BETWEEN PLOT POINTS (DTPLT):	3.5000E+00
STARTING TIME OF PLOT (TTSRT):	0.0000E+00
ENDING TIME OF PLOT (TTEND):	3.5000E+01
DATA POINTS AT EVENTS (KKEVT):	YES

DEPENDENT VARIABLES

VARIABLE	SYMBOL	IDENTIFIER	LOW ORDINATE VALUE		HIGH ORDINATE VALUE	
SS(1)	A	F	MIN TO NEAREST	0.0000E+00	MAX TO NEAREST	0.0000E+00
SS(3)	B	FE1	MIN TO NEAREST	0.0000E+00	MAX TO NEAREST	0.0000E+00
SS(4)	C	FC	MIN TO NEAREST	0.0000E+00	MAX TO NEAREST	0.0000E+00
SS(6)	D	FCE2	MIN TO NEAREST	0.0000E+00	MAX TO NEAREST	0.0000E+00
SS(7)	E	UC	MIN TO NEAREST	0.0000E+00	MAX TO NEAREST	0.0000E+00
SS(10)	F	UCLE3	MIN TO NEAREST	0.0000E+00	MAX TO NEAREST	0.0000E+00
SS(11)	G	PU	MIN TO NEAREST	0.0000E+00	MAX TO NEAREST	0.0000E+00
SS(12)	H	FCLE3	MIN TO NEAREST	0.0000E+00	MAX TO NEAREST	0.0000E+00

TABLE 36 CONTINUED

SS(13) I PF MIN TO NEAREST 0.0000E+00 MAX TO NEAREST 0.0000E+00

RANDOM NUMBER STREAMS

STREAM NUMBER	SEED VALUE	REINITIALIZATION OF STREAM
1	428956419	NO
2	1954324947	NO
3	1145991099	NO
4	1835732737	NO
5	794161987	NO
6	1329531353	NO
7	20049a737	NO
8	63381o299	NO
9	1410143303	NO
10	1282538739	NO

INITIALIZATION OPTIONS

BEGINNING TIME OF SIMULATION (TTBEG):	0.0000E+00
ENDING TIME OF SIMULATION (TTFIN):	0.5000E+01
STATISTICAL ARRAYS CLEARED (JJCLR):	YES
VARIABLES INITIALIZED (JJVAR):	YES
FILES INITIALIZED (JJFIL):	YES

NSET/QSET STORAGE ALLOCATION

DIMENSION OF NSET/QSET (MNSET):	5000
WORDS ALLOCATED TO FILING SYSTEM:	0
WORDS ALLOCATED TO VARIABLES:	19
WORDS AVAILABLE FOR PLOTS/TABLES:	4981

INPUT ERRORS DETECTED: 0

EXECUTION WILL BE ATTEMPTED

TABLE 36 CONTINUED

_MSCDUD$DUA4:[USERS.NBI.SIK]MODEL35.LOG;1 19-S[illegible]-1991 11:06 Page 6

INTERMEDIATE RESULTS

TABLE 36 CONTINUED

MSCOJDS$DUA4:[USERS.MRI.SIK]MODEL35.LOG;1 19-SEP-1991 11:08 Page 7

S L A M I I S U M M A R Y R E P O R T

SIMULATION PROJECT DESAT MODEL BY ZIMAN

DATE 24/10/1989 RUN NUMBER 1 OF 1

CURRENT TIME 0.5000E+01
STATISTICAL ARRAYS CLEARED AT TIME 0.0000E+00

STATE AND DERIVATIVE VARIABLES

(I)	SS(I)	DD(I)
1	0.9222E+00	0.1091E+00
2	0.6512E-01	-0.1069E-01
3	0.5921E-02	-0.2187E-01
4	0.2139E+01	-0.1888E+00
5	0.2115E-01	0.1078E-02
6	0.2885E-01	-0.1078E-02
7	0.1502E+00	0.3160E-01
8	0.7466E+00	-0.7100E-01
9	0.3519E-01	-0.1182E-01
10	0.2976E-02	-0.6265E-03
11	0.2873E-01	0.5952E-02
12	0.4421E-01	-0.2275E-01
13	0.1378E+01	0.8842E-01
14	0.5790E+00	0.3256E-01
15	0.0000E+00	0.0000E+00
16	0.4176E+00	0.3519E-01
17	0.0000E+00	0.0000E+00
18	0.0000E+00	0.0000E+00

TABLE 36 CONTINUED

MSC0005$DUA4:[USERS.MAT.SIK]MODEL35.LOG;21 19-SEP-1991 11:08 Page 8

TABLE NUMBER 1
RUN NUMBER 1

TIME	F	FE1	FC	FCE2	UC	UCLE3	PU	FCLE3	PF
0.0000E+00	0.4700E+01	0.0000E+00	0.0000E+00	0.0000E+00	0.0000E+00	0.0000E+00	0.0000E+00	0.0000E+00	0.0000E+00
0.0000E+00	0.4700E+01	0.0000E+00	0.0000E+00	0.0000E+00	0.0000E+00	0.0000E+00	0.0000E+00	0.0000E+00	0.0000E+00
0.2000E+00	0.3654E+01	0.1600E+00	0.6717E+00	0.1461E-01	0.1773E-02	0.3064E-03	0.3960E-04	0.1663E+00	0.3131E-01
0.4000E+00	0.2991E+01	0.1277E+00	0.1206E+01	0.2157E-01	0.5725E-02	0.8439E-03	0.2714E-03	0.2325E+00	0.1146E+00
0.6000E+00	0.2477E+01	0.1019E+00	0.1630E+01	0.2540E-01	0.1088E-01	0.1317E-02	0.7057E-03	0.2419E+00	0.2102E+00
0.8000E+00	0.2082E+01	0.8127E-01	0.1945E+01	0.2764E-01	0.1665E-01	0.1732E-02	0.1318E-02	0.2375E+00	0.3063E+00
0.1000E+01	0.1778E+01	0.6550E-01	0.2172E+01	0.2901E-01	0.2279E-01	0.2096E-02	0.2085E-02	0.2284E+00	0.3996E+00
0.1200E+01	0.1545E+01	0.5304E-01	0.2332E+01	0.2987E-01	0.2912E-01	0.2417E-02	0.2989E-02	0.2173E+00	0.4888E+00
0.1400E+01	0.1365E+01	0.4384E-01	0.2439E+01	0.3042E-01	0.3553E-01	0.2698E-02	0.4013E-02	0.2054E+00	0.5733E+00
0.1600E+01	0.1228E+01	0.3645E-01	0.2509E+01	0.3074E-01	0.4199E-01	0.2944E-02	0.5143E-02	0.1932E+00	0.6530E+00
0.1800E+01	0.1121E+01	0.3099E-01	0.2550E+01	0.3095E-01	0.4845E-01	0.3154E-02	0.6363E-02	0.1809E+00	0.7278E+00
0.2000E+01	0.1040E+01	0.2636E-01	0.2570E+01	0.3105E-01	0.5493E-01	0.3331E-02	0.7662E-02	0.1688E+00	0.7978E+00
0.2200E+01	0.9791E+00	0.2242E-01	0.2574E+01	0.3106E-01	0.6137E-01	0.3474E-02	0.9024E-02	0.1570E+00	0.8629E+00
0.2400E+01	0.9326E+00	0.1972E-01	0.2566E+01	0.3103E-01	0.6780E-01	0.3585E-02	0.1044E-01	0.1456E+00	0.9234E+00
0.2600E+01	0.8933E+00	0.1745E-01	0.2550E+01	0.3096E-01	0.7423E-01	0.3665E-02	0.1189E-01	0.1346E+00	0.9794E+00
0.2800E+01	0.8741E+00	0.1531E-01	0.2527E+01	0.3085E-01	0.8059E-01	0.3716E-02	0.1336E-01	0.1241E+00	0.1031E+01
0.3000E+01	0.8574E+00	0.1401E-01	0.2499E+01	0.3072E-01	0.8695E-01	0.3739E-02	0.1486E-01	0.1141E+00	0.1079E+01
0.3200E+01	0.8477E+00	0.1231E-01	0.2469E+01	0.3058E-01	0.9331E-01	0.3737E-02	0.1635E-01	0.1047E+00	0.1123E+01
0.3400E+01	0.8428E+00	0.1151E-01	0.2436E+01	0.3042E-01	0.9965E-01	0.3711E-02	0.1784E-01	0.9585E-01	0.1163E+01
0.3600E+01	0.8429E+00	0.1034E-01	0.2401E+01	0.3024E-01	0.1060E+00	0.3666E-02	0.1932E-01	0.8756E-01	0.1199E+01
0.3800E+01	0.8468E+00	0.9274E-02	0.2365E+01	0.3006E-01	0.1123E+00	0.3603E-02	0.2077E-01	0.7982E-01	0.1233E+01
0.4000E+01	0.8535E+00	0.8713E-02	0.2328E+01	0.2987E-01	0.1186E+00	0.3524E-02	0.2220E-01	0.7263E-01	0.1263E+01
0.4200E+01	0.8634E+00	0.7795E-02	0.2290E+01	0.2968E-01	0.1250E+00	0.3432E-02	0.2359E-01	0.6597E-01	0.1291E+01
0.4400E+01	0.8751E+00	0.7440E-02	0.2253E+01	0.2949E-01	0.1313E+00	0.3329E-02	0.2494E-01	0.5983E-01	0.1316E+01
0.4600E+01	0.8889E+00	0.7122E-02	0.2215E+01	0.2927E-01	0.1376E+00	0.3218E-02	0.2625E-01	0.5417E-01	0.1339E+01
0.4800E+01	0.9050E+00	0.6772E-02	0.2177E+01	0.2906E-01	0.1439E+00	0.3099E-02	0.2752E-01	0.4897E-01	0.1359E+01
0.5000E+01	0.9225E+00	0.6561E-02	0.2139E+01	0.2885E-01	0.1502E+00	0.2976E-02	0.2873E-01	0.4421E-01	0.1378E+01
0.5000E+01	0.9222E+00	0.5921E-02	0.2139E+01	0.2885E-01	0.1502E+00	0.2976E-02	0.2873E-01	0.4421E-01	0.1378E+01
MINIMUM	0.8428E+00	0.0000E+00	0.0000E+00	0.0000E+00	0.0000E+00	0.0000E+00	0.0000E+00	0.0000E+00	0.0000E+00
MAXIMUM	0.4700E+01	0.1600E+00	0.2574E+01	0.3106E-01	0.1502E+00	0.3739E-02	0.2873E-01	0.2419E+00	0.1378E+01

TABLE 36 CONTINUED

```
MSC000$DUA4:[USERS.MBI.SIK]MODEL35.LOG;1            19-SEP-1991 11:08                    Page 9
                                          **PLOT NUMBER  1**
                                            RUN  NUMBER  1
                                            SCALES OF PLOT
A=F        0.8428E+00        0.1807E+01        0.2771E+01        0.3736E+01        0.4700E+01
B=FE1      0.0000E+00        0.4001E-01        0.8002E-01        0.1200E+00        0.1600E+00
C=FC       0.0000E+00        0.6434E+00        0.1287E+01        0.1930E+01        0.2574E+01
D=FCE2     0.0000E+00        0.7766E-02        0.1553E-01        0.2330E-01        0.3106E-01
E=UC       0.0000E+00        0.3756E-01        0.7512E-01        0.1127E+00        0.1502E+00
F=UCLE3    0.0000E+00        0.9347E-03        0.1869E-02        0.2804E-02        0.3739E-02
G=PU       0.0000E+00        0.7183E-02        0.1437E-01        0.2155E-01        0.2873E-01
H=FCLE3    0.0000E+00        0.6047E-01        0.1209E+00        0.1814E+00        0.2419E+00
I=PF       0.0000E+00        0.3445E+00        0.6890E+00        0.1034E+01        0.1378E+01
```

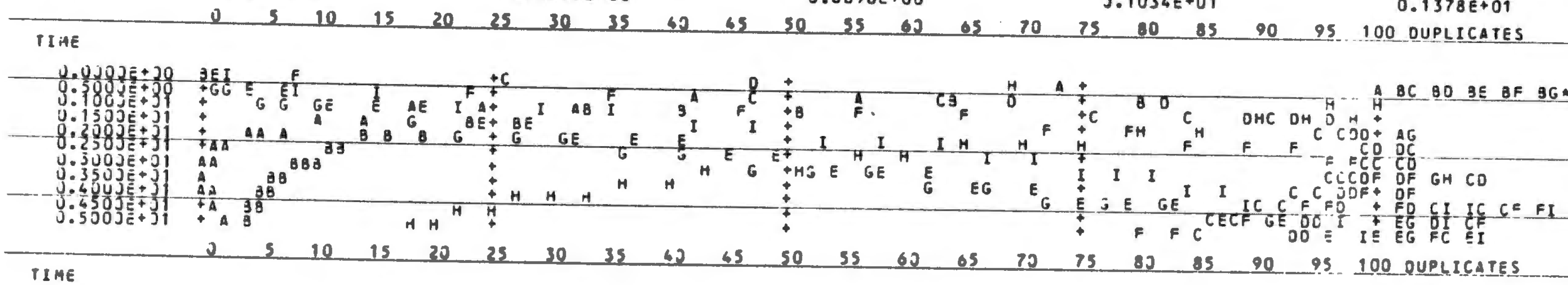

```
OUTPUT  CONSISTS  OF      28 POINT SETS (    252 POINTS)
STORAGE ALLOCATED FOR    498 POINT SETS (   4983 WORDS )
STORAGE  NEEDED   FOR     28 POINT SETS (    280 WORDS )
FORTRAN STOP
SIK          Job terminated at 19-SEP-1991 11:08:54.35

Accounting information:
Buffered I/O count:              72      Peak working set size:     1001
Direct I/O count:                97      Peak page file size:       3999
Page faults:                    813      Mounted volumes:              0
Charged CPU time:     0 00:00:36.70      Elapsed time:     0 00:00:37.27
```

TABLE 37

VALUES OF RATE CONSTANTS AS A FUNCTION OF COMPUTER MODELLING RUN

k	RUN 1	2	3	4	5	6	7	8	9	10	11
1	500	**150**	150	150	150	150	150	150	150	150	150
2	300	300	**1500**	**4500**	4500	4500	**1000**	**1500**	**1800**	1500	1500
3	30	30	30	30	**45**	**60**	30	30	30	30	30
4	55	55	55	55	55	55	55	55	55	55	55
5	22	22	22	22	22	22	22	22	22	22	22
6	2.2	2.2	2.2	2.2	**3**	**3**	**2.6**	**2.6**	**2.6**	**2**	2
7	110	**5.5**	5.5	5.5	5.5	5.5	5.5	5.5	5.5	5.5	**2.5**
8	5.5	5.5	**16**	16	16	16	5.5	5.5	5.5	5.5	5.5
9	0.55	0.55	0.55	0.55	**0.4**	**0.4**	0.55	0.55	0.55	0.55	**2**
10	110	**5.5**	5.5	5.5	5.5	5.5	5.5	5.5	5.5	5.5	**2.5**
11	5.5	5.5	**16**	16	16	16	5.5	5.5	5.5	5.5	5.5
12	0.55	0.55	0.55	0.55	**0.4**	**0.4**	0.55	0.55	0.55	0.55	**2**
13	0.11	0.11	0.11	0.11	0.11	0.11	0.11	0.11	0.11	0.11	0.11
14											
15											
16											
CALCULATED EQUILIBRIUM CONSTANTS AND Kcat VALUES											
K E1	0.66	2.20	10.20	30.20	30.30	30.40	6.87	10.20	12.20	10.20	10.20
K E2	0.44	0.44	0.44	0.44	0.45	0.45	0.45	0.45	0.45	0.44	0.44
K E3	0.06	1.10	3.01	3.01	2.98	2.98	1.10	1.10	1.10	1.10	3.00
kcat E1	30.00	30.00	30.00	30.00	45.00	60.00	30.00	30.00	30.00	30.00	30.00
kcat E2	2.20	2.20	2.20	2.20	3.00	3.00	2.60	2.60	2.60	2.00	2.00
kcat E3	0.55	0.55	0.55	0.55	0.40	0.40	0.55	0.55	0.55	0.55	2.00

Abbreviations used are E1, acyl-CoA synthetase, E2; Δ6-desaturase; E3, lysophospholipid acyltransferase.

TABLE 37 CONTINUED

k	12	13	14	RUN 15	16	17	18	19	20	21	22
1	150	150	150	150	150	150	150	150	150	150	150
2	1500	1500	1500	1500	1500	1500	1500	1500	1500	1500	1500
3	**25**	**15**	**25**	25	25	25	25	25	25	25	25
4	55	55	55	55	55	55	55	55	55	55	55
5	22	22	22	22	22	22	22	22	22	22	22
6	2	2	2	2	2	2	2	2	2	2	2
7	5.5	5.5	5.5	5.5	5.5	5.5	5.5	5.5	5.5	5.5	5.5
8	5.5	5.5	5.5	5.5	5.5	5.5	5.5	5.5	5.5	5.5	5.5
9	0.55	0.55	**2**	0.55	0.55	0.55	0.55	0.55	0.55	0.55	0.55
10	5.5	5.5	5.5	5.5	5.5	5.5	5.5	5.5	5.5	5.5	5.5
11	5.5	5.5	5.5	5.5	5.5	5.5	5.5	5.5	5.5	5.5	5.5
12	0.55	0.55	**2**	0.55	0.55	0.55	0.55	0.55	0.55	0.55	0.55
13	0.11	0.11	0.11	0.11	0.11	0.11	0.11	0.11	0.11	0.11	0.11
14				**0.02**	**0.8**			**0.3**	**0.1**	**0.3**	**0.3**
15											
16						**0.05**	**0.2**			**1**	**10**

CALCULATED EQUILIBRIUM CONSTANTS AND Kcat VALUES

K E1	10.17	10.10	10.17	10.17	10.17	10.17	10.17	10.17	10.17	10.17	10.17
K E2	0.44	0.44	0.44	0.44	0.44	0.44	0.44	0.44	0.44	0.44	0.44
K E3	1.10	1.10	1.36	1.10	1.10	1.10	1.10	1.10	1.10	1.10	1.10
kcat E1	25.00	15.00	25.00	25.00	25.00	25.00	25.00	25.00	25.00	25.00	25.00
kcat E2	2.00	2.00	2.00	2.00	2.00	2.00	2.00	2.00	2.00	2.00	2.00
kcat E3	0.55	0.55	2.00	0.55	0.55	0.55	0.55	0.55	0.55	0.55	0.55

TABLE 37 CONTINUED

k	23	24	25	26	27	28	29
1	150	150	**120**	**120**	150	150	150
2	1500	1500	1500	1500	1500	1500	1500
3	25	25	25	**30**	25	25	25
4	55	55	55	55	55	55	55
5	22	22	22	22	22	22	22
6	2	2	2	2	**1.6**	**1.72**	**1.85**
7	5.5	5.5	5.5	5.5	5.5	5.5	5.5
8	5.5	5.5	5.5	5.5	5.5	5.5	5.5
9	0.55	0.55	0.55	0.55	0.55	0.55	0.55
10	5.5	5.5	5.5	5.5	5.5	5.5	5.5
11	5.5	5.5	5.5	5.5	5.5	5.5	5.5
12	0.55	0.55	0.55	0.55	0.55	0.55	0.55
13	0.11	0.11	0.11	0.11	0.11	0.11	0.11
14	**0.5**	**0.5**	**0.5**	**0.5**	0.5	0.5	0.5
15							
16	**1**	**4**	**4**	**4**	1	1	1
CALCULATED EQUILIBRIUM CONSTANTS AND Kcat VALUES							
K E1	10.17	10.17	12.71	12.75	10.17	10.17	10.17
K E2	0.44	0.44	0.44	0.44	0.43	0.43	0.43
K E3	1.10	1.10	1.10	1.10	1.10	1.10	1.10
kcat E1	25.00	25.00	25.00	30.00	25.00	25.00	25.00
kcat E2	2.00	2.00	2.00	2.00	1.60	1.72	1.85
kcat E3	0.55	0.55	0.55	0.55	0.55	0.55	0.55

TABLE 37 CONTINUED

	Modelled on run 27, 2.2 uM lysophospholipid, 0.5 uM E3				Modelled on run 33			Modelled on run 35
k	30	31	32	33	34	*35*	36	35A
1	150	150	150	150	150	*150*	150	150
2	1500	1500	1500	1500	1500	*1500*	1500	1500
3	25	25	25	25	25	*25*	25	25
4	55	55	55	55	55	*55*	**65**	**46**
5	22	22	22	22	**70**	***85***	**85**	85
6	1.6	1.6	1.6	1.6	**1.28**	***1.28***	**1.28**	1.28
7	5.5	5.5	5.5	5.5	5.5	*5.5*	5.5	5.5
8	5.5	5.5	5.5	5.5	5.5	*5.5*	5.5	5.5
9	0.55	**1.1**	**1.7**	**2.2**	**2**	***2***	**2**	2
10	5.5	5.5	5.5	5.5	5.5	*5.5*	5.5	5.5
11	5.5	5.5	5.5	5.5	5.5	*5.5*	5.5	5.5
12	0.55	**1.1**	**1.7**	**2.2**	**2**	***2***	**2**	2
13	0.11	0.11	0.11	0.11	0.11	*0.11*	0.11	0.11
14	0.5	0.5	0.5	0.5	0.5	*0.5*	0.5	0.5
15								
16	1	1	1	1	1	*1*	1	1
CALCULATED EQUILIBRIUM CONSTANTS AND Kcat VALUES								
K E1	10.17	10.17	10.17	10.17	10.17	*10.17*	10.17	10.17
K E2	0.43	0.43	0.43	0.43	1.30	*1.57*	1.33	1.88
K E3	1.10	1.20	1.31	1.40	1.36	*1.36*	1.36	1.36
kcat E1	25.00	25.00	25.00	25.00	25.00	*25.00*	25.00	25.00
kcat E2	1.60	1.60	1.60	1.60	1.28	*1.28*	1.28	1.28
kcat E3	0.55	1.10	1.70	2.20	2.00	*2.00*	2.00	2.00

Data from several runs are overlaid on a single plot. Included in each plot for reference is the relevant experimental data.

In models 2 - 4 (Figures 39, 40, 41 and 42), fatty acid concentration decayed towards zero in an exponential, while the experimental data appeared to be biphasic (Figure 39). No model fitted the shape of the curve well. Increasing k_2 by a factor of 15 (compare model 4 to model 2), decreased the loss of linoleic acid. The production of acyl-CoA esters was at too fast an initial rate in models 2 and 3, and too slow an initial rate in model 4 (Figure 40). All three models showed too striking a secondary decay of acyl-CoA levels after about 1 to 3 minutes. All three models approximated the Δ6-desaturase reaction (Figure 41). None of the three modelled the shape of the curve for phospholipid formation, although values of phospholipid formation were within 50 to 100% of the experimental data (Figure 42).

Models 7, 8 and 9 were compared to model 2 and the experimental data in Figures 43, 44, 45 and 46. k_2 was increased in models 7, 8 and 9 relative to model 2 by a factor of 3 to 6, but was ca. two- to five-fold below the value in model 6. k_6 was also intermediate between models 2 and 6; k_8 and k_{11} were unchanged relative to model 2. Models 7, 8 and 9 modelled the experimental data for fatty acid disappearance closer than did model 2 (Figure 43), with model 9 better than 8, and 8 better than 7, respectively. This correlated with and reflected the increase in k_2. With regard to acyl-CoA formation, model 9 most closely mimicked the data, but in all three models, acyl-CoA levels increased too strikingly up to 2 minutes and decreased faster than the experimental data thereafter (Figure 44). Models 7, 8 and 9 were, however, an improvement on model 2 for fitting acyl-CoA formation with time. Models 7, 8

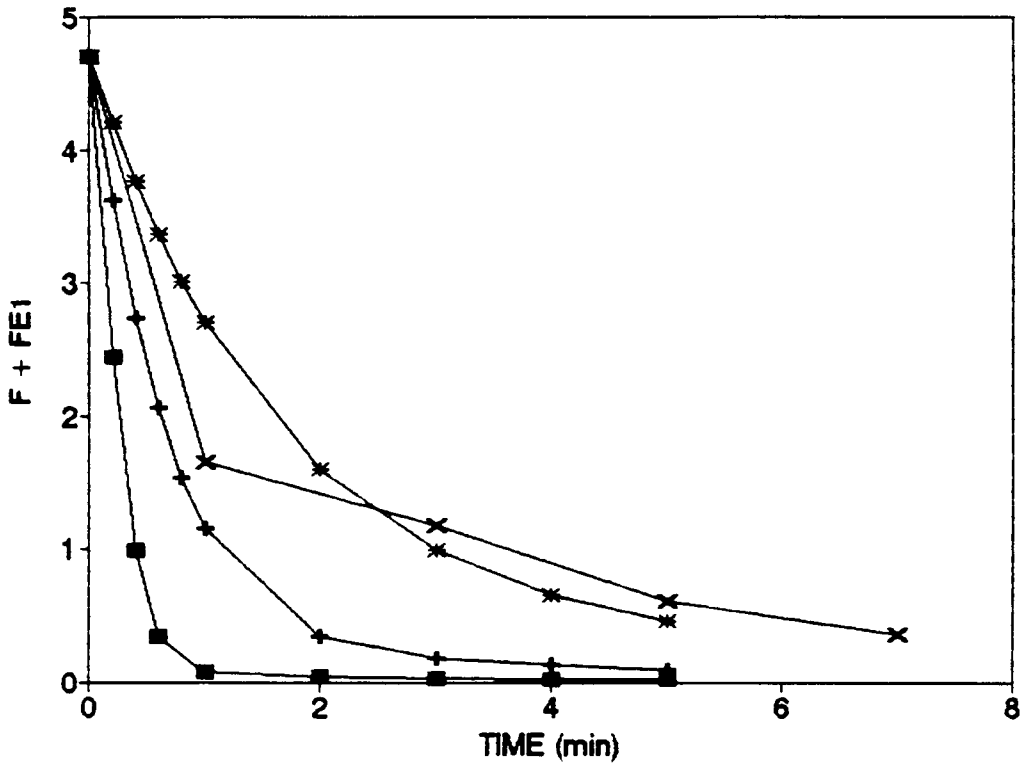

FIGURE 39 **Overlay plots of the effect of time on the disappearance of linoleic acid measured during the metabolism of linoleic acid (4.7 μM) using data from models 2 (■), 3 (+), 4 (*), and the experimental data from Figure 30 (X).**

F + FE1, μM free linoleic acid plus that bound to the acyl-CoA synthetase.

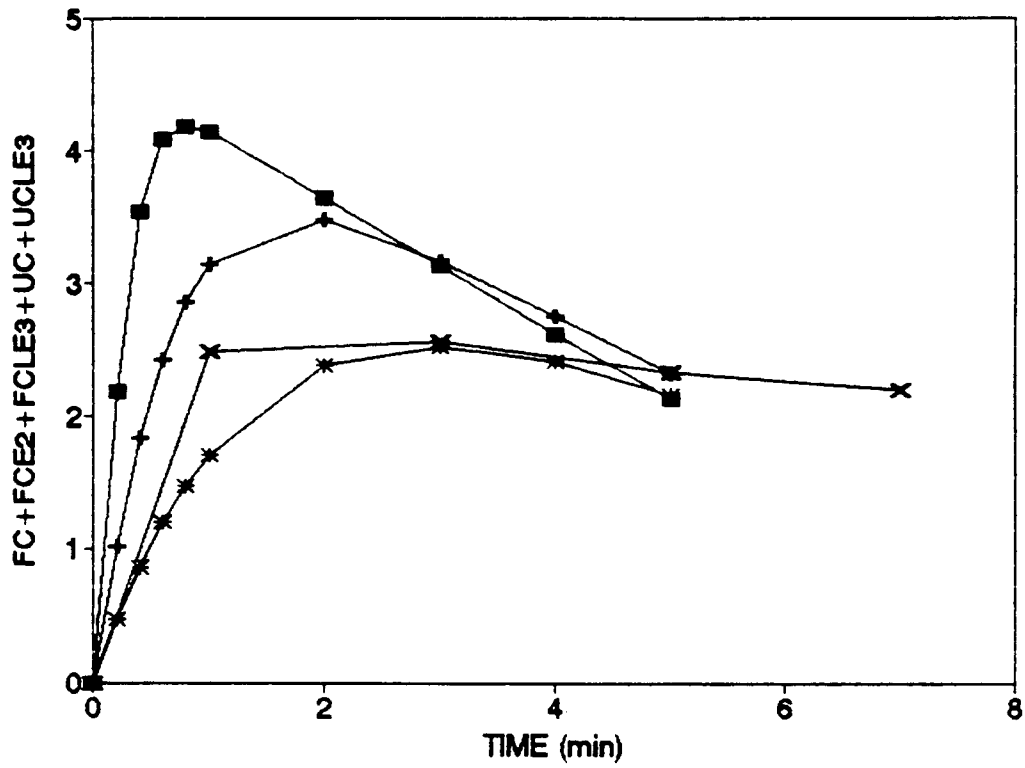

FIGURE 40 **Overlay plots of the effect of time on the formation of acyl-CoA measured during the metabolism of linoleic acid (4.7 μM) using data from models 2 (■), 3 (+), 4 (*), and the experimental data from Figure 30 (X).**

FC + FCE2 + FCLE3 + UC + UCLE3, μM free linoleoyl-CoA plus γ-linolenoyl-CoA plus that bound to the Δ6-desaturase and lysophospholipid acyltransferase.

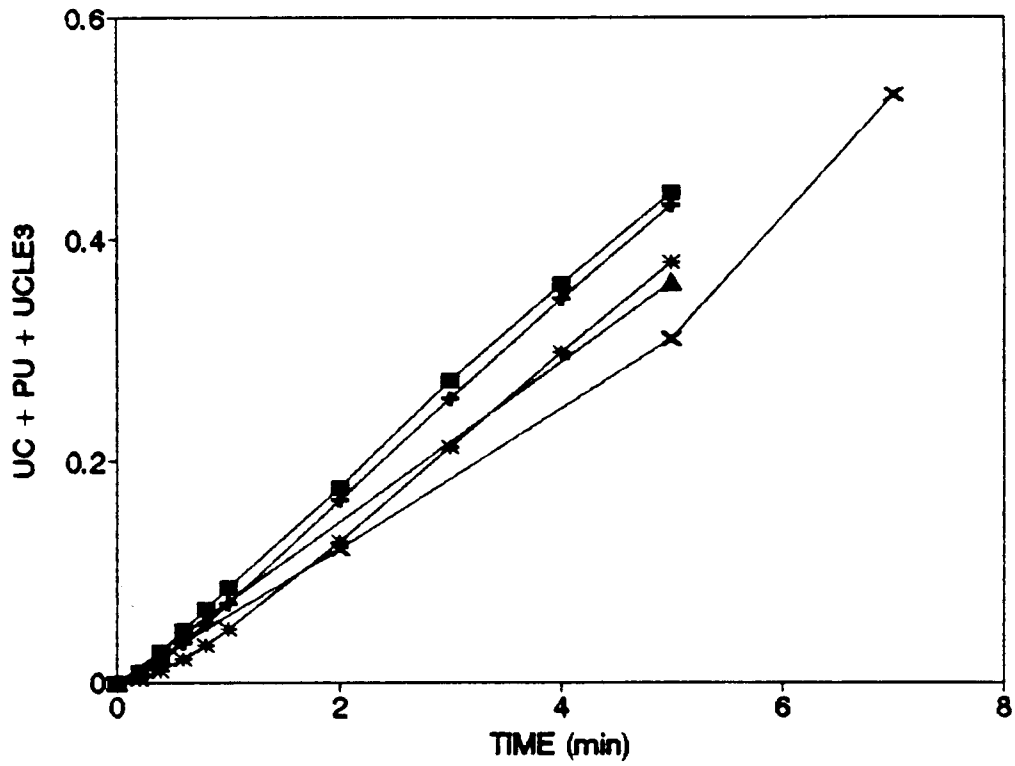

FIGURE 41

Overlay plots of the effect of time on the Δ6-desaturation of linoleic acid (4.7 μM) using data from models 2 (■), 3 (+), 4 (*), and the experimental data from Figures 19 (▲) and 20 (X).

UC + PU + UCLE3, μM free γ-linolenoyl-CoA plus that bound to the lysophospholipid acyltransferase plus that acylated into phospholipids.

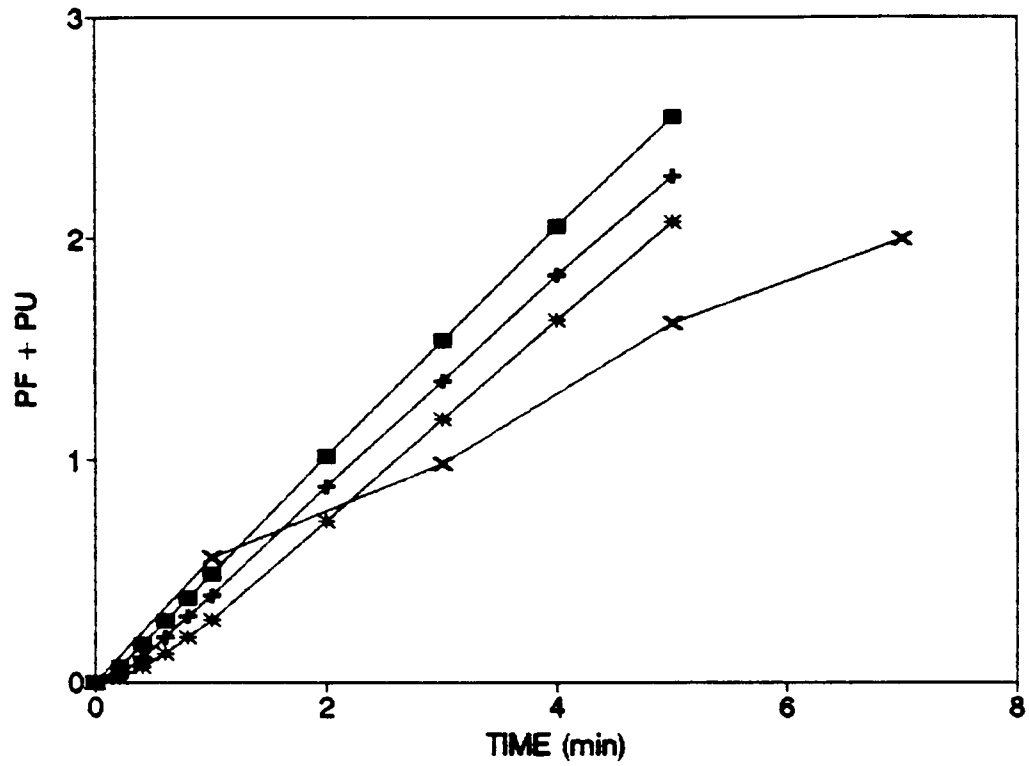

FIGURE 42 **Overlay plots of the effect of time on the acylation of phospholipids measured during the metabolism of linoleic acid (4.7 μM) using data from models 2 (■), 3 (+), 4 (*), and the experimental data from Figure 30 (X).**

PF + PU, μM linoleoyl-CoA acid plus γ-linolenoyl-CoA acylated into phospholipids.

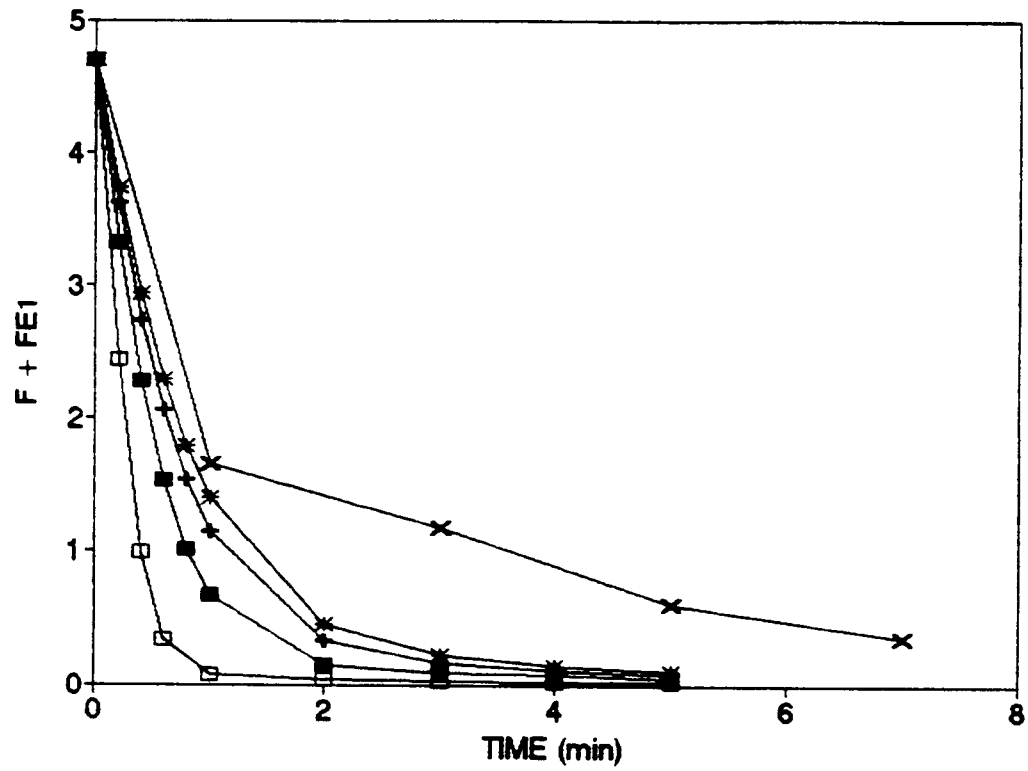

FIGURE 43 **Overlay plots of the effect of time on the disappearance of linoleic acid measured during the metabolism of linoleic acid (4.7 μM) using data from models 2 (□), 7 (■), 8 (+), 9 (*) and the experimental data from Figure 30 (X).**

F + FE1, μM free linoleic acid plus that bound to the acyl-CoA synthetase.

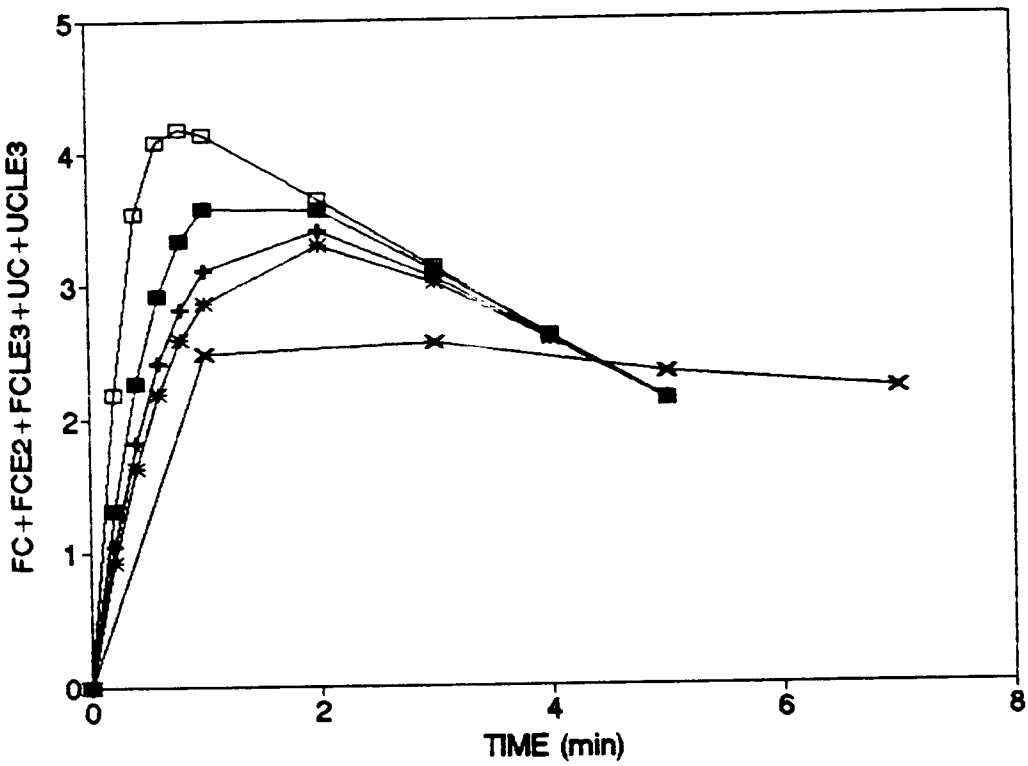

FIGURE 44 **Overlay plots of the effect of time on the formation of acyl-CoA measured during the metabolism of linoleic acid (4.7 μM) using data from models 2 (□), 7 (■), 8 (+), 9 (*) and the experimental data from Figure 30 (X).**

FC + FCE2 + FCLE3 + UC + UCLE3, μM free linoleoyl-CoA plus γ-linolenoyl-CoA plus that bound to the Δ6-desaturase and lysophospholipid acyltransferase.

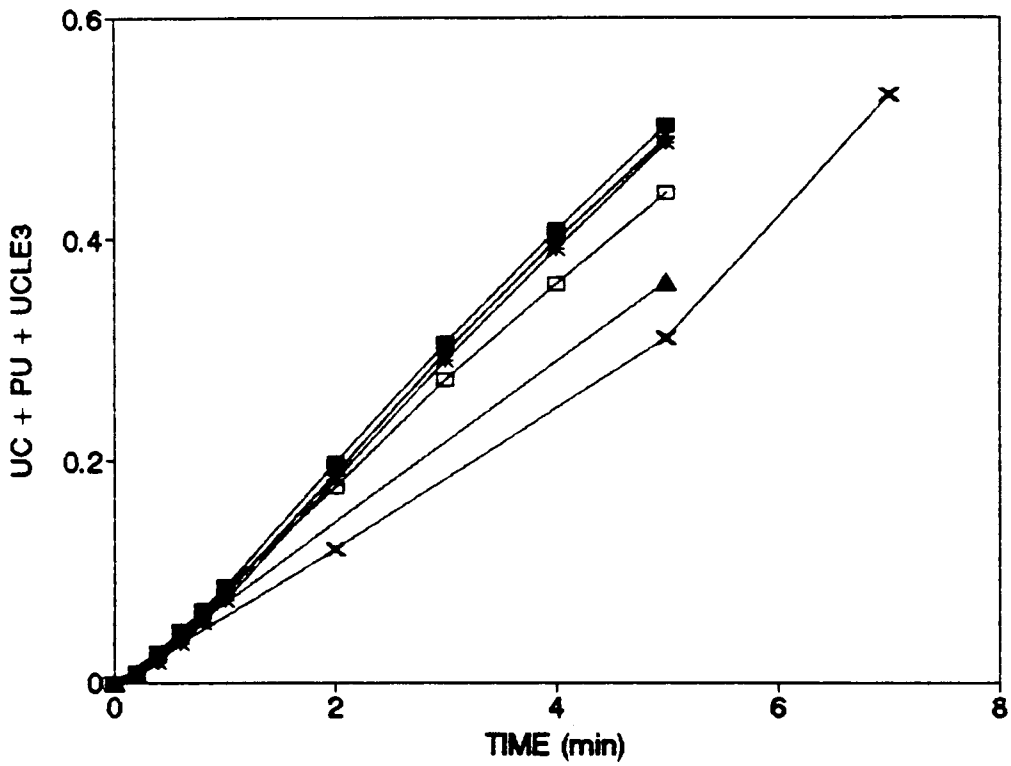

FIGURE 45 **Overlay plots of the effect of time on the Δ6-desaturation of linoleic acid (4.7 μM) using data from models 2 (□), 7 (■), 8 (+), 9 (*) and the experimental data from Figures 19 (▲) and 20 (X).**

UC + PU + UCLE3, μM free γ-linolenoyl-CoA plus that bound to the lysophospholipid acyltransferase plus that acylated into phospholipids.

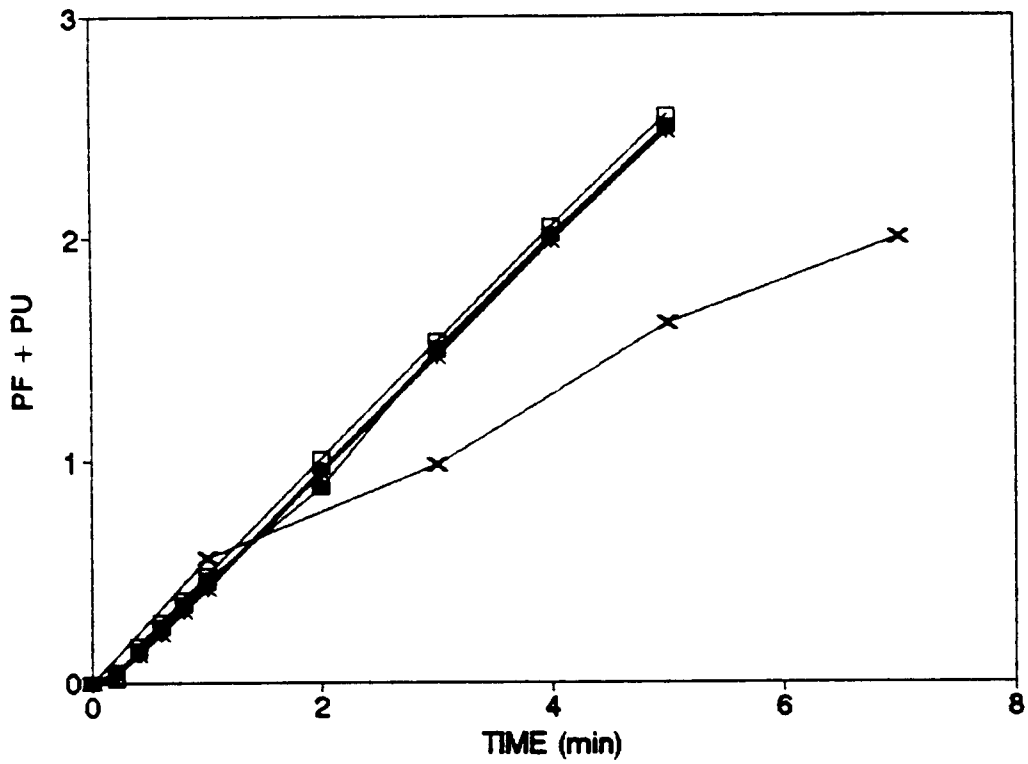

FIGURE 46 **Overlay plots of the effect of time on the acylation of phospholipids measured during the metabolism of linoleic acid (4.7 μM) using data from models 2 (□), 7 (■), 8 (+), 9 (*) and the experimental data from Figure 30 (X).**

PF + PU, μM linoleoyl-CoA acid plus γ-linolenoyl-CoA acylated into phospholipids.

and 9 approximated the Δ6-desaturase reaction, but were ca. 50% above the experimental data (Figure 45). Models 7, 8, 9 and 2 all approximated phospholipid formation over 1 minute but exceeded experimental phospholipid formation thereafter (Figure 46).

Figures 47, 48, 49 and 50 compare the results of models 8, 12, 13 and 14 to the experimental data. Relative to models 8 or 10, models 12 and 13 diminished k_3 by up to two-fold. In models 12 to 14, k_6 was decreased by approximately 25% relative to model 8, and model 14 additionally increased k_9 and k_{12} by 3.6-fold relative to models 8 and 10. As with previous runs, although the computer generated data bracketed the experimental data, the computer generated data followed a smooth exponential or linear curves, while the experimental data appeared biphasic for fatty acid disappearance and phospholipid formation, respectively (Figures 47 and 50). This led us to introduce additional constants for the decay of activity of E_1, E_2 and E_3 in subsequent runs in an attempt to model the biphasic curves. Models 8, 12 and 14 generated almost identical curves for fatty acid disappearance with time (Figure 47); this reflected identical k_1, k_2, k_4, k_5, k_7, k_8, k_{10}, k_{11} and k_{13} values in these models. k_3 differed only by 20% among the models and this slight variation in k_3 appeared to be without striking effect on fatty acid disappearance. The differences in k_9 and k_{12} between models 13 and 14 were so late in the reaction pathway as apparently to be without significant effect on the first step in linoleic acid metabolism, viz: its conversion to acyl-CoA.

Models 8, 12 and 14 showed acyl-CoA formation exceeding the experimental data over an initial period of from 0.5 to 4 minutes (Figure 48). After ca. 1 to 2 minutes, acyl-CoA levels in these models declined at a far greater rate than did

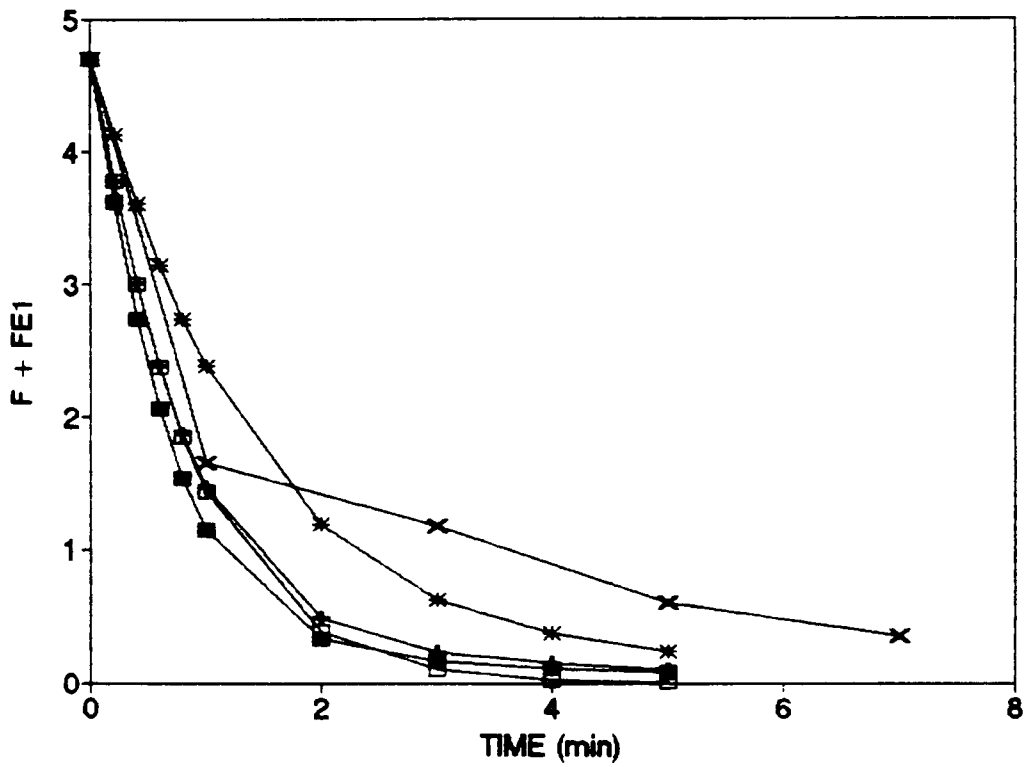

FIGURE 47 **Overlay plots of the effect of time on the disappearance of linoleic acid measured during the metabolism of linoleic acid (4.7 μM) using data from models 8 (■), 12 (+), 13 (*), 14 (□) and the experimental data from Figure 30 (X).**

F + FE1, μM free linoleic acid plus that bound to the acyl-CoA synthetase.

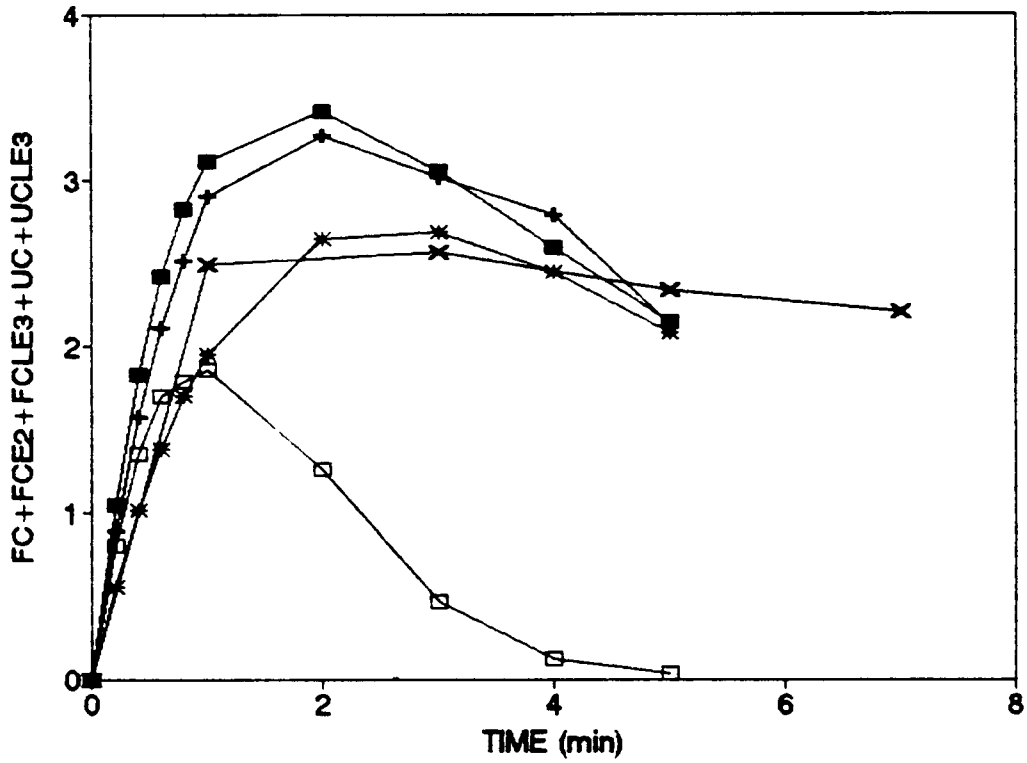

FIGURE 48 **Overlay plots of the effect of time on the formation of acyl-CoA measured during the metabolism of linoleic acid (4.7 μM) using data from models 8 (■), 12 (+), 13 (*), 14 (□) and the experimental data from Figure 30 (X).**

FC + FCE2 + FCLE3 + UC + UCLE3, μM free linoleoyl-CoA plus γ-linolenoyl-CoA plus that bound to the Δ6-desaturase and lysophospholipid acyltransferase.

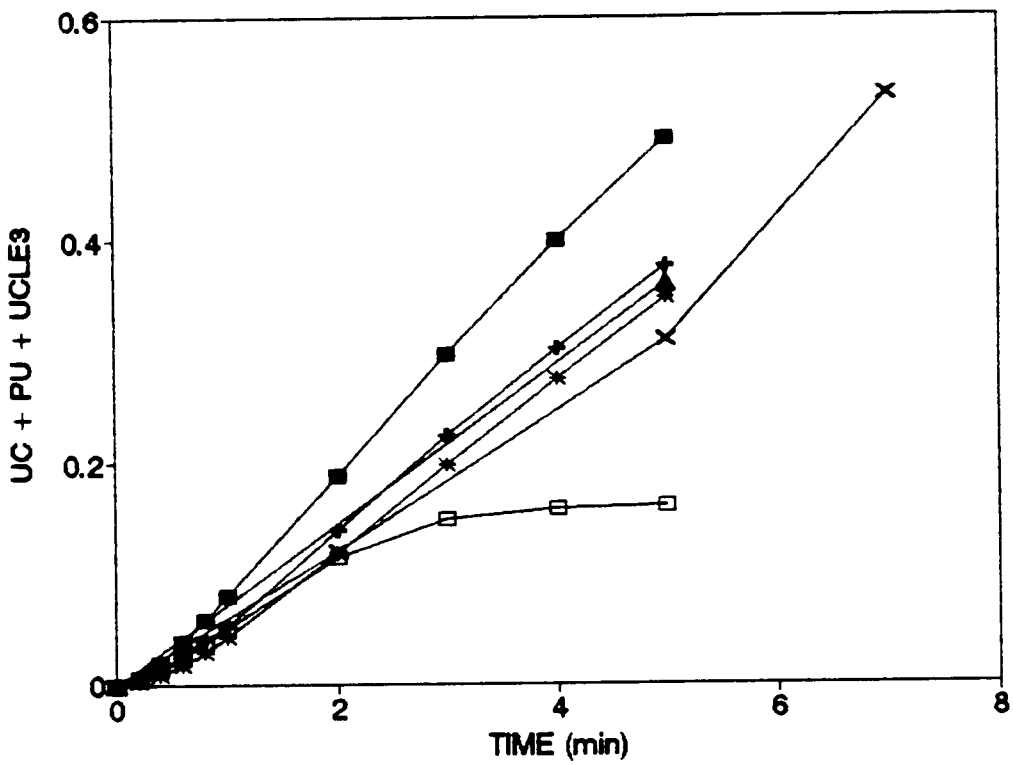

FIGURE 49 **Overlay plots of the effect of time on the Δ6-desaturation of linoleic acid (4.7 μM) using data from models 8 (■), 12 (+), 13 (*), 14 (□) and the experimental data from Figures 19 (▲) and 20 (X).**

UC + PU + UCLE3, μM free γ-linolenoyl-CoA plus that bound to the lysophospholipid acyltransferase plus that acylated into phospholipids.

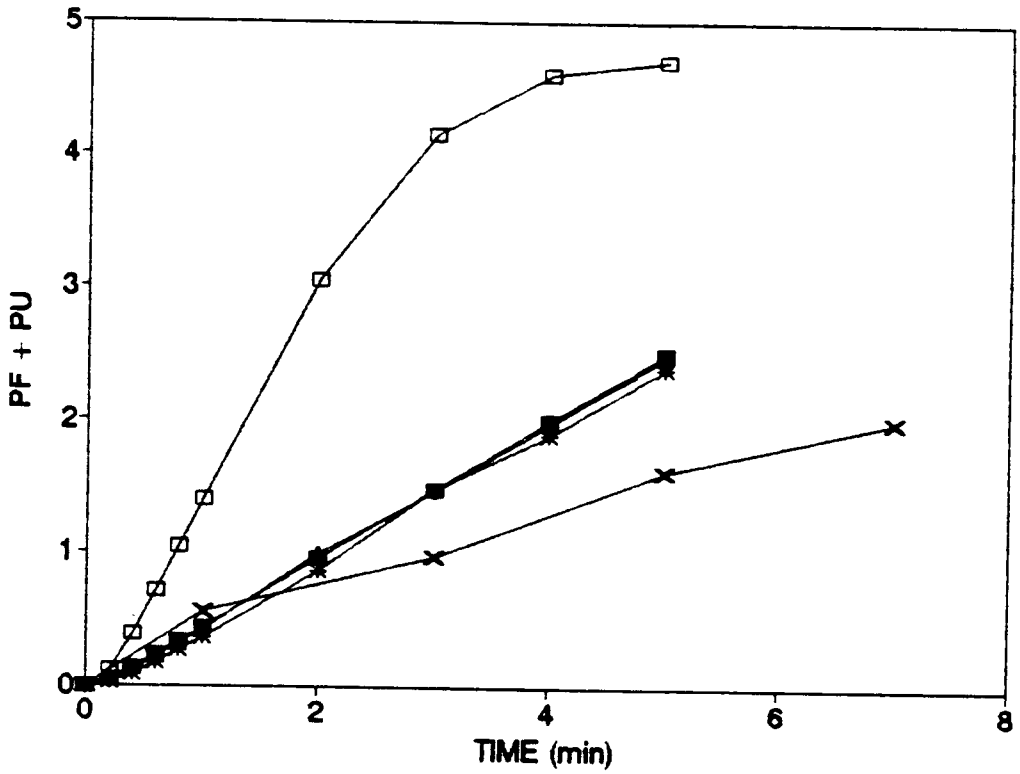

FIGURE 50 **Overlay plots of the effect of time on the acylation of phospholipids measured during the metabolism of linoleic acid (4.7 μM) using data from models 8 (■), 12 (+), 13 (⋆), 14 (□) and the experimental data from Figure 30 (X).**

PF + PU, μM linoleoyl-CoA acid plus γ-linolenoyl-CoA acylated into phospholipids.

the experimental data. Model 13 mimicked acyl-CoA formation well up to ca. 0.5 minutes, then plateaued at approximately the same acyl-CoA levels as the experimental data and showed a slight decline after ca. 2 minutes. For the Δ6-desaturase reaction, model 8 provided data above experimental levels, and model 14, data well below the experimental (Figure 49). For the latter model, Δ6-desaturase product tapered off to a plateau not seen in the experimental data. Models 12 and 13 mimicked the experimental data for the Δ6-desaturase well. For phospholipid formation, model 14 far exceeded the experimental data; the remaining models were virtually superimposible on each other, and on the experimental data for ca. 2 minutes. Thereafter, the modelled levels of phospholipid formation exceeded the experimental data (Figure 50).

Figures 51, 52, 53 and 54 compare the results of models 16, 19, 20, 21 and 22 to experimental data. In this set of models, non-zero values for rate constants 14 and/or 16 are used. These constants allow for decay of the activity of E_1 and E_3. k_{15} remained zero, since the shape of the curve for the Δ6-desaturase enzyme, E_2, was modelled by the computer generated data. Values for k_{14} varied from 0.1 to 0.8, and for k_{16} from 0 to 10. Fatty acid disappearance over the first minute was closely approximated by models 19, 20, 21 and 22 (Figure 51). Model 16 gave slightly lower loss of fatty acid over the first minute. The increasing value of k_{14} in models 20, 19 and 16 respectively resulted in the plateauing of the slower phase of fatty acid disappearance between 2 and 5 minutes at increasing levels of fatty acid remaining. The introduction of k_{16} of 1 in model 21 did not significantly affect the plot relative to model 19, while increasing this constant to 10 in model 22 resulted in a non-plateau in fatty acid concentration with time, but a trough and subsequent upswing.

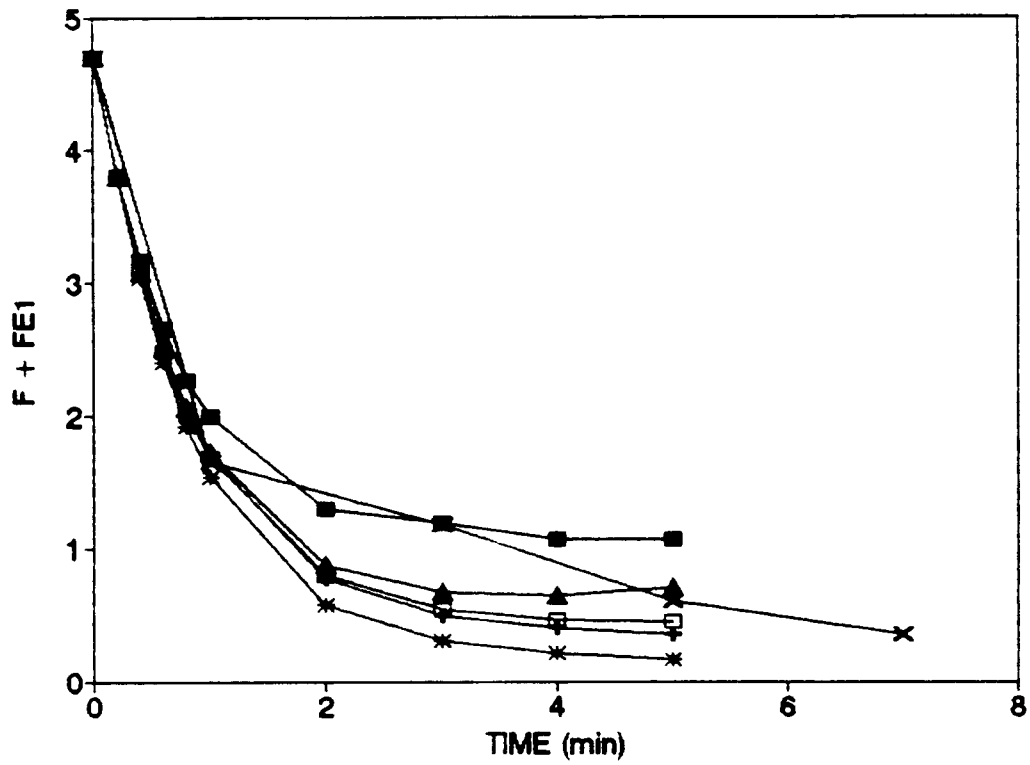

FIGURE 51 **Overlay plots of the effect of time on the disappearance of linoleic acid measured during the metabolism of linoleic acid (4.7 μM) using data from models 16 (■), 19 (+), 20 (*), 21 (□), 22 (▲) and the experimental data from Figure 30 (X).**

F + FE1, μM free linoleic acid plus that bound to the acyl-CoA synthetase.

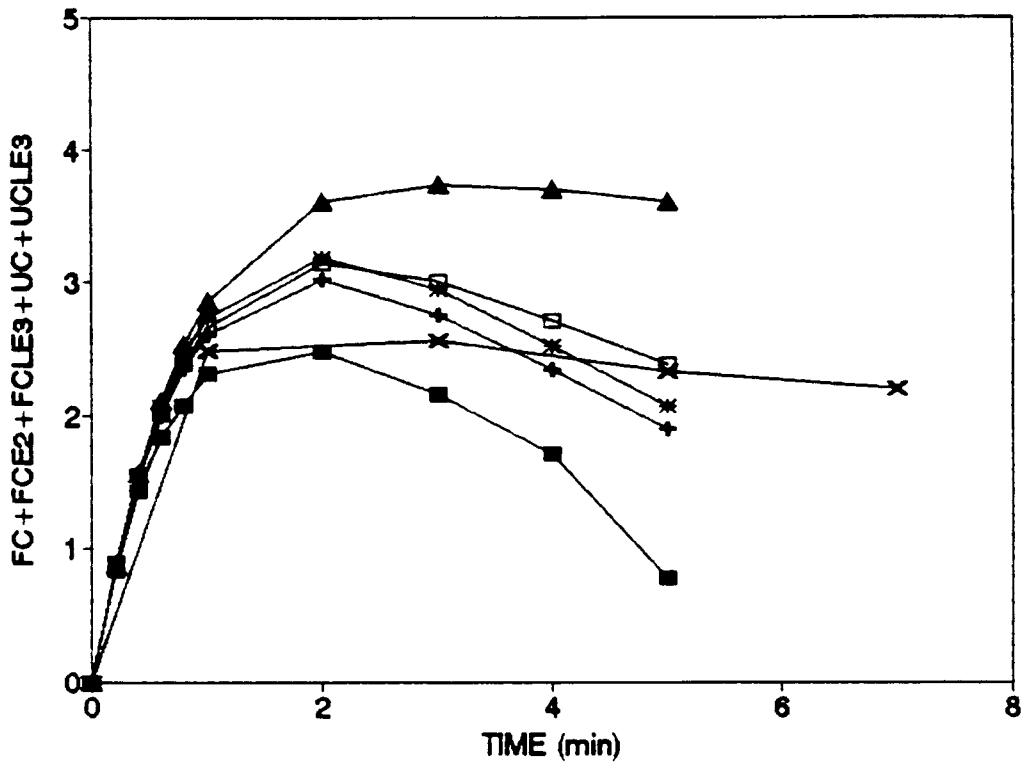

FIGURE 52 **Overlay plots of the effect of time on the formation of acyl-CoA measured during the metabolism of linoleic acid (4.7 μM) using data from models 16 (■), 19 (+), 20 (*), 21 (□), 22 (▲) and the experimental data from Figure 30 (X).**

FC + FCE2 + FCLE3 + UC + UCLE3, μM free linoleoyl-CoA plus γ-linolenoyl-CoA plus that bound to the Δ6-desaturase and lysophospholipid acyltransferase.

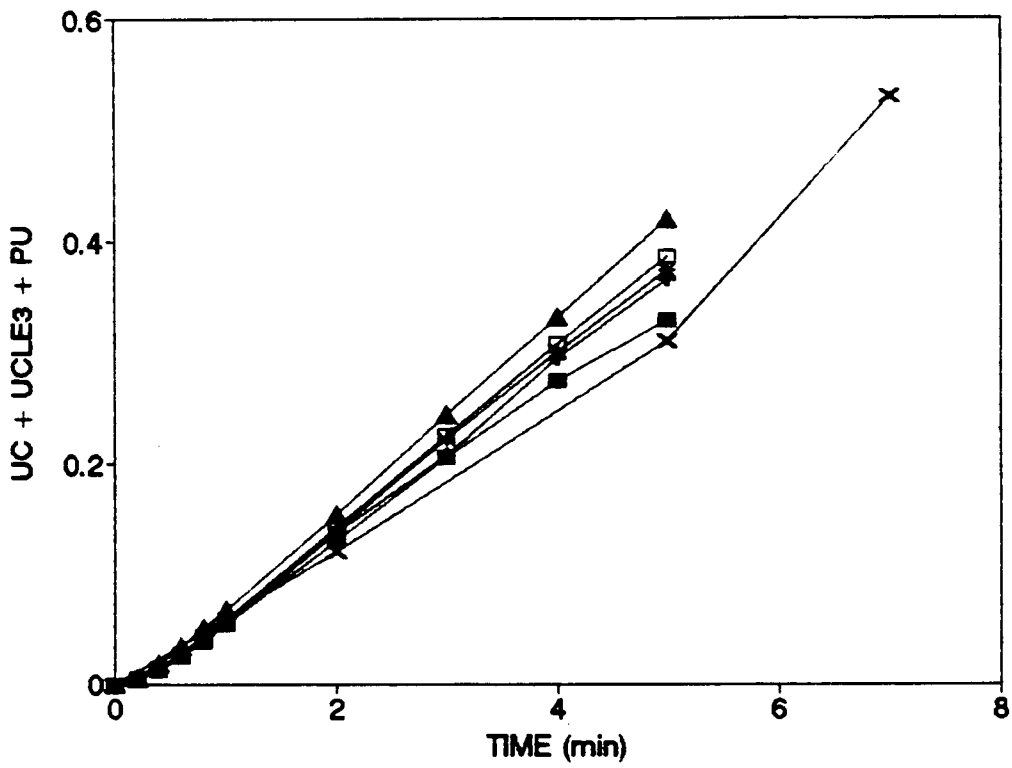

FIGURE 53 **Overlay plots of the effect of time on the Δ6-desaturation of linoleic acid (4.7 μM) using data from models 16 (■), 19 (+), 20 (*), 21 (□), 22 (▲) and the experimental data from Figure 20 (X).**

UC + PU + UCLE3, μM free γ-linolenoyl-CoA plus that bound to the lysophospholipid acyltransferase plus that acylated into phospholipids.

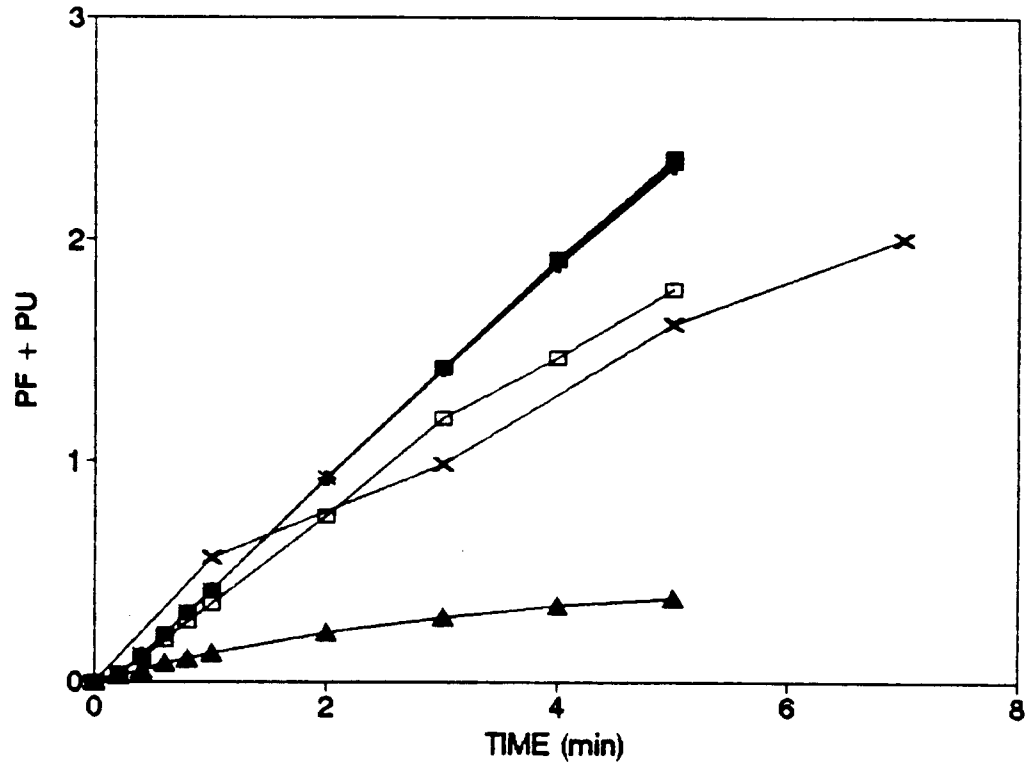

FIGURE 54 **Overlay plots of the effect of time on the acylation of phospholipids measured during the metabolism of linoleic acid (4.7 μM) using data from models 16 (■), 19 (+), 20 (*), 21 (□), 22 (▲) and the experimental data from Figure 30 (X).**

PF + PU, μM linoleoyl-CoA acid plus γ-linolenoyl-CoA acylated into phospholipids.

In models 16, 19, 20, 21 and 22, the first minute of acyl-CoA production was modelled reasonably well; thereafter, however, models 19, 20 and 21 predicted decay of acyl-CoA levels in excess of the very slight decline found experimentally (Figure 52). Model 22 showed a plateau of acyl-CoA levels after ca. 2 minutes, but at ca. 50% above experimental levels. The Δ6-desaturase was well mimicked by all models (Figure 53). Models 16, 19, 20 and 21 were within 50 to 100% of the phospholipid formation with time up to five minutes, but did not model the shape of the time course well (Figure 54). Run 22 provided data up to six-fold below the experimental data at longer time points.

Models 23 to 26 (Figures 55, 56, 57 and 58) were based on model 21. Models 23 to 26 had a ca. 70% increase in k_{14} and no change to four-fold change in k_{16} relative to model 21. Models 25 and 26, compared to model 24, adjusted k_1 downward and in model 26, in addition, k_3 was increased by ca. 20%. This set of models provided the best approximation to the time course for fatty acid disappearance compared to previous models (see especially Figures 39 and 43) and for acyl-CoA formation (see Figures 40, 44 and 48). Models 23 and 24 approximated the fatty acid disappearance curve slightly better than model 21 (Figure 55). Models 25 and 26 plateaued above the experimental data. All models were reasonably close to modelling acyl-CoA formation, with model 23 being closer to the data than the other models (Figure 56). Δ6-Desaturation was essentially equivalently modelled by the computer runs 21, 23, 24, 25 and 26 (Figure 57). This set of runs showed a tightening of output into a narrower range. Since the modelling of the Δ6-desaturase component has been close throughout previous runs (see Figures 41, 45, 49 and 53), the current runs at most show a slight improvement in fit. Phospholipid formation was modelled most closely by models 21 and 23,

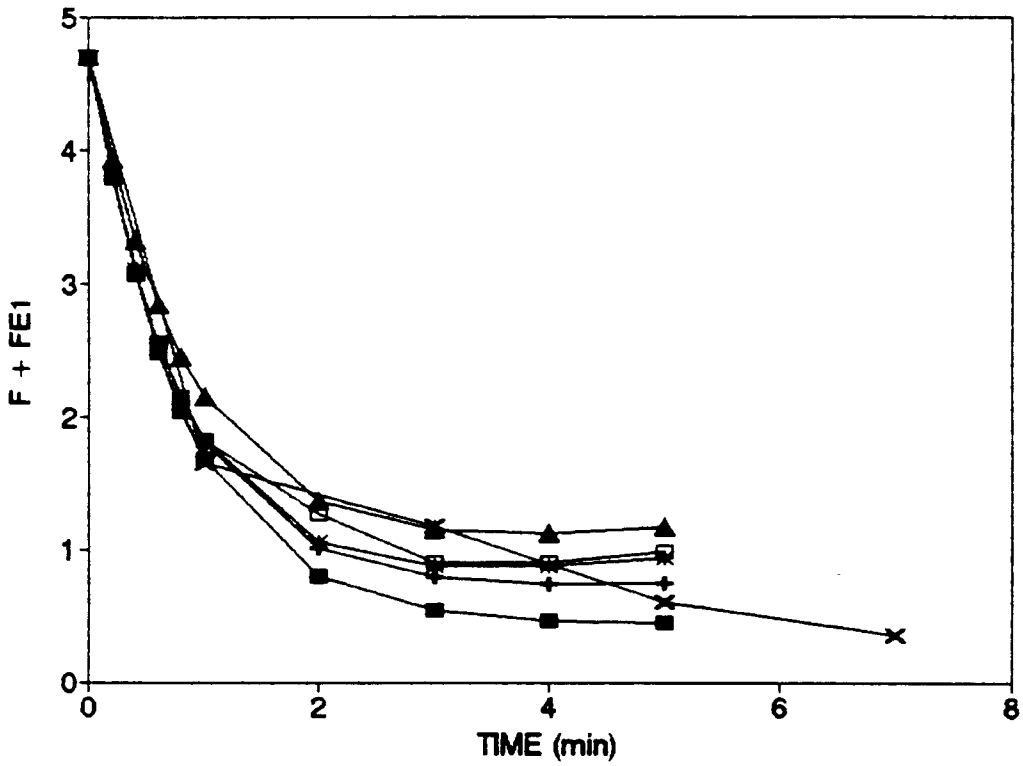

FIGURE 55 **Overlay plots of the effect of time on the disappearance of linoleic acid measured during the metabolism of linoleic acid (4.7 μM) using data from models 21 (■), 23 (+), 24 (*), 25 (□), 26 (▲) and the experimental data from Figure 30 (X).**

F + FE1, μM free linoleic acid plus that bound to the acyl-CoA synthetase.

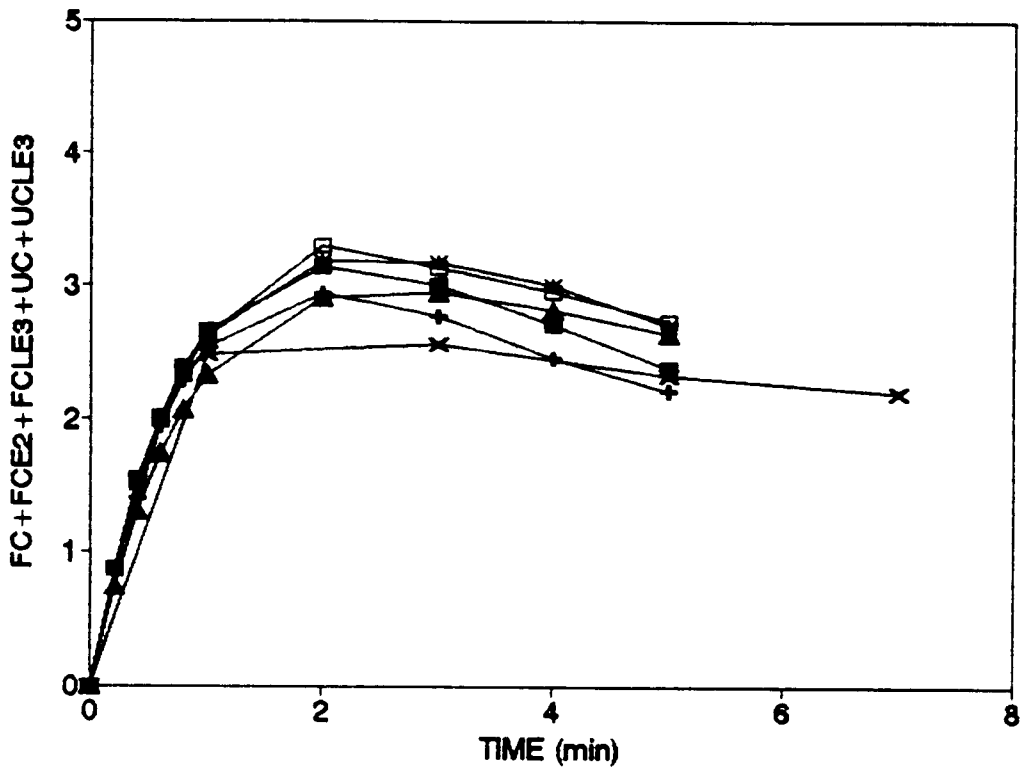

FIGURE 56 **Overlay plots of the effect of time on the formation of acyl-CoA measured during the metabolism of linoleic acid (4.7 μM) using data from models 21 (■), 23 (+), 24 (*), 25 (□), 26 (▲) and the experimental data from Figure 30 (X).**

FC + FCE2 + FCLE3 + UC + UCLE3, μM free linoleoyl-CoA plus γ-linolenoyl-CoA plus that bound to the Δ6-desaturase and lysophospholipid acyltransferase.

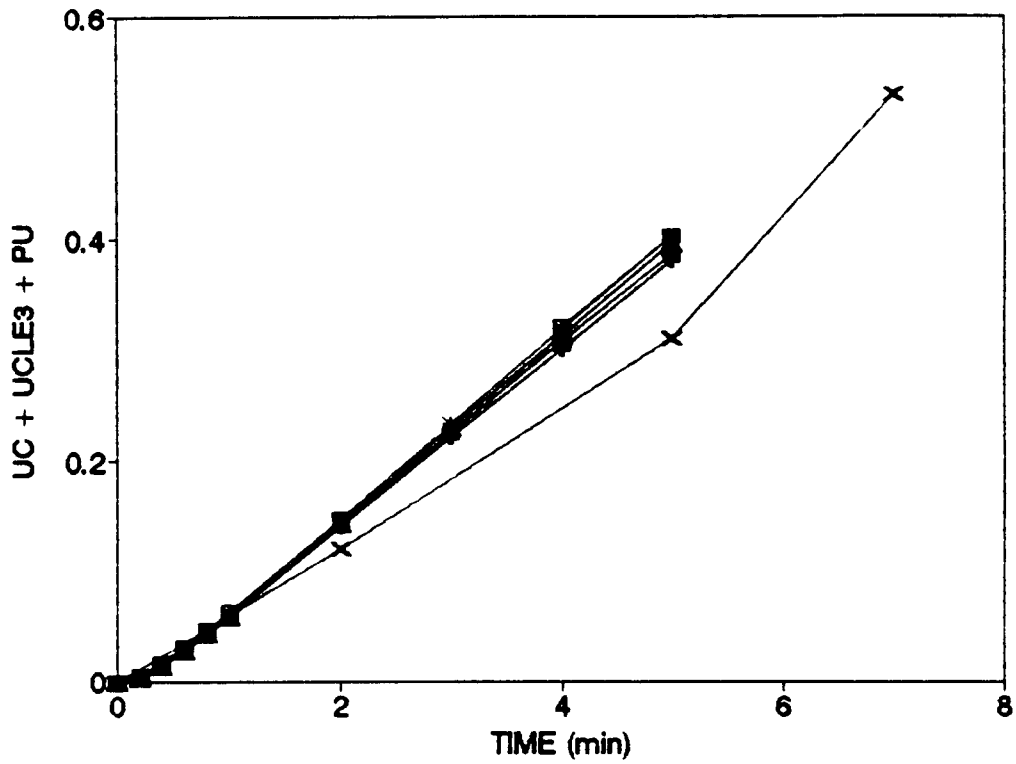

FIGURE 57

Overlay plots of the effect of time on the Δ6-desaturation of linoleic acid (4.7 μM) using data from models 21 (■), 23 (+), 24 (*), 25 (□), 26 (▲) and the experimental data from Figure 20 (X).

UC + PU + UCLE3, μM free γ-linolenoyl-CoA plus that bound to the lysophospholipid acyltransferase plus that acylated into phospholipids.

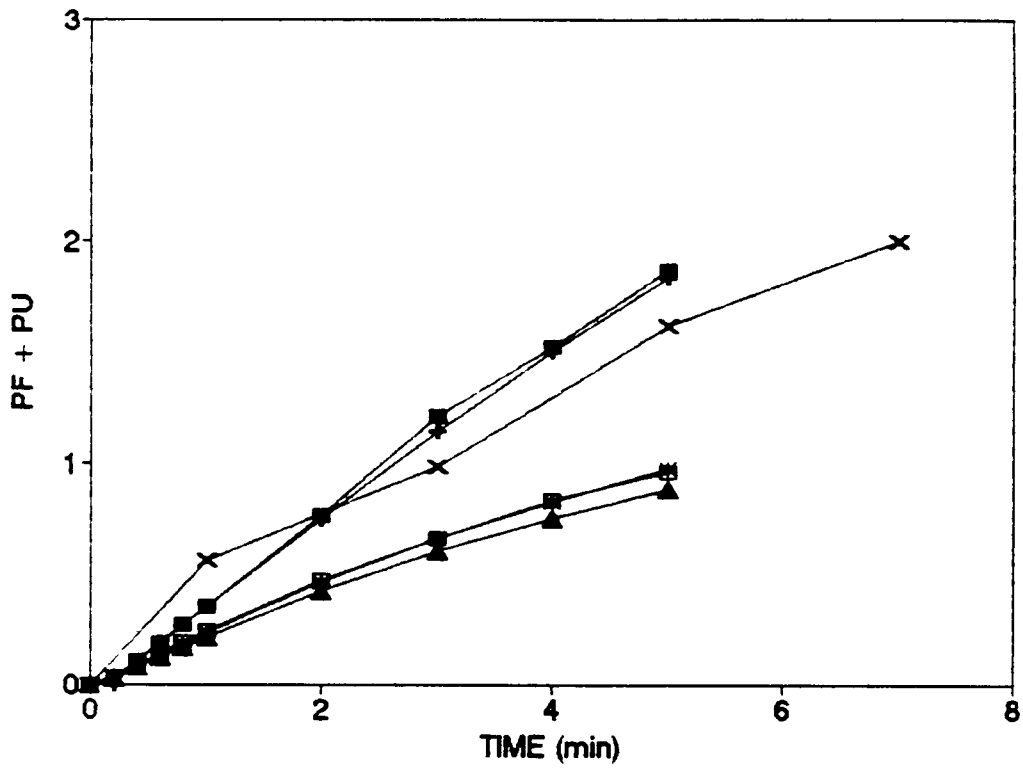

FIGURE 58 **Overlay plots of the effect of time on the acylation of phospholipids measured during the metabolism of linoleic acid (4.7 μM) using data from models 21 (■), 23 (+), 24 (*), 25 (□), 26 (▲) and the experimental data from Figure 30 (X).**

PF + PU, μM linoleoyl-CoA acid plus γ-linolenoyl-CoA acylated into phospholipids.

with models 24, 25 and 26 predicting ca. two-fold lower formation than the experimental data (Figure 58). The former runs provide a closer fit to the experimental data than previous runs (see Figures 42, 46, 50 and 54).

Finer tuning of the model was performed with models 27, 28 and 29 (see Figures 59, 60, 61 and 62). These models were based on model 23, and only k_6 was altered, being decreased in the order model 23>29>28>27. All these models generated identical plots for fatty acid disappearance, acyl-CoA formation and phospholipid acylation (Figures 59, 60 and 62). Only the plot of the Δ6-desaturase reaction was affected, with the data approximating the experimental data in the following order 23<29<28<27, with model 27 fitting the data up to 5 minutes extremely well (Figure 61).

Prior to the modelling described in the thesis, we made a number of earlier runs on the SLAM II program. In these earlier runs, we were unable to model the data at all closely without altering the concentrations of two of the components needed for the computer modelling. The components are lysophospholipid and lysophospholipid acyltransferase. The concentrations of both of these were set higher than the literature values (Table 35). At this current point in our modelling, we wished to check whether we could lower the levels of these components and still model the data. The relevant data is shown in Figures 63, 64, 65 and 66 where data from model 27, run at 11 μM and 2.2 μM lysophospholipid concentration is presented with the experimental data. The decrease in lysophospholipid concentration was accompanied by a significant, but managable decrease in phospholipid formation (Figure 66). Therefore, the concentrations of lysophospholipid and lysophospholipid acyltransferase reported in hepatic microsomes at 0.5 mg protein/ml were used in subsequent

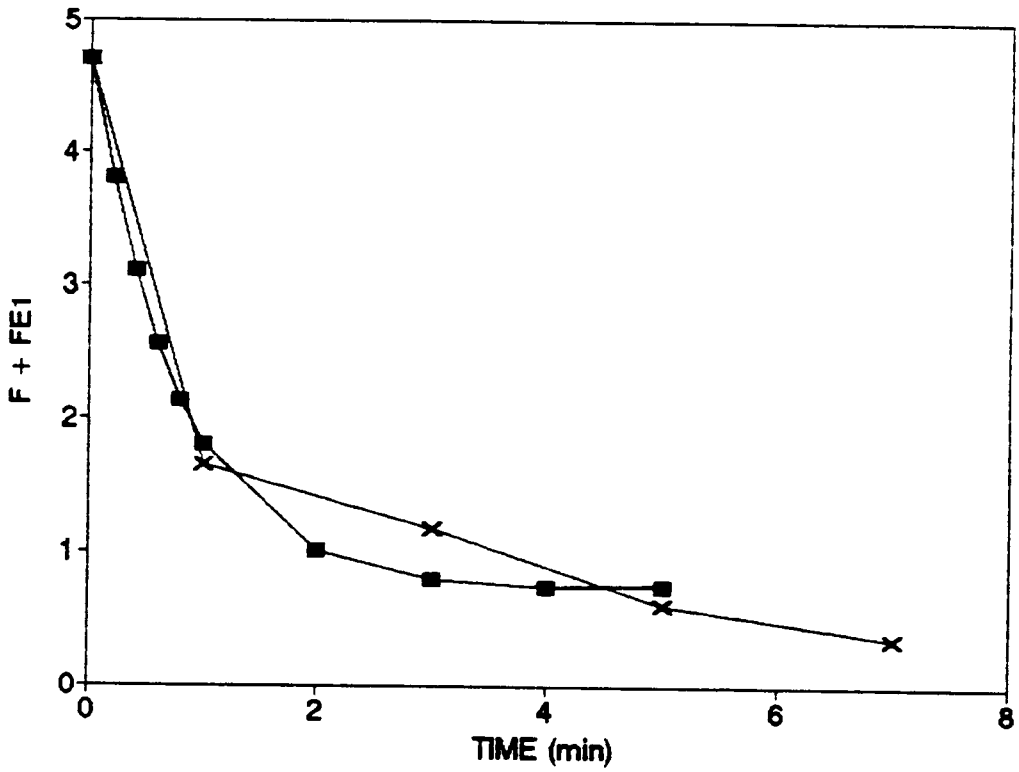

FIGURE 59 **Overlay plots of the effect of time on the disappearance of linoleic acid measured during the metabolism of linoleic acid (4.7 μM) using data from models 23, 27, 28, 29 (■), and the experimental data from Figure 30 (X).**

F + FE1, μM free linoleic acid plus that bound to the acyl-CoA synthetase.

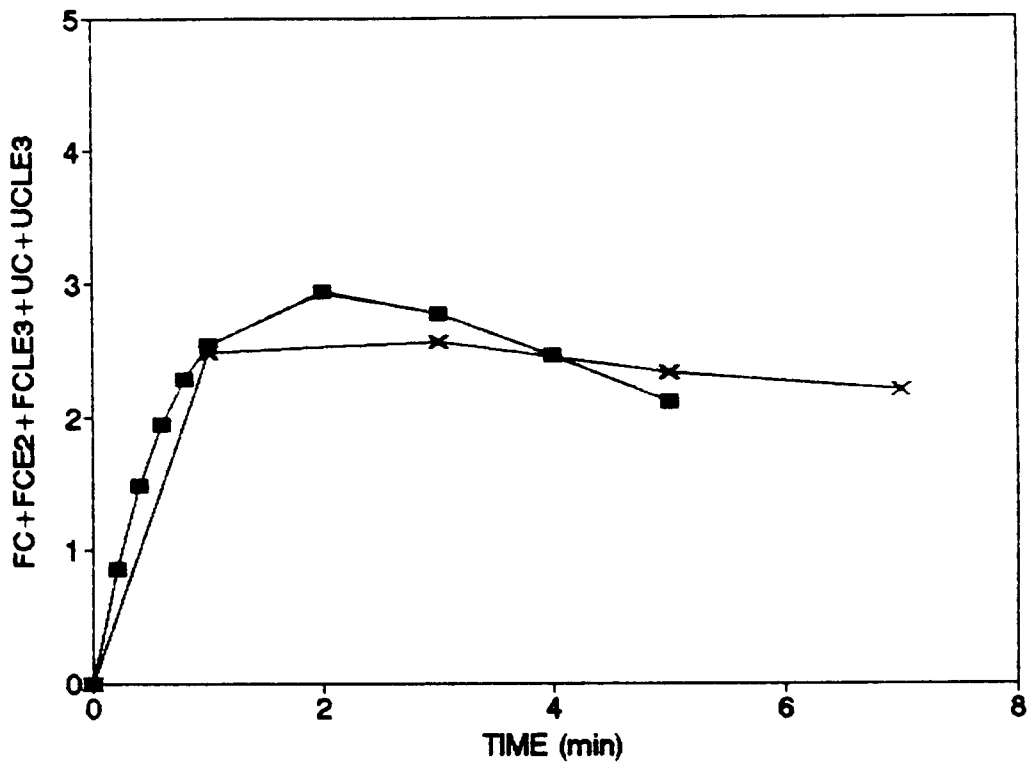

FIGURE 60 **Overlay plots of the effect of time on the formation of acyl-CoA measured during the metabolism of linoleic acid (4.7 μM) using data from models 23, 27, 28, 29 (■), and the experimental data from Figure 30 (X).**

FC + FCE2 + FCLE3 + UC + UCLE3, μM free linoleoyl-CoA plus γ-linolenoyl-CoA plus that bound to the Δ6-desaturase and lysophospholipid acyltransferase.

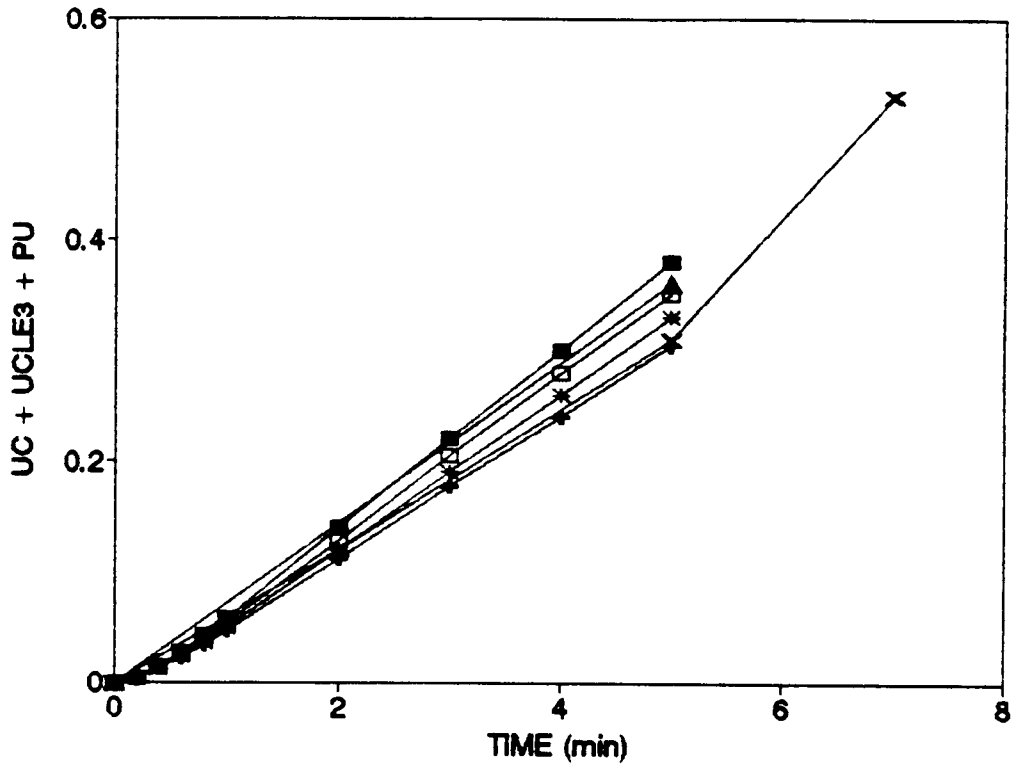

FIGURE 61 **Overlay plots of the effect of time on the Δ6-desaturation of linoleic acid (4.7 μM) using data from models 23 (■), 27 (+), 28 (*), 29 (□), and the experimental data from Figures 19 (▲) and 20 (X).**

UC + PU + UCLE3. μM free γ-linolenoyl-CoA plus that bound to the lysophospholipid acyltransferases plus that acylated into phospholipids.

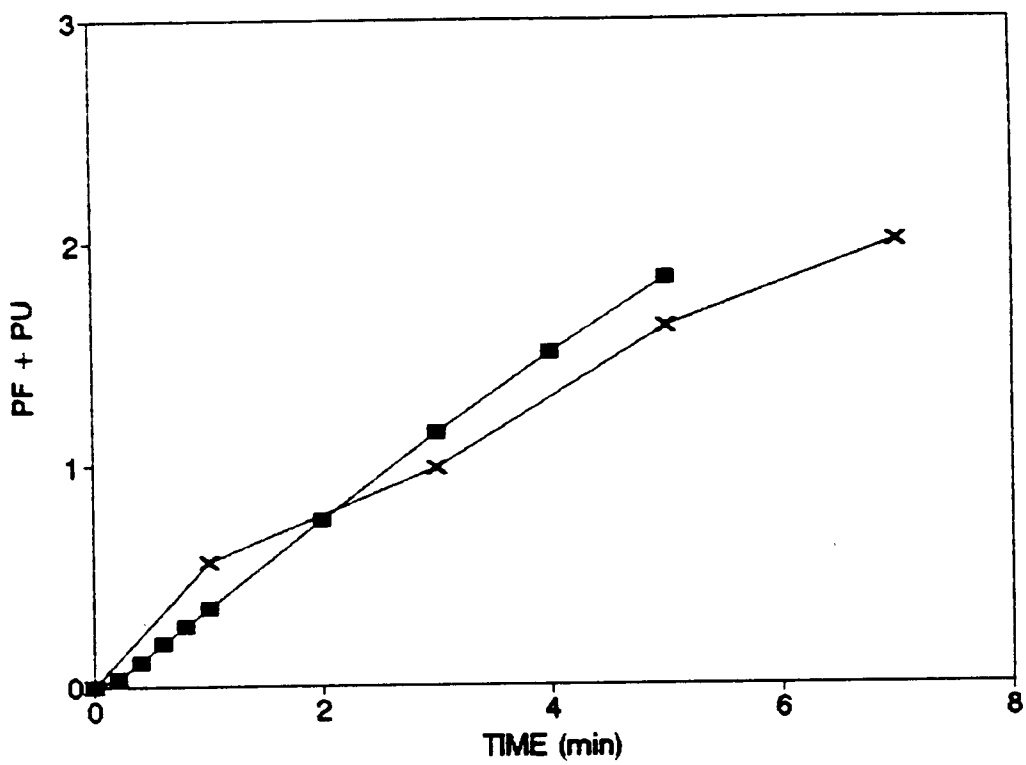

FIGURE 62 **Overlay plots of the effect of time on the acylation of phospholipids measured during the metabolism of linoleic acid (4.7 μM) using data from models 23, 27, 28, 29 (■), and the experimental data from Figure 30 (X).**

PF + PU, μM linoleoyl-CoA acid plus γ-linolenoyl-CoA acylated into phospholipids.

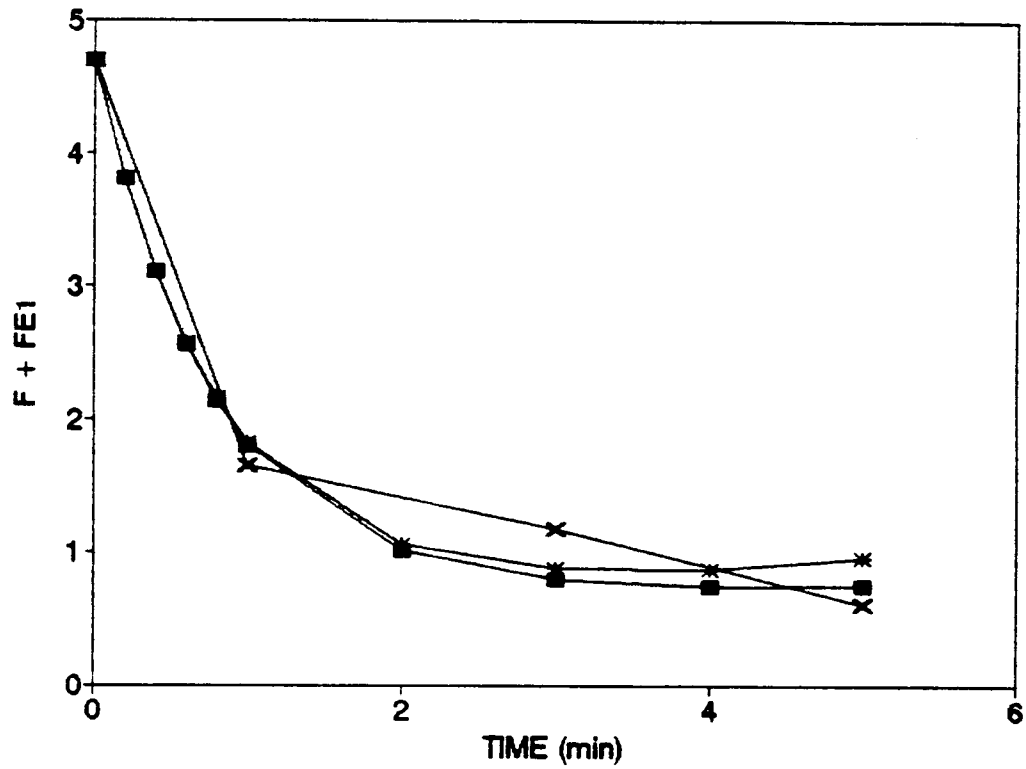

FIGURE 63 **Overlay plots of the effect of time on the disappearance of linoleic acid measured during the metabolism of linoleic acid (4.7 μM) using data from model 27 run at concentrations of 11 μM (■) and 2.2 μM (*) lysophospholipid, and the experimental data from Figure 30 (X).**

F + FE1, μM free linoleic acid plus that bound to the acyl-CoA synthetase.

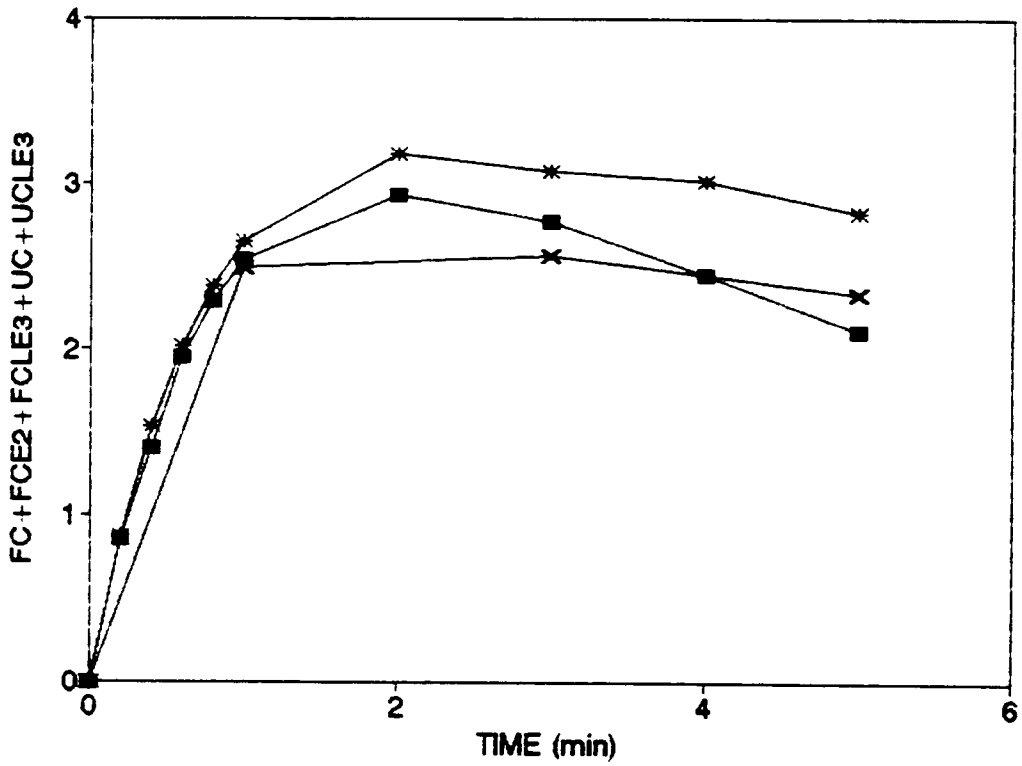

FIGURE 64 **Overlay plots of the effect of time on the formation of acyl-CoA measured during the metabolism of linoleic acid (4.7 μM) using data from model 27 run at concentrations of 11 μM (■) and 2.2 μM (*) lysophospholipid, and the experimental data from Figure 30 (X).**

FC + FCE2 + FCLE3 + UC + UCLE3, μM free linoleoyl-CoA plus γ-linolenoyl-CoA plus that bound to the Δ6-desaturase and lysophospholipid acyltransferase.

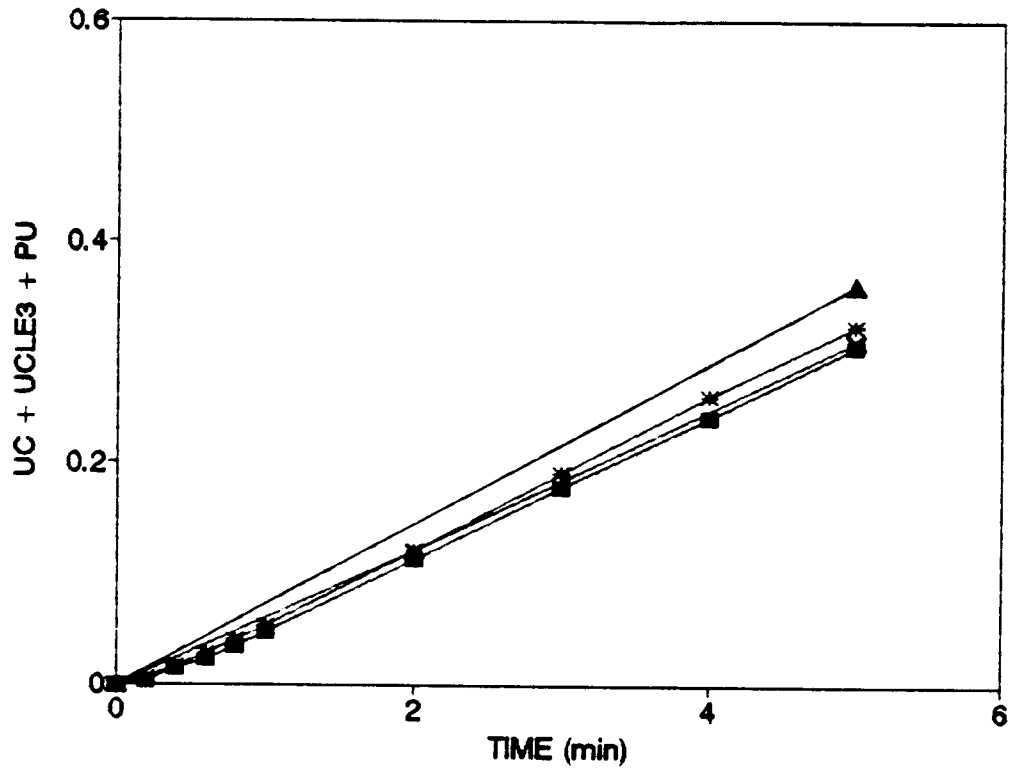

FIGURE 65

Overlay plots of the effect of time on the Δ6-desaturation of linoleic acid (4.7 μM) using data from model 27 run at concentrations of 11 μM (■) and 2.2 μM (*) lysophospholipid, and the experimental data from Figures 19 (Δ) and 20 (X).

UC + PU + UCLE3, μM free γ-linolenoyl-CoA plus that bound to the lysophospholipid acyltransferases plus that acylated into phospholipids.

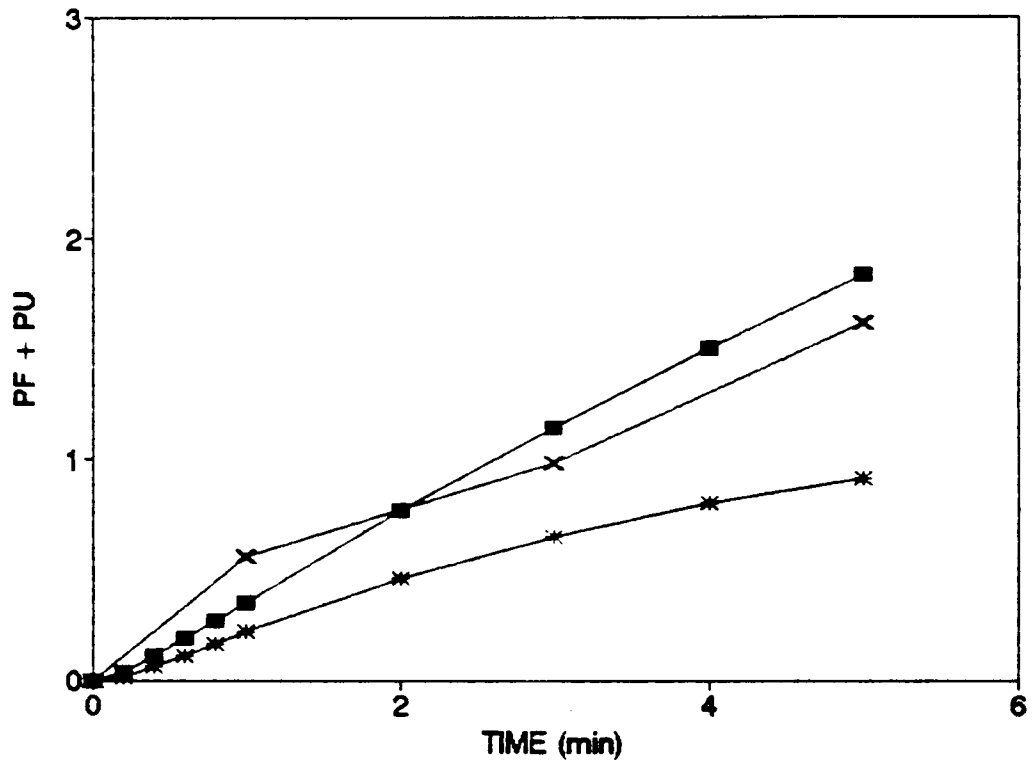

FIGURE 66 **Overlay plots of the effect of time on the acylation of phospholipids measured during the metabolism of linoleic acid (4.7 μM) using data from model 27 run at concentrations of 11 μM (■) and 2.2 μM (⋆) lysophospholipid, and the experimental data from Figure 30 (X).**

PF + PU, μM linoleoyl-CoA acid plus γ-linolenoyl-CoA acylated into phospholipids.

models (Table 35). The constants in the model were adjusted to increase the activity of the lysophospholipid acyltransferase (Figure 66).

In models 30, 31, 32 and 33, concentrations of 2.2 μM lysophospholipid and 0.5 μM lysophospholipid acyltransferase were used, and the values of k_9 and k_{12} were adjusted to compensate for decreased lysophospholipid acyltransferase activity accompaning the changes in component concentration. The results are given together with the data from model 27 and the experimental data in Figures 67, 68, 69 and 70. The decrease in the concentration of lysophospholipid and lysophospholipid acyltransferase without change in rate constants (compare models 27 and 30) was accompanied by very small changes in fatty acid disappearance (Figure 67) and Δ6-desaturase activity (Figure 69), but striking changes in acyl-CoA formation (Figure 68) and lysophospholipid acyltransferase activity (Figure 70). At the lower concentrations of lysophospholipid and lysophospholipid acyltransferase, the four-fold increase in k_9 and k_{12} in model 30 to model 33 (Table 37) appears to be sufficient for the simulated data to approximately model the experimental data (Figures 67, 68, 69, and 70).

Now that the simulated data for model 33 approximately modelled the experimentally determined data for substrate disappearance and product formation as a function of time, it was necessary to see if the simulated data for product formation with time for the acyl-CoA synthetase, Δ6-desaturase and lysophospholipid acyltransferase versus initial linoleic acid concentration mimicked the experimental data in Figures 32, 33 and 34, as outlined in the following sections.

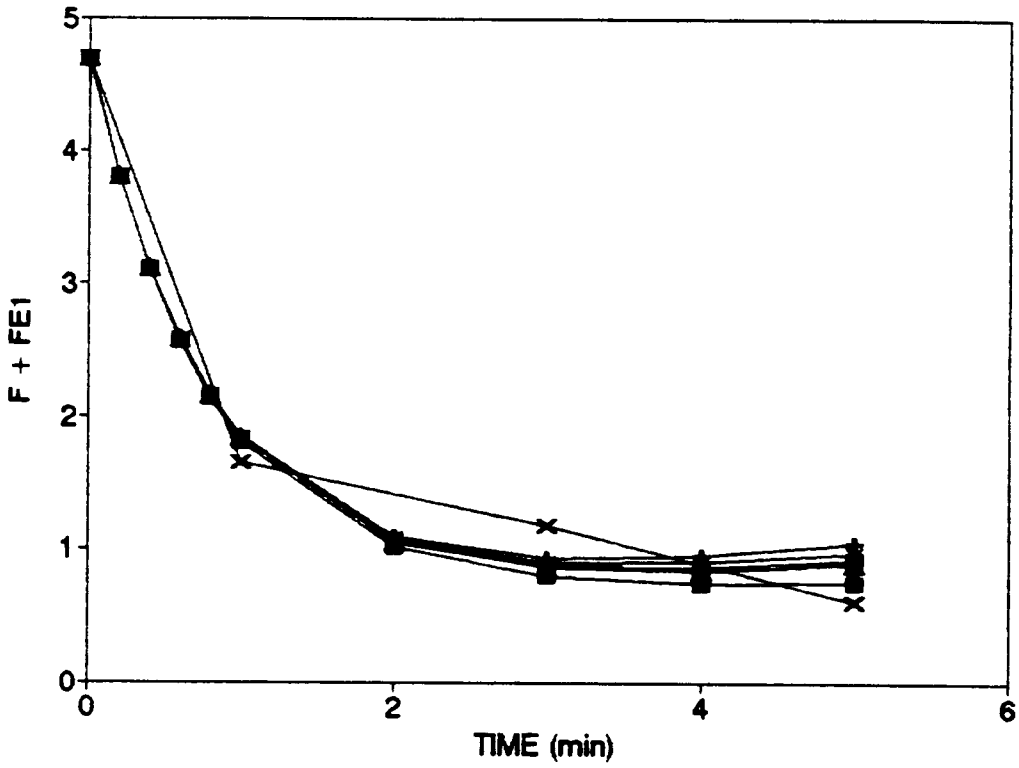

FIGURE 67 **Overlay plots of the effect of time on the disappearance of linoleic acid measured during the metabolism of linoleic acid (4.7 μM) using data from models 27 (■), 30 (+), 31 (*), 32 (□), 33 (▲) and the experimental data from Figure 30 (X).**

F + FE1, μM free linoleic acid plus that bound to the acyl-CoA synthetase.

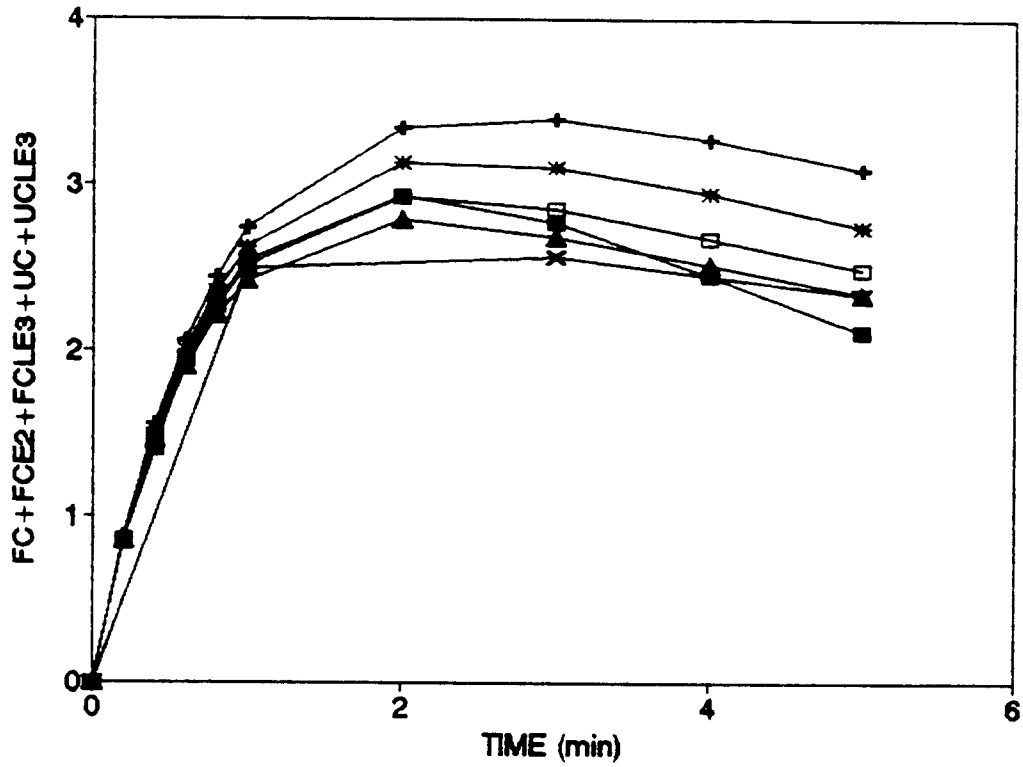

FIGURE 68

Overlay plots of the effect of time on the formation of acyl-CoA measured during the metabolism of linoleic acid (4.7 μM) using data from models 27 (■), 30 (+), 31 (*), 32 (□), 33 (▲) and the experimental data from Figure 30 (X).

FC + FCE2 + FCLE3 + UC + UCLE3, μM free linoleoyl-CoA plus γ-linolenoyl-CoA plus that bound to the Δ6-desaturase and lysophospholipid acyltransferase.

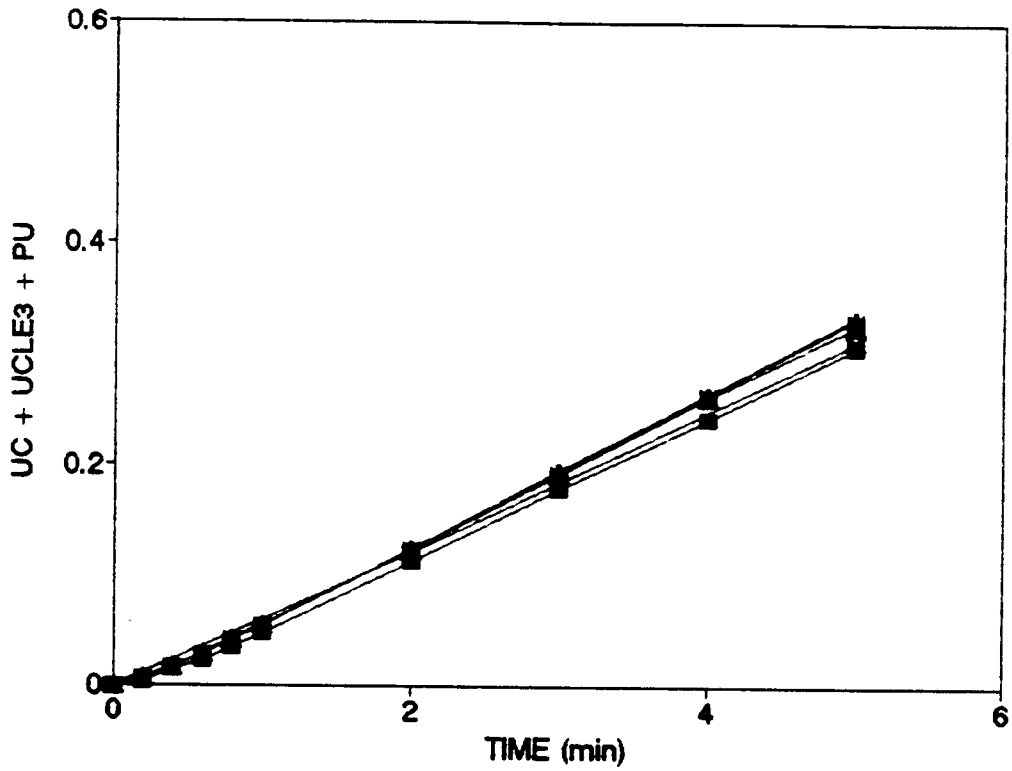

FIGURE 69

Overlay plots of the effect of time on the Δ6-desaturation of linoleic acid (4.7 μM) using data from models 27 (■), 30 (+), 31 (*), 32 (□), 33 (▲) and the experimental data from Figure 20 (X).

UC + PU + UCLE3, μM free γ-linolenoyl-CoA plus that bound to the lysophospholipid acyltransferases plus that acylated into phospholipids.

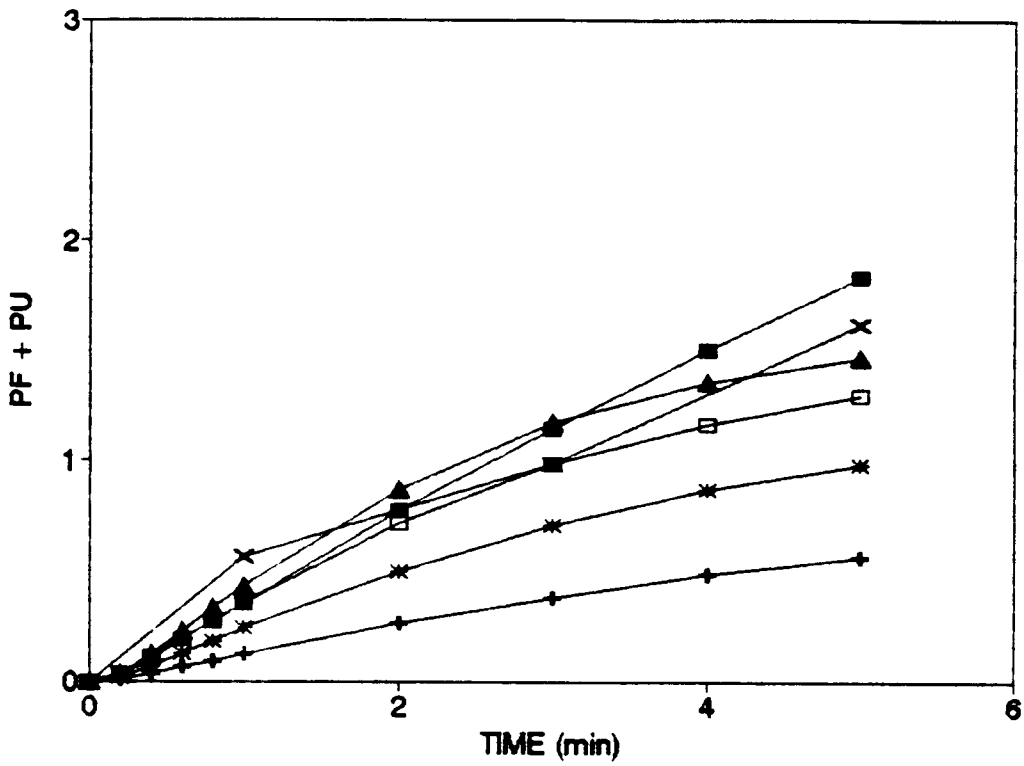

FIGURE 70 **Overlay plots of the effect of time on the acylation of phospholipids measured during the metabolism of linoleic acid (4.7 μM) using data from models 27 (■), 30 (+), 31 (*), 32 (□), 33 (▲) and the experimental data from Figure 30 (X).**

PF + PU, μM linoleoyl-CoA acid plus γ-linolenoyl-CoA acylated into phospholipids.

Using the constants from model 33 in Table 37 and the SLAM II program, data for product formation with time at various linoleic acid concentrations for the acyl-CoA synthetase, Δ6-desaturase and lysophospholipid acyltransferase was obtained. The time period was chosen as 3 minutes, since this was the time period over which the experimental data was collected. The enzyme activities were measured as follows:

i) for the acyl-CoA synthetase, the formation of the sum of the two acyl-CoA products plus all enzyme-bound acyl-CoA (linoleoyl-CoA, γ-linolenoyl-CoA, [linoleoyl-CoA.E_2], [linoleoyl-CoA.E_3] plus [γ-linolenoyl-CoA.E_3] in Figure 38) over 3 minutes, normalised to 1 minute, from the computer output is plotted versus initial linoleic acid concentration with the experimentally determined data (Figure 32 B) in Figure 71.

ii) for the Δ6-desaturase, the formation of free γ-linolenic acid plus that fatty acid esterified to CoA or phospholipid plus all enzyme-bound γ-linolenoyl-CoA (γ-linolenoyl-CoA, [γ-linolenoyl-CoA.E_3], and 2-γ-linolenoyl-phospholipid in Figure 38) over 3 minutes, normalised to 1 minute, from the computer output is plotted versus initial linoleic acid concentration together with the experimentally determined data (Figure 33 B) in Figure 72.

iii) for the lysophospholipid acyltransferases, the formation of 2-linoleoyl-phospholipid plus 2-γ-linolenoyl-phospholipid (Figure 38) over 3 minutes, normalised to 1 minute, from the computer output is

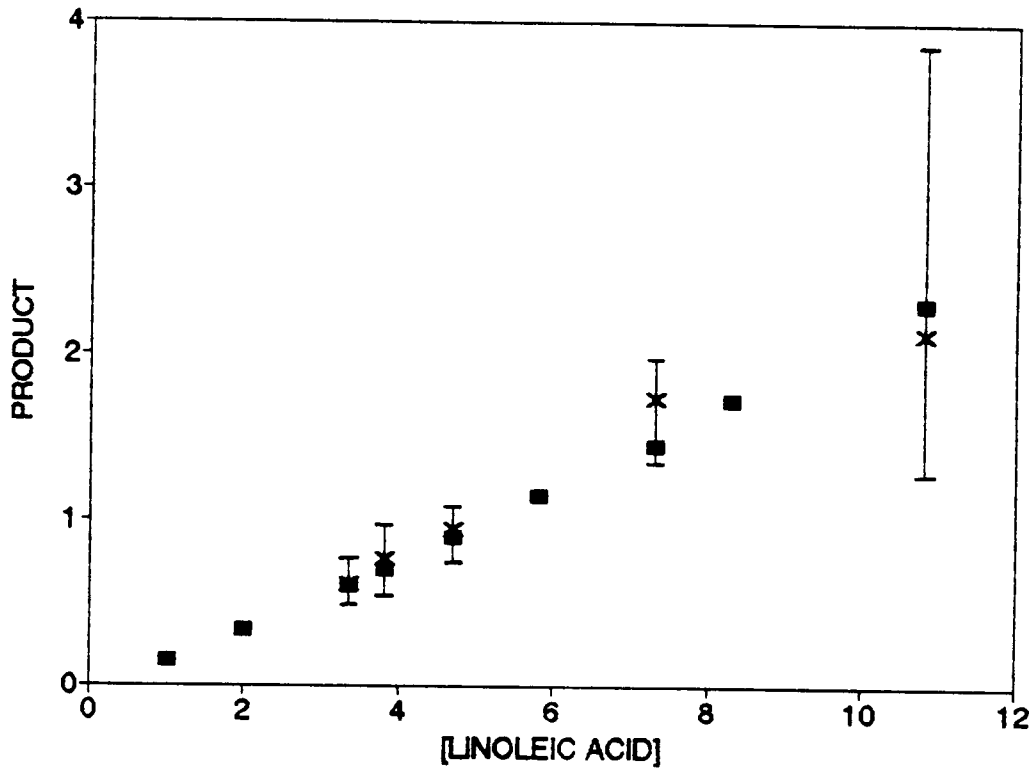

FIGURE 71

Overlay plots of the effect of linoleic acid concentration on the formation of acyl-CoA measured during the metabolism of linoleic acid using data from model 33 (■) and the experimental data from Figure 32 B (X).

Product, μM [1-^{14}C] linoleoyl-CoA + [1-^{14}C] γ-linolenoyl-CoA formed/min for the experimental data and linoleoyl-CoA + γ-linolenoyl-CoA + [linoleoyl-CoA.E_2] + [γ-linolenoyl-CoA.E_3] + [linoleoyl-CoA.E_3] formed/min for the simulated data; linoleic acid concentration, μM linoleic acid. Product formation was measured at 3 min and was normalised to 1 min by dividing by 3.

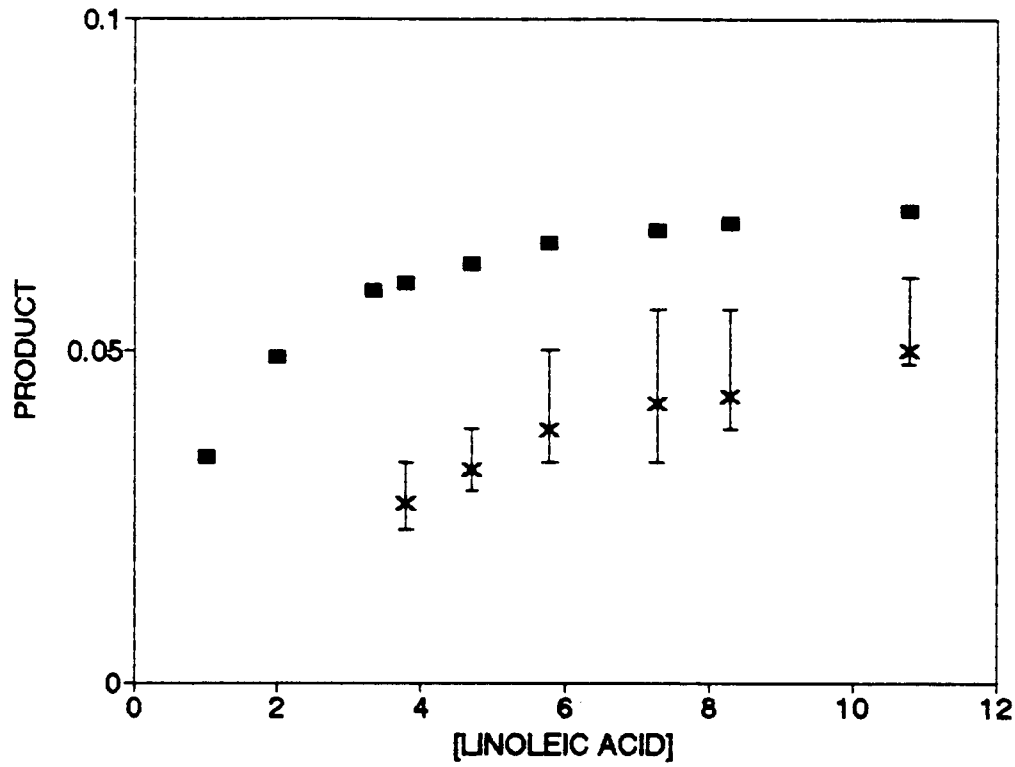

FIGURE 72 **Overlay plots of the effect of linoleic acid concentration on the Δ6-desaturation of linoleic acid using data from model 33 (■) and the experimental data from Figure 33 B (X).**

Product, μM [1^{-14}C] γ-linolenoyl-CoA + [1^{-14}C] γ-linolenoyl-phospholipid formed/min for the experimental data and μM γ-linolenoyl-CoA + γ-linolenoyl-phospholipid + [γ-linolenoyl-CoA.E_3] formed/min for the simulated data; linoleic acid concentration, μM linoleic acid. Product formation was measured at 3 min and was normalised to 1 min by dividing by 3.

plotted versus initial linoleic acid concentration together with the experimentally determined data (Figure 34 B) in Figure 73.

In the overlay plots of the experimental data and the simulated data using the constants from model 33 as outlined above, there was good correlation between the experimental data and the simulated data for the acyl-CoA synthetase and lysophospholipid acyltransferase (Figures 71 and 73). However, for the Δ6-desaturase, the rate of product formation calculated from the simulated reaction scheme using model 33 was ca. two-fold higher than that obtained experimentally (Figure 72). Further modelling was aimed at improving the agreement between the experimentally determined data and the data from the simulated reaction scheme for the Δ6-desaturation of linoleic acid as a function of linoleic acid concentration.

Overlay plots of the experimental data and simulated data from models 34, 35 and 36 of product formation as a function of time are illustrated in Figures 74, 75, 76 and 77. No changes were made to the rate constants for the acyl-CoA synthetase (k_1, k_2 and k_3), and very small differences in the disappearance of fatty acid and formation of acyl-CoA were observed between models 33, 34, 35 and 36. These changes did not affect the agreement between the experimental data and the simulated data plotted for linoleic acid disappearance or acyl-CoA formation as a function of time (Figures 74 and 75). In models 34, 35 and 36, k_9 and k_{12} for the lysophospholipid acyltransferase were decreased by ca. 10%, resulting in small changes in the overlay plots for phospholipid formation without affecting the correlation between experimental and simulated data (Figure 77).

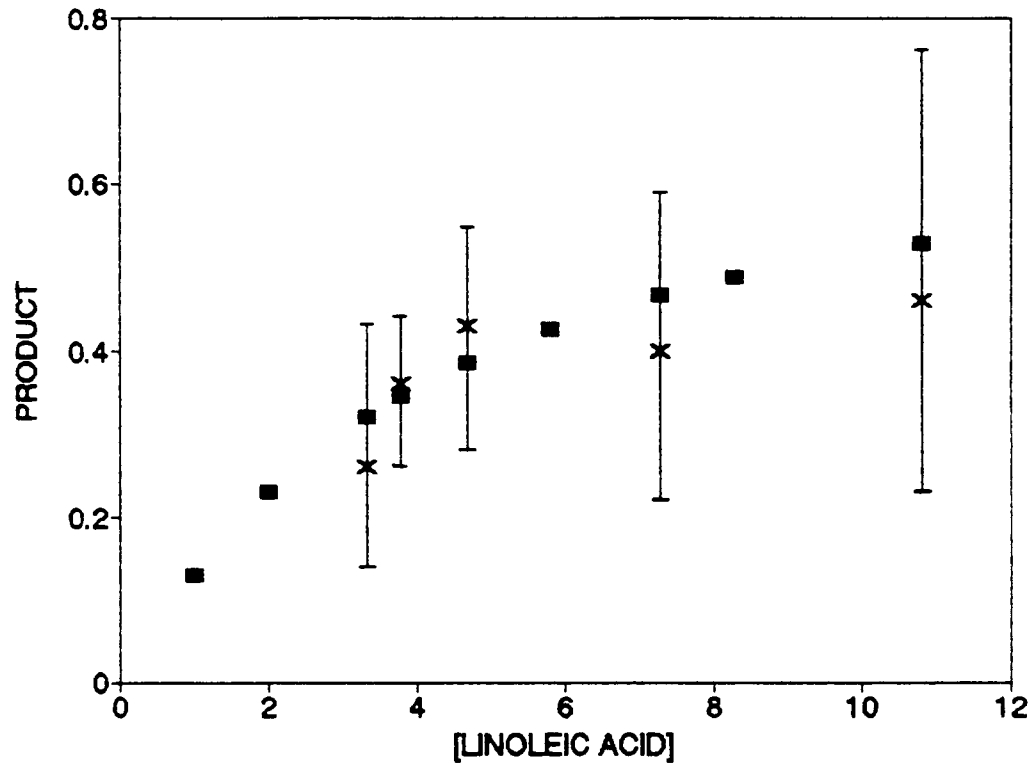

FIGURE 73 **Overlay plots of the effect of linoleic acid concentration on the acylation of phospholipids measured during the metabolism of linoleic acid using data from model 33 (■) and the experimental data from Figure 34 B (X).**

Product, μM [1-^{14}C] linoleoyl-phospholipid + [1-^{14}C] γ-linolenoyl-phospholipid formed/min for the experimental data and μM linoleoyl-phospholipid + γ-linolenoyl-phospholipid formed/min for the simulated data; linoleic acid concentration, μM linoleic acid. Product formation was measured at 3 min and was normalised to 1 min by dividing by 3.

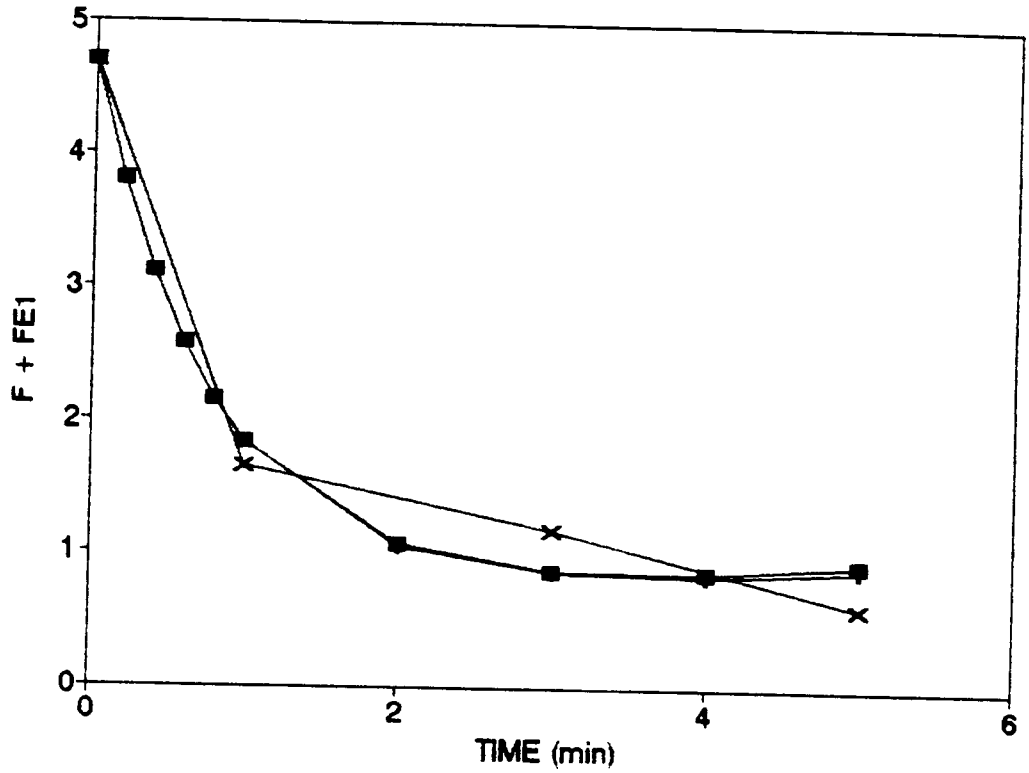

FIGURE 74 **Overlay plots of the effect of time on the disappearance of linoleic acid measured during the metabolism of linoleic acid (4.7 μM) using data from models 33 (+), 34, 35, 36 (■) and the experimental data from Figure 30 (X).**

F + FE1, μM free linoleic acid plus that bound to the acyl-CoA synthetase.

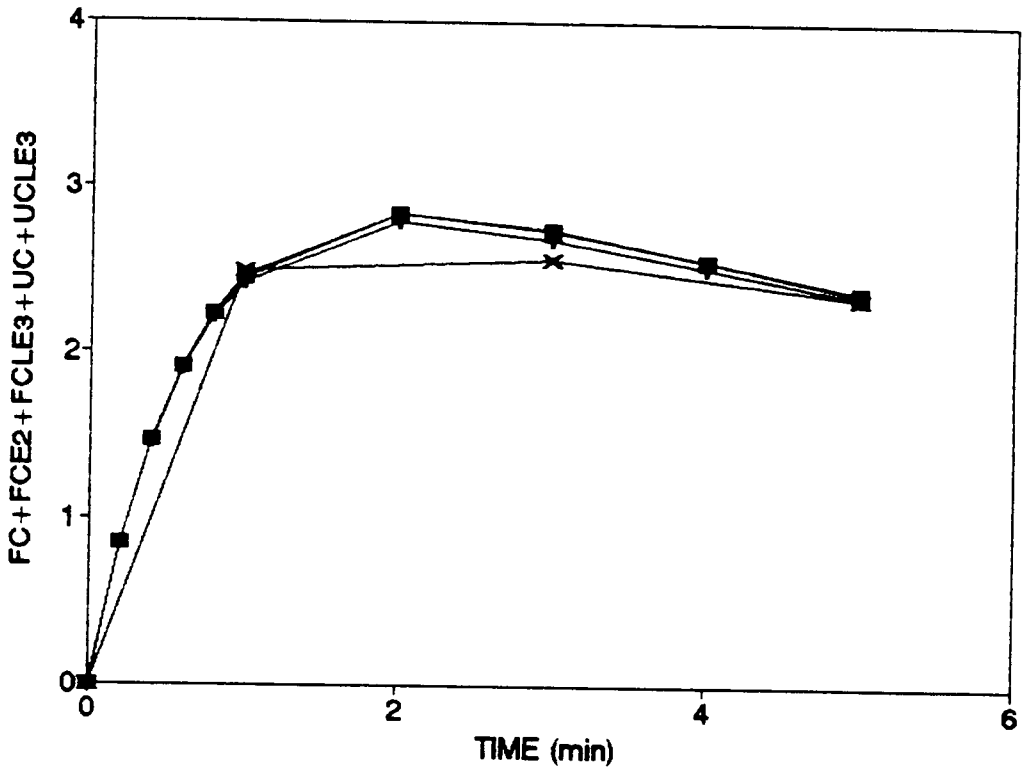

FIGURE 75

Overlay plots of the effect of time on the formation of acyl-CoA measured during the metabolism of linoleic acid (4.7 μM) using data from models 33 (+), 34, 35, 36 (■) and the experimental data from Figure 30 (X).

FC + FCE2 + FCLE3 + UC + UCLE3, μM free linoleoyl-CoA plus γ-linolenoyl-CoA plus that bound to the Δ6-desaturase and lysophospholipid acyltransferase.

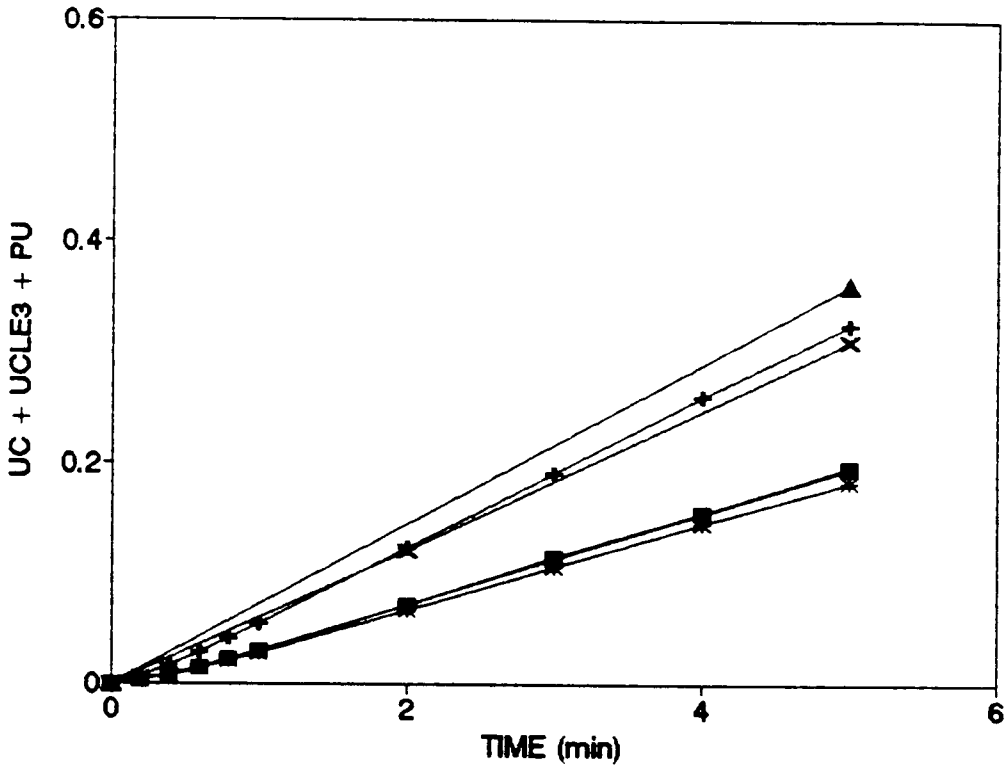

FIGURE 76 **Overlay plots of the effect of time on the Δ6-desaturation of linoleic acid (4.7 μM) using data from models 33 (+), 34 (■), 35 (*), 36 (□) and the experimental data from Figures 19 (▲) and 20 (X).**

UC + PU + UCLE3, μM free γ-linolenoyl-CoA plus that bound to the lysophospholipid acyltransferase plus that acylated into phospholipids.

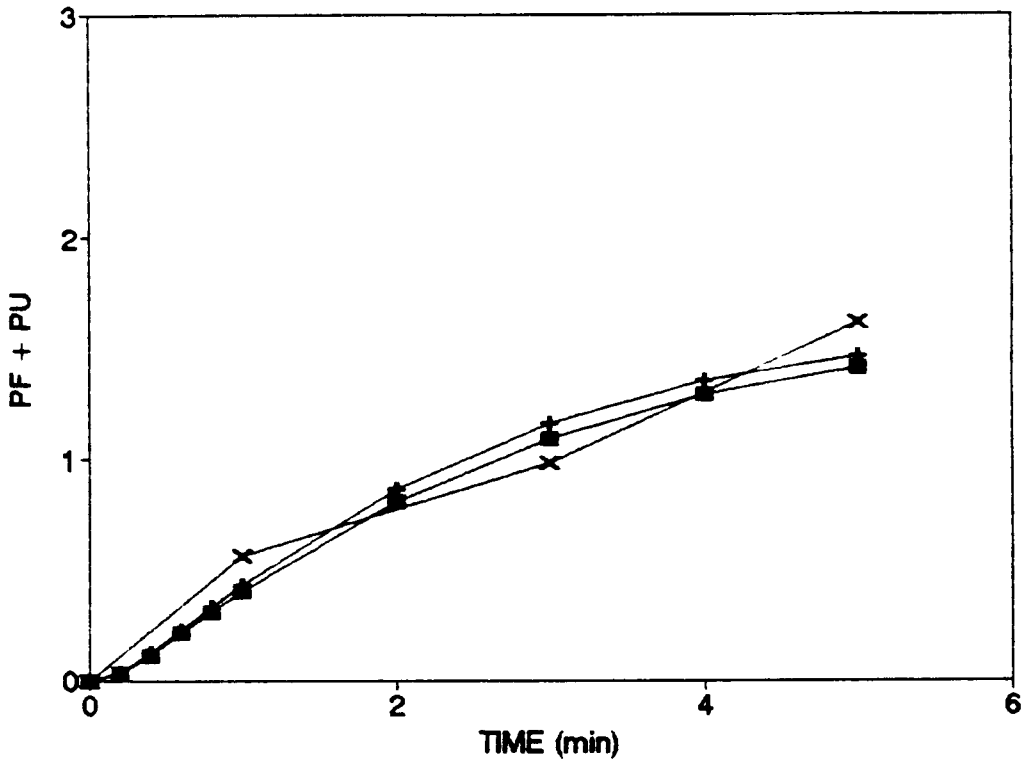

FIGURE 77 **Overlay plots of the effect of time on the acylation of phospholipids measured during the metabolism of linoleic acid (4.7 μM) using data from models 33 (+), 34, 35, 36 (■), and the experimental data from Figure 30 (X).**

PF + PU, μM linoleoyl-CoA acid plus γ-linolenoyl-CoA acylated into phospholipids.

For the Δ6-desaturase, in model 34, the values of k_5 and k_6 were increased three-fold, and decreased 20%, respectively. These changes resulted in a ca. two-fold decrease in the rate of product formation with time (Figure 76) and the simulated data no longer mimicked the experimental data closely, except that the shape of the curve appeared to be unaffected. Since the activity of the Δ6-desaturase varied up to 50% in different preparations of hepatic microsomes (see, for example, Table 28) and the data in Figures 19 and 20 were reported for a single preparation of hepatic microsomes, we attempted to maintain the linear shape, rather than the absolute activity value. Therefore, the changes in values of k_4, k_5 and k_6 for the Δ6-desaturase from models 34, 35 and 36 were aimed at improving the correlation between the data for the plot of product formation with linoleic acid concentration (Figure 33 B), while maintaining the linear nature of the plot of product formation with time (Figures 19 and 20).

In the overlay plots of the experimental and simulated data for rate of product formation versus linoleic acid concentration for models 34, 35 and 36 (Figures 78, 79 and 80), there was excellent agreement between the simulated data and the experimental data for all three models for the acyl-CoA synthetase and lysophospholipid acyltransferase (Figures 78 and 80). For the Δ6-desaturase, all three models were an improvement on model 33, with model 35 giving the closest agreement to the experimental data (Figure 79).

Therefore, the constants from model 35 provided the best correlation between the experimentally determined product formation with time for the disappearance of linoleic acid, acyl-CoA formation, Δ6-desaturase and acylation of lysophospholipid and the product formation simulated using the SLAM II program as outlined above. The experimentally determined product formation

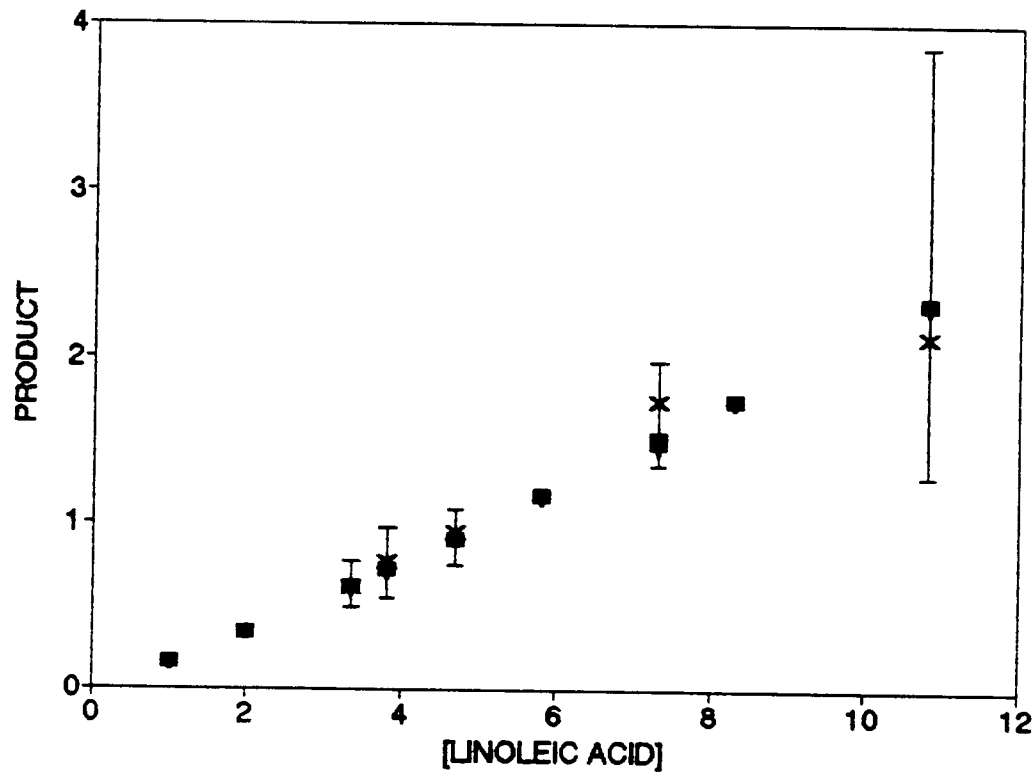

FIGURE 78 **Overlay plots of the effect of linoleic acid concentration on the formation of acyl-CoA measured during the metabolism of linoleic acid using data from models 33 (+), 34, 35, 36 (■) and the experimental data from Figure 32 B (X).**

Product, μM [$1^{-14}C$] linoleoyl-CoA + [$1^{-14}C$] γ-linolenoyl-CoA formed/min for the experimental data and linoleoyl-CoA + γ-linolenoyl-CoA + [linoleoyl-CoA.E_2] + [γ-linolenoyl-CoA.E_3] + [linoleoyl-CoA.E_3] formed/min for the simulated data; linoleic acid concentration, μM linoleic acid. Product formation was measured at 3 min and was normalised to 1 min by dividing by 3.

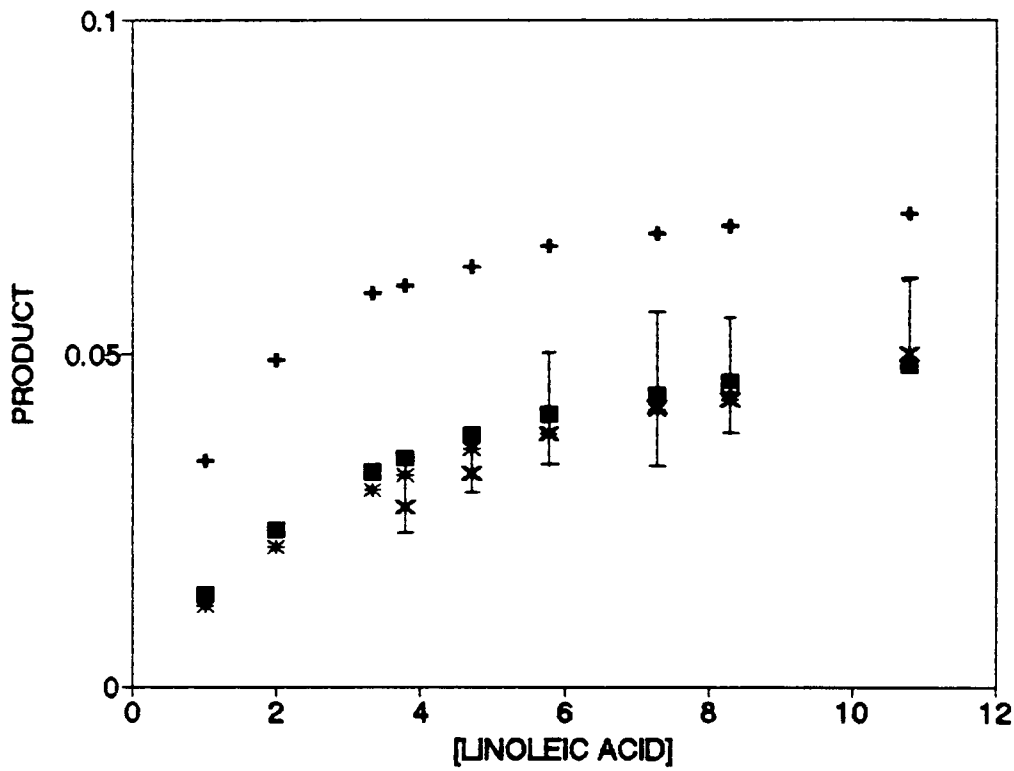

FIGURE 79

Overlay plots of the effect of linoleic acid concentration on the Δ6-desaturation of linoleic acid using data from models 33 (+), 34 (■), 35 (*), 36 (□) and the experimental data from Figure 33 B (X).

Product, [1^{-14}C] μM γ-linolenoyl-CoA + [1^{-14}C] γ-linolenoyl-phospholipid formed/min for the experimental data and μM γ-linolenoyl-CoA + γ-linolenoyl-phospholipid + [γ-linolenoyl-CoA.E_3] formed/min for the simulated data; linoleic acid concentration, μM linoleic acid. Product formation was measured at 3 min and was normalised to 1 min by dividing by 3.

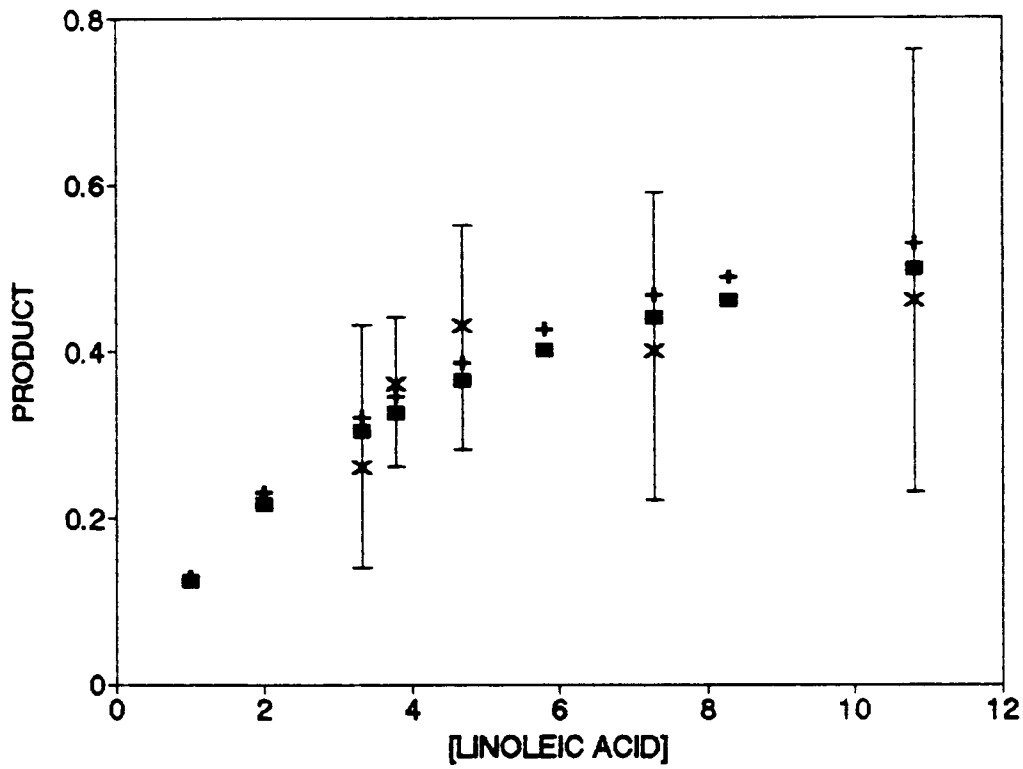

FIGURE 80 **Overlay plots of the effect of linoleic acid concentration on the acylation of phospholipids measured during the metabolism of linoleic acid using data from models 33 (+), 34, 35, 36 (■), and the experimental data from Figure 34 B (X).**

Product, μM [1-^{14}C] linoleoyl-phospholipid + [1-^{14}C] γ-linolenoyl-phospholipid formed/min for the experimental data and μM linoleoyl-phospholipid + γ-linolenoyl-phospholipid formed/min for the simulated data; linoleic acid concentration, μM linoleic acid. Product formation was measured at 3 min and was normalised to 1 min by dividing by 3.

with time together with the simulated data for disappearance of fatty acid, acyl-CoA formation, Δ6-desaturation of linoleic acid and acylation of lysophospholipid at 4.7 μM linoleic acid are illustrated in Figures 81, 82, 83 and 84, respectively. Similarly, the experimentally determined rate of product formation versus linoleic acid concentration is illustrated in Figures 85, 86 and 87, together with the rate determined from simulation of the reaction scheme using the constants from model 35 for the acyl-CoA synthetase, Δ6-desaturase and lysophospholipid acyltransferase, respectively. The rate constants from model 35, and the apparent k_{cat}, K_m and V_{max} values calculated therefrom are given in Table 38.

Once the overall reaction scheme had been simulated at several substrate concentrations, the output from model 35 was used to assess the kinetics of E_2, the Δ6-desaturase, removing the contributions from lysophospholipid acyltransferase and acyl-CoA synthetase to the experimentally obtained data (Figure 38). This process was performed as follows: the tabulated output of product verus time (see, for example, Table 36, page 215), was examined for model 35 at each initial substrate concentration. A region in time where the concentration of acyl-CoA (free plus enzyme-bound forms) was relatively constant was found and chosen as illustrated in Figure 88 A (Table 39). The values of FC plus FCE_2 with time chosen as essentially constant for each initial linoleic acid concentration are given in Table 39. This concentration of linoleoyl-CoA was used in Lineweaver-Burk and Eadie-Hofstee plots for the Δ6-desaturase. The product formation (all forms of γ-linolenoyl-CoA, i.e. UC, $UCLE_3$ and PU) over this time period at 0.2 minute intervals is given in Table 39. Product formation was plotted versus time and each plot checked for linearity (see, for example, Figure 88 B). The product formation (all forms of

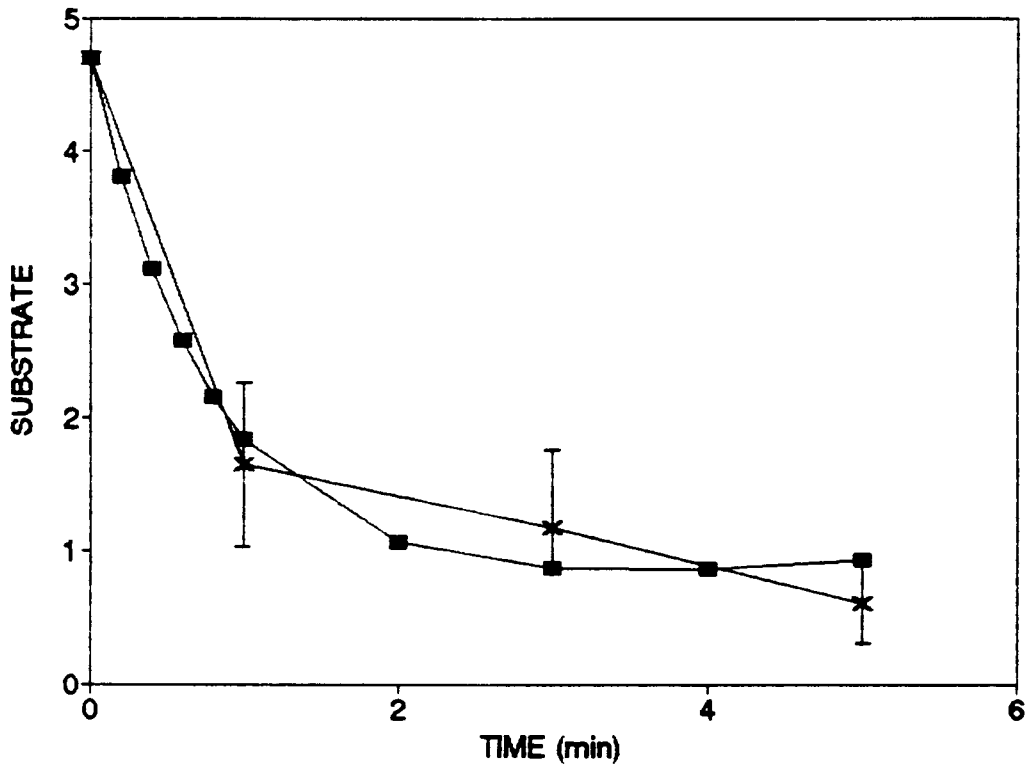

FIGURE 81 **The effect of time on the disappearance of fatty acid (substrate) measured during the metabolism of linoleic acid (4.7 μM) in hepatic microsomes using experimentally obtained data from Figure 30 (X) and data obtained from model 35 of the simulated reaction scheme (■).**

Substrate, μM [1^{-14}C] linoleic acid formed for the experimental data and [linoleic acid + linoleic acid.E_1] formed for the simulated data. For the experimental data, BSA concentration was 11.5 μg/μg linoleic acid added. Separation of the fatty acid, phospholipid and acyl-CoA from hepatic microsomes was carried out by differential organic extractions (Section 2.2.3.8a, Method B). Data represents quintipulate determinations on one preparation of hepatic microsomes.

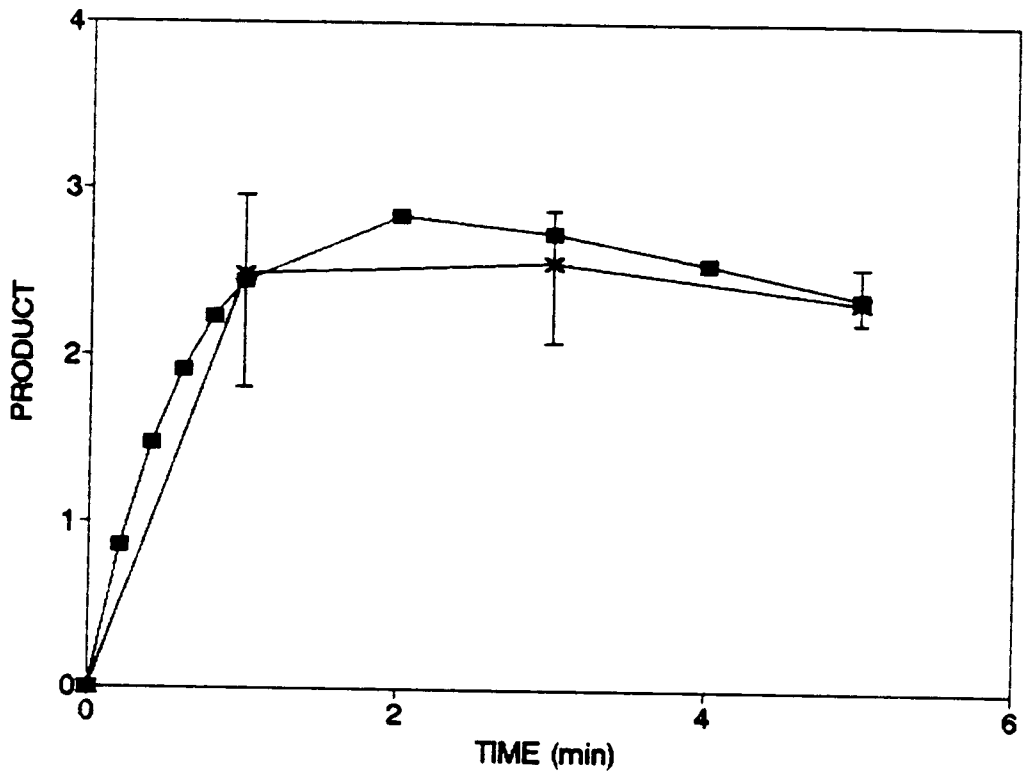

FIGURE 82

The effect of time on the formation of acyl-CoA measured during the metabolism of linoleic acid (4.7 μM) in hepatic microsomes using experimentally obtained data from Figure 30 (X) and data obtained from model 35 of the simulated reaction scheme (■).

Product, μM [1-^{14}C] linoleoyl-CoA + [1-^{14}C] γ-linolenoyl-CoA formed for the experimental data and linoleoyl-CoA + γ-linolenoyl-CoA + [linoleoyl-CoA.E_2] + [γ-linolenoyl-CoA.E_3] + [linoleoyl-CoA.E_3] formed for the simulated data. For the experimental data, BSA concentration was 11.5 μg/μg linoleic acid added. Separation of the fatty acid, phospholipid and acyl-CoA from hepatic microsomes was carried out by differential organic extractions (Section 2.2.3.8a, Method B). Data represents quintipulate determinations on one preparation of hepatic microsomes.

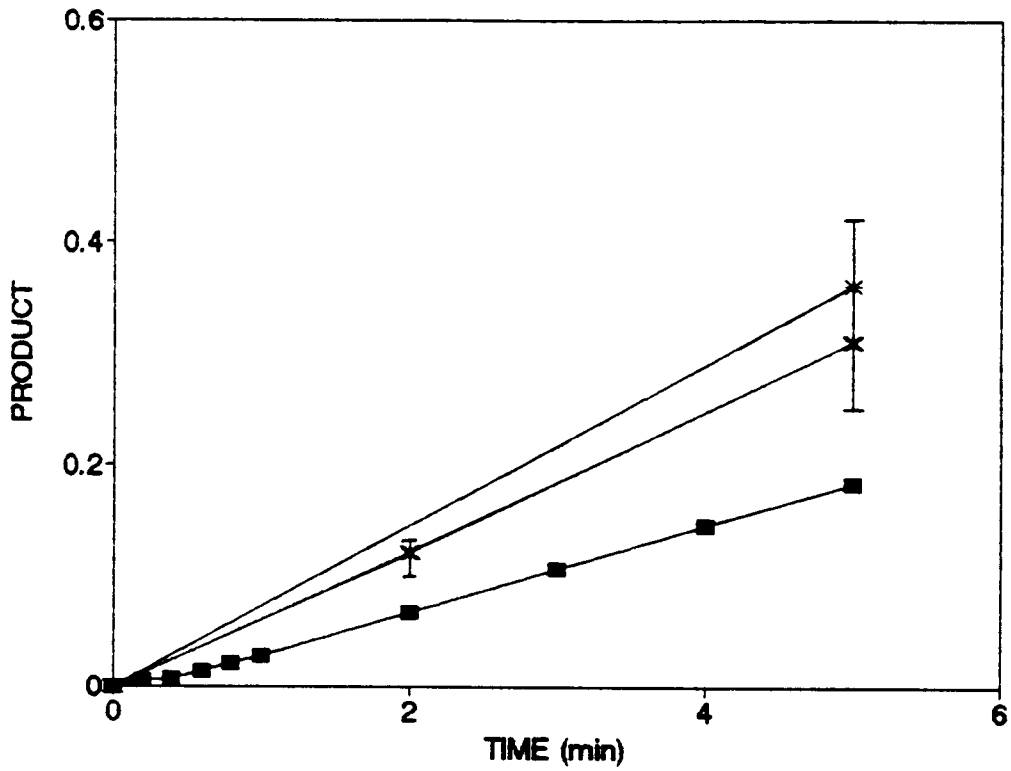

FIGURE 83

The effect time on the Δ6-desaturation of linoleic acid (4.7 μM) in hepatic microsomes using experimentally obtained data from Figures 19 (*) and 20 (X) and data obtained from model 35 of the simulated reaction scheme (■).

Product, μM [$1^{-14}C$] γ-linolenoyl-CoA + [$1^{-14}C$] γ-linolenoyl-phospholipid formed for the experimental data and μM γ-linolenoyl-CoA + γ-linolenoyl-phospholipid + [γ-linolenoyl-CoA.E_3] formed for the simulated data; linoleic acid concentration was 4.7 μM. Δ6-Desaturase activity in hepatic microsomes was measured using Methods 1 (*) and 2 (X). For the experimental data, BSA concentration was 11.5 μg/μg linoleic acid added in Method 1 (*), and 115 μg/μg linoleic acid added in Method 2 (X). In both cases, data represents triplicate determinations on one preparation of hepatic microsomes. The shape of the curve is typical of that obtained with two other microsomal preparations, but product formation varied up to ca. 50% depending on the preparation.

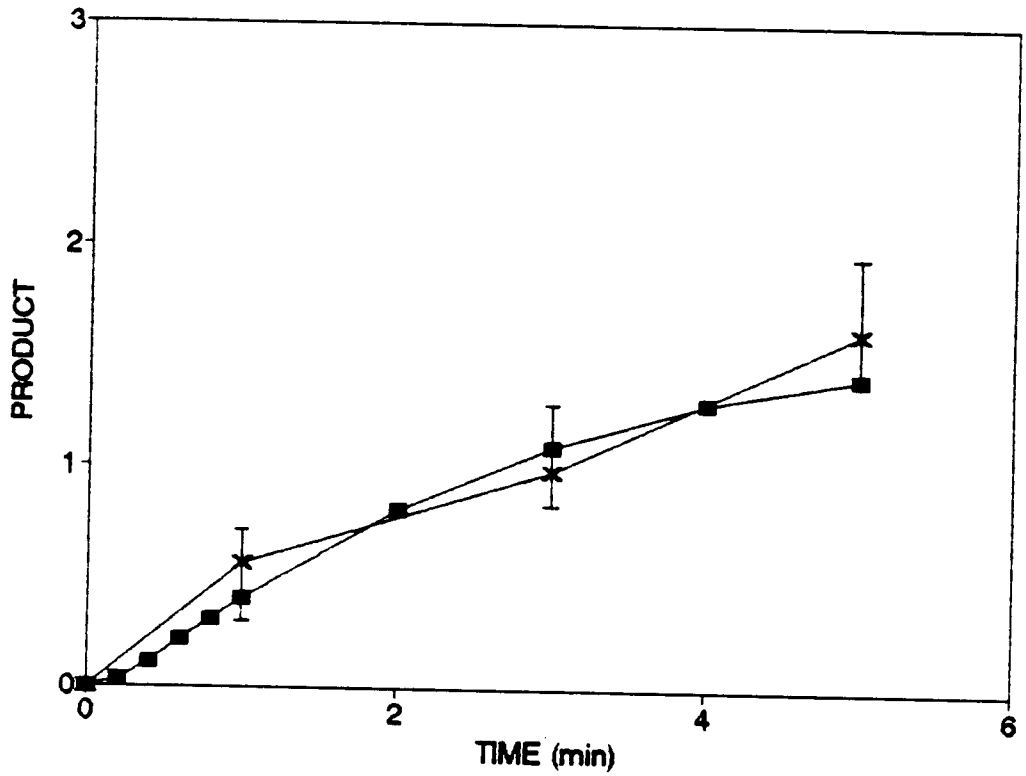

FIGURE 84

The effect of time on the acylation of phospholipids during the metabolism of linoleic acid (4.7 μM) in hepatic microsomes using experimentally determined data from Figure 30 (X) and data obtained from model 35 of the simulated reaction scheme (■).

Product, μM [1-^{14}C] 2-linoleoyl- + [1-^{14}C] 2-γ-linolenoyl-phospholipid formed for the experimental and simulated data. For the experimental data, BSA concentration was 11.5 μg/μg linoleic acid added. Separation of the fatty acid, phospholipid and acyl-CoA from hepatic microsomes was carried out by differential organic extractions (Section 2.2.3.8a, Method B). Data represents quintipulate determinations on one preparation of hepatic microsomes.

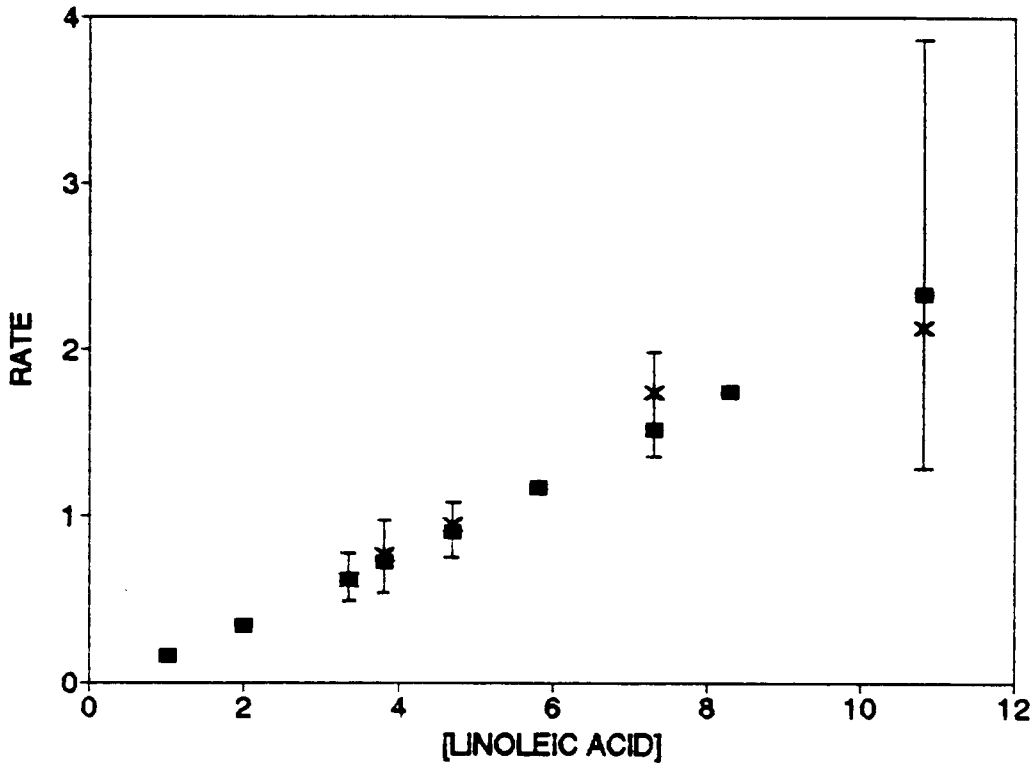

FIGURE 85 **Plot of formation of acyl-CoA by acyl-CoA synthetase versus linoleic acid concentration using experimentally obtained data from Figure 32 B (X) and data obtained from model 35 of the simulated reaction scheme (■).**

Rate, μM [1-^{14}C] linoleoyl-CoA + [1-^{14}C] γ-linolenoyl-CoA formed/min for the experimental data and linoleoyl-CoA + γ-linolenoyl-CoA + [linoleoyl-CoA.E_2] + [γ-linolenoyl-CoA.E_3] + [linoleoyl-CoA.E_3] formed/min for the simulated data; linoleic acid concentration, μM linoleic acid. Product formation was measured at 3 min and was normalised to 1 min by dividing by 3. For the experimental data, BSA concentration was 11.5 μg/μg linoleic acid added. Separation of the fatty acid, phospholipid and acyl-CoA from hepatic microsomes was carried out by differential organic extractions (Section 2.2.3.8a, Method B). Data represents the average of three to five determinations obtained from three preparations of hepatic microsomes.

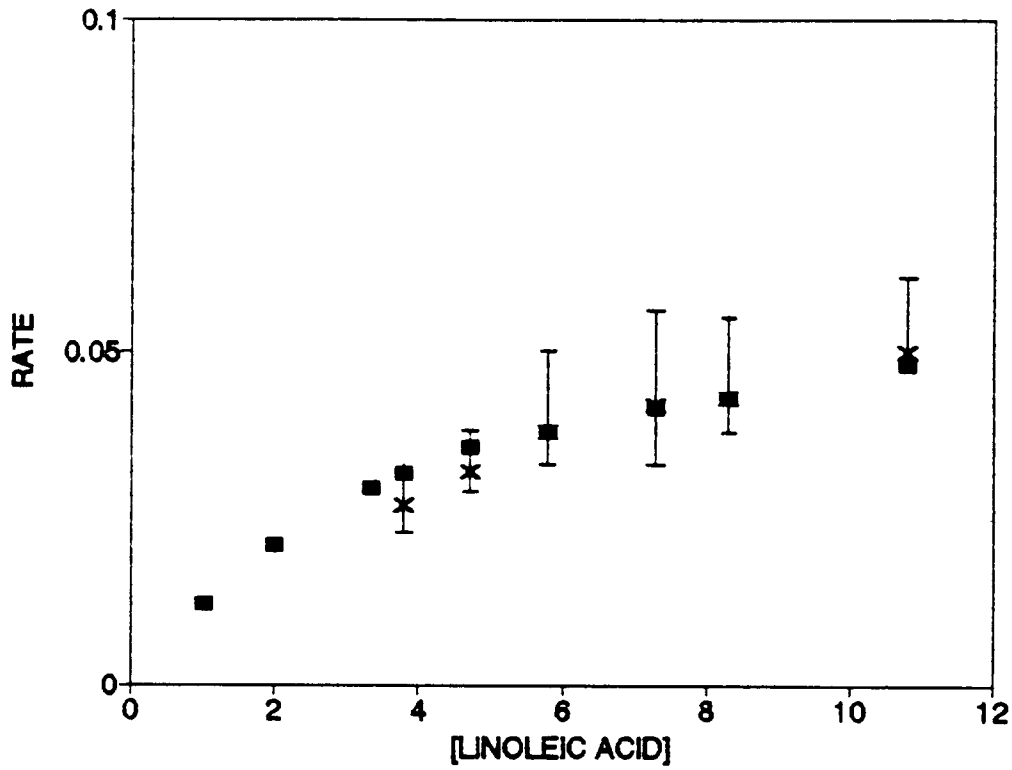

FIGURE 86

Plot of rate of formation of γ-linolenic acid by Δ6-desaturase versus linoleic acid concentration using experimentally obtained data from Figure 33 B (X) and data obtained from model 35 of the simulated reaction scheme (■).

Rate, μM [1-^{14}C] γ-linolenoyl-CoA + [1-^{14}C] γ-linolenoyl-phospholipid formed/min for the experimental data and μM γ-linolenoyl-CoA + γ-linolenoyl-phospholipid + [γ-linolenoyl-CoA.E_3] formed/min for the simulated data; linoleic acid concentration, μM linoleic acid. Product formation was measured at 3 min and was normalised to 1 min by dividing by 3. For the experimental data, BSA concentration was 11.5 μg/μg linoleic acid added. Δ6-Desaturase activity in hepatic microsomes was measured using Method 2. Data represents the average of that obtained in triplicate from three preparations of hepatic microsomes.

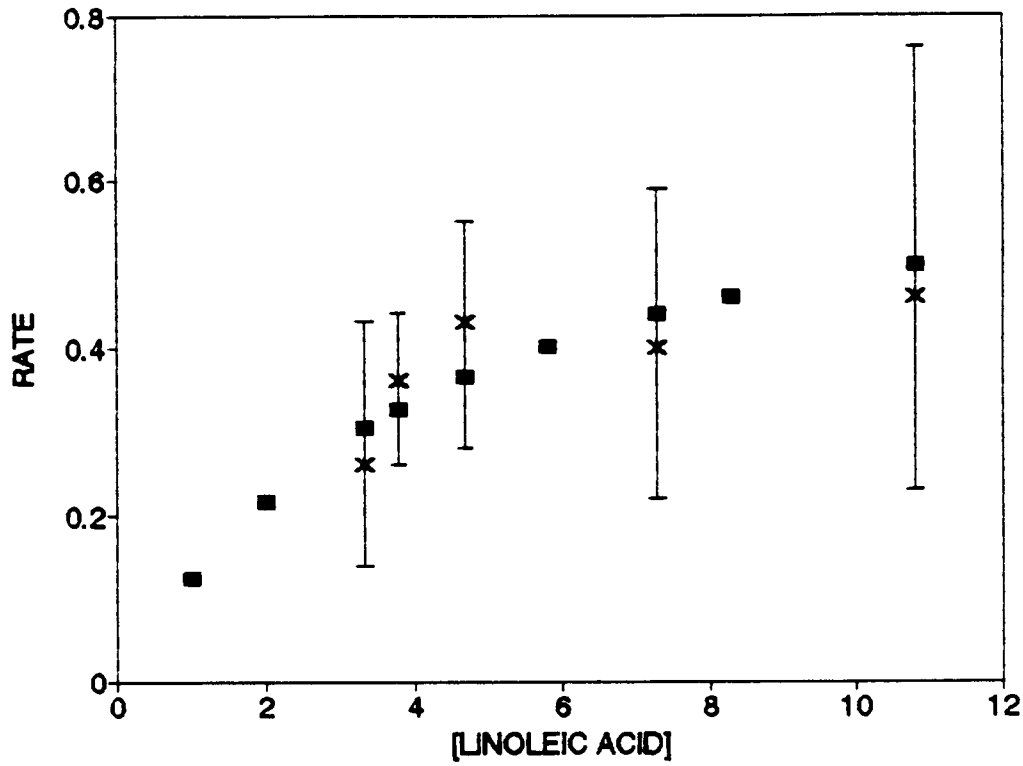

FIGURE 87

Plot of rate of acylation of phospholipids by the lysophospholipid acytransferases versus linoleic acid concentration using experimentally obtained data from Figure 34 B (X) and data obtained from model 35 of the simulated reaction scheme (■).

Rate, μM [1-^{14}C] 2-linoleoyl- + [1-^{14}C] 2-γ-linolenoyl-phospholipid formed/min for the experimental and simulated data; linoleic acid concentration, μM linoleic acid. Product formation was measured at 3 min and was normalised to 1 min by dividing by 3. For the experimental data, BSA concentration was 11.5 μg/μg linoleic acid added. Separation of the fatty acid, phospholipid and acyl-CoA from hepatic microsomes was carried out by differential organic extractions (Section 2.2.3.8a, Method B). Data represents the average three to five determinations obtained from three preparations of hepatic microsomes.

TABLE 38

RATE CONSTANTS FROM COMPUTER MODELLING OF MODEL 35 AND PARAMETERS CALCULATED THEREFROM

Enzyme	Rate Constant	Value	Apparent K_m (μM)	Apparent k_{cat} (min^{-1})	Apparent V_{max} ($\mu M/min^{-1}$)
Acyl-CoA	k_1	1.5×10^2 *			
synthetase	k_2	1.5×10^3 †	$(k_2+k_3)/k_1 = 10.17$	$k_3 = 25$	16.25
	k_3	2.5×10^1 †			
Δ6-Desaturase	k_4	5.5×10^1 *			
	k_5	8.5×10^1 †	$(k_5+k_6)/k_4 = 1.57$	$k_6 = 1.28$	0.064
	k_6	1.28 †			
Lysophospholipid	$k_7 = k_{10}$	5.5 *	$(k_8+k_9)/k_7 =$	$k_9 = k_{12} =$	1.0
acyltransferase	$k_8 = k_{11}$	5.5 †	$(k_{11}+k_{12})/k_{10} =$	2.0	
	$k_9 = k_{12}$	2.0 †	1.36		
Acyl-CoA hydrolase	k_{13}	1.1×10^{-1} †			
	k_{14}	5.0×10^{-1} †			
	k_{15}	0			
	k_{16}	1.0 †			

* in μM^{-1}, min^{-1}

† in min^{-1}

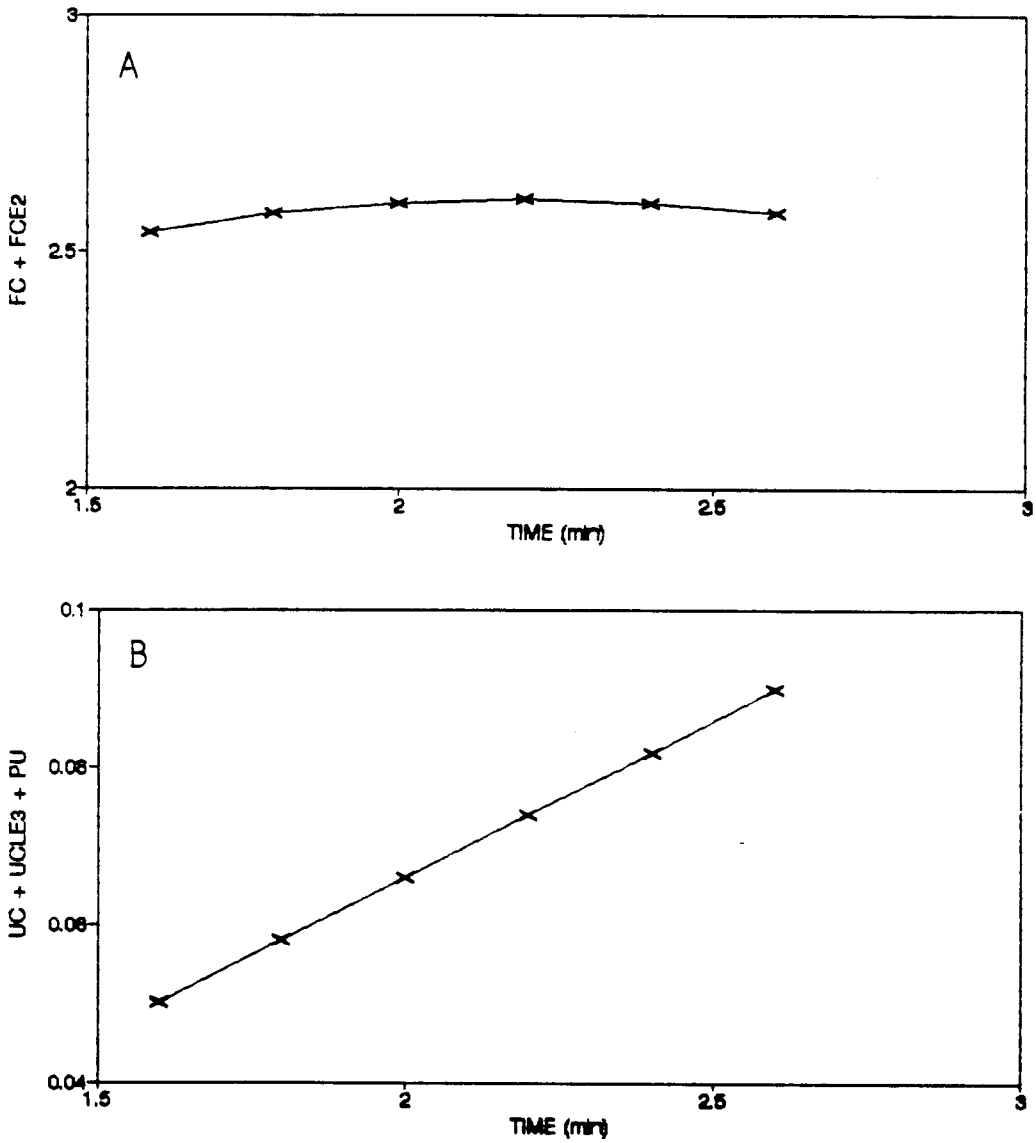

FIGURE 88 **Formation of all the species of linoleoyl-CoA (A) and γ-linolenoyl-CoA (B) from linoleic acid (4.7 μM) with time using data from model 35 of the simulated reaction scheme.**

FC + FCE2, free linoleoyl-CoA + linoleoyl-CoA bound to the acyl-CoA synthetase; UC + UCLE3 + PU, free γ-linolenoyl-CoA + γ-linolenoyl-CoA bound to the lysophospholipid acyltransferase and acylated into phospholipids.

TABLE 39

THE EFFECT OF TIME ON THE CONCENTRATIONS OF INTERMEDIATES GENERATED FROM COMPUTER MODELLING OF MODEL 35 AT DIFFERENT INITIAL CONCENTRATIONS OF LINOLEIC ACID

Intermediates*	Time (min)	Total Concentration of Intermediates (μM)						
Initial linoleic acid concentration (μM)		3.35	3.8	4.7	5.8	7.3	8.3	10.8
FC + FCE_2†	1.4	1.27	1.52					
	1.6	1.29	1.56	2.08				
	1.8	1.30	1.57	2.12	2.82			
	2.0	1.30	1.57	2.13	2.85	3.82	4.47	
	2.2	1.28	1.55	2.12	2.85	3.85	4.51	
	2.4	1.26	1.53	2.10	2.85	3.85	4.54	6.21
	2.6				2.84	3.84	4.53	6.24
	2.8					2.80	4.50	6.25
	3.0							6.23
UC + $UCLE_3$ + PU	1.4	0.062	0.066					
	1.6	0.074	0.078	0.088				
	1.8	0.086	0.091	0.098	0.105			
	2.0	0.098	0.103	0.112	0.119	0.125	0.128	
	2.2	0.110	0.116	0.125	0.133	0.139	0.142	
	2.4	0.122	0.129	0.139	0.147	0.154	0.157	0.162
	2.6				0.161	0.168	0.172	0.177
	2.8					0.182	0.186	0.192
	3.0							0.207

* FC + FCE_2, linoleoyl-CoA plus linoleoyl-CoA bound to the Δ6-desaturase; UC + $UCLE_3$ + PU, γ-linolenoyl-CoA plus γ-linolenoyl-CoA bound to the lysophospholipid acyltransferase plus that acylated into phospholipids (see Figure 38).

† Underlined concentrations were used as the initial substrate concentration for linoleoyl-CoA for reciprocal plots of the Δ6-desaturase activity shown in Figure 89.

γ-linolenoyl-CoA, i.e. UC, $UCLE_3$ and PU) at the beginning of this time period was subtracted from product levels at the end of this time period and normalised to 1 minute. The output, viz: total γ-linolenoyl-CoA formed per minute, was used as the initial rate data for Lineweaver-Burk and Eadie-Hofstee plots for the Δ6-desaturase.

Lineweaver-Burk and Eadie-Hofstee plots constructed using the linoleoyl-CoA concentration and the rate of product formation calculated from the simulated data from model 35 as outlined above, are shown in Figure 89. The Lineweaver-Burk and Eadie-Hofstee plots for the conversion of linoleoyl-CoA to γ-linolenoyl-CoA by the Δ6-desaturase were linear (Figure 89).

The apparent K_m and k_{cat} (or V_{max}) values for this reaction were calculated in two different ways as follows:

i) first, they were calculated directly from the rate constants from model 35 viz: $(k_5 + k_6)/k_4$ equal to K_m; and k_6 equal to k_{cat}, as shown in Table 38.

ii) second, the data in Figure 89 was curve fit using the Michaelis Menten equation; the K_m value calculated from this plot was 1.52 ± 0.04 μM and the V_{max} value was 0.063 ± 0.001 μM/min.

The inhibition of the Δ6-desaturase by isoflurane using computer modelling of the reaction scheme was examined. In model 35A, the value of k_4 was decreased relative to model 35. The overlay plot of simulation of the reaction

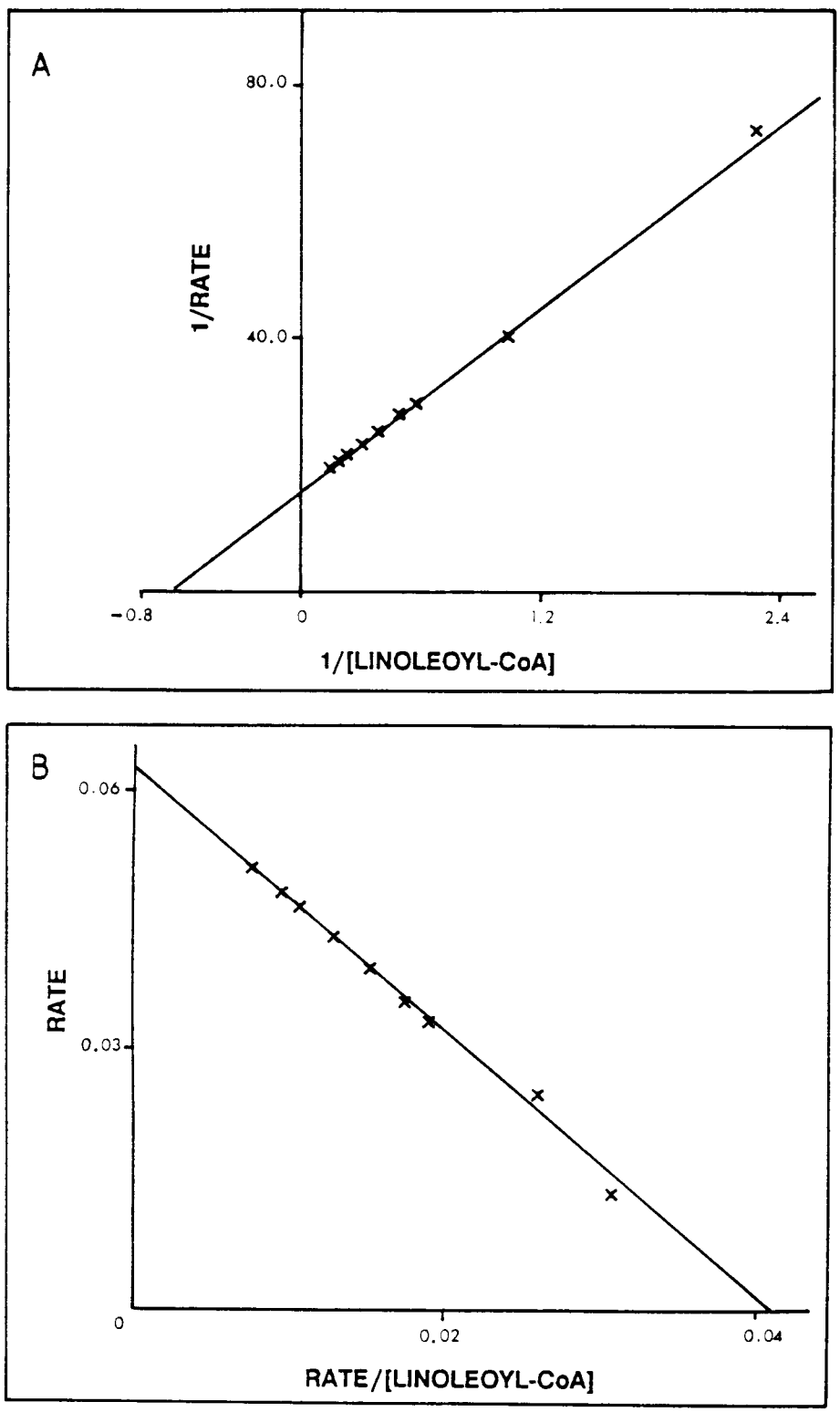

FIGURE 89 **Lineweaver-Burk (A) and Eadie-Hofstee (B) plots for the Δ6-desaturation of linoleoyl-CoA using data from model 35 the simulated reaction scheme.**

Rate, μM γ-linolenoyl-CoA + γ-linolenoyl-CoA bound to the lysophospholipid acyltransferases and acylated into phospholipids formed/min; linoleoyl-CoA concentration, μM linoleoyl-CoA. Lines were drawn by Enzfitter (Section 2.2.3.10).

scheme using data from model 35A and the experimental data for the rate of product formation as a function of linoleic acid concentration for the Δ6-desaturase in the presence of isoflurane*, are illustrated in Figure 90. In order to adjust the output of the computer model to fit the experimental data for the inhibition of the Δ6-desaturase by isoflurane, only one rate constant had to be changed: k_4 was reduced to 4.6×10^1 μM^{-1} min^{-1}. By adjusting k_4, the K_m value for the Δ6-desaturase in the presence of isoflurane calculated from the constants $(k_5 + k_6)/k_4$ was increased to 1.88 μM from 1.57 μM, the value seen in the absense of isoflurane (Table 38). The k_{cat} value was unaffected, and remained 1.28 min^{-1}. For the modelled data of the inhibition of the Δ6-desaturase by isoflurane, reciprocal plots of the output rates versus linoleoyl-CoA concentration were determined in an analogous manner to that shown in Table 39. The double reciprocal for the presence of isoflurane was linear, and intersected on the Y-axis with the line for minus isoflurane (Figure 91). The K_m value for E_2 in the presence of isoflurane calculated from fitting the Michaelis-Menten equation to the data in Figure 91 was 1.89 ± 0.01 μM, which differed from the value calculated in the absence of isoflurane (1.52 ± 0.04). The V_{max} value for the Δ6-desaturase was the same whether calculated from the data in the presence or absence of isoflurane, viz: 0.064 ± 0.001 μM/min and 0.063 ± 0.001 μM/min for the presence and absence of isoflurane, respectively.

* Experimental data for Δ6-desaturase activity measured in the presence and absence of isoflurane was obtained from the same three preparations of hepatic microsomes.

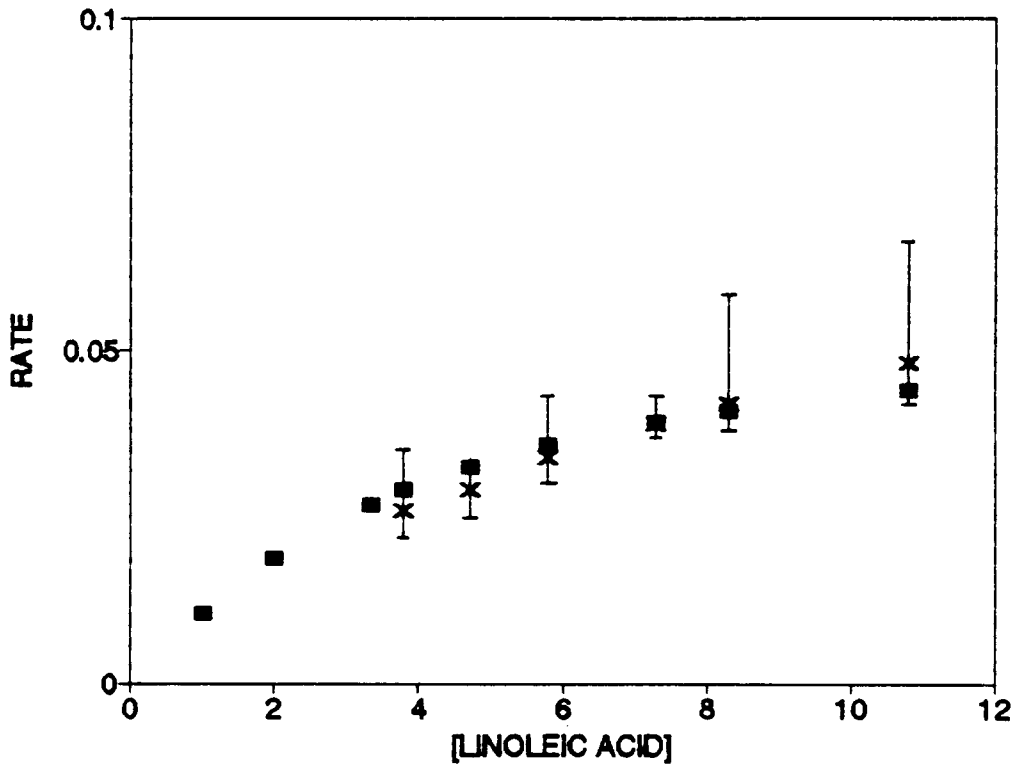

FIGURE 90 **Plot of rate of formation of γ-linolenic acid by Δ6-desaturase versus linoleic acid concentration in the presence of isoflurane (2mM) using experimentally obtained data (X) and data obtained from model 35A of the simulated reaction scheme (■).**

Rate, μM [1^{-14}C] γ-linolenoyl-CoA + [1^{-14}C] γ-linolenoyl-phospholipid formed/min for the experimental data and μM γ-linolenoyl-CoA + γ-linolenoyl-phospholipid + [γ-linolenoyl-CoA.E_3] formed/min for the simulated data; linoleic acid concentration, μM linoleic acid. Product formation was measured at 3 min and was normalised to 1 min by dividing by 3. For the experimental data, BSA concentration was 11.5 μg/μg linoleic acid added. Δ6-Desaturase activity in hepatic microsomes was measured using Method 2. Data represents the average of that obtained in triplicate from three preparations of hepatic microsomes.

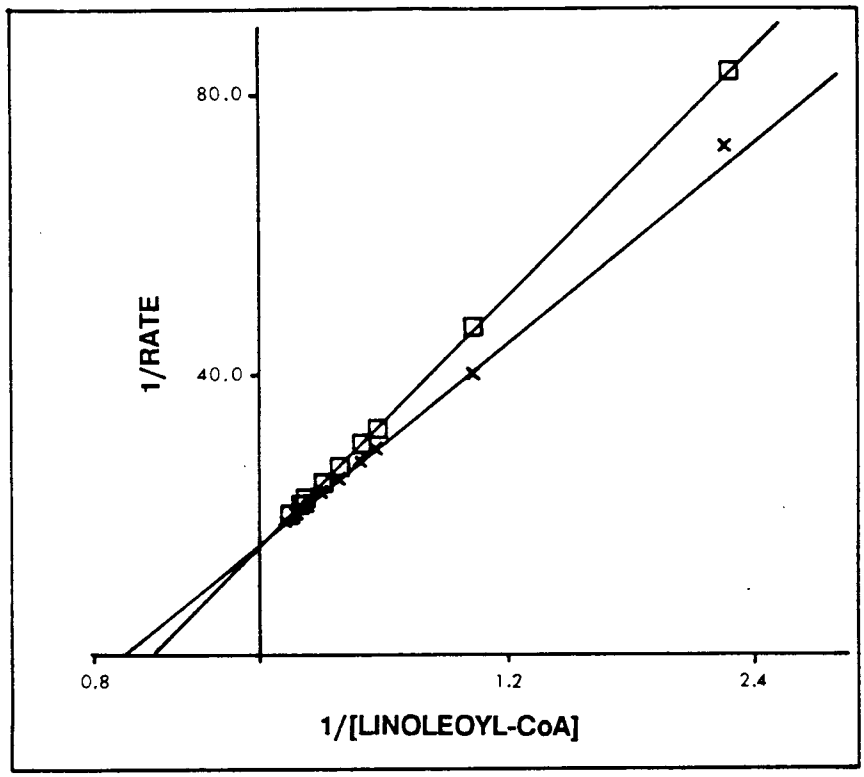

FIGURE 91 **Lineweaver-Burk plot for the Δ6-desaturation of linoleoyl-CoA in the absence (X) and presence (□) of isoflurane using data from models 35 and 35A of the simulated reaction scheme.**

Rate, μM γ-linolenoyl-CoA + γ-linolenoyl-CoA bound to the lysophospholipid acyltransferases and acylated into phospholipids formed/min; linoleoyl-CoA concentration, μM linoleoyl-CoA. Lines were drawn by Enzfitter (Section 2.2.3.10).

4. DISCUSSION

Since many of the deleterious effects of volatile anaesthetics can be attributed to their metabolism, much attention has focussed on understanding the details of anaesthetic metabolism, including the binding of the drug and their metabolites to cellular macromolecules and the influence of administered drugs on anaesthetic metabolism. In this study we have attempted to contribute to the understanding of the metabolism of the anaesthetic agent isoflurane, by investigating the following:

i) the metabolism of isoflurane by rat hepatic cytochrome P-450 isozymes which are members of the gene families I, II and III, and by cytochrome P-450 in human hepatic microsomes.

ii) the identification of the organofluoride metabolites of isoflurane in rat and human hepatic microsomes resulting in further elucidation of the pathways of isoflurane metabolism.

iii) the interaction of isoflurane (and other anaesthetic agents) with the fatty acid desaturases.

iv) the inhibition of the Δ6-desaturase by isoflurane.

Firstly, the metabolism of isoflurane by rat and human hepatic cytochrome P-450 is discussed.

4.1 THE INTERACTION OF ISOFLURANE WITH RAT AND HUMAN HEPATIC CYTOCHROME P-450

The results presented in this thesis confirm that the major non-volatile metabolite of isoflurane is fluoride ion (4,184,193,194). The K_m and V_{max} values for isoflurane defluorination in microsomes from phenobarbital-pretreated rats herein can now be compared with those for enflurane and methoxyflurane defluorination reported by Ivanetich et al (182). From a comparison of the V_{max} values (per nmol cytochrome P-450) for the rates of defluorination of these anaesthetic agents, it appears that the rate of defluorination in vitro increased in the same order as the relative extent of their metabolism in vivo (182,191), as follows: isoflurane (V_{max} = 0.017 nmol fluoride ion/nmol cytochrome P-450/min) < enflurane (V_{max} = 0.055 nmol fluoride ion/nmol cytochrome P-450/min) < methoxyflurane (V_{max} = 0.42 nmol fluoride ion/nmol cytochrome P-450/min). In contrast, the K_m values decreased in the same order, viz: isoflurane (K_m = 0.86 mM) > enflurane (K_m = 0.355 mM) > methoxyflurane (K_m = 0.099 mM) (182).

The decrease in the K_m values and increase in V_{max} in the series isoflurane, enflurane and methoxyflurane is consistent with their reactivities towards O-dealkylation and dechlorination proposed by Loew et al (183), and with the in vitro rates of defluorination (182).

Although fluoride ion production from isoflurane in rat hepatic microsomes was dependent on the presence of NADPH, NADH supported the defluorination of isoflurane to a greater extent (73%) than that observed for most cytochrome P-450 dependent reactions (5 - 10%) (Table 14) (34,62). The high extent to which NADH supported the defluorination of isoflurane suggests that

cytochrome b_5 may play a role in electron transfer to cytochrome P-450 during the reaction. Alternatively, NADH may in part support the defluorination of isoflurane by another enzyme system. This possibility was not investigated, but could occur since isoflurane interacted with the Δ6-desaturase (which will be discussed later), and possibly other enzyme systems.

Although inhibition of NADPH and/or NADH supported hepatic microsomal metabolic reactions by CO is often used to identify a cytochrome-P-450-catalysed reaction, the extent of CO-inhibition of isoflurane defluorination was very small (Table 13). There are a number of other cytochrome P-450-catalysed reactions which are poorly inhibited by CO, such as those catalysed by the biosynthetic cytochrome P-450 isozymes (111). The extent of inhibition by CO is known to vary with the substrate and the isozyme (377). The significant, if small, inhibition of isoflurane defluorination by CO and metyrapone, nevertheless, suggests that cytochrome P-450 catalyses this reaction, at least in part. The greater extent of inhibition of isoflurane defluorination observed with metyrapone than with CO may result from inhibition of the reaction at both the substrate- and ligand-binding sites by metyrapone; metyrapone has been shown to bind to both sites and is reported to be more effective in inhibiting cytochrome P-450-dependent reactions than CO (111,113).

Further evidence that cytochrome P-450 catalysed the defluorination of isoflurane is provided by the rates of fluoride ion production following induction of the different cytochrome P-450 isozymes (Table 12). By comparing the rates of defluorination of isoflurane in hepatic microsomes from rats which had received pretreatments resulting in preferential induction of different cytochrome

P-450 isozymes, it was possible to ascertain which of the isozyme(s) primarily catalysed this reaction in microsomal preparations.

Since pretreatment of rats with β-naphthoflavone had no effect on the rate of defluorination of isoflurane, the β-naphthoflavone-inducible cytochrome P-450 isozymes (cytochrome P-450c and d) appeared to play no role in this reaction (Table 12). These results are consistent with the report by Mazze and Hitt that pretreatment of rats with 3-methylcholanthrene, also an inducer of cytochrome P-450c and cytochrome P-450d, did not increase the rate of isoflurane defluorination in rat hepatic microsomes (184).

Pretreatment of rats with phenobarbital or pregnenolone-16α-carbonitrile enhanced the rate of isoflurane defluorination in rat hepatic microsomes (Table 12) suggesting that one or more of the isozymes induced by these agents may catalyse isoflurane metabolism. Phenobarbital induces cytochrome P-450 isozymes of the P450IIB gene subfamily, including cytochrome P-450b and e, as well members of the P450IIIA gene subfamily, cytochrome P-450PCN1 and cytochrome P-450PCN2 (119,126). Pregnenolone-16α-carbonitrile pretreatment of animals elevates the levels of only cytochrome P-450PCN1 (119,126), and that to a greater extent than phenobarbital.

From the results presented in Table 12, it can be seen that the defluorination of isoflurane in hepatic microsomes from phenobarbital- and pregnenolone-16α-carbonitrile-pretreated rats proceeded at rates respectively 3.7-fold and 7.9-fold (pmol fluoride ion/mg microsomal protein) higher than that in uninduced hepatic microsomes. Since pregnenolone-16α-carbonitrile

induction enhanced the rate of isoflurane defluorination to a greater extent than phenobarbital induction of cytochrome P-450, it appears that the cytochrome P-450 isozyme preferentially induced by pregnenolone-16α-carbonitrile, and significantly induced by phenobarbital, viz: cytochrome P-450PCN1, catalysed the defluorination of isoflurane. Our results did not eliminate a possible role for cytochrome P-450b and cytochrome P-450e in isoflurane defluorination. Confirmation of the involvement of cytochrome P-450PCN1, and not cytochrome P-450b or cytochrome P-450e in the metabolism of isoflurane, can only be obtained from a study of the defluorination of isoflurane using the purified isozymes in a reconstituted system together with the other components necessary for catalytic activity (Figure 2).

A comparison of the K_m and V_{max} values for fluoride ion production from isoflurane in hepatic microsomes from phenobarbital- and pregnenolone-16α-carbonitrile-pretreated rats provided further evidence that cytochrome P-450PCN1 catalysed the defluorination of isoflurane. Since the K_m values were the same in hepatic microsomes from both phenobarbital- and pregnenolone-16α-carbonitrile-pretreated rats (0.86 ± 0.05 mM), a single isozyme of cytochrome P-450 may catalyse the defluorination of isoflurane. The V_{max} value was approximately two-fold higher in hepatic microsomes from pregnenolone-16α-carbonitrile-pretreated rats (Section 3.1.2) indicating that the isozyme which catalysed the defluorination of isoflurane was induced to a greater extent by pregnenolone-16α-carbonitrile than phenobarbital, i.e. cytochrome P-450PCN1.

Until fairly recently, most studies of the defluorination of anaesthetic agents have focussed on the phenobarbital-inducible isozymes (cytochrome P-450b

and/or cytochrome P-450e) or the polycyclic aromatic hydrocarbon-inducible isozymes (cytochrome P-450c and/or cytochrome P-450d) (182,184). The results reported herein confirmed earlier reports that phenobarbital pretreatment of rats enhances the rate of isoflurane defluorination in vitro whereas the polycyclic aromatic hydrocarbon inducing agents, e.g. β-napthoflavone and 3-methylcholanthrene, do not (184). These results also suggested that cytochrome P-450PCN1 participates in anaesthetic metabolism but the role played by cytochrome P-450PCN1 in the metabolism of other anaesthetic agents is still unknown. The recent report that isoflurane inhibits the oxidative, but not the reductive metabolism of halothane suggests that oxidative metabolism of halothane and defluorination of isoflurane may be catalysed by the same cytochrome P-450 isozyme, namely cytochrome P-450PCN1 and/or cytochrome P-450 3a (178,179,185,186). Cytochrome P-450 3a is the ethanol-inducible isozyme shown to metabolise isoflurane (186). In contrast, isoflurane does not inhibit the reductive metabolism of halothane (378,379). The reductive metabolism of halothane has been shown to be catalysed by the major phenobarbital-inducible cytochrome P-450 isozyme from rabbit liver, cytochrome P-450LM_2 (175,176), confirming that this isozyme does not appear to catalyse the defluorination of isoflurane.

The metabolism of isoflurane was also measured indirectly by the CO-inhibitable NADPH consumption (Table 10). The rate of NADPH oxidation was far higher than the rate of fluoride ion production from isoflurane; in hepatic microsomes from phenobarbital-, β-naphthoflavone-pretreated and untreated rats, the rate of NADPH oxidation was approximately 100-fold higher than the rate of fluoride ion production, whereas in hepatic microsomes from pregnenolone-16α-carbonitrile-pretreated rats, the rate of NADPH oxidation was approximately

10-fold higher than the rate of fluoride ion production (Tables 10 and 12). Since two fluoride ions are produced for every isoflurane molecule metabolised, the difference between NADPH oxidation and fluoride ion production was a factor of two higher than that measured, i.e. 20- to 200-fold.

The observed stoichiometry for defluorination of isoflurane in phenobarbital-induced hepatic microsomes was as follows: 5.7 nmol NADPH oxidised:2.12 nmol hydrogen peroxide generated:0.06 nmol fluoride produced (Tables 10, 12 and 16). In the absence of isoflurane, 5.19 nmol hydrogen peroxide is produced (Table 16); on the addition of isoflurane, the hydrogen peroxide produced is reduced by 3.07 nmol, but only 0.06 nmol fluoride is produced. Therefore, considering the combined stoichiometry of cytochrome P-450 monooxygenase and oxidase activities (Introduction, equations 1 and 2, pages 14 and 19, respectively), there was a difference between the NADPH oxidation and hydrogen peroxide generation (3.58 nmol more NADPH oxidised) which was not quantitatively balanced by fluoride ion production (0.06 nmol). Since the discrepancy between NADPH oxidation, hydrogen peroxide generation and fluoride ion production could not be explained, the experimental conditions of hydrogen peroxide measurement were examined. Optimum conditions for accurate measurement of hydrogen peroxide measurement by the spectrophotometric method were determined (Table 15) and finally the rate of hydrogen peroxide generation was measured using two different assays. The results from the two assays were identical (Table 16).

The exact fate of the extra reducing equivalents utilised in the defluorination of

isoflurane is still not clear. However, possible fates may be as follows:

i) a four-electron transfer may be required by cytochrome P-450 during the defluorination of isoflurane, similar to that which occurs during the oxidation of ethanol (82); the occurrence of a four-electron transfer is reported to depend on the substrate (380). However, this would account for only 0.06 nmol of the extra 3.58 nmol NADPH utilised.

ii) a four-electron transfer may occur in the presence of substrate, resulting in the production of water instead of active oxygen species or fluoride ion (Figure 4)(83).

Since water production was not measured, this remains a possible fate for the extra reducing equivalents. In pregnenolone-16α-carbonitrile-induced hepatic microsomes, the difference between NADPH oxidation and fluoride ion production was far less than that observed in phenobarbital- or β-naphthoflavone-induced hepatic microsomes. It is therefore possible that the phenobarbital- and β-naphthoflavone-inducible isozymes are involved in a four-electron transfer to water, but not the pregnenolone-16α-carbonitrile-inducible isozyme.

It is apparent from the results presented herein that isoflurane does not enhance the production of hydrogen peroxide relative to experiments in the absence of the drug (Table 16), thereby uncoupling the cytochrome P-450 electron transfer pathway. The stoichiometry of the cytochrome P-450-catalysed defluorination of isoflurane was not investigated further.

Since fresh human liver was available from transplant donors, it was possible to study isoflurane metabolism in human hepatic microsomes: isoflurane was shown to be defluorinated at a rate comparable to that of untreated male Long Evans rats (Tables 12 and 17). Such a measurement of the rate of isoflurane defluorination by human hepatic microsomes does not allow for any comparison with the rate of defluorination of other anaesthetic agents, or with the in vivo rate of defluorination of isoflurane in other individuals following isoflurane anaesthesia. Therefore, further studies on the metabolism of isoflurane by human and phenobarbital-induced rat hepatic microsomes focussed on the identification of the organofluorine metabolites of isoflurane metabolism in vitro, and subsequent extension of the pathways of isoflurane metabolism (Figure 5).

4.1.1 Identification of Organofluorine Metabolites of Isoflurane

Possible metabolites of isoflurane are trifluoroacetic acid or trifluoroacetaldehyde, depending on the pathway of isoflurane metabolism; O-dealkylation results in trifluoroacetaldehyde (Pathway I, Figure 5) and O-insertion followed by dechlorination or O-dealkylation results in trifluoroacetic acid (Pathway II, Figure 5). The fluoride ion production was accurately measured as inorganic fluoride. Accurate measurement of trifluoroacetic acid production from isoflurane in rat hepatic microsomes was attempted using gas chromatography, which proved too insensitive to detect the small amounts of trifluoroacetic acid produced (results not shown). An alternative method reported by Soltis and Gandolfi (365) for the detection of small quantities of fluorinated metabolites of volatile anaesthetic agents was attempted but was found not to be able to quantitate the total metabolites of fluorinated anaesthetic

agents. Essential conditions for utilisation of the method of Soltis and Gandolfi (365) for the quantitation of metabolites of isoflurane were found to be:

i) that the fluorinated anaesthetic agent was volatile

ii) that the fluorinated metabolites of the anaesthetic agent were non-volatile (see Table 18).

Although isoflurane is a volatile anaesthetic agent and was almost completely removed by lyophilisation, a small, but significant amount remained in hepatic microsomes (Table 19). The amount remaining was small in comparison to the initial isoflurane concentration, but significant compared to metabolite production (Table 19). Isoflurane has 5 fluoride ions per molecule in contrast to only 3 in the expected organofluorine metabolites. The amount of isoflurane which remained in the microsomes after lyophilisation was corrected for by subtracting out fluoride measurements in zero-time samples which contained isoflurane, an NADPH-generating system and EDTA (Table 19).

Since the fluorinated metabolites had to be in a non-volatile form for measurement by the method of Soltis and Gandolfi (365), this method was modified in our laboratory (Section 2.2.2.6) (396) to ensure that either trifluoroacetic acid or trifluoroacetaldehyde were non-volatile as outlined in Sections 3.1.5 and 3.1.6.

The standard curves for fluoride ion (sodium fluoride) measured as described in Section 2.2.2.6 were slightly different from that where the fluoride was derived from either trifluoroacetic acid, trifluoroacetaldehyde or sodium

fluoride (Figures 16 and 17). Therefore, accurate quantitation of total non-volatile organic fluoride (trifluoroacetic acid or trifluoroacetaldehyde plus fluoride ion) in a single sample was not possible. Results were sufficiently accurate, however, to further elucidate the pathways of metabolism of isoflurane in rat and human hepatic microsomes.

Metabolism of isoflurane via either Pathway I or Pathway II (Figure 5) should result in the production of 1 molecule of trifluoroacetaldehyde or trifluoroacetic acid for every 2 fluoride ions produced. Therefore, a comparison of total fluoride (trifluoroacetic acid or trifluoroacetaldehyde plus fluoride ion) to fluoride ion production alone should give a ratio of 5/2, i.e. 2.5. Where fluoride ion alone is measured, i.e. under conditions designed to ensure that the trifluoroacetic acid or trifluoroacetaldehyde produced was volatile during total fluoride analysis (Figure 11), this ratio should be 1. Therefore, this ratio, together with the method of total fluoride analysis (Figure 11), can be used as an qualitative indicator of the pathway of isoflurane metabolism in rat and human hepatic microsomes.

In phenobarbital-induced rat hepatic microsomes, the ratio of production of total fluoride to fluoride ion was 11.4 where trifluoroacetaldehyde was measured as a phenylhydrazone, and 6.2 where it was measured as a Schiff base bound to microsomes (Table 19). These two ratios far exceeded the calculated ratio of 2.5 for total fluoride to fluoride ion. In contrast, the ratio of total fluoride to fluoride ion where trifluoroacetic acid was measured in phenobarbital-induced rat hepatic microsomes, was <1. From the comparison of these ratios for total fluoride to fluoride ion, it is apparent that in phenobarbital-induced rat hepatic microsomes, isoflurane was primarily metabolised via Pathway I, i.e. to fluoride

ion and trifluoroacetaldehyde (Figure 5). Since trifluoroacetaldehyde was detected in a non-volatile form either as a phenylhydrazone or under conditions where it was normally volatile (Table 18), it appeared that some of the trifluoroacetaldehyde produced binds as a Schiff base to cellular macromolecules, thus converting it to a non-volatile form. The lower yield of trifluoroacetaldehyde when measured without added phenylhydrazone suggested, however, that not all the trifluoroacetaldehyde produced was bound to cellular macromolecules, and that some was lost during lyophilisation (Table 19). Thus, trifluoroacetaldehyde appears to be a product of isoflurane metabolism in rat hepatic microsomes measured by a modification of the method of Soltis and Gandolfi.

The measurement of trifluoroacetaldehyde as a metabolite of isoflurane in phenobarbital-induced rat hepatic microsomes confirmed the results in which trifluoroacetaldehyde produced from isoflurane defluorination was identified by an indirect method (Section 3.1.6). In this method, trifluoroacetaldehyde was oxidised to trifluoroacetic acid, separated by TLC and the trifluoroacetic acid identified by comparison of R_f values with those of standards. These results showed that trifluoroacetaldehyde is a metabolite of isoflurane in rat hepatic microsomes and provide the first identification of trifluoroacetaldehyde as a metabolite of an anaesthetic agent. The binding of trifluoroacetaldehyde to microsomal macromolecules may result in the formation of a protein adduct, which serves as an antigen resulting in cross-sensitisation and hepatotoxicity. Such immunoreactive protein adducts have been identified in rat liver following isoflurane anaesthesia (387).

In human hepatic microsomes, only trifluoroacetic acid was measured following defluorination of isoflurane since insufficient material was available for measurement of trifluoroacetaldehyde. Using the modified method of Soltis and Gandolfi (Section 2.2.2.6) to determine trifluoroacetic acid, ratios for total fluoride to fluoride ion of 6.2 and 2.2 were obtained in the case of livers 2 and 3, respectively (Table 19). A comparison of the ratio of total fluoride to fluoride ion obtained when trifluoroacetic acid was measured in human hepatic microsomes (6.2 and 2.2) with that obtained in rat hepatic microsomes (<1) (Table 19), suggested that in human hepatic microsomes, isoflurane was metabolised primarily via Pathway II (Figure 5), i.e. to fluoride ion and trifluoroacetic acid. Since measurement of trifluoroacetaldehyde as a metabolite of isoflurane in human hepatic microsomes was not possible, the metabolism of isoflurane via Pathway I to trifluoroacetaldehyde in human hepatic microsomes cannot be excluded. From the results presented herein, however, trifluoroacetic acid appears to be the major metabolite of isoflurane (besides fluoride ion) in human hepatic microsomes, although trifluoroacetaldehyde may be produced in small, possibly insignificant, amounts.

The results of this investigation may explain the differences in the ratios of urinary metabolites of isoflurane in the rat and human reported by Hitt et al (195). In rats exposed to isoflurane, the low urinary ratio of non-volatile fluoride (non-ionic fluoride) to fluoride ion may be explained by the insignificant production of non-volatile organofluorine metabolites, i.e. trifluoroacetic acid. Because trifluoroacetic acid is found in small amounts in rats exposed to isoflurane, it would appear that a low, but significant capability for the oxidation of trifluoroacetaldehyde exists in liver cytosol (which was not demonstrated herein, Section 3.1.7), or elsewhere in the rat. In contrast, in humans, ionic

fluoride (fluoride ion) and non-ionic fluoride in the form of trifluoroacetic acid were recovered in the urine. The source of this trifluoroacetic acid could presumably have been

i) from direct metabolism of isoflurane via Pathway II to trifluoroacetic acid, or, less likely

ii) via Pathway I to trifluoroacetaldehyde which could be directly oxidised in the liver cytosol to trifluoroacetic acid.

The ability of human hepatic microsomes to metabolise isoflurane to trifluoroacetaldehyde has not been proved to be a general phenomenon. Human liver cytosol from a single individual oxidised trifluoroacetaldehyde to trifluoroacetic acid but not the livers of the other two individuals (Section 3.1.7).

Identification of the metabolites of isoflurane by Hitt et at (195) and herein, indicate that in human liver, Pathway II is the favoured pathway for isoflurane metabolism (Figure 5). Fluoride ion and trifluoroacetic acid have been identified as metabolites of cytochrome P-450-dependent metabolism in vitro and as urinary metabolites following in vivo biotransformation of isoflurane (195). Consequently, isoflurane appears to undergo metabolism primarily in a single step catalysed by hepatic cytochrome P-450, and the metabolites of this step are readily excreted in the urine. In contrast, in rat liver, Pathway I is favoured for isoflurane metabolism (Figure 5), since fluoride ion and trifluoroacetaldehyde have been identified as metabolites of cytochrome P-450 metabolism in vitro. Fluoride ion has been identified as the major urinary metabolite following in vivo biotransformation of isoflurane (195), and a small

amount of trifluoroacetic acid, which could result from a low, but significant oxidation of trifluoroacetaldehyde in the rat. It is apparent, however, that the majority of the trifluoroacetaldehyde undergoes an alternate fate, viz: the binding of trifluoroacetaldehyde to cellular macromolecules as a Schiff base (which was demonstrated in this thesis) or perhaps reduction to trifluoroethanol followed by conjugation.

The major conclusions of the study of the metabolism of isoflurane by cytochrome P-450 in hepatic microsomes can, therefore, be summarised as follows:

i) Another isozyme of cytochrome P-450, besides cytochrome P-450 3a (178,179,185,186), appears to catalyse the defluorination of isoflurane in the rat; this isozyme is probably cytochrome P-450PCN1.

ii) Isoflurane appears to be metabolised primarily by different pathways in the rat and human liver; consequently the rat appears to be an unsuitable model for studying the effects of biotransformation of this anaesthetic agent and another more suitable model should be sought.

iii) The the newly identified metabolite of isoflurane in the rat (trifluoracetaldehyde) may contribute to the toxic potential of the anaesthetic in this species, especially as it has been shown to bind to cellular macromolecules in the liver. This effect could account for the hepatic centrilobular necrosis observed after exposure of rats to isoflurane which has been reported by Van Dyke (381). In contrast, the metabolites of isoflurane in the human were shown not to bind to cellular

macromolecules. It seems unlikely that metabolism of isoflurane to low levels of trifluoroacetic acid in humans would contribute to the toxic potential of this anaesthetic.

After identification of the metabolites of isoflurane in rat and human hepatic microsomes, we went on to investigate the interaction of isoflurane with the rat hepatic cyanide-sensitive factors, including the fatty acid desaturases.

4.2 THE INTERACTION OF ISOFLURANE AND OTHER ANAESTHETIC AGENTS WITH THE CYANIDE-SENSITIVE FACTORS

A study of the interaction of isoflurane with the cyanide-sensitive factors was prompted by reports by Ivanetich and co-workers which concluded that halothane, methoxyflurane and enflurane interact with hepatic microsomal Δ9-desaturase (313,314). Although these anaesthetic agents did not inhibit the Δ9-desaturation of stearoyl-CoA, they stimulated the cyanide-sensitive re-oxidation of cytochrome b_5, suggesting that these drugs interacted with the cyanide-sensitive factors, which include the fatty acid desaturases (314). Since cytochrome b_5 is an electron carrier for a number of metabolic pathways in hepatic microsomes, the enzyme system(s) responsible for the stimulation of re-oxidation of cytochrome b_5 by a particular compound can only be identified indirectly. The biochemical pathways in which cytochrome b_5 participates in hepatic microsomes are fatty acid chain elongation (335,337), cholesterol biosynthesis (316,342), plasminogen biosynthesis (316,342), desaturation of fatty acids (198) and some cytochrome P-450 drug oxidation (95-99). The autooxidation of cytochrome b_5 can also be stimulated (313).

The ability of a compound to stimulate the reoxidation of cytochrome b_5 in hepatic microsomes suggests that it interacts with one or more of the above enzymes. If the stimulation of electron transfer is inhibited by low concentrations of cyanide, the compound probably interacts with either the fatty acid desaturases or enzymes of cholesterol biosynthesis (Δ7-sterol 5-desaturase and 4-methyl sterol oxidase (382))(235,316). Cytochrome P-450 is inhibited by cyanide, but at higher concentrations (236).

The ability of isoflurane to stimulate the re-oxidation of cytochrome b_5 and the inhibition of this effect by cyanide (0.5 mM) (Table 24) suggests that isoflurane interacts with one or more of the cyanide-sensitive factor(s), viz: the fatty acid desaturases and/or enzymes of cholesterol biosynthesis. Our subsequent experiments focussed on assessing whether isoflurane interacted with the fatty acid desaturases.

The interaction of isoflurane with the Δ9-desaturase was assessed indirectly by the reoxidation of microsomal cytochrome b_5 as an index of fatty acid desaturase activity, and directly, by the effect on Δ9-desaturation of stearoyl-CoA.

The Δ9-desaturase is induced by a high-carbohydrate diet, but the Δ5- and Δ6-desaturases are not (Table 8)(284-288). Dietary treatment was thus used to distinguish the Δ9-desaturase from the Δ5- and Δ6-desaturases. In hepatic microsomes from rats fed a high-carbohydrate diet, stearoyl-CoA (the substrate for the Δ9-desaturase) stimulated re-oxidation of cytochrome b_5 5-fold confirming induction of the Δ9-desaturase (Table 25). In hepatic microsomes from rats fed a normal diet which does not strikingly induce the Δ9-desaturase,

stearoyl-CoA stimulated the rate of re-oxidation of cytochrome b_5 only 1.8-fold (Table 25).

Linoleoyl-CoA (the substrate for the Δ6-desaturase) stimulated the re-oxidation of cytochrome b_5 similarly in microsomes from rats fed normal, or high-carbohydrate diets (1.2- and 1.6-fold stimulation, respectively)(Table 25).

From the above comparison of the effects of stearoyl-CoA and linoleoyl-CoA on the cytochrome b_5 reoxidation in hepatic microsomes from differently pretreated rats, it appeared that we succeeded in reproducing induction of Δ9-desaturase by high-carbohydrate diets (284-286,288) and that the Δ6-desaturase was not induced by a high-carbohydrate diet.

From literature data (314) we can compare the extent of interaction of halothane, methoxyflurane and enflurane with the fatty acid desaturases in hepatic microsomes from rats fed high-carbohydrate or normal diets. Halothane, methoxyflurane and enflurane stimulated cytochrome b_5 reoxidation 1.5-, 1.6- and 2.0-fold, respectively, in hepatic microsomes from rats fed a high-carbohydrate diet, and 1.6-, 1.2- and 1.5-fold, respectively from rats fed a normal diet; the stimulation of cytochrome b_5 reoxidation by stearoyl-CoA was 3.8- versus 1.3-fold for high-carbohydrate and normal diets (314). Since there is not much difference between the extents to which these anaesthetic agent stimulate the re-oxidation of cytochrome b_5 in microsomes from rats fed the different diets (compared to stearoyl-CoA), it appears that these anaesthetic agents may not interact primarily with the Δ9-desaturase, but may stimulate electron flow through cytochrome b_5 to some extent by interacting with other cyanide-sensitive factors (314).

By the same argument, since isoflurane stimulated the re-oxidation of cytochrome b_5 similarly in hepatic microsomes from rats fed high-carbohydrate and normal diets (1.7-fold and 1.4-fold, respectively) (Table 25) it appears that isoflurane does not interact preferentially with the Δ9-desaturase. This is consistent with the lack of effect of isoflurane on the Δ9-desaturation of stearoyl-CoA: isoflurane did not inhibit the Δ9-desaturase using NADH as electron donor and only slightly diminished activity with NADPH as electron donor (Table 26). The latter effect may reflect a small amount of inhibition by isoflurane, or may reflect the high rate of utilisation and perhaps the consequent depletion of NADPH by cytochrome P-450 in the presence of isoflurane (see Table 10). In any event, the extent, if any, of the effect of isoflurane on the Δ9-desaturase was of too low magnitude to pursue.

It would therefore appear that isoflurane may stimulate cytochrome b_5 reoxidation by interacting with the Δ6-desaturase, the Δ5-desaturase or other cyanide sensitive factors, which are not induced by high-carbohydrate diet. The effects of isoflurane on the Δ5- and Δ6-desaturases were studied directly by measuring the Δ6-desaturation of linoleic and α-linolenic acids and the Δ5-desaturation of eicosa-8,11,14-trienoic acid.

Isoflurane inhibited the Δ6-desaturation of linoleic acid at physiologically achievable concentrations of the anaesthetic (Figure 26). In contrast, isoflurane did not inhibit the Δ6-desaturation of another physiologically important fatty acid substrate, α-linolenic acid (Section 3.2.3.3). The lack of effect of isoflurane on the latter reaction suggested that a) isoflurane is not a competitive inhibitor of the Δ6-desaturase, viz: it does not bind directly to the fatty acyl-CoA binding site, and b) isoflurane inhibited the Δ6-desaturase with linoleic acid as substrate by

interacting directly with the fatty acid desaturase rather than by disrupting electron transfer to this enzyme. The latter effect has been reported for the anti-inflammatory drug, ebselen (388).

Isoflurane appeared also to interact with the Δ5-desaturase; isoflurane inhibited the Δ5-desaturase slightly and in a significant manner (Table 27). The inhibition of the Δ5-desaturase by isoflurane was achieved at ca. 10-fold higher concentration than for inhibition of the Δ6-desaturase. Inhibition of the Δ5-desaturase would not be expected to be significant in vivo since blood isoflurane levels do not exceed ca. 1 mM (4), while half maximal inhibition of the Δ5-desaturase is predicted to occur only above 8 mM isoflurane (Table 27).

Since isoflurane inhibited the Δ6-desaturation of linoleic acid most strikingly, we anticipated that other fluorinated anaesthetics might also inhibit the Δ6-desaturase. However, neither halothane, methoxyflurane nor enflurane inhibited Δ6-desaturase activity toward linoleic acid (Table 30), even though the latter two anaesthetic ethers are close structural analogues of isoflurane. We conclude that either these three anaesthetic agents did not bind to the Δ6-desaturase, or interacted with the Δ6-desaturase at a site which does not affect enzyme activity.

The activity of the Δ6-desaturase appeared to depend on the BSA concentration in reaction mixtures. Increasing the BSA concentration ten-fold increased the apparent activity of the enzyme, evidenced by the reaction rates for the Δ6-desaturase at two different BSA concentrations (Figure 33). Similarly, the

apparent V_{max} value for the Δ6-desaturase was increased by additional BSA (0.09 ± 0.01 and 0.15 ± .01 μM γ-linolenic acid formed/min at the low and high BSA concentrations, respectively), whereas the apparent K_m value remained essentially the same (ca. 8 μM) (Table 34). The stimulation of the Δ6-desaturase activity by BSA reported here is consistent with similar reports in the literature, where BSA was reported to increase the activity of the Δ6-desaturase by 50% in unwashed microsomes (276). The stimulation in activity observed in the presence of BSA both here and in the literature suggests that BSA may possibly have protected the enzyme from surface denaturation (276,383). Alternatively, the apparent effect of increasing BSA concentration on Δ6-desaturase activity may be an artifact resulting from the observed daily variations in activity (see e.g. Table 28)(247,249).

Although the inhibition of the Δ6-desaturase by isoflurane was not reversed by bubbling with air (Table 29), no estimation of the isoflurane concentration subsequent to bubbling was made. Lyophilisation of hepatic microsomes resulted in 0.15 μM isoflurane remaining with microsomal membranes (calculated from data in Section 3.1.5). Assuming that bubbling with air for 5 minutes was not as effective in removing isoflurane from hepatic microsomes as was lyophilisation, it is possible that the concentration of isoflurane was not lowered sufficiently by bubbling to prevent Δ6-desaturase inhibition or that the binding of isoflurane to the Δ6-desaturase is tight.

Isoflurane has been demonstrated to be defluorinated by cytochrome P-450 (Section 4.1). We addressed the question as to whether it was possible that this drug was also defluorinated during the course of its interaction with the

Δ6-desaturase, and found some evidence that could be construed as supporting this possibility:

i) NADH is the preferential electron donor for the Δ6-desaturase, although it can donate electrons to cytochrome P-450 (34,62), and, in some cases, is the preferential electron donor (32). The extent (73%) to which NADH supports the defluorination of isoflurane relative to NADPH (Table 14) suggested that isoflurane may also be defluorinated by a microsomal enzyme which utilises NADH as preferential electron donor, such as the fatty acid desaturases.

ii) isoflurane defluorination in hepatic microsomes was not greatly inhibited by CO (viz: 24% inhibition, Table 13), suggesting that either a) the cytochrome P-450 isozyme in question is not susceptible to CO inhibition, for which there is precedent (111), or b) another pathway which can utilise NADPH as electron donor and is not very sensitive to CO, such as the fatty acid desaturases, also metabolises isoflurane.

iii) metyrapone inhibited the NADH-supported defluorination of isoflurane by cytochrome P-450 to a greater extent than that supported by NADPH (Tables 13 and 14). Metyrapone also inhibits the desaturation of linoleic acid to a far greater extent than CO (Table 28). Therefore, the relative extents of metyrapone and CO inhibition of the defluorination of isoflurane is consistent with metabolism by both cytochrome P-450 and the Δ6-desaturase.

The low levels of fluoride ion production from isoflurane in hepatic microsomes from uninduced rats (Table 12) precluded determination whether fluoride production from isoflurane was cyanide inhibitable, and thus attributable to fatty acid desaturase activity (unpublished results). In any event, whatever enzymes defluorinate isoflurane in vivo and in vitro, the reaction proceeds with reluctance, slowly and to a small extent relative to analogues such as methoxyflurane or enflurane (182,191).

Since isoflurane inhibited the Δ6-desaturation of linoleic acid, it is surprising that it did not inhibit Δ6-desaturation of the close structural analogue, α-linolenic acid. Isoflurane may inhibit the Δ6-desaturation of linoleic acid selectively by interacting with a Δ6-desaturase isozyme that preferentially metabolises linoleic acid. However, there is no evidence for Δ6-desaturase isozymes of similar or differing substrate specificities. Alternatively, isoflurane may bind to a site outside of the acyl-CoA binding site and indirectly affect enzyme activity toward one substrate but not another.

The following conclusions were drawn from the study of the interaction of isoflurane with the cyanide-sensitive factors:

i) Isoflurane interacted with one or more of the cyanide-sensitive factors.

ii) Isoflurane did not appear to interact with the Δ9-desaturase.

iii) Isoflurane weakly and slightly inhibited the Δ5-desaturation of eicosa-8,11,14-trienoic acid.

iv) Isoflurane, at physiological achievable concentrations, inhibited the Δ6-desaturation of linoleic acid but not α-linolenic acid.

v) For reasons that are not clear, close structural analogues of isoflurane, such as enflurane and methoxyflurane, were not similarly efficaceous.

It is possible that isoflurane affected other cyanide-sensitive factors, but this was beyond the scope of our investigations. We then went on to characterise kinetically the inhibition of the Δ6-desaturase by isoflurane.

4.2.1 Investigations into Factors Which Could Influence Δ6-Desaturase Activity in Hepatic Microsomes

In the course of attempting to characterise isoflurane inhibition of the hepatic microsomal Δ6-desaturase, we began to realise that the experimental kinetics of the Δ6-desaturase, even in the absence of isoflurane, were complex. There are, in fact, a number of reasons why the kinetics of the fatty acid desaturases are more complex than generally appears to be appreciated. The complexity of the experimental kinetics of the Δ6-desaturase (and other fatty acid desaturases) in hepatic microsomes reflects the following factors:

i) Other enzymes compete with the Δ6-desaturase for the acyl-CoA substrate; this includes enzymes such as the lysophospholipid acyltransferases.

ii) The acyl-CoA substrate can partition between the aqueous and lipid phases, rendering exact calculations of substrate levels available to the enzyme problematic.

iii) Endogenous fatty acids are present in significant amounts in the microsomal membrane (Table 23)(397) and can act as alternate substrates or inhibitors. Many fatty acids are substrates for the acyl-CoA synthetase (213). Thus, endogenous fatty acid substrates for the acyl-CoA synthetase would be converted to acyl-CoA derivatives that could act as alternate substrates or inhibitors of the Δ6-desaturase. In this way, endogenous fatty acids can affect apparent Δ6-desaturase activity. For example, for the desaturation of linoleic acid, possible competing substrates found in the microsomal membrane in significant amounts would include oleate (found but not quantitated) and α-linolenate (see Section 3.2.2.2, Figure 24 and Table 23). Furthermore, endogenous unlabelled microsomal linoleate would dilute out the added radiolabelled substrate thus directly affecting true substrate levels, the specific activity of both the substrate and product and apparent rate of product formation. The effect of endogenous substrate was found to be highly significant for linoleic acid Δ6-desaturation and, to a lesser extent, α-linolenic acid desaturation and would be a factor for any enzyme system using as substrates the fatty acids shown in Table 23 and Figure 24. These endogenous fatty acids would affect apparent kinetics whether or not radioisotopic assay methods were used (376).

iv) Most fatty acid desaturase assay systems use added fatty acid plus an acyl-CoA generating system to generate the acyl-CoA substrate for the

fatty acid desaturase (see, for example, 266-270). It has not been fully established that this esterification reaction is pre-rate determining under all experimental conditions.

Some or all of the above factors may have influenced measurement of desaturase activity and the effect of isoflurane on this process under our experimental conditions. We attempted to remove, isolate or correct for these processes and clarify the underlying kinetics of the Δ6-desaturase before trying to superimpose the inhibition by isoflurane thereon. In particular, we attempted to establish and correct for the effects of endogenous substrate on Δ6-desaturase activity in hepatic microsomes, and to dissociate the kinetics of the Δ6-desaturase from the acyl-CoA synthetase pre-reaction and lipid synthesis post-reactions.

The kinetic parameters that we measured for apparent Δ6-desaturase activity in hepatic microsomes (Table 34) were consistent with those reported in the literature; linear Lineweaver-Burk plots were obtained and the apparent K_m for linoleic acid value fell within the range reported in the literature (ca. 10 μM compared to the values in Table 40). However, the apparent K_m values reported for the Δ6-desaturase for linoleic acid in the literature (Table 40) fell over an extremely wide range.

The breadth of the K_m range could be explained by several factors: firstly, several plots contained an insufficient number of data points for accurate calculation of an apparent K_m. For example, the reciprocal plots shown in four publications contained only three points each (see e.g. 266,269,270,395). Second, in some reports, the range of substrate concentrations was too small

TABLE 40

LITERATURE DATA FOR THE Δ6-DESATURASE

Δ6-Desaturase Source (concentration in mg protein/ml)	K_m (μM)	Substrate *	Range of Substrate Concentration (fold)	Ref.
Hepatic microsomes from rats fed a fat free diet (1.3)	2.5	Linoleic acid (0.25 - 2 μM)	8	269
Hepatic microsomes from rats fed a fat deficient diet (2.0)	160	Linoleic acid (40 - 100 μM)	2.5	266
Hepatic microsomes from rats fed a fat deficient diet (2.0)	200	Linoleoyl-CoA (50 - 100 μM)	2	266
Hepatic microsomes from rats fed a normal diet (0.053)	≈ 0.5	Linoleic acid (0.4 - 2 μM)	5	267 (Figure 1)
Hepatic microsomes from rats fed a fat deficient diet (3.3)	≈ 27	Linoleic acid (12.3 - 93 μM)	7.5	268 (Figure 1)
Hepatic microsomes from rats fed a fat deficient diet (1.3)	13	Linoleic acid ≈ 1-20 μM	≈ 20	270
Hepatic microsomes from rats fed a fat deficient diet (1.3)	39	Linoleic acid ≈ 0.8-4.0 μM	≈ 5	395
Hepatic microsomes from rats fed a normal diet (0.5)	9.6	Linoleic acid (0.45-10.8 μM)	24	Table 34
Purified from rat hepatic microsomes	45	Linoleoyl-CoA	unknown	255

* Concentrations are of added substrate.

to obtain an accurate apparent K_m value; the substrate concentrations do not, in fact, span the apparent K_m value in four of the studies of Δ6-desaturase activity shown in Table 40. With two other studies, the substrate concentration range did not extend to more than 10% below the apparent K_m (Table 40).

In none of the above studies was the effect of endogenous linoleic acid concentrations recognised, measured or corrected for.

In measuring apparent Δ6-desaturase activity, we did, however, take into account the level of endogenous linoleic acid in hepatic microsomes. We report in this thesis that endogenous linoleic acid concentrations are approximately 3 μM in the rat hepatic microsomal preparations used (Table 23). The level of endogenous linoleic acid is highly significant compared to the lower end of the range of added linoleic acid concentrations used in determination of kinetic constants for the Δ6-desaturase in this thesis and the range of linoleic acid concentrations used in the literature (ca. 0.25 μM to 40 μM, Table 40). For a clear demonstration of how reciprocal plots can be affected by endogenous substrate levels, see Figure 25 for treatment of the data in this thesis, as well as I.H. Segel, pages 93 and 94 (376). The apparent K_m is particularly sensitive to levels of endogenous substrate. The omission of consideration of the effects of endogenous substrate levels by investigators using linoleic acid as substrate provided a basis for doubting the validity of most of the reported kinetic parameters for the Δ6-desaturase obtained with microsomal preparations.

Although we avoided the aforementioned problems of unsuitable substrate concentration range and lack of correction for endogenous substrate in our studies, there were factors that, because of their complexity, were ignored both

here and in the literature (266-270,395). For example, the possible effects of endogenous alternate substrates and endogenous inhibitors on the Δ6-desaturase were ignored (266-270,395). α-Linolenic acid, which is an alternate physiological substrate for the Δ6-desaturase and is metabolised at a greater rate than linoleic acid (197,198,237), is present in hepatic microsomal preparations. The concentration of this compound in hepatic microsomes is low (ca. 0.3 μM, Table 23) relative to the concentration of linoleic acid, but the extent of its effects on the kinetics of the Δ6-desaturase is not known.

In addition, the well documented ability of fatty acids and acyl-CoA derivatives to form micelles is known to affect kinetics (218). The critical micelle concentration of linoleoyl-CoA is reported to be 5.5 μM in aqueous solution (218); it is likely to be higher in the presence of both hepatic microsomes and BSA due to binding to these components (278,279). In our kinetic studies, all but the highest concentration of linoleic acid added (7.9 μM linoleic acid added, 10.8 μM total linoleic acid (added plus endogenous)) appeared to produce maximal concentrations of linoleoyl-CoA that were below the critical micelle concentration of linoleoyl-CoA. However, the total concentration of all acyl-CoA species is unknown (due to the presence of endogenous fatty acids), as is the question of whether micelle formation affected the kinetics of the Δ6-desaturase under the conditions of our experiments. This effect has been ignored in the kinetic studies reported here. It has to our knowledge been ignored in all literature studies of the Δ6-desaturation of linoleic acid.

In our studies and most of those in the literature (see, for example, 266-270), apparent Δ6-desaturase activity measured with hepatic microsomes reflects a combination of the activity of the Δ6-desaturase plus acyl-CoA synthetase and

lysophospholipid acyltransferase activities. The activity of all three enzymes is measured because (i) acyl-CoA synthetase is a pre-reaction that produces the substrate for the Δ6-desaturase, and (ii) microsomal reaction mixtures are saponified prior to quantitation of fatty acid substrate and product resulting in measurement of unesterified (or free fatty acids) together with fatty acids esterified into lipids or into acyl-CoA. The effects of these enzymes on Δ6-desaturase activity will be discussed in more detail.

In addition to the acyl-CoA synthetase and lysophospholipid acyltransferase, other enzymes which may influence apparent Δ6-desaturase activity are the fatty acid elongase and the phospholipases (Figure 7). Some of these enzymes could influence Δ6-desaturase activity by competing for acyl-CoA substrate, e.g., fatty acid elongase. Others, e.g., phospholipases, could release fatty acid from membrane lipids, thus diluting the radiolabelled fatty acid substrate. The activity of these enzymes was investigated or considered under our experimental conditions.

Firstly, fatty acid elongase was inactive under the conditions used: the radioactivity from the Δ6-desaturase reaction was recovered quantitatively as [1-^{14}C] linoleic acid plus [1-^{14}C] γ-linolenic acid (see Section 3.2.1.2). This was not unexpected since acetyl-CoA, the cofactor required for chain elongation was not added to reaction mixtures (335).

Secondly, the phospholipases, in particular phospholipase A_2 (Figure 7), could have influenced apparent fatty acid desaturase activity measurements by decreasing the specific activity of the radiolabelled substrate and/or providing

endogenous alternate substrates. If active, phospholipase would release unlabelled linoleic acid from membrane phospholipids.

The activity of phospholipase A_2 was measured in hepatic microsomes under the experimental conditions used to measure Δ6-desaturase activity; this enzyme was shown to be essentially inactive (Section 3.2.5.1). Phospholipase A_2 activity was measured rather than phospholipase A_1 activity because linoleic acid is esterified primarily in the second position of phospholipids which is the site attacked by phospholipase A_2 (222). Phospholipase C, which, together with diglyceride lipase, catalyses the release of fatty acids from phospholipids, was not considered since it is cytosolic rather than microsomal in origin and specifically attacks phosphotidylinositol releasing arachidonic acid (230-233). The phospholipases appear not to influence hepatic microsomal Δ6-desaturase activity under our experimental conditions.

The two enzymes already mentioned which are closely linked to the methods by which Δ6-desaturase activity was measured in hepatic microsomes, may affect Δ6-desaturase activity as follows: firstly, the acyl-CoA synthetase generates the substrate for the Δ6-desaturase (linoleoyl-CoA) from the commonly added, far less expensive precursor, linoleic acid. Secondly, the lysophospholipid acyltransferase competes with the Δ6-desaturase for the linoleoyl-CoA substrate. The generation of linoleoyl-CoA from linoleic acid which is catalysed by the acyl-CoA synthetase has been reported to be rapid and pre-rate determining (266,384). This reaction has been reported to essentially go to completion, and therefore not to influence the activity of the Δ6-desaturase in microsomes (266,384). In contrast, the lysophospholipid acyltransferases are reported to affect the activity of the Δ6-desaturase in hepatic microsomes

(269-270,395). Another enzyme in hepatic microsomes which also uses acyl-CoA substrate, is the acyl-CoA hydrolase. This enzyme was not investigated because it is reported to be relatively inactive compared to the lysophopholipid acyltransferases (218).

The effects of the acyl-CoA synthetase and lysophospholipid acyltransferase on the kinetic parameters of the Δ6-desaturase were assessed using computer modelling.

4.2.2 Computer Modelling

The data for the Δ6-desaturase, acyl-CoA synthetase and lysophospholipid acyltransferase in hepatic microsomes were subjected to computer modelling in order to dissect the kinetic parameters for these enzymes, and remove the kinetic contributions from the other enzymes. Our focus was on obtaining more accurate kinetic parameters for the Δ6-desaturase. All experimental data used in this operation were corrected for endogenous substrate levels.

In hepatic microsomes, the Δ6-desaturase reaction measured was (Figure 38):

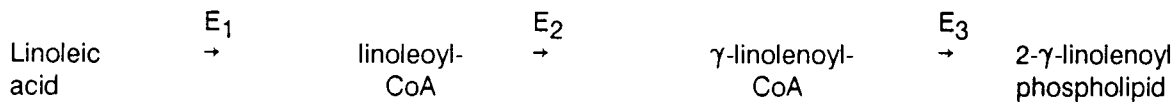

i.e. a series of coupled reactions catalysed by three different enzymes. The reason why the Δ6-desaturase reaction is measured as a coupled reaction is because the substrate, added as linoleic acid, and the product (γ-linolenic acid)

are quantitated after saponification of the microsomes, a process which splits the ester bonds in acyl-CoA and lipids, releasing all fatty acids.

The reaction scheme incorporating these enzymic reactions, shown in Figure 38, was modelled using the SLAM II program (see Section 2.2.3.11 to Section 2.2.3.12.4). The effects of variations of the individual rate constants in the different models (Table 37) were considered in the Results (Section 3.2.6) and will not be further discussed here. However, some generalities about the modelling are relevant to discuss.

The rate constants reported for model 35 (the final model) in Table 37 comprise one set of rate constants that model the experimental data with sufficient accuracy compared to experimental error. Using the existing computer program, we had no mechanism for searching for all possible combinations of rate constants and other parameters that would do so. We would like to emphasise that we have presented one possible solution, but others may be equally reasonable. The large errors associated with some of the data points make us wary of overmodelling the data and overinterpreting the results of the modelling.

The initial values of the rate constants in the model were such that all of the reactions were assumed to follow rapid equilibrium kinetics (399). This is still true for the final values of the constants for E_1 and E_2, where $k_2 >> k_3$ and $k_5 >> k_6$ (Table 38). For E_3, however, k_8 is only 2.25-fold greater than k_9. This difference is not sufficiently large to maintain rapid equilibrium kinetics.

The K_m and k_{cat} values from the literature for E_1, E_2 and E_3 utilised to generate constants for the initial model (previous to the models shown in Table 37) and the K_m and k_{cat} values for E_1, E_2 and E_3 calculated from the rate constants in the final run (Model 35) are compared in Table 41. The calculated K_m for E_1 is 5-fold greater than the literature value used, but between the two reported values of 2 μM and 30 μM (386,392). The generated K_m for E_2 is within the broad range reported in the literature (Table 40). The remaining modelled K_m and k_{cat} values approximate the experimental data except for the k_{cat} for E_3; the literature k_{cat} was generated under saturating conditions of the acyl acceptor, while our experiments were conducted with only endogenous microsomal lipid levels of acyl acceptor present (see Table 42 and references therein). Therefore, the modelled results are in no case providing unreasonable values compared to experimental and literature data (Tables 40, 41 and 42).

Coupling of the Δ6-desaturase with the acyl-CoA synthetase is reported to have no effect on the activity of the Δ6-desaturase (266,384). This proposal is not consistent with the experimental results or the output of the computer modelling of the desaturase reaction reported in this thesis. Firstly, the experimentally determined utilisation of linoleic acid with time does not show instantaneous disappearance of linoleate (see Figures 30 and 31). Especially at an initial linoleic acid concentration of 10.8 μM, utilisation of linoleate is slow, with only ca. 40% of the substrate being utilised within 3 minutes. The computer modelling confirms for 4.7 μM linoleic acid initial concentration, that over one minute, the linoleate concentration declines by ca. 75% (Figure 81) and production of acyl-CoA increases significantly in 0.2 minute increments up to ca. 2 minutes (Figure 82). This is slow enough to affect the subsequent desaturation reaction.

TABLE 41

A COMPARISON OF THE THE LITERATURE K_m AND k_{cat} VALUES USED INITIALLY IN THE COMPUTER MODELLING WITH THE FINAL VALUES FROM MODEL 35

Enzyme	Parameter	Initial value taken * from the literature	Final value † calculated from model 35
E_1, Acyl-CoA synthetase	K_m	2 μM	10.2 μM
E_2, Δ6-Desaturase	K_m	10 μM	1.6 μM
E_3, Lysophospholipid acyltransferase	K_m	3 μM	1.4 μM
E_1, Acyl-CoA synthetase	k_{cat}	41 min^{-1}	25 min^{-1}
E_2, Δ6-Desaturase	k_{cat}	1 - 4 min^{-1}	1.3 min^{-1}
E_3, Lysophospholipid acyltransferase	k_{cat}	26 min^{-1}	2 min^{-1}

* Taken from Tables 40, 42, and references cited therein.

† Calculated from rate constants in model 35 (Table 37).

TABLE 42

LITERATURE DATA FOR LYSOPHOSPHOLIPID ACYLTRANSFERASES

Enzyme	K_m for Acyl Donor (μM)	Acyl Donor (varying in concentration)	Acyl Acceptor (fixed concentration)	Ref.*
Partially purified lysolecithin acyltransferase from rat hepatic microsomes	3.5	linoleoyl-CoA	1-acyl-sn-glycero-3-phosphatidylcholine (100 μM)	228
Lysolecithin acyltransferase in rat hepatic microsomes	3.0	eicosa- 8, 11, 14 - trienoyl-CoA	1-acyl-sn-glycero-phosphatidylcholine (50 μM)	371 (Figure 4)
Partially purified lysolecithin acyltransferase from rat hepatic microsomes	1.5	linoleoyl-CoA	1-stearoyl-sn-glycero-3-phosphatidylcholine (50 μM)	224 (Figure 4)
Purified lysolecithin acyltransferase from rat hepatic microsomes	3.3	linoleoyl-CoA	1-acyl-sn-glycero-3-phosphatidylcholine (60 μM)	227 (Figure 3)

* All assays were spectrophotometric.

The relative values of K_m and V_{max} calculated from the modelling also support the conclusion that under certain conditions the acyl-CoA synthetase reaction could significantly affect the apparent kinetics of the Δ6-desaturase. The K_m for the acyl-CoA synthetase is ca. 6-fold higher than that for the desaturase, while the calculated V_{max} value for the acyl-CoA synthetase is approximately 250-fold greater than that for the Δ6-desaturase (Table 38). From these comparisons, it would appear that at least at substrate concentrations in the low μM range, which is in the experimentally achievable range, the lower K_m for the Δ6-desaturase would to some extent compensate for its relatively low V_{max} and the acyl-CoA synthetase activity would significantly affect measurement of Δ6-desaturase activity using linoleic acid as the source of the substrate.

The modelling of the reaction scheme showed that the lysophospholipid acyltransferase affected the kinetics of the Δ6-desaturase, which is in accord with literature reports (268-270,395). Firstly, the lysophospholipid acyltransferase competes with the Δ6-desaturase for the same acyl-CoA substrate. From the computer modelling, the K_m value for the lysophospholipid acyltransferase is, within experimental error, equivalent to the K_m for the Δ6-desaturase for linoleoyl-CoA substrate. Both K_m values were ca. 1 μM (Table 38); the calculated V_{max} values for the lysophospholipid acyltransferase exceed that for the Δ6-desaturase by between ca. six- and fifteen-fold (modelling results, Table 38, and experimentally determined value, Table 34). Therefore, it would appear likely that the lysophospholipid acyltransferase would significantly affect the apparent activity of the Δ6-desaturase measured in hepatic microsomes using a typical assay system.

The apparent K_m value for the lysophospholipid acyltransferases (ca. 2 μM) determined experimentally in hepatic microsomes (Section 3.2.5.4, Figure 34 and Table 34) was compared with that determined from the modelling (ca. 1 μM, Table 38). Both values agreed closely with those reported in the literature (ca. 1.5 μM to 3 μM from Table 42 and references therein). In determining the K_m values for this enzyme in the literature and in our modelling studies, linoleoyl-CoA was used as substrate while linoleic acid was used for our experimentally determined K_m value. Nevertheless, possibly because of competing factors, the V_{max} for the experimental data and computer modelling are surprisingly close for this enzyme (compare Tables 34 and 38).

Although the apparent K_m values for the Δ6-desaturase obtained from hepatic microsomes in the literature are subject to some doubt on theoretical bases, they do bracket the computer generated K_m for the Δ6-desaturase (see Section 3.2.6). The single report of an apparent K_m value for the isolated enzyme (255) of 45 μM is ca. 40-fold greater than the K_m value of 1.5 μM calculated using data from the simulated reaction scheme (Table 38). This difference could reflect the differences in enzyme preparation: the isolated Δ6-desaturase was solubilised in detergent (255) while our data is for the membrane-bound enzyme. Detergent solubilisation and the structure of the detergent are well known to affect kinetic parameters.

When the kinetics of the Δ6-desaturase were dissected free of contributions from the acyl-CoA synthetase and lysophosphilipid acyltransferases, the initial rate data plotted versus the concentration of the authentic substrate, linoleoyl-CoA, provided reciprocal plots that were excellent approximations to Michaelis Menten kinetics, with calculated K_m of 1.5 μM and V_{max} of

0.063 μM/min (Section 3.2.6). The K_m differed considerably from the apparent K_m value calculated directly from the identical experimental data utilised in the computer modelling. The experimentally determined K_m values was 9.6 μM (Table 34). The experimentally determined V_{max} of 0.09 μM/min was similar to the modelling result (Tables 34 and 38). It should be noted that the discrepancy in the K_m value does not reflect endogenous substrate (which was corrected for in both cases), but probably reflects interference from E_1, and E_3 in accurate determination of K_m for E_2 in hepatic microsomes.

The main conclusions arising from this study of the computer modelling of competing reactions on measurement of the kinetics of the Δ6-desaturase in hepatic microsomes were as follows:

i) Neither chain elongation nor the phospholipases appeared to influence the Δ6-desaturase activity in hepatic microsomes.

ii) The acyl-CoA synthetase is coupled with the Δ6-desaturase and is responsible for production of its acyl-CoA substrate when fatty acid is added as precursor; the kinetics of the acyl-CoA synthetase are such that it is anticipated that, at least at some concentrations of substrate, the acyl-CoA synthetase reaction is not rapid and pre-equilibrium for desaturation. The acyl-CoA synthetase, therefore, appears to influence the kinetics of the Δ6-desaturase in hepatic microsomes, when fatty acid is added as the source of substrate.

iii) The lysophospholipid acyltransferases also affected the activity of Δ6-desaturase. These enzymes compete with the Δ6-desaturase for the linoleoyl-CoA substrate. Secondly, the lysophospholipid acyltransferases would remove the product of desaturation of linoleate, viz: linolenoyl-CoA, thus preventing potential product inhibition of the Δ6-desaturase; the extent of this latter effect and whether it would be kinetically significant is not known.

iv) Using the kinetic data for the Δ6-desaturase generated from the simulated reaction scheme, the Δ6-desaturase was shown to follow simple Michaelis-Menten kinetics resulting in linear reciprocal and double reciprocal plots (Figure 89).

The kinetics of the inhibition of the Δ6-desaturase by isoflurane were also assessed by computer modelling. Isoflurane had no effect on either acyl-CoA synthetase or lysophospholipid acyltransferase (Section 3.2.5.5). Therefore, only the kinetic constants for E_2, the Δ6-desaturase, were adjusted until the model output approximated the experimental rate versus substrate concentration curve in the presence of isoflurane. Double reciprocal plots of the kinetics of the inhibition of the Δ6-desaturase by isoflurane showed that it apparently acts like a competitive inhibitor, i.e., it alters the K_m value of the enzyme without affecting the V_{max} value (Figure 91). Because isoflurane competitively inhibits the Δ6-desaturation of linoleic acid, it appears to bind in such a manner as to affect the linoleoyl-CoA binding site of the enzyme. Since isoflurane does not inhibit the Δ6-desaturation of α-linolenic acid, it would appear that the inhibitor does not compete by fully blocking the site for

acyl-CoA binding, if we assume that the same isozyme desaturates both α-linolenoyl-CoA and linoleoyl-CoA.

It is obvious that many of the complications in the kinetics of the Δ6-desaturase are a function of the enzyme source used, namely hepatic microsomes. Problems such as endogenous substrate, competing enzymes, etc. could be avoided entirely by using a purified reconstituted Δ6-desaturase enzyme system including the Δ6-desaturase and electron transfer protein(s) plus lipid with linoleoyl-CoA as substrate.

The purification and reconstitution of the Δ9-desaturase and Δ6-desaturase systems has been reported (255). In the initial stages of our studies we planned to investigate the effects of anaesthetic agents on the Δ9-desaturase and successfully purified the electron transfer proteins, but were repeatedly unable to purify the Δ9-desaturase (unpublished results). More than one laboratory report using the isolated reconstitued Δ9-desaturase system (251,254,258,259), whereas there is only a single report using the Δ6-desaturase system (255). After our lack of success in purifying the Δ9-desaturase, we did not attempt isolation of the Δ6-desaturase as the procedure was lengthy, yielding very little enzyme. To our knowledge, no reports in the literature cite the use of the isolated Δ6-desaturase by the reported method.

Of necessity, we resorted to the kinetic modelling to characterise the kinetics of the Δ6-desaturase, and until the Δ6-desaturase isolation and reconstitution is successfully used, we feel that ours was a reasonable and fruitfull approach.

4.2.3 Physiological Significance of the Interaction of Isoflurane with the Δ6-Desaturase, and Possible Future Areas of Research

The inhibition of the Δ6-desaturase by isoflurane could influence prostglandin biosynthesis as well as Δ6-desaturation. The role of the Δ6-desaturase in prostaglandin biosynthesis (in particular, the 1-series) is presently uncertain; it has been speculated that Δ6-desaturase is the controlling step in PGE_1 synthesis (350). This may be possible, if not likely, since direct the fatty acid precursor of the 1-series of prostaglandins, dihommogammalinolenic acid, is not quantitatively an important fatty acid constituent of membrane phospholipids and the total cellular phospholipid pool, excepting in seminal vesicles where PGE_1 is produced in abnormally high amounts (201). Thus, it might be anticipated that it would be biosynthesised via Δ6-desaturation of linoleate as needed. Little appears to be known about the rate-limiting step in the biosynthesis of the 1-series of prostaglandins. Therefore the inhibition of the Δ6-desaturase by isoflurane may or may not directly affect this pathway (Figure 10), and may or may not have any physiological significance. The extent of the inhibition is slight in vitro; nevertheless, the apparent K_i is in the low mM range, which is physiologically achievable. Further studies of PGE_1 synthesis are required before we would feel comfortable speculating on this issue.

It might be of interest to assess the effects of the inhibition of the Δ6-desaturase on PGE_1 in a whole cell system. The cell system often used to study the synthesis of the 2-series of prostaglandins is polymorphonuclear leukocytes because the latter is reported to have a high activity of cyclo-oxygenase, the enzyme catalysing the synthesis of prostaglandins from fatty acids. A

preliminary investigation into a cell system suitable to use for the study of the inhibition of the Δ6-desaturase by isoflurane and effects on PGE_1 synthesis, showed that polymorphonuclear leukocytes lacked Δ6-desaturase activity (unpublished results) (389). Therefore, in order to study the relationship between the Δ6-desaturase and PGE_1 synthesis, a cell system containing both Δ6-desaturase and cyclo-oxygenase activity will have to be found. Recently, a mouse fibrosarcoma line has been used to study the mass production of PGE_1 and PGE_2 and the role of the Δ5-desaturase in the PGE_2/PGE_1 ratio (393). Should this cell line have an active Δ6-desaturase, isoflurane may help in the study of the relationship between Δ6-desaturase activity and PGE_1 synthesis. It is, however, anticipated that the chances of success in such an endeavour would be enhanced with a more potent inhibitor than isoflurane. Nevertheless, since this is one of the few non-physiological, xenobiotic compounds known to inhibit the Δ6-desaturase, it is, at present, a reasonable starting point for further investigations.

5. REFERENCES

1. Wade, J.G. and Stevens, W.C. Isoflurane: An Anesthetic for the Eighties? Anesth. Analg., **60** (9), 666-682, 1981.

2. Stevens, W.C., From Ether to Isoflurane: Comparison of General Anesthetics. 34th Annual Refresher Course Lectures and Clinical Update Program, 1-4, 1983.

3. Vitcha, J.F. A History of Forane. Anesthesiology **35** (1), 4-7, 1971.

4. Eger II, E.I. Isoflurane: A Review. Anesthesiology, **55** (5), 559-576, 1981.

5. Pohl, L.R. and Gillette, J.R. A Perspective on Halothane-Induced Hepatotoxicity. Anesth. Analg. **61** (10), 809-811, 1982.

6. Neuberger, J. and Williams, R. Halothane Anaesthesia and Liver Damage. Br. Med. J. **289**, 1136-1139, 1984.

7. Van Dyke, R.A. Metabolism of Anesthetic Agents: Toxic Implications. Acta Anaesth. Scand. Suppl. **75**, 7-9, 1982.

8. Plummer, J.L., Hall, P. de la M., Jenner, M.A., Ilsley, A.H. and Cousins, M.J. Hepatic and Renal Effects of Prolonged Exposure of Rats to 50 p.p.m. Methoxyflurane. Acta Pharmacol. et Toxicol., **57**, 176-183, 1985.

9. Mazze, R.I. Biotransformation and Nephrotoxicity following Enflurane Anesthesia. Hiroshima J. Anesth., **21**.Suppl., 65-73, 1985.

10. Mazze, R.I. and Hitt, B.A. Methoxyflurane Metabolism. Anesthesiology **44** (5), 369-371, 1976.

11. Cook, T.L., Beppu, W.J., Hitt, B.A., Kosek, J.C. and Mazze, R.I. A Comparison of the Renal Effects and Metabolism of Sevoflurane and Methoxyflurane in Enzyme-Induced Rats. Anesth. Analg. **54**, 829-835, 1975.

12. Fry, B.W., Taves, D.R. and Merin,R.G. Fluorometabolites of Methoxyflurane. Anesthesiology **38** (1), 38-44, 1973.

13. Mazze, R.I. and Cousins, M.J. Renal Toxicity of Anaesthetics: With Specific Reference to the Nephrotoxicity of Methoxyflurane. Canad. Anaesth. Soc. J., **20** (1), 64-80, 1973.

14. Carter, R., Heerdt, M. and Acchiardo, S. Fluoride Kinetics after Enflurane Anesthesia in Healthy and Anephric Patients and in Patients with Poor Renal Function. Clin. Pharmacol. Ther., **20** (5), 565-570, 1976.

15. Corall, I.M., Knights, K.M. and Strunin, L. Enflurane Anaesthesia in Man. Br. J. Anaesth., **49**, 881-885, 1977.

16. Prys-Roberts, C. Isoflurane. Br. J. Anaesth., **53** (12), 1243-1245, 1981.

17. Corbett, T.H. Cancer and Congenital Anomalies Associated with Anesthetics. Annals N.Y. Acad. Sci., **271** , 58-66, 1976 .

18. Eger II, E.I., White, A.E., Brown, C.L., Biava, C.G. Corbett, T.H. and Stevens, W.C. A Test of the Carcinogenicity of Enflurane, Isoflurane, Halothane, Methoxyflurane, and Nitrous Oxide in Mice. Anesth. Analg., **57**, 678-694, 1978.

19. Baden, J.M., Kelley, M., Wharton, R.S., Hitt, B.A., Simmon, V.F. and Mazze, R.I. Mutagenicity of Halogenated Ether Anesthetics. Anesthesiology, **46** (5), 346-350, 1977.

20. Stoelting, R.K., Blitt, C.D., Cohen, P.J. and Merin, R.G. Hepatic Dysfunction after Isoflurane Anesthesia. Anesth. Analg., **66**, 147-153, 1987.

21. Wills, E.D. Metabolism of Xenobiotics. ; Xenobiochemistry; in Biochemical Basis of Medicine, John Wright and Sons Limited, 445-465, 1985

22. Blumberg, W.E. Enzymic Modification of Environmental Intoxicants: the Role of Cytochrome P-450. Quarterely Rev. Biophys. II, **4**, 481-542, 1978.

23. Guengerich, F.P. Effects of Nutritive Factors on Metabolic Processes Involving Bioactivation and Detoxification of Chemicals. Ann. Rev. Nutr., **4**, 207-231, 1984.

24. Gillette, J.R. Effects of Induction of Cytochrome P-450 Enzymes on the Concentration of Foreign Compounds and Their Metabolites and on the Toxicological Effects of These Compounds. Drug Metab. Rev., **10** (1), 59-87, 1979.

25. Pelkonen, O., and Vähäkangas, K. Metabolic Activation and Inactivation of Chemical Carcinogens. J. Toxicol. Environ. Health, **6**, 989-999, 1980.

26. Gillette, J.R., Mitchell, J.R. and Brodie, B.B. Biochemical Mechanisms of Drug Toxicity. Drug Toxicity, 271-288, 1974.

27. Miller, E.C. and Miller, J.A. Mechanisms of Chemical Carcinogenesis. Cancer, **47** (5), 1055-1064, 1981.

28. Pelkonen, O. and Nebert, D.W. Metabolism of Polycyclic Aromatic Hydrocarbons: Etiologic Role in Carcinogenesis. Pharmacol. Rev., **34** (2), 189-222, 1982.

29. Weisburger, E.K. Metabolic Activation of Chemical Carcinogens. Prog. Drug Res., **26**, 143-166, 1982.

30. Farber, J.L. and Gerson, R.J. Mechanisms of Cell Injury with Hepatotoxic Chemicals. Pharmacol. Rev., **36** (2), 71S-75S, 1984.

31. Kappus, H., Bolt, H.M., Buchter, A. and Bolt, W. Rat Liver Microsomes Catalyse Covalent Binding of ^{14}C-Vinyl Chloride to Macromolecules. Nature, **257**, 134-135, 1975.

32. Black, S.D. and Coon, M.J. P-450 Cytochromes: Structure and Function. Advances in Enzymol., **60**, 35-87, 1987.

33. Bridges, J.W. The Role of the Drug-Metabolizing Enzymes. Ciba Giegy Found. Symp. 76 (Environ. Chem. Enzyme Funct. and Hum. Dis.), 5-17, 1980.

34. Paine, A.J. Hepatic Cytochrome P-450; in Essays in Biochemistry, eds., P.N.Campbell and R.D.Marshall, Academic Press, London, **17**, 85-126, 1981.

35. Omura, T. and Sato, R. A New Cytochrome in Rat Liver Microsomes. J. Biol. Chem., **237**, PC 1375-1376, 1962.

36. Omura, T. and Sato, R. The Carbon Monoxide-binding Pigment of Liver Microsomes. I. Evidence for its Hemoprotein Nature. J. Biol. Chem., **239** (7), 2370-2378, 1964.

37. Omura, T. and Sato, R. The Carbon Monoxide-binding Pigment of Liver Microsomes. II. Solubilization, Purification, and Properties. J. Biol. Chem., **239** (7), 2379-2385, 1964.

38. Mannering, G.J. Microsomal Enzyme Systems which Catalyze Drug Metabolism; in Fundamentals of Drug Metabolism and Disposition, eds. B.N.La Du, H.G.Mandel and E.L.Way. Williams and Wilkens Company, Baltimore, 206-251, 1971.

39. Kappas, A. and Alvares, A.P. How the Liver Metabolizes Foreign Substances. Sci. Am., **232**, 22-32, 1975.

40. Lu, A.Y.H., Junk, K.W. and Coon, M.J. Resolution of the Cytochrome P-450-containing ω-Hydroxylation System of Liver Microsomes into Three Components. J. Biol. Chem., **244** (13), 3714-3721, 1969.

41. Omura, T., Sanders, E., Estabrook, R.W., Cooper, D.Y. and Rosenthal, O. Isolation from Adrenal Cortex of a Non Heme Iron Protein and a Flavoprotein Functional as a Reduced Triphosphopyridine Nucleotide-Cytochrome P-450 Reductase. Arch. Biochem. Biophys., **117**, 660-673, 1966.

42. Lu, A.Y.H. and West, S.B. Multiplicity of Mammalian Microsomal Cytochromes P-450. Pharmacol. Rev., **31** (4), 277-295, 1980.

43. Bansal, S.K., Love, J.H. and Gurtoo, H.L. Resolution of Multipte Forms of Cytochrome P-450 by High-Performance Liquid Chromatography. J. Chromatog., **297**, 119-127, 1984.

44. Bansal, S.K., Love, J. and Gurtoo, H.L. High Pressure Liquid Chromatographic Separation of Multiple Forms of Cytochrome P-450. Biochem. Biophys. Res Commun., **117** (1), 268-274, 1983.

45. Björkhem, I. Rate Limiting Step in Microsomal Cytochrome P-450 Catalyzed Hydroxylations. Pharmac. Ther. A., **1**, 327-348, 1977

46. Ryan, D.E., Thomas, P.E. and Levin, W. Hepatic Microsomal Cytochrome P-450 from Rats Treated with Isosafrole. J. Biol. Chem., **255** (16), 7941-7955, 1980.

47. Elshourbagy, N.A. and Guzelian, P.S. Separation, Purification, and Characterization of a Novel Form of Hepatic Cytochrome P-450 from Rats Treated With Pregnenolone-16α-carbonitrile. J. Biol. Chem., **255** (4), 1279-1285, 1980.

48. Tamburini, P.P., Masson, H.A., Bains, S.K., Makowski, R.J., Morris, B. and Gibson, G.G. Multiple Forms of Hepatic Cytochrome P-450. Eur. J. Biochem., **139**, 235-246, 1984.

49. Koop, D.R. and Coon, M.J. Purification of Liver Microsomal Cytochrome P-450 Isozymes 3a and 6 from Imidazole-Treated Rabbits. Mol. Pharmacol., **25**, 494-501, 1984.

50. White, R.E. and Coon, M.J. Oxygen Activation by Cytochrome P-450. Ann. Rev. Biochem., **49**, 315-356, 1980.

51. Loew G.H., Collins, J., Luke, B., Waleh, A., and Pudzianowski, A. Theoretical Studies of Cytochrome P-450. Enzyme, **36**, 54-78, 1986.

52. Coon, M.J. and Inouye, K. Biochemical Properties of Cytochrome P-450 in Relation to Steriod Oxygenation. Annals N.Y. Acad. Sci., **458**, 216-224, 1985.

53. Sakurai, H., Hatayama, E., Yoshimura, T., Maeda, M., Tamura, H. and Kawasaki, K. Thiol-Containing Peptide-Hemin Complexes as Models of Cytochrome P-450. Biochem. Biophys. Res Commun., **115** (2), 590-597, 1983.

54. Groves, J.T. Key Elements of the Chemistry of Cytochrome P-450. J. Chem. Educat., **62** (11), 928-931, 1985.

55. Kumaki, K. and Nebert, D.W. Spectral Evidence for Weak Ligand in Sixth Position of Hepatic Microsomal Cytochrome P-450 Low Spin Ferric Iron *in vivo*. Pharmacology, **17**, 262-279, 1978.

56. White, R.E. and Coon, M.J. Heme Ligand Replacement Reactions of Cytochrome P-450. J. Biol. Chem., **257** (6), 3073-3083, 1982.

57. Yoshida, Y., Imai, Y. and Hashimoto-Yutsudo, C. Spectrophotometric Examination of Exogenous-Ligand Complexes of Ferric Cytochrome P-450. Characterization of the Axial Ligand *trans* to the Thiolate in the Native Ferric Low-Spin Form. J. Biochem., **91**, 1651-1659, 1982.

58. Nebert, D.W. and Gonzales, F.J. Cytochrome P-450 Gene Expression and Regulation. TIPS, **6** (4), 160-164, 1985.

59. Lu, A.Y.H., Levin, W., Ryan, D., West, S.B., Thomas, P., Kawalek, J., Kuntzman, R. and Conney, A.H. Induction of Different Types of Cytochrome P-450 in Microsomes by Drugs and Carcinogens. Anticonvulsant Drugs and Enzyme Induction. Associated Scientific Publishers, 169-183, 1976.

60. Whitlock, Jr., J.P. The Regulation of Cytochrome P-450 Gene Expression. Ann. Rev. Pharmacol. Toxicol., **26**, 333-369, 1986.

61. Gillette, J.R., Davis, D.C. and Sasame, H.A. Cytochrome P-450 and its Role in Drug Metabolism. Ann. Rev. Pharmacol., **12**, 57-83, 1972.

62. Peterson, J.A. and Prough, R.A. Cytochrome P-450 Reductase and Cytochrome b_5 in Cytochrome P-450 Catalysis; in Cytochrome P-450, eds. P.R.O. de Montellano, Plenum Press, New York, London, 89-111, 1986.

63. Schenkman, J.B., Remmer, H. and Estabrook, R.W. Spectral Studies of Drug Interaction with Hepatic Microsomal Cytochrome. Mol. Pharmacol., **3**, 113-123, 1967.

64. Sligar, S.G. Coupling of Spin, Substrate, and Redox Equilibria in Cytochrome P450. Biochemistry, **15** (24), 5399-5406, 1976.

65. Kumaki, K., Sato, M., Kon, H. and Nebert, D.W. Correlation of Type I, Type II, and Reverse Type I Difference Spectra with Absolute Changes in Spin State of Hepatic Microsomal Cytochrome P-450 Iron from Five Mammalian Species. J. Biol. Chem., **253** (4), 1048-1058, 1978.

66. Kumaki, K. and Nebert, D.W. Spectral Evidence for Weak Ligand in Sixth Position of Hepatic Microsomal Cytochrome P-450 Low Spin Ferric Iron *in vivo*. Pharmacol. **17**, 262-279, 1978.

67. Rein, H., and Ristau, O. The Importance of the High spin / Low Spin Equilibrium Existing in Cytochrome P-450 for the Enzymatic Mechanism. Pharmazie **33,** H. 6, 325-328, 1978.

68. Gibson, G.G. and Tamburini, P.P. Cytochrome P-450 Spin State: Inorganic Biochemistry of Haem Iron Ligation and Functional Significance. Xenobiotica, **14** (1/2), 27-47, 1984.

69. Lu, A.Y.H., Kuntzman, R. and Conney, A.H. The Liver Microsomal Hydroxylation Enzyme System. Front. Gastrointest. Res., **2**, 1-31, 1976.

70. Dus, K.M. Insights into the Active Site of the Cytochrome P-450 Haemoprotein Family - a Unifying Concept based on Structural Considerations. Xenobiotica, **12** (11), 745-772, 1982.

71. Estabrook, R.W., Franklin, M.R. and Hilderbrandt, A.G. Factors Influencing the Inhibitory Effect of Carbon Monoxide on Cytochrome P-450-catalyzed Mixed Function Oxidation Reactions. Ann. N.Y. Acad. Sci. **174**, 218-232, 1970.

72. Estabrook, R.W., Matsubara, T., Mason, J.I., Werringloer, J. and Baron, J. Studies on the Molecular Function of Cytochrome P-450 during Drug Metabolism. Drug Metab. Dispos., **1** (1), 98-110, 1973.

73. Ullrich, V., Ruf, H.H. and Wende, P. The Structure and Mechanism of Cytochrome P-450. Croatica Chemica Acta, **49** (2), 213-222, 1977.

74. Guengerich, F.P. and Macdonald, T.L. Chemical Mechanisms of Catalysis by Cytochromes P-450: a Unified View. Accounts Chem. Res., **17**, 9-16, 1984.

75. De Montellano, P.R.O. Oxygen Activation and Transfer; in Cytochrome P-450, eds., P.R.O. de Montellano, Plenum Press, New York, London, 217-271, 1986.

76. Bast, A. and Haenen, G.R.M.M. Cytochrome P-450 and Glutathione: What is the Significance of Their Interrelationship in Lipid Peroxidation? TIBS, 510-513, 1984.

77. Kuthan, H. and Ullrich, V. Oxidase and Oxygenase Function of the Microsomal Cytochrome P-450 Monooxygenase System. Eur. J. Biochem., **126**, 583-588, 1982.

78. Bast, A. Is Formation of Reactive Oxygen by Cytochrome P-450 Perilous and Predictable. TIPS, **7** (7), 266-270, 1986.

79. Winston, G.W. and Cederbaum, A.I. NADPH-dependent Production of Oxy Radicals by Purified Components of the Rat Liver Mixed Function Oxidase System. J. Biol. Chem., **258** (3), 1508-1513, 1983.

80. Heinemeyer, G., Nigam, S. and Hildebrandt, A.G. Hexobarbital-Binding, Hydroxylation and Hexobarbital-Dependent Hydrogen Peroxide Production in Hepatic Microsomes of Guinea Pig, Rat and Rabbit. Naunyn-Schmiedeberg's Arch. Pharmacol., **314**, 201-210, 1980.

81. Gorsky, L.D. Koop, D.R. and Coon, M.J. On the Stoichiometry of the Oxidase and Monooxygenase Reactions Catalysed by Liver Microsomal Cytochrome P-450. J. Biol. Chem., **259** (11), 6812-6817, 1984.

82. Morgan, E.T., Koop, D.R. and Coon, M.J. Catalytic Activity of Cytochrome P-450 Isozyme 3a Isolated from Liver Microsomes of Ethanol-treated Rabbits. J. Biol. Chem., **257** (23), 13951-13957, 1982.

83. Zhukov, A.A and Archakov. A.I. Complete Stoichiometry of Free NADPH Oxidation in Liver Microsomes. Biochem. Biophys. Res. Commun., **109** (3), 813-818, 1982.

84. Nordblom, G.D. and Coon, M.J. Hydrogen Peroxide Formation and Stoichiometry of Hydroxylation Reactions Catalyzed by Highly Purified Liver Microsomal Cytochrome P-450. Arch. Biochem. Biophys., **180**, 343-347, 1977.

85. Takazawa, R.S. and Strobel. H.W. Cytochrome P-450 Mediated Reductive Dehalogenation of the Perhalogenated Aromatic Compound Hexachlorobenzene. Biochemistry, **25**, 4804-4809, 1986.

86. Brault, D. Model Studies in Cytochrome P-450-Mediated Toxicity of Halogenated Compounds: Radical Processes Involving Iron Porphyrins. Environ. Health Perspec., **64**, 53-60, 1985.

87. Van Dyke, R.A., Baker, M.T, Jansson, I. and Schenkman, J. Reductive Metabolism of Halothane by Purified Cytochrome P-450. Biochem. Pharmacol., **37** (12), 2357-2361, 1988.

88. Pohl, L.R., Schulick, R.D., Highet, R.J. and George, J.W. Reductive-Oxygenation Mechanism of Metabolism of Carbon Tetrachloride to Phosgene by Cytochrome P-450. Mol. Pharmacol., **25**, 318-321, 1984.

89. Bösterling, B., Trudell, J.R., Trevor, A.J and Bendix, M. Lipid-Protein Interactions as Determinants of Activation or Inhibition by Cytochrome b_5 of Cytochrome P-450-mediated Oxidations. J. Biol. Chem., **257** (8), 4375-4380, 1982.

90. Ingelman-Sundberg, M. Cytochrome P-450 Organization and Membrane Interaction; in Cytochrome P-450, eds., P.R.O. de Montellano, Plenum Press, New York, London, 119-160, 1986.

91. Guengerich, F.P., Ballou, D.P. and Coon, M.J. Purified Liver Microsomal Cytochrome P-450. J. Biol. Chem., **250** (18), 7405-7414, 1975.

92. Mannering, G.J. Role of Cytochrome b_5 in the NADH Synergism of NADPH-dependent Reactions of the Cytochrome P-450 Monooxygenase System of Hepatic Microsomes. Adv. Exper. Med. and Biol., **58**, 405-434, 1975.

93. Imai, Y. and Sato, R. The Roles of Cytochrome b_5 in a Reconstituted N-Demethylase System Containing Cytochrome P-450. Biochem. Biophys. Res. Commun., **75** (2), 420-426, 1977.

94. Ingelman-Sundberg, M. and Johansson, I. Cytochrome b_5 as Electron Donor to Rabbit Liver Cytochrome $P\text{-}450_{LM_2}$ in Reconstituted Phospholipid Vesicles. Biochem. Biophys. Res. Commun., **97** (2), 582-589, 1980.

95. Lipka, J.J. and Waskell, L. Methoxyflurane Acts at the Substrate Binding Site of Cytochrome $P\text{-}450LM_2$ to induce a Dependence on Cytochrome b_5. Arch. Biochem. Biophys., **268** (1), 152-160, 1989.

96. Kuwahara, S. and Omura, T. Different Requirement for Cytochrome b_5 in NADPH-supported O-Deethylation of p-Nitrophenetole Catalyzed by Two Types of Microsomal Cytochrome P-450. Biochem. Biophys. Res. Commun., **96** (4), 1562-1568, 1980.

97. Chiang, J.Y.L. Interaction of Purified Microsomal Cytochrome P-450 with Cytochrome b_5. Arch. Biochem. Biophys., **211** (2), 662-673, 1981.

98. Waxman, D.J. and Walsh, C. Cytochrome P-450 Isozyme 1 from Phenobarbital-Induced Rat Liver: Purification, Characterization, and Interactions with Metyrapone and Cytochrome b_5. Biochemistry, **22**, 4846-4855, 1983.

99. Vatsis, K.P., Theoharides, A.D., Kupfer, D. and Coon, M.J. Hydroxylation of Prostaglandins by Inducible Isozymes of Rabbit Liver Microsomal Cytochrome P-450. J. Biol. Chem., **257** (19), 11221-11229, 1982.

100. Hlavica, P. On the Function of Cytochrome b_5 in the Cytochrome P-450-Dependent Oxygenase System. Arch. Biochem. Biophys. **228** (2), 600-608, 1984.

101. Tamburini, P.P. and Schenkman, J.B. Mechanism of Interaction between Cytochrome P-450 RLM5 and Cytochrome b_5: Evidence for an Electrostatic Mechanism Involving Cytochrome b_5 Heme Propionate Groups. Arch. Biochem. Biophys., **245** (2), 512-522, 1986.

102. Tamburini, P.P and Schenkman, J.B. Purification to Homogeneity and Enzymological Characterization of a Functional Covalent Complex Composed of Cytochromes P-450 Isozymes 2 and b_5 from Rabbit Liver. Proc. Natl. Acad. Sci. USA., **84**, 11-15, 1987.

103. Tamburini, P.P., White, R.E. and Schenkman, J.B. Chemical Characterization of Protein-Protein Interactions between Cytochrome P-450 and Cytochrome b_5. J. Biol. Chem., **260** (7), 4007-4015, 1985.

104. Tamburini, P.P., MacFarquhar, S. and Schenkman, J.B. Evidence of Binary Complex Formations between Cytochrome P-450, Cytochrome b_5, and NADPH-Cytochrome P-450 Reductase of Hepatic Microsomes. Biochem. Biophys. Res. Commun., **134** (2), 519-526, 1986.

105. Tamburini, P.P. and Schenkman, J.B. Differences in the Mechanism of Functional Interaction between NADPH-Cytochrome P-450 Reductase and Its Redox Partners. Mol. Pharmacol., **30**, 178-185, 1986.

106. Bernhardt, R., Pommerening, K. and Ruckpaul, K. Modification of Carboxyl Groups on NADPH-Cytochrome P-450 Reductase Involved in Binding of Cytochrome c amd P-450 LM2. Biochem. Int., **14** (5), 823-832, 1987.

107. Nadler, S.G. and Strobel, H.W. Role of Electrostatic Interactions in the Reaction of NADPH-Cytochrome P-450 Reductase with Cytochromes P-450. Arch. Biochem. Biophys., **261** (2), 418-429, 1988.

108. Taniguchi, H., Imai, Y. and Sato, R. Protein-Protein and Lipid-Protein Interactions in a Reconstituted Cytochrome-P-450 Dependent Microsomal Monooxygenase. Biochemistry, **26** (22), 7084-7090, 1987.

109. Backes, W.L. and Reker-Backes, C.E. The Effect of NADPH Concentration on the Reduction of Cytochrome P-450 LM_2. J. Biol. Chem., **263** (1), 247-253, 1988.

110. Backes, W.L. and Eyer, C.S. Cytochrome P-450 LM2 Reduction. Substrate Effects on the Rate of Reductase-LM2 Association. J. Biol. Chem., **264** (11), 6252-6259, 1989.

111. De Montellano, P.R.O.and Reich, N.O. Inhibition of Cytochrome P-450 Enzymes; in Cytochrome P-450, eds., P.R.O. de Montellano, Plenum Press, New York, London, 273-314, 1986.

112. Testa, B. and Jenner, P. Inhibitors of Cytochrome P-450s and their Mechanism of Action. Drug Metab. Rev., **12**, 1-117,

113. Netter, K.J. Inhibition of Oxidative Drug Metabolism in Microsomes. Pharmacol. Ther., **10**, 515-535, 1980.

114. Franklin, M.R. Inhibition of Mixed-Function Oxidations by Substrates Forming Reduced Cytochrome P-450 Metabolic-Intermediate Complexes. Pharmac. Ther. A., **2**, 227-245, 1977.

115. De Maties, F., Gibbs, A.H., Cantoni, L. and Francis, J. Substrate-Dependent Irreversible Inactivation of Cytochrome P-450: Conversion of its Haem Moiety into Modified Porphryns.Ciba Giegy Found. Symp. 76 (Environ. Chem. Enzyme Funct. and Hum. Dis.), 119-139, 1980.

116. Marks, G.S., McCluskey, S.A., Mackie, J.E., Riddick, D.S. and James, C.A. Disruption of Hepatic Heme Biosynthesis after Interaction of Xenobiotics with Cytochrome P-450. FASEB. J., **2**, 2774-2783, 1988.

117. Walsh, C.T. Suicide Substrates, Mechanism-Based Enzyme Inactivators: Recent Developments. Ann. Rev. Biochem., **53**, 493-535, 1984.

118. Conney, A.H., Brown R.R., Miller, J.A. and Miller, E.L. The Metabolism of Methylated Aminoazo Dyes. VI. Intracellular Distribution and Properties of Demethylase System. Cancer Res., **17**, 628-633, 1957.

119. Gonzales, F.J. The Molecular Biology of Cytochrome P-450. Pharmacol. Rev., **40** (2), 243-288. 1989.

120. Goldstein, J.A. Mechanism of Induction of Hepatic Drug Metabolizing Enzymes: Recent Advances. TIPS, **5** (7), 290-292, 1984.

121. Nebert, D.W. P-450 Genes and Their Regulation. TIPS, **6** (7), 270-273, 1985.

122. Nebert, D.W., Nelson, D.R., Adesnik, M., Coon, M.J., Estabrook, R.W., Gonzalez, F.J., Guengerich, F.P., Gunsalus, I.C., Johnson, E.F., Kemper, B., Levin, W., Phillips, I.R., Sato, R. and Waterman, M.R. The Cytochrome P-450 Superfamily: Updated listing of all Genes and Recommended Nomenclature for Chromasomal Loci. DNA, **8** (1), 1-13, 1989.

123. Hardwick, J.P., Song, B-J, Huberman, E. and Gonzalez, F.J. Isolation, Complementary DNA Sequence, and Regulation of Rat Hepatic Lauric Acid ω-Hydroxylase (Cytochrome $P\text{-}450_{LA\omega}$). J. Biol. Chem., **262** (2), 801-810, 1987.

124. Friedberg, T., Waxman, D.J., Atchison, M., Kumar, A., Haarparante, T., Raphael, C. and Adesnik, M. Isolation and Characterization of cDNA Clones for Cytochrome P-450 Immunochemically Related to Rat Hepatic P-450 Form PB-1. Biochemistry, **25**, 7975-7983, 1986.

125. Wolf. C.R., Miles, J.S., Seilman, S., Burke, M.D., Rospendowski, B.N., Kelly, K. and Smith, W.E. Evidence That the Catalytic Differences of Two Structurally Homologous Forms of Cytochrome P-450 Relate to Their Heme Environment. Biochemistry, **27**, 1597-1603, 1988.

126. Halpert, J.R. Multiplicity of Steroid-Inducible Cytochromes P-450 in Rat Liver Microsomes. Arch. Biochem. Biophys., **263** (1), 59-68, 1988.

127. Haniu, M., Ryan, D.E., Levin, W. and Shively, J.E. Structures of Cysteine-Containing Peptides in Isosafrole-Inducible Rat Hepatic Microsomal Cytochrome P-450d: Sequence Homology with 3-Methylcholanthrene-Induced Cytochrome P-450c. Proc. Natl. Acad. Sci. USA, **81**, 4298-4301, 1984.

128. Nebert, D.W. and Jones, J.E. Minireview: Regulation of the Mammalian Cytochrome P_1-450 (CYP1A1) gene. Int. J. Biochem., **21** (3), 243-252, 1989.

129. Imai, Y., Komori, M. and Sato. R. Comparison of Primary Structures Deduced from cDNA Nucleotide Sequences for Various Forms of Liver Microsomal Cytochrome P-450 from Phenobarbital-Treated Rabbits. Biochemistry, **27**, 80-88, 1988.

130. Kumar, A., Raphael, C. and Adesnik, M. Cloned Cytochrome P-450 cDNA. J. Biol. Chem., **258** (18), 11280-11284, 1983.

131. Walz, F.G., Vlasuk, G.P., Omiecinski, C.J., Bresnick, E., Thomas, P.E., Ryan, D.E. and Levin, W. Multiple, Immunoidentical Forms of Phenobarbital-Induced Rat Liver Cytochromes P-450 are Encoded by Different mRNAs. J. Biol. Chem., **257** (8), 4023-4026, 1982.

132. Waxman, D.J. Rat Hepatic Cytochrome P-450; in Cytochrome P-450, eds., P.R.O. de Montellano, Plenum Press, New York, London, 525-539, 1986.

133. Ryan, D.E., Thomas, P.E., Reik, L.M. and Levin, W. Purification, Characterization and Regulation of Five Rat Hepatic Microsomal Cytochrome P-450 Isozymes. Xenobiotica, **12** (11), 727-744, 1982.

134. Conney, A.H. Pharmacological Implications of Microsomal Enzyme Induction. Pharmacol. Rev., **19** (3), 317-366, 1967.

135. Komori, M., Imai, Y., Tsunasawa, S. and Sato, R. Microheterogeneity in the Major Phenobarbital-Inducible Forms of Rabbit Liver Microsomal Cytochrome P-450 ss Revealed by Nucleotide Sequencing of Cloned cDNAs. Biochemistry **27**, 73-80, 1988.

136. Rampersaud, A. and Walz, Jr., F.G. At Least Six Forms of Extremely Homologous Cytochromes P-450 in Rat Liver are Encoded at Two Closely Linked Genetic Loci. Proc. Natl. Acad. Sci. USA., **80**, 6542-6546, 1983.

137. Waxman, D.J. and Walsh, C. Phenobarbital-Induced Rat Liver Cytochrome P-450. J. Biol. Chem., **257** (17), 10446-10457, 1982.

138. Vlasuk, G.P., Ryan, D.E., Thomas, P.E., Levin, W. and Walz, Jr., F.G. Polypeptide Patterns of Hepatic Microsomes from Long-Evans Rats Treated with Different Xenobiotics. Biochemistry, **21**, 6288-6292, 1982.

139. Omiecinski, C.J., Walz, Jr., F.G. and Vlasuk, G.P. Phenobarbital Induction of Rat Liver Cytochrome P-450b and P-450e. J. Biol. Chem., **260** (6), 3247-3250, 1985.

140. Eisen, H.J. Induction of Hepatic P-450 Isozymes. Evidence for Specific Receptors in Cytochrome P-450; in Cytochrome P-450, ed., P.R.O. de Montellano, Plenum Press, New York, London, 315-344, 1986.

141. Miller, J.A. Carcinogenesis by Chemicals: an Overview-G.H.A. Clowes Memorial Lecture. Cancer Research, **30**, 559-576, 1970.

142. Conney, A.H. Induction of Microsomal Enzymes by Foreign Chemicals and Carcinogenesis by Polycyclic Aromatic Hydrocarbons: G.H.A. Clowes Memorial Lecture. Cancer Research, **42**, 4875-4917, 1982.

143. Gelboin, H.V. Benzo[α]Pyrene Metabolism, Activation, and Carcinogenesis: Role and Regulation of Mixed-Function Oxidases and Related Enzymes. Physiol. Rev., **60** (4), 1107-1154, 1980.

144. Morville, A.L., Thomas, P., Levin, W., Reik, L., Ryan, D.E., Raphael, C. and Adesnik, M. The Accumulation of Distinct mRNAs for the Immunochemically Related Cytochromes P-450c and P-450d in Rat Liver Following 3-Methylcholanthrene Treatment. J. Biol. Chem., **258** (6), 3901-3906, 1983.

145. Thomas, P.E., Reik, L.M., Ryan, D.E. and Levin, W. Induction of Two Immunochemically Related Rat Liver Cytochrome P-450 Isozymes, Cytochrome P-450c and P-450d, by Structurally Diverse Xenobiotics. J. Biol. Chem., **258** (7), 4590-4598, 1983.

146. Kawajiri, K., Gotoh, O., Sogawa, K., Tagashira, Y., Muramatsu, M. and Fujii-Kuriyama, Y. Coding Nucleotide Sequence of 3-Methylcholanthrene-Inducible Cytochrome P-450d cDNA from Rat Liver. Proc. Natl. Acad. Sci. USA, **81**, 1649-1653, 1984.

147. Sogawa, K., Gotoh, O., Kawajiri, K. and Fujii-Kuriyama, Y. Distinct Organization of Methylcholanthrene-and Phenobarbital-Inducible Cytochrome P-450 Genes in the Rat. Proc. Natl. Acad. Sci. USA., **81**, 5066-5070, 1984.

148. Reik, L.M., Levin, W., Ryan, D.E. and Thomas, P.E. Immunochemical Relatedness of Rat Hepatic Microsomal Cytochromes P-450c and P-450d. J. Biol. Chem., **257**, (7), 3950-3957, 1982.

149. Schuetz, E.G., Wrighton, S.A., Barwick, J.L. and Guzelian, P.S. Induction of Cytochrome P-450 by Glucocorticoids in Rat Liver. J. Biol. Chem., **259**, (3), 1999-2006, 1984.

150. Hardwick, J.P., Gonzalez, F.J. and Kasper, C.B. Cloning of DNA Complementary to Cytochrome P-450 Induced by Pregnenolone-16α-carbonitrile. J. Biol. Chem., **258** (16), 10182-10186, 1983.

151. Guengerich, F.P. Characterization of Human Microsomal Cytochrome P-450 Enzymes. Annu. Rev. Pharmacol. Toxicol., **29**, 241-164, 1989.

152. Gibson, G.G. and Bains, S.K. Cytochrome P-450 Isoenzymes Involved in Fatty Acid Metabolism. Biochem. Soc. Transac., **13**, 850-852, 1985.

153. Ryan, D.E., Koop, D.R., Thomas, P.E., Coon, M.J., and Levin, W. Evidence that Isoniazid and Ethanol Induce the Same Microsomal Cytochrome P-450 in Rat Liver, an Isozyme Homologous to Rabbit Liver Cytochrome P-450 Isozyme 3a. Arch. Biochem. Biophys., **246** (2), 633-644, 1986.

154. Khani, S.C., Zaphiropoulos, P.G., Fujita, V.S., Porter, T.D., Koop, D.R. and Coon, M.J. cDNA and Derived Amino Acid sequence of Ethanol-inducible Rabbit Liver Cytochrome P-450 Isozyme 3a ($P\text{-}450_{ALC}$). Proc. Natl. Acad. Sci. USA., **84**, 638-642, 1987.

155. Guengerich, F.P., Dannan, G.A., Wright, S.T., Martin, M.V and Kaminsky, L.S. Purification and Characterization of Liver Microsomal Cytochromes P-450: Electrophoretic, Spectral, Catalytic and Immunochemical Properties and Inducibility of Eight Isozymes Isolated from Rats Treated with Phenobarbital or β-Naphthoflavone. Biochemistry, **21**, 6019-6030, 1982.

156. Guengerich, F.P., Distlerath, L.M., Reilly, P.E.B., Wolff, T., Shimada, T., Umbenhauer, D.R. and Martin, M.V. Human-Liver Cytochromes P-450 Involved in Polymorphisms of Drug Oxidation. Xenobiotica, **16** (5), 367-378, 1986.

157. Guengerich, F.P., Beaune, P., Umbenhauer, D.R., Churchhill, P.F., Bork, R.W., Dannan. G.A., Knodell, R.G., Lloyd, R.S. and Martin, M.V. Cytochrome P-450 Enzymes Involved in Genetic Polymorphism of Drug Oxidations in Humans. Biochem. Soc. Transac., **15**, 576-578, 1987.

158. Meehan, R.R., Gosden, J.R., Rout, D., Hastie, N.D., Friedberg, T., Asdenik, M., Budkland, R., Van Heyningen, V., Fletcher, J., Spurr, N.K., et al. Human Cytochrome P-450 PB-1: a Multigene Family Involved in Mephenytoin and Steroid Oxidations that Maps to Chromosome 10. Am. J. Hum. Genet., **42** (1), 26-37, 1988.

159. Guengerich, F.P. Polymophism of Cytochrome P-450 in Humans. TIPS, **10** (3), 107-109, 1989.

160. Guengerich, F.P., Umbenhauer, D.R., Churchill, P.F., Beaune, P.H., Böcker, R., Knodell, R.G., Martin, M.V. and Lloyd, R.S. Polymorphism of Human Cytochrome P-450. Xenobiotica, **17** (3), 311-316, 1987.

161. Guengerich, F.P., Martin, M.V., Beaune, P.H., Kremers, P., Wolff, T. and Waxman, D.J. Characterization of Rat and Human Liver Microsomal Cytochrome P-450 Forms Involved in Nifedipine Oxidation, a Prototype for Genetic Polymorphism in Oxidative Drug Metabolism. J. Biol. Chem., **261** (11), 5051-5060, 1986.

162. Smith, R.L. Introduction. Xenobiotica, **16** (5), 361-365, 1986.

163. Mahgoub, A., Idle, J.R., Dring, L.G., Lancaster, R. and Smith, R.L. Polymorphic Hydroxylation of Debrisoquine in Man. Lancet, **2**, 584-586, 1977.

164. Eichelbaum, M., Bertilsson, L., Säwe, J. and Zekorn, C. Polymorphic Oxidation of Sparteine and Debrisoquine: Related Pharmacogenetic Entities. Clin. Pharmacol. Ther., **31** (2),184-186, 1982.

165. Distlerath, L.M. and Guengerich, F.P. Characterization of a Human Liver Cytochrome P-450 Involved in the Oxidation of Debrisoquine and Other Drugs by Using Antibodies Raised to the Analogous Rat Enzyme. Proc. Natl. Acad. Sci. USA., **81**, 7348-7352, 1984.

166. Gut, J., Catin, T., Dayer, P., Kronbach, T., Zanger, U. and Meyer, U.A. Debrisoquine/Sparteine-type Polymorphism of Drug Oxidation. J. Biol.Chem., **261** (25), 11734-11743, 1986.

167. Meyer, U.A., Gut, J., Kronbach, T., Skoda, C., Meier, U.T. and Catin, T. The Molecular Mechanism of Two Common Polymorphisms of Drug Oxidation - Evidence for Functional Changes in Cytochrome P-450 Isozymes Catalysing Bufuralol and Mephenytoin Oxidation. Xenobiotica, **16** (5), 449-464, 1986.

168. Dignam, J.D. and Strobel, H.W. Preparation of Homogeneous NADPH-Cytochrome P-450 Reductase from Rat Liver. Biochem. Biophys. Res. Commun., **63** (4), 845-851, 1975.

169. Iyanagi, T., Makino, R. and Anan, F.K. Studies on the Microsomal Mixed-Function Oxidase System: Mechanism of Action of Hepatic NADPH-Cytochrome P-450 Reductase. Biochemistry, **20** (7), 1722-1730, 1981.

170. Knapp, J.A., Dignam, J.D.and Strobel, H.W. NADPH-Cytochrome P-450 Reductase. J. Biol. Chem., **252** (2), 437-443, 1977.

171. Dignam, J.D. and Strobel, H.W. NADPH-Cytochrome P-450 Reductase from Rat Liver: Purification by Affinity Chromatography and Characterization. Biochemistry, **16** (6), 1116-1122, 1977.

173. Van Dyke, R.A. and Gandolfi, A.J. Anaerobic Release of Fluoride from Halothane. Drug Metab. Dispos., **4** (1), 40-44, 1976.

174. Baker, M.T., Nelson, R.M. and Van Dyke, R.A. The Release of Inorganic Fluoride from Halothane and Halothane Metabolites by Cytochrome P-450, Hemin, and Hemoglobin. Drug Metab. Dispos. **11**, (4), 308-311, 1983.

175. Fujii, K., Morio, M. and Kikuchi, H. A Possible Role of Cytochrome P-450 in Anaerobic Dehalogenation of Halothane. Biochem. Biophys. Res. Commun., **101** (4), 1158-1163, 1981.

176. Fujii, K., Miki, N., Sugiyama, T., Morio, M., Yamano, T. and Miyake, Y. Anaerobic Dehalogenation of Halothane by Reconstituted Liver Microsomal Cytochrome P-450 Enzyme System. Biochem. Biophys. Res. Commun., **102** (1), 507-512, 1981.

177. Rice, S.A., Maze, M., Smith, C.M., Kosek, J.C. and Mazze, R.I. Halothane Hepatotoxicity in Fischer 344 Rats Pretreated with Isoniazid. Toxicol. Appl. Pharmacol., **87**, 411-419, 1987.

178 Gruenke, L.D., Konopka, K., Koop, D.R. and Waskell, L.A. Characterization of Halothane Oxidation by Hepatic Microsomes and Purified Cytochromes P-450 using a Gas Chromatographic Mass Spectrometric Assay. J. Pharmacol. Exp. Ther., **246**, (2), 454-459, 1988.

179. Rice, S.A., Sbordone, L. and Mazze, R.I. Metabolism by Rat Hepatic Microsomes of Fluorinated Ether Anesthetics Following Isoniazid Administration. Anesthesiology, **53**, 489-493, 1980.

180. Van Dyke, R.A. and Chenowith, M.B. The Metabolism of Volatile Anesthetics-II. *In vitro* Metabolism of Methoxyflurane and Halothane in Rat Liver Slices and Cell Fractions. Biochem. Pharmacol., **14**, 603-609, 1965.

181. Waskell, L. and Gonzales, J. Dependence of Microsomal Methoxyflurane O-Demethelation on Cytochrome P-450 Reductase and the Stoichiometry of Fluoride Ion and Formaldehyde Release. Anesth. Analg., **61** (7), 609-613, 1982.

182. Ivanetich, K.M., Lucas, S.A. and Marsh, J.A. Enflurane and Methoxyflurane. Their Interaction with Hepatic Cytochrome P-450 *in vitro*. Biochem. Pharmacol., **28**, 785-792, 1979.

183. Loew, G., Motulsky, H., Trudell, J., Cohen, E. and Hjelmeland, L. Quantum Chemical Studies of the Metabolism of the Inhalation Anesthetics Methoxyflurane, Enflurane, and Isoflurane. Mol. Pharmacol., **10**, 406-418, 1974.

184. Mazze, R.I. and Hitt, B. Effects of Phenobarbital and 3-Methylcholanthrene on Anesthetic Defluorination in Fischer 344 Rats. Drug Metab. Dispos., **6** (6), 680-681, 1978.

185. Rice, S A., Dooley, J.R. and Mazze, R.I. Metabolism by Rat Hepatic Microsomes of Fluorinated Ether Anesthetics Following Ethanol Consumption. Anesthesiology, **58**, 237-241, 1983.

186. Van Dyke, R.A. Enflurane, Isoflurane, and Methoxyflurane Metabolism in Rat Hepatic Microsomes from Ethanol-treated Animals. Anesthesiology, **58**, 221-224, 1983.

187. Mazze, R.I., Hitt, B.A. and Cousins, M.J. Effect of Enzyme Induction with Phenobarbital on the *in Vivo* and *in Vitro* Defluorination of Isoflurane and Methoxyflurane. J. Pharmacol. Exper. Ther., **190** (3), 523-529, 1974.

188. Waskell, L., Canova-Davis, E., Philpot, R., Parandoush, Z. and Chiang, J.Y.L. Identification of the Enzymes Catalyzing Metabolism of Methoxyflurane. Drug Metab. Dispos., **14** (6), 643-648, 1986.

189. Burke, T.R., Branchflower, R.V., Lees, D.E. and Pohl, L.R. Mechanism of Defluorination of Enflurane. Identification of an Organic Metabolite in Rat and Man. Drug Metab. Dispos., **9** (1), 19-24, 1981.

190. Hitt, B.A., Mazze, R.I., Beppu, W.J., Stevens, W.C. and Eger II, E.I. Enflurane Metabolism in Rats and Man. J. Pharmacol. Exper. Ther., **203** (1), 193-202, 1977.

191. Carpenter, R.L., Eger II, E.I. Johnson, B.H., Unadkat, J.D. and Sheiner, L.B. The Extent of Metabolism of Inhaled Anesthetics in Humans. Anesthesiology, **65**, 201-205, 1986.

192. Holaday, D.A., Fiserova-Bergerova, V., Latto, I.P. and Zumbiel, M.A. Resistance of Isoflurane to Biotransformation in Man. Anesthesiology, **43** (3), 325-332, 1975.

193. Mazze, R.I., Cousins, M.J. and Barr, G.A. Renal Effects and Metabolism of Isoflurane in Man. Anesthesiology, **40** (6), 536-542, 1974.

194. Cousins, M.J., Mazze, R.I., Barr, G.A. and Kosek, J.C. A Comparison of the Renal Effects of Isoflurane and Methoxyflurane in Fischer 344 Rats. Anesthesiology, **38**, (6) 557-564, 1973.

195. Hitt, B.A., Mazze, R.I., Cousins, M.J., Edmunds, H.N., Barr, G.A. and Trudell, J.R. Metabolism of Isoflurane in Fischer 344 Rats and Man. Anesthesiology, **40** (1), 62-67, 1974.

196. Gurr, I.I. and James, A.T. Fatty Acids; in Lipid Biochemistry: an Introduction. Chapman and Hall, London, New York, 18-89, 1980.

197. Mead, J.F., Alfin-Slater, R.B., Howton, D.R.and Pojak,G. Desaturation of Fatty Acids - The Essential Fatty Acids; in Lipids, Plenum Press, New York and London, 133-147, 1986.

198. Jeffcoat, R. and James, A.T. The Regulation of Desaturation and Elongation of Fatty Acids in Mammals; in Fatty Acid Metabolism and Its Regulation, Ed. S.Numa, Elsevier, Amsterdam, New York, London, 85-112, 1984.

199. Sinclair, H.M. Essential Fatty Acids in Perspective. Human Nutr.: Clin. Nutr., **38C**, 245-260, 1984.

200. Alfin-Slater, R.B. and Aftergood, L. Essential Fatty Acids Reinvestigated. Physiol. Rev., **48** (4), 758-784, 1968.

201. Willis, A.L. Nutritional and Pharmacological Factors in Eicosanoid Biology. Nutr. Rev., **39** (8), 289-301, 1981 .

202. Cunnane, S.C. Essential Fatty-Acid/Mineral Interactions with Reference to the Pig; in Fats in Animal Nutrition. Ed. J. Wiseman, Butterworths, London, 167-183, 1984.

203. Burr, G.O. and Burr, M.M. A New Deficiency Disease Produced by the Rigid Exclusion of Fat From the Diet. J. Biol. Chem., **82**, (2), 345-367, 1929.

204. Hansen, H.S. The Essential Nature of Linoleic Acid in Mammals. TIBS, **11**, 263-265, 1986.

205. Mead, J.F. The Non-Eicosanoid Functions of the Essential Fatty Acids. J. Lipid. Res., **25**, 1517-1521, 1984.

206. Wahle, K.W.J. Fatty acid Modification and Membrane Lipids. Proc. Nutr. Soc., **42**, 273-287, 1983.

207. Brenner, R.R. Effect of Unsaturated Acids on Membrane Structure and Enzyme Kinetics. Prog. Lipid Res., **23**, 69-96, 1984.

208. Kates, M., Pugh, E.L. and Ferrante, G. Regulation of Membrane Fluidity by Lipid Desaturases. Biomembranes, **12**, 379-395, 1984.

209. Essential Fatty Acids and Maintenance of the Epidermal Water Barrier. Nutr. Rev., **44** (4), 151-154, 1986.

210. Irvine, R.F. How is the Level of Free Arachidonic Acid Controlled in Mammalian Cells? Biochem. J., **204**, 3-16, 1982.

211. Philipp, D.P. and Parson, P. Isolation and Purification of Long Chain Fatty Acyl Coenzyme A Ligase from Rat Liver Mitochondria. J. Biol. Chem., **254**, (21), 10776-10784, 1979.

212. Maes, E. and Bar-Tana, J. Rat Liver Microsomal Palmitoyl-CoA Synthetase: Subunit Structure. Biochim. Biophys. Acta, **480**, 527-530, 1977.

213. Bremer, J. and Osmundsen, H. Fatty Acid Oxidation and its Regulation; in Fatty Acid Metabolism and its Regulation, ed., S.Numa, Elsevier Science Publishers B.V., 113-154, 1984.

214. Rose, G., Bar-Tana, J. and Shapiro, B. Palmitoyl Coenzyme Synthetase Activation by Uncomplexed ATP. Biochim. Biophys. Acta, **573**, 126-135, 1979.

215. Bar-Tana, J,. Rose, G., Brandes, R, and Shapiro, B. Palmitoyl-Coenzyme A Synthetase. Mechanism of Reaction. Biochem. J., **131**, 199-209, 1973.

216. Bar-Tana, J., Rose, G. and Shapiro, B. Palmitoyl-Coenzyme A Synthetase. Isolation of an Enzyme-Bound Intermediate. Biochem. J., **135**, 411-416, 1973.

217. Berge, R.K. Purification and Characterization of a Long-Chain Acyl-CoA Hydrolase from Rat Liver Microsomes. Biochim. Biophys. Acta, **574**, 321-333, 1979.

218. Barden, R.E and Cleland, W.W. 1-Acylglycerol 3-Phosphate Acyltransferase from Rat Liver. J. Biol. Chem., **244** (13), 3677-3684, 1969.

219. Sun, G.Y., Smith, R.E., Chan, K. and MacQuarrie, R. Inhibition of Acyl-CoA Hydrolase Activity in Liver Microsomes by Lyso-phospholipids. Biochem. Biophys. Res. Commun., **94** (4), 1278-1284, 1980.

220. Yamashita, S., Hosaka, K., Miki, Y. and Numa, S. Glycerolipid Acyltransferases from Rat Liver: 1-Acylglycerophosphate Acyltransferase, 1-Acylglycerophosphorylcholine Acyltransferase, and Diacylglycerol Acyltransferase. Meth. Enzymol., **71**, 528-536, 1981.

221. Possmayer, F., Scherphof, G.L., Dubbelman, T.M.A.R., Van Golde, L.M.G. and Van Deenen, L.L.M. Positional Specificity of Saturated and Unsaturated Fatty Acids in Phosphatidic Acid from Rat Liver. Biochim. Biophys. Acta, **176**, 95-110, 1969.

222. Lands, W.E.M., Inoue, M., Sugiura, Y. and Okuyama, H. Selective Incorporation of Polyunsaturated Fatty Acids into Phosphatidylcholine by Rat Liver Microsomes. J. Biol. Chem., **257**, (24), 14968-14972, 1982.

223. Okuyama, H., Eibl, H. and Lands, W.E.M. Acyl Coenzyme A: 2-Acyl-*sn*-Glycerol-3-Phosphate Acyltransferase Activity in Rat Liver Microsomes. Biochim. Biophys. Acta, **248**, 263-273, 1971.

224. Miki, Y., Hosaka, K. Yamashita, S., Handa, H. and Numa, S. Acyl-Acceptor Specificities of 1-Acylglycerolphosphate Acyltransferase and 1-Acylglycerophosphorylcholine Acyltransferase Resolved from Rat Liver Microsomes. Eur. J. Biochem., **81**, 433-441, 1977.

225. Okuyama, H., Yamada, K. and Ikezawa, H. Acceptor Concentration Effect in the Selectivity of Acyl Coenzyme A:1-Acylglycerylphosphorylcholine Acyltransferase System in Rat Liver. J. Biol.Chem., **250** (5), 1710-1713, 1975.

226. Gavino, V.C. and Deamer, D.W. Purifiction of Acyl CoA:1-acyl-*sn*-glycero-3-phosphorylcholine Acyltransferase. J. Bioenergetics Biomembranes, **14** (5/6), 513-526, 1982.

227. Yamashita, S., Nakaya, N., Miki, Y. and Numa, S. Separation of 1-Acylglycerolphosphate Acyltransferase and 1-Acylglycerolphosphorylcholine Acyltransferase of Rat Liver Microsomes. Proc. Nat. Acad. Sci. USA., **72** (2), 600-603, 1975.

228. Hasegawa-Sasaki, H. and Ohno, K. Extraction and Partial Purification of Acyl-CoA:1-Acyl-*sn*-Glycero-3-Phosphocholine Acyltransferase from Rat Liver Microsomes. Biochim. Biophys. Acta, **617**, 205-217, 1980.

229. Deka, N., Sun, G.Y. and MacQuarrie, R. Purification and Properties of Acyl-CoA:1-Acyl-sn-Glycero-3-phosphocholine-O-Acyltransferase from Bovine Brain Microsomes. Arch. Biochem. Biophys., **246**, (2), 554-563, 1986.

230. Van Den Bosch, H. Phospholipases: Link between Membrane Phospholipids and Arachidonate Metabolites. NATO Adv. Sci. Inst. Ser., Ser A, **54**, 1-14, 1983.

231. Blackwell, G.J. and Flower, R.J. Inhibition of Phospholipase. Brit. Med. Bull., **39** (3), 260-264, 1983.

232. Waite, M. Approaches to the Study of Mammalian Cellular Phospholipases. J. Lipid Res., **26**, 1379-1387, 1985.

233. Lapetina, E.G. Regulation of Arachidonic Acid Production: Role of Phospholipases C and A_2. TIPS, **3** (3), 115-118, 1982.

234. Van Den Bosch, H. Intracellular Phospholipases A. Biochim. Biophys. Acta, **604**, 191-246, 1980.

235. Oshino, N., Imai, Y. and Sato, R. Electron-Transfer Mechanism Associated with Fatty Acid Desaturation Catalyzed by Liver Microsomes. Biochim. Biophys. Acta, **128**, 13-28, 1966.

236. Oshino, N., Imai, Y. and Sato, R. A Function of Cytochrome b_5 in Fatty Acid Desaturation by Rat Liver Microsomes. J. Biochem., **69**, 155-167, 1971.

237. Brenner, R.R. The Desaturation Step in the Animal Biosynthesis of Polyunsaturated Fatty Acids. Lipids, **6** (8), 567-575, 1971.

238. Jeffcoat, R. The Biosynthesis of Unsaturated Fatty Acids and its Control in Mammalian Liver; in Essays in Biochemistry ed., P.N.Campbell and R.D.Marshall, Academic Press, London, **15**, 1-36, 1979.

239. Oshino, N. and Omura, T. Immunochemical Evidence for the Participation of Cytochrome b_5 in Microsomal Stearoyl-CoA Desaturation Reaction. Arch. Biochem. Biophys., **157** (2), 395-404, 1973.

240. Lee, T., Baker, R.C. Stephens, N. and Snyder, F. Evidence for Participation of Cytochrome b_5 in Microsomal Δ6-Desaturation of Fatty Acids. Biochim. Biophys. Acta, **489**, 25-31, 1977.

241. Jones, P.D., Holloway, P.W., Peluffo, R.O. and Wakil, S.J. A Requirement for Lipids by the Microsomal Stearyl Coenzyme A Desaturase. J. Biol. Chem., **244** (3), 744-754, 1969.

242. Holloway, P.W. and Wakil, S.J. Requirement for Reduced Diphosphopyridine Nucleotide-Cytochrome b_5 Reductase in Stearyl Coenzyme A Desaturation. J. Biol. Chem., **245** (7), 1862-1865, 1970.

243. Holloway, P.W. A Requirement for Three Protein Components in Microsomal Stearyl Coenzyme A Desaturation. Biochemistry, **10** (9), 1556-1560, 1971.

244. Holloway, P.W., Roseman, M. and Calabro, A. The Role of Lipid in Stearyl CoA Desaturation. Adv. Exper. Med. Biol., **83**, 23-32, 1977.

245. Jeffcoat, R., Brawn, P.R. and James, A.T. The Effect of Soluble Rat Liver Proteins on the Activity of Microsomal Stearoyl-CoA and Linoleoyl-CoA Desaturase. Biochim. Biophys. Acta, **431**, 33-44, 1976.

246. Leiken, A.I., Nervi, A.M. and Brenner, R.R. Lipid Binding Properties of a Factor Necessary for Linoleic Acid Desaturation. Lipids, **14** (12), 1021-1026, 1979.

247. Leiken, A.I. and Brenner, R.R. Regulation of Linoleic Acid Δ6-Desaturation by a Cytosolic Lipoprotein-like Fraction in Isolated Rat Liver Microsomes. Biochim. Biophys. Acta, **876**, 300-308, 1986.

248. Jones, D.P. and Gaylor, J.L. Regulation of Microsomal Stearoyl-Coenzyme A Desaturase. Biochem. J., **183**, 405-415, 1979.

249. Catalá, A., Nervi, A.M. and Brenner, R.R. Separation of a Protein Factor Necessary for the Oxidative Desaturation of Fatty Acids in the Rat. J. Biol. Chem., **250** (18), 7481-7484, 1975.

250. Bloch, K. Enzymatic Synthesis of Monounsaturated Fatty Acids. Accounts Chem. Res., **2** (7), 193-202, 1969.

251. Strittmatter, P. and Enoch, H.G. Purification of Stearyl-CoA Desaturase from Rat Liver. Meth. Enzymol., **52**, 188-193, 1978.

252. Brenner, R.R. Nutritional and Hormonal Factors Influencing Desaturation of Essential Fatty Acids. Prog. Lipid Res., **20**, 41-47, 1981.

253. Fujiwara, Y., Okayasu, T., Ishibashi, T. and Imai, Y. Immunochemical Evidence for the Enzymatic Difference of Δ6-Desaturase from Δ9-and Δ5-Desaturase in Rat Liver Microsomes. Biochem. Biophys. Res. Commun., **110** (1), 36-41, 1983.

254. Strittmatter, P., Spatz, L., Corcoran, D., Rogers, M.J., Setlow, B. and Redline, R. Purification and Properties of Rat Liver Microsomal Stearyl Coenzyme A Desaturase. Proc. Nat. Acad. Sci. USA, **71** (11), 4565-4569, 1974.

255. Okayasu, T., Nagao, M., Ishibashi, T. and Imai, Y. Purification and Partial Characterization of Linoleoyl-CoA Desaturase from Rat Liver Microsomes. Arch. Biochem. Biophys., **206** (1), 21-28, 1981.

256. Horrobin, D.F. and Cunnane, S.C. Is the Triene/Tetraene Ratio always a Valid Indicator of Functional Essential Fatty Acid Deficiency? Prog. Lipid Res., **20**, 831-833, 1981.

257. Jeffcoat, R. The Physiological Role and Control of Mammalian Fatty Acyl-Coenzyme A Desaturases. Biochem. Soc. Transac., **5**, 811-818, 1977.

258. Prasad, M.R. and Joshi, V.C. Purification and Properties of Hen Liver Microsomal Terminal Enzyme Involved in Stearoyl Coenzyme A Desaturation and Its Quantitation in Neonatal Chicks. J. Biol. Chem., **254** (14), 6362-6369, 1979.

259. Joshi, V.C., Prasad, M.R. and Sreekrishna, K. Terminal Enzyme of Stearoyl-CoA Desaturation from Chicken Liver. Meth. Enzymol., **71**, 252-258, 1981.

260. Thiede, M. A., Ozols, J. and Strittmatter, P. Construction and Sequence of cDNA for Rat Liver Stearyl Coenzyme A Desaturase. J. Biol. Chem., **261** (28), 13230-13235, 1986.

261. Jeffcoat, R. and James, A.T. Problems Involved with the Purification of Stearoyl-CoA Desaturase. Lipids, **1**, 1-9, 1976.

262. Enoch, H.G., Catalá, A. and Strittmattter, P. Mechanism of Rat Liver Microsomal Stearyl-CoA Desaturase. J. Biol. Chem., **251** (16), 5095-5103, 1976.

263. Okayasu, T., Nagao, M, and Imai, Y. Solubilization of Linoleoyl-Coenzyme A Desaturase of Rat Liver Microsomes. FEBS Lett., **104** (2), 241-243, 1979.

264. Prasad, M.R., Sreekrishna, K. and Joshi, V.C. Topology of the Δ9 Terminal Desaturase in Chicken Liver Microsomes and Artificial Micelles. J. Biol. Chem., **255** (6), 2583-2589, 1980.

265. Fujiwara, Y., Ishibashi, T. and Imai, Y. Cytoplasmic Location of Linoleoyl-CoA Desaturase in Microsomal Membranes of Rat Liver. Arch. Biochem. Biophys., **233** (2), 402-407, 1984.

266. Mahfouz, M.M., Johnson, S. and Holman, R.T. The Effect of Isomeric trans-18:1 acids on the Desaturation of Palmitic, Linoleic and Eicosa-8,11,14-trienoic Acids by Rat Liver Microsomes. Lipids, **15** (2), 100-107, 1980.

267. Okayasu, T., Ono, T., Shinojima, K. and Imai, Y. Involvement of Cytochrome b_5 in the Oxidative Desaturation of Linoleic Acid to γ-Linolenic Acid in Rat Liver Microsomes. Lipids, **12** (3), 267-271, 1977.

268. Ullman, D. and Sprecher, H. An *in vitro* Study of the Effects of Linoleic, Eicosa-8,11,14-trienoic and Arachidonic Acids on the Desaturation of Stearic, Oleic and Eicosa-8,11-dienoic Acids. Biochim. Biophys. Acta, **248**, 61-70, 1971.

269. Brenner, R.R. and Peluffo, R.O. Effect of Saturated and Unsaturated Fatty Acids on the Desaturation *in Vitro* of Palmitic, Stearic, Oleic, Linoleic, and Linolenic Acids. J. Biol. Chem., **241** (22), 5213-5219, 1966.

270. Brenner, R.R and Peluffo, R.O. Regulation of Unsaturated Fatty Acid Biosynthesis. 1. Effect of Unsaturated Fatty Acid of 18 Carbons on the Microsomal Desaturation of Linoleic Acid into γ-Linolenic Acid. Biochim. Biophys. Acta, **176**, 471-479, 1969.

271. Pollard, M.R., Gunstone, F.D., Morris, L.J. and James, A.T. The Δ5 and Δ6 Desaturation of Fatty Acids of Varying Chain Length by Rat Liver: A Preliminary Report. Lipids, **15** (9), 690-693, 1980.

272. Castuma, J.C., Brenner, R.R. and Kunau, W. Specificity of Δ6-Desaturase - Effect of Chain Length and Number of Double Bonds. Adv. Exper. Med. Biol., **83**, 127-134, 1977.

273. Pugh, E.L. and Kates, M. Direct Desaturation of Eicosatrienoyl Lecithin to Arachidonoyl Lecithin by Rat Liver Microsomes. J. Biol. Chem., **252** (1), 68-73, 1977.

274. Pugh, E. L. and Kates, M. Membrane-Bound Phospholipid Desaturases. Lipids, **14** (2), 159-165, 1978.

275. Stymne, S. and Appelqvist, L. The Biosynthesis of Linoleate from Oleoyl-CoA via Oleoyl-Phosphatidylcholine in Microsomes of Developing Safflower Seeds. Eur. J. Biochem., **90**,223-229, 1978.

276. Jeffcoat, R., Dunton, A.P. and James, A.T. Evidence for the Different Responses of Δ9-, Δ6- and Δ5-Fatty Acyl-CoA Desaturases to Cytoplasmic Proteins. Biochim. Biophys. Acta, 528, 28-35, 1978.

277. Leiken, A.I. and Brenner, R.R. Microsomal Δ5-Desaturation of Eicosa-8,11,14-trienoic Acid is Activated by a Cytosolic Fraction. Lipids, **24** (2),101-104, 1989.

278. Lamb, R.G. and Fallon, H.J. Inhibition of Monoacylglycerophosphate Formation by Chlorophenoxyisobutyrate and β-benzalbutyrate. J. Biol. Chem., **247** (4), 1281-1287, 1972.

279. Constantinides, P.P. and Steim, J.M. Physical Properties of Fatty Acyl-CoA. J. Biol. Chem., **260** (12), 7573-7580, 1985.

280. Jeffcoat, R., Brawn, P.R., Safford, R. and James, A.T. Properties of Rat Liver Microsomal Stearoyl-Coenzyme A Desaturase. Biochem. J., **161**, 431-437, 1977.

281. Brenner, R.R. The Oxidative Desaturation of Unsaturated Fatty Acids in Animals. Mol. Cell. Biochem., **3** (1), 41-52, 1974.

282. Brenner, R.R. Regulatory Function of Δ6-Desaturase -Key Enzyme of Polyunsaturated Fatty Acid Synthesis. Adv. Exper. Med. Biol., **83**, 85-101, 1977.

283. Clandinin, M.T., Wong, K. and Hacker, R.R. Synthesis of Chain Elongation-Desaturation Products of Linoleic Acid by Liver and Brain Microsomes During Developement of the Pig. Biochem. J., **226**, 305-309, 1985.

284. Prasad, M.R. and Joshi, V.C. Regulation of Rat Hepatic Stearoyl Coenzyme A Desaturase. J. Biol. Chem., **254** (4), 997-999, 1979.

285. Wilson, A.C., Wakil, S.J. and Joshi, V.C. Induction of Microsomal Stearyl Coenzyme A Desaturase in Newly Hatched Chicks. Arch. Biochem. Biophys., **173**, 154-161, 1976.

286. Oshino, N. and Sato, R. The Dietary Control of Microsomal Stearyl CoA Desaturation Enzyme System in Rat Liver. Arch. Biochem. Biophys., **149**, 369-377, 1972.

287. Jeffcoat, R. and James, A.T. Interrelationship between the Dietary Regulation of Fatty Acid Synthesis and the Fatty Acyl-CoA Desaturases. Lipids, **12** (6), 469-474, 1977.

288. Inkpen, C.A., Harris, R.A. and Quackenbush, F.W. Differential Responses to Fasting and Subsequent Feeding by Microsomal Systems of Rat Liver: 6-and 9-Desaturation of Fatty Acids. J. Lipid. Res., **10**, 277-282, 1969.

289. De Gómez Dumm, I.N.T., Peluffo, R.O. and Brenner, R.R. Comparative Effect of a Protein Diet on the Desaturation, Elongation and Simultaneous Desaturation and Elongation of Linoleic Acid. Lipids, **7** (9), 590-592, 1972.

290. Peluffo, R.O., Nervi, A.M., Gonzales, M.S. and Brenner, R.R. Effect of Different Amino Acid Diets on Δ5, Δ6 and Δ9 Desaturases. Lipids, **19** (2), 154-157, 1984.

291. De Alaniz, M.J.T., De Gómez Dumm, I.N.T. and Brenner, R.R. Effect of Fasting on Δ5 Desaturation Activity in Rat Liver Microsomes and HTC cells. Mol. Cell. Biochem., **33**, 165-170, 1980.

292. Jeffcoat, R. and James, A.T. The Control of Stearoyl-CoA Desaturase by Dietary Linoleic Acid. FEBS Lett., **85** (1), 114-118, 1978.

293. De Gómez Dumm, I.N.T., De Alaniz, M.J.T. and Brenner, R.R. Effect of Dietary Fatty Acids on Δ5 Desaturase Activity and Biosynthesis of Arachidonic Acid in Rat Liver Microsomes. Lipids, **18** (11), 781-788, 1983.

294. Peluffo, R.O., Nervi, A.M. and Brenner, R.R. Linoleic Acid Desaturation Activity of Liver Microsomes of Essential Fatty Acid Deficient and Sufficient Rats. Biochim. Biophys. Acta, **441**, 25-31, 1976.

295. Kinsella, J.E., Bruckner, G., Mai, J. and Shimp, J. Metabolism of *trans* Fatty Acids with Emphasis on the Effects of *trans,trans*-Octadecadienoate on Lipid Composition, Esssential Fatty Acid, and Prostagladins: an Overview. Am. J. Clin, Nutr, **34**, 2307-2381, 1981.

296. Blomstrand, R., Diczfalusy, U., Sisfontes, L and Svensson, L. Influence of Dietary Partially Hydrogenated Vegetable and Marine Oils on Membrane Composition and Function of Liver Microsomes and Platelets in the Rat. Lipids, **20** (5), 283-295, 1985.

297. Mahfouz, M. Effect of Dietary trans Fatty Acids on the Δ5, Δ6 and Δ9 Desaturases of Rat Liver Microsomes in vivo. Acta. Biol. Med Germ, **40**, 1699-1705, 1981.

298. Kirstein, D., Hoy, C.-E. and Holmer, G. Effect of Dietary Fats on the Δ6- and Δ5-Desaturation of Fatty Acids in Rat Liver Microsomes. Brit. J. Nutr., **50**, 749-756, 1983.

299. Pollard, M.R., Gunstone, F.D., James, A.T. and Morris, L.J. Desaturation of Positional and Geometric Isomers of Monoenoic Fatty Acids by Microsomal Preparations from Rat Liver. Lipids, **15** (5), 306-314, 1980.

300. Mahfouz, M.M., Valicenti, A.J. and Holman, R.T. Desaturation of Isomeric *trans*-Octadecenoic Acids by Rat Liver Microsomes. Biochim. Biophys. Acta., **618**, 1-12, 1980.

301. Mahfouz, M. and Holman, R.T. Desaturation of Isomeric *cis* 18:1 Acids. Lipids, **15** (1), 63-65, 1980.

302. Hill, E.G., Johnson S.B., Lawson, L.D. Mahfouz, M.M. and Holman, R.T. Peturbation of the Metabolism of Essential Fatty Acids by Dietary Partially Hydrogenated Vegetable Oil. Proc. Natl. Acad. Sci. USA, **79**, 953-957, 1982.

303. De Schrijver, R. and Privett, O.S. Effects of Dietary Long-Chain Fatty Acids on the Biosynthesis of Unsaturated Fatty Acids in the Rat. J. Nutr., **112**, 619-626, 1982.

304. Mahfouz, M.M., Smith, T.L. and Kummerow, F.A. Effect of Dietary Fats on Desaturase Activities and the Biosynthesis of Fatty Acids in Rat-Liver Microsomes. Lipids, **19** (3), 214-222, 1984.

305. Mikhailidis, D.P., Kirtland, S.J., Barradas, M.A., Mahadeviah, S. and Dandona, P. The Effect of Dihomogammalinolenic Acid on Platelet Aggregation and Prostaglandin Release, Erythrocyte Membrane Fatty Acids and Serum Lipids: Evidence for Defects in PGE_1 Synthesis and Δ5-Desaturase Activity in Insulin-Dependent Diabetics. Diabetes Res., **3**, 7-12, 1986.

306. Poisson, J.-P. Comparative in Vivo and in Vitro Study of the Influence of Experimental Diabetes on Rat Liver Linoleic Acid Δ6- and Δ5-Desaturation. Enzyme, **34**, 1-14, 1985.

307. Jeffcoat, R., Roberts, P.A., Ormesher, J. and James, A.T. Stearoyl-CoA Desaturase: A Control Enzyme in Hepatic Lipogenesis. Eur. J. Biochem., **101**, 439-445, 1979.

308. Faas, F.H. and Carter, W.J. Fatty Acid Desaturation and Microsomal Lipid Fatty Acid Composition in Experimental Hypothyroidism. Biochem. J., **207**, 29-35, 1982.

309. De Gómez Dumm, I.N.T., De Alaniz, M.J.T. and Brenner, R.R. Effect of Glucocorticoids on the Oxidative Desaturation of Fatty Acids by Rat Liver Microsomes. J. Lipid Res., **20**, 834-839, 1979.

310. Leiken, A.I. and Brenner, R.R. Cholesterol-induced Microsomal Changes Modulate Desaturase Activities. Biochim. Biophys. Acta, **922**, 294-303, 1987.

311. Wang, D.L. and Reitz, R.C. Ethanol Ingestion and Polyunsaturated Fatty Acids: Effects on the Acyl-CoA Desaturases. Alcoholism: Clin. Exper. Res., **7** (2), 220-226, 1983.

312. Reitz, R.C. Relationship of the Acyl-CoA Desaturases to Certain Membrane Fatty Acid Changes Induced by Ethanol Consumption. Proc. West. Pharmacol. Soc., **27**, 247-249, 1984.

313. Berman, M.C., Ivanetich, K.M. and Kench, J.E. The Effects of Halothane on Hepatic Microsomal Electron Transfer. Biochem. J., **148**, 179-186, 1975.

314. Ivanetich, K.M., Manca, V., Harrison, G.G. and Berman, M. Enflurane and Methoxyflurane: Their Interaction with Hepatic Microsomal Stearate Desaturase. Biochem. Pharmacol., **29**, 27-34, 1980.

315. Sreekrishna, K., Prasad, M.R., Wakil, A.S. and Joshi, V.C. Interaction of Phenols with Δ9- Terminal Desaturase and other Cyanide-sensitive Factors in Chicken Liver Microsomes. Biochim. Biophys. Acta, **665**, 427-433, 1981.

316. Umeki, S. and Nozawa, Y. Effect of Local Anesthetics on Stearoyl-CoA Desaturase of *Tetrahymena* Microsomes. Biol. Chem. Hoppe-Seyler, **367**, 61-65, 1986.

317. De Gómez Dumm, I.N.T. and Brenner, R.R. Oxidative Desaturation of α-Linolenic, Linoleic, and Stearic Acids by Human Liver Microsomes. Lipids, **10** (6), 315-317, 1975.

318. Hughs, S. and York, D.A. Hepatic Δ6-Desaturase Activity in Lean and Genetically Obese *ob/ob* Mice. Biochem. J., **225**, 307-313, 1985.

319. Willis, A.L. Essential Fatty Acids, Prostaglandins and Related Eicosanoids. in 90-115

320. Rivers, J.P.W., Hassam, A.G., Crawford, M.A. and Brambell, M.R. The Inability of the Lion, *Panthera Leo*, L. to Desaturate Linoleic Acid. FEBS Lett., 67, (3), 269-270, 1976.

321. Clark, D.L. and Queener, S.F. Effects of Diabetes Mellitus on Renal Fatty Acid Activation and Desaturation. Biochem. Pharmacol., **34** (24), 4305-4310, 1985.

322. Mandon, E.C., De Gómez Dumm, I.N. and Brenner, R.R. Effect of High Carbohydrate and High Protein Diets on Microsomal Fatty Acid Composition, Fluidity and Delta 6 Desaturation Activity in Kidney and Lung. Acta. Physiol. Pharmacol. Latinoam., **38**(1), 49-58, 1988.

323. Ayala, S., Gaspar, G., Brenner, R.R., Peluffo, R.O. and Kunau, W. Fate of Linoleic, Arachidonic, and Docosa-7,10,13,16-tetraenoic Acid in Rat Testicles. J. Lipid Res., **14**, 296-305, 1973.

324. McDonald, T.M. and Kinsella, J.E. Stearyl-CoA Desaturase of Bovine Mammary Microsomes. Arch. Biochem. Biophys., **156**, 223-231, 1973.

325. Salviati, G., Betto, R., Salvatori, S. and Margreth, A. Evidence for the Presence of the Stearyl-CoA Desaturase System in the Sarcoplasmic Reticulum of Rabbit Slow Muscle. Biochim. Biophys. Acta, **574**, 280-289, 1979.

326. Mandon, E.C., De Gomez Dumm, I.N. and Brenner, R.R. Effect of Epinephrine on the Oxidative Desaturation of Fatty Acids in the Rat Adrenal Gland. Lipids, **21** (6), 401-404, 1986.

327. Chapkin, R.S. and Ziboh, V.A. Inability of Skin Enzyme Preparations to Biosynthesize Arachidonic Acid from Linoleic Acid. Biochem. Biophys. Res. Commun., **124** (3), 784-792, 1984.

328. Chapkin, R.S., Ziboh, V.A., Marcello, C.L. and Voorhees, J.J. Metabolism of Essential Fatty Acids by Human Epidermal Enzyme Preparations: Evidence of Chain Elongation. J. Lipid Res., **27**, 945-954, 1986.

329. De Bravo, M.M.G., De Tomás, M.E. and Mecuri, O. Metabolism of Gammalinolenic Acid by Human Blood Platelet Microsomes. Biochem. Int., **10** (6), 889-896, 1985.

330. Rao, G.A. and Abraham, S. Stearoyl-CoA Desaturase Activity in Mammary Adrenocarcinomas Carried by C_3H Mice. Lipids, **10** (12), 835-839, 1975.

331. Morton, R.E., Hartz, J.W., Reitz, R.C., Waite, B.M. and Morris, H.P. The Acyl-CoA Desaturases of Microsomes from Rat Liver and the Morris 7777 Hepatoma. Biochim. Biophys. Acta, **573**, 321-331, 1979.

332. Dunbar, L.M. and Bailey, J.M. Enzyme Deletions and Essential Fatty Acid Metabolism in Cultured Cells. J. Biol. Chem., **250** (3), 1152-1153, 1975.

333. Dippenaar, N., Booyens, J., Fabbri, D. and Katzeff, I.E. The Reversibility of Cancer: Evidence that Malignancy in Melanoma Cells is Gamma-Linolenic Acid Deficiency-Dependent. SA Med. J., **62**, 505-509, 1982.

334. Nugteren, D.H. The Enzymic Chain Elongation of Fatty Acids by Rat-Liver Microsomes. Biochim. Biophys. Acta, **106**, 280-290, 1965.

335. Keyes, S.R. and Cinti, D.L. Biochemical Properties of Cytochrome b_5-Dependent Microsomal Fatty Acid Elongation and Identification of Products. J. Biol. Chem., **255** (23), 11357-11364, 1980.

336. Nagi, M., Cook, L., Prasad, M.R. and Cinti, D.L. Do Rat Hepatic Microsomes Contain Multiple NADPH-Supported Fatty Acid Chain Elongation Pathways or a Single Pathway? Biochem. Biophys. Res. Commun., **140** (1), 74-80, 1986.

337. Nagi, M., Cook, L., Prasad, M.R. and Cinti, D.L. Site of Participation of Cytochrome b_5 in Hepatic Microsomal Fatty Acid Chain Elongation. J. Biol. Chem., **258** (24), 14823-14828, 1983.

338. Nagao, M., Ishibashi, T., Okayasu, T. and Imai, Y. Possible Involvement of NADPH-Cytochrome P450 Reductase and Cytochrome b_5 on β-Ketostearoyl-CoA Reduction in Microsomal Fatty Acid Chain Elongation Supported by NADPH. FEBS Lett., **155** (1), 11-14, 1983.

339. Ilan, Z., Ilan, R. and Cinti, D.L. Evidence for a New Physiological Role of Hepatic NADPH:Ferricytochrome (P450) Oxidoreductase. J. Biol. Chem., **256** (19), 10066-10072, 1981.

340. Osei, P., Suneja, S.K., Laguna, J.C., Nagi, M., Cook, L., Prasad, M.R. and Cinti, D.L. Topography of the Rat Hepatic Microsomal Enzymatic Components of the Fatty Acid Chain Elongation System. J. Biol. Chem., **264** (12), 6844-6949, 1989.

341. Bernert, Jr., J.T. and Sprecher, H. Studies to Determine the Role Rates of Chain Elongation and Desaturation Play in Regulating the Unsaturated Fatty Acid Composition of Rat Liver Lipids. Biochim. Biophys Acta, **398**, 354-363, 1975.

342. Strittmatter, P. and Dailey, H.A. Essential Structural Features and Orientation of Cytochrome b_5 in Membranes; in Membrane and Transport,**1**, ed., A. Martonosi, Plenum Press, New York and London, 71-82, 1982.

343. Omura, T. and Takesue, S. A New Method for Simultaneous Purification of Cytochrome b_5 and NADPH-Cytochrome c Reductase from Rat Liver Microsomes. J. Biochem., **67** (2), 249-257, 1970.

344. Oshino, N. Cytochrome b_5 and its Physiological Significance. Pharmac. Ther. A., **2**, 477-515, 1978.

345. Spatz, L. and Strittmatter, P. A Form of Reduced Nicotinamide Adenine Dinucleotide-Cytochrome b_5 Reductase Containing Both the Catalytic Site and an Additional Hydrophobic Membrane-binding Segment. J. Biol. Chem., **248** (3), 793-799, 1973.

346. Dailey, H.A. and Strittmatter, P. Characterization of the Interaction of Amphipathic Cytochrome b_5 with Stearyl Coenzyme A Desaturase and NADPH:Cytochrome P-450 Reductase. J. Biol. Chem., **255** (11), 5184-5189, 1980.

347. Dailey, H.A. and Strittmatter, P. Modification and Identification of Cytochrome b_5 Carboxyl Groups Involved in Protein-Protein Interaction with Cytochrome b_5 Reductase. J. Biol. Chem., **254** (12), 5388-5396, 1979.

348. Wolfe, L.S. Eicosanoids: Prostaglandins, Thromboxanes, Leukotrienes, and Other Derivatives of Carbon-20 Unsaturated Fatty Acids. J. Neurochem., **38** (1), 1-14, 1982.

349. Konturek, S.J. and Pawlik, W. Physiology and Pharmacology of Prostaglandins. Digestive Diseases and Sciences, **31** (2), 6S-19S, 1986.

350. Crawford, M.A. Background to Essential Fatty Acids and their Prostanoid Derivatives. Brit. Med. Bull., **39** (3), 210-213, 1983.

351. Willis, A.L. Unanswered Questions in EFA and PG Research. Prog. Lipid Res., **20**, 839-849, 1981.

352. Moncada, S. and Vane, J.R. Pharmacology and Endogenous Roles of Prostaglandin Endoperoxides, Thromboxane A_2, and Prostacyclin. Pharm. Rev., **30** (3), 293-331, 1979.

353. Needleman, P., Turk, J., Jakschik, B.A., Morrison, A.R. and Lefkowith, J.B. Arachidonic Acid Metabolism. Ann. Rev. Biochem., **55**, 69-102, 1986.

354. Mead, J.F., Alfin-Slater, R.B., Howton, D.R. and Popjak, G. Prostaglandins, Thromboxanes and Prostacyclin; in Lipids, Chemistry, Biochemistry and Nutrition. Plenum Press, London, New York, 149-215. 1986.

355. Lloyd-Davies, K.A. and Brindley, D.N. Palmitate Activation and Esterification in Microsomal Fractions of Rat Liver. Biochem. J., **152**, 39-49, 1975.

356. Saynor, R., Gillott, T., Doyle, T., Allen, D., Field, P. and Scott, M. Clinical Studies on the Effect of Dietary *n*-3 and *n*-6 Fatty Acids on Serum Lipids, Haemostasis and GTN Consumption. Prog. Lipid Res., **25**, 211-217, 1986.

357. Zipser, R.D and Laffi, G. Prostaglandins, Thromboxanes and Leukotrienes in Clinical Medicine. West J. Med., **143**, 485-497, 1985.

358. Salmon, J.A. and Higgs, G.A. Prostaglandins and Leukotrienes as Inflamatory Mediators. Brit. Med. Bull., **43** (2), 285-296, 1987.

359. Holtzman, J.L. and Carr, M.L. The Temperature Dependence of Components of the Hepatic Microsomal Mixed Function Oxidases. Arch. Biochem. Biophys., **150**, 227-234, 1972.

360. Lowry, O., Rosenbourgh, N., Farr, A. and Randell, R. Protein measurements with Folin Phenol Reagent. J. Biol. Chem., **193**, 265-275, 1951.

361. Chaykin, S. Biochemistry Laboratory Techniques, John Wiley, New York, 20, 1966.

362. Stripp, B., Zampaglione, N., Hamrick, M. and Gillette, J.R. An Approach Measurement of the Stoichiometric Relationship between Hepatic Microsomal Drug Metabolism and the Oxidation of Reduced Nicotinamide Adenine Dinucleotide Phosphate. Mol. Pharmacol., **8**, 189-196, 1972.

363. Dippy, J.F.J., Hughes, S.R.C. and Rosanski, A. Chemical Constitution and Dissociation Constants of Monocarboxylic Acids. J. Chem. Soc., **1959**, 2492, 1959.

364. Costa, A.K. and Ivanetich, K.M. The 1,2-Dichloroethylenes: their Metabolism by Hepatic Cytochrome P-450 in vitro. Biochem. Pharmacol., **31**, 2093-2102, 1982.

365. Soltis, J.J. and Gandolfi, A.J. Detection of Fluorinated Anesthetic Metabolites by Sodium Fusion. Anesth. Analg., **59**, 61-64, 1980.

366. Hilderbrandt, A.G., Speck, M. and Roots, I. Possible Control of Hydrogen Peroxide Production and Degradation in Microsomes during Mixed Function Oxidation Reactions. Biochem. Biophys. Res. Commun., **54** (3), 968- 975, 1973.

367. Hilderbrandt, A.G., Roots, I., Tjoe, M. and Heinemeyer, G. Hydrogen Peroxide in Hepatic Microsomes. Determination of H_2O_2 in the Presence of Catalase and Absence of Sodium Azide; in Methods in Enzymology III Part C, eds. S.Fleisher and C.Pacher, Academic Press, New York, 345-346, 1978.

368. Aveldano, M.I., VanRollins, M. and Horrocks, L.A. Separation and Quantitation of Free Fatty Acids and Fatty Acid Methyl Esters by Reverse Phase High Pressure Liquid Chromatography. J.Lipid Res., **24**, 83-91, 1983.

369. McIntosh, D.B., Berman, M.C. and Kench, J.E. Characteristics of Sarcoplasmic Reticulum from Slowly Glycolysing and from Rapidly Glycolysing Pig Skeletal Muscle *post mortem.* Biochem. J., **166**, 387-398, 1977.

370. Saunders, R.D. and Horrocks, L.A. Simultaneous Extraction and Preparation for High-Performance Liquid Chromatography of Prostaglandins and Phospholipids. Anal. Biochem., **143**, 71-75, 1984.

371. Pugh, E.L. and Kates, M. The Dietary Regulation of Acyltransferase and Desaturase Activities in Microsomal Membranes of Rat Liver. Lipids, **19** (1), 48-55, 1984.

372. Folch, J., Lees, M. and Sloan Stanley, G.H. A Simple Method for the Isolation and Purification of Total Lipides from Animal Tissue. J. Biol. Chem., **226** , 497-509, 1957.

373. Skipski, V.P. and Barclay, M. Thin-Layer Chromatography. Meth. Enzymol., **14**, 530-599, 1969.

374. Lands, W.E.M. Metabolism of Glycerolipids. II. The Enzymatic Acylation of Lysolecithin. J. Biol. Chem., **235** (8), 2233-2237, 1960.

375. Stadman, E.R. Acyl Coenzyme A and other Thiol Esters. Meth. Enzymol., **3**, 921-941, 1957.

376. Segel, I.H., Kinetics of Unireactant Enzymes. Effect of Endogenous Substrates; in Enzyme Kinetics, John Wiley and Sons, New York/ London/ Sydney/ Toronto, 89-97, 1975.

377. Schröder, U. and Diehl, H. Substrate Specificity of the Carbon Monoxide-Dependent Cytochrome P-450 Kinetics. Biochim. Biophys. Acta, **913**, 185-194, 1987.

378. Fiserova-Bergerova, V. Inhibitory Effect of Isoflurane upon Oxidative Metabolism of Halothane. Anesth. Analg., **63**, 399-404, 1984.

379. Fiserova-Bergerova, V. and Dolan, F.D. Transient Inhibitory Effect of Isoflurane upon Oxidative Halothane Metabolism. Anesth. Analg., **64**, 1171-1177, 1985.

380. Jansson, I. and Schenkman, J.B. Influence of Cytochrome b_5 on the Stoichiometry of the Different Oxidative Reactions Catalyzed by Liver Microsomal Cytochrome P-450. Drug Metab. Dispos., **15** (3), 846-851, 1987.

381. Van Dyke, R.A. Hepatic Centrilobular Necrosis in Rats after Exposure to Halothane, Enflurane, or Isoflurane. Anesth. Analg., **61**, 812-819, 1982.

382. Kawata, S., Trzaskos, J.M. and Gaylor, J.L. Microsomal Enzymes of Cholesterol Biosynthesis from Lanosterol. J. Biol. Chem., **260** (11), 6609-6617, 1985.

383. Neet, K.E. and Ainslie Jnr., G.R. Hysteretic Enzymes. Meth. Enzymol., **64**, 192-227, 1980.

384. Larsson, O.M. and Brimer, L. NADH- and NADPH-dependent Desaturation of Linoleic Acid in the Extracted Microsomal Fraction of Rat Liver, and Related Effects of Catalase and Hydrogen Peroxide. Biochim. Biophys. Acta, **572**, 395-403, 1979.

385. Iritani, N., Ikeda, Y. and Kajitani, H. Selectivities of 1-Acylglycerophosphorylcholine Acyltransferase and Acyl-CoA Synthetase for *n*-3 Polyunsaturated Fatty Acids in Platelets and Liver Microsomes. Biochim. Biophys. Acta, **793**, 416-422, 1984.

386. Normann, P.T., Thomassen, M.S., Christiansen, E.L. and Flatmark, T. Acyl-CoA Synthetase Activity of Rat Liver Microsomes. Substrate Specificity with Special Reference to Very-Long-Chain and Isomeric Fatty Acids. Biochim. Biophys. Acta, **664**, 416-427, 1981.

387. Christ, D.D., Satoh, H., Kenna, J,G. and Pohl, L.R. Potential Metabolic Basis for Enflurane Hepatitis and the Cross-sensitization between Enflurane and Halothane. Drug Metab. Dispos., **16** (1), 135-140, 1988.

388. Laguna, J.C., Nagi, M.N., Cook, L. and Cinti, D.L. Action of Ebselen on Rat Hepatic Microsomal Enzyme-Catalyzed Fatty Acid Chain Elongation, Desaturation, and Drug Biotransformation. Arch. Biochem. Biophys. **269** (1), 272-283, 1989.

389 Chapkin, R.S., Somers, S.D. and Erickson, K.L. Inability of Murine Peritoneal Macrophages to Convert Linoleic Acid into Arachidonic Acid. J. Immunol., **140** (7), 2350-2355, 1988.

390. Holloway, P.W. and Mantsch, H.H. Structure of Cytochrome b_5 in Solution by Fourier-Transform Infrared Spectroscopy. Biochemistry, **28**, 931-935, 1989.

391. Rigby, J.S., Bull, P.C., Ashworth, A., Shephard, E.A., Santisteban, I. and Phillips, I.R. Isolation and Characterization of the Genes Coding for Cytochrome b_5 and Cytochrome-b_5 Reductase. Biochem. Soc. Trans.,**17** (1), 194-195, 1989.

392. Marcel, Y.L. and Suzue, G. Kinetic Studies on the Specificity of Long Chain Acyl Coenzyme A Synthetase from Rat Liver Microsomes. J. Biol. Chem., **247**, (14). 4433-4436, 1972.

393. Rubin, D. and Laposata, M. Regulation of Antagonist-induced Prostaglandin E_1 *versus* Prostaglandid E_2 Production. J. Biol. Chem., **266** (35), 23618-23623, 1991.

394. Bar-Tana, J., Rose, G. and Shapiro, B. The Purification and Properties of Microsomal Palmitoyl-Coenzyme A Synthetase. Biochem. J., **122**, 353-362, 1971.

395. Nervi, A.M., Brenner, R.R. and Peluffo, R.O. Effect of Arachidonic Acid on the Microsomal Desaturation of Linoleic into γ-Linolenic Acid and Their Simultaneous Incorporation into the Phospholipids. Biochim. Biophys. Acta, **152**, 539-551, 1968.

396. Ivanetich, K.M. and Bradshaw, J.J. Limitations of the Sodium Fusion Assay for Fluorinated Metabolites. Anesth. Analg., **61** (9), 61-64, 1980.

397. Gibson, G.G, Cinti, D.L., Sligar, S.G. and Schenkman, J.B. The Effect of Microsomal Fatty Acids and Other Lipids on the Spin State of Purified Cytochrome P-450. J. Biol. Chem., **255** (5), 1867-1872, 1980.

398. Emilsson, A. and Sundler, R. Studies on the Enzymatic Pathways of Calcium Ionophore-Induced Phospholipid Degradation and Arachidonic Acid Mobilization in Peritoneal Macrophages. Biochim. Biophys. Acta, **816**, 265-274, 1985.

399. Segel, I.H. Kinetics of Unireactant Enzymes. The Henri and Michaelis-Menten Equation; in Enzyme Kinetics, John Wiley and Sons, New York/ London/ Sydney/ Toronto, 18-22, 1975.

400. Cunningham, C.C, Filus, S., Bottenus, R.E. and Spach, P.I. Effect of Ethanol Consumption on the Phospholipis Composition of Rat Liver Microsomes and Mitochondria. Biochim. Biophys. Acta, **712**, 225-233, 1982.